72-26,337

SHILLING, Norman Zethward, 1944-
THE EFFECT OF VARIABLE PROPERTIES ON THE LAMINAR FLOW OF GASES IN CYLINDRICAL TUBES AT LOW WALL TO BULK TEMPERATURE RATIOS.

Newark College of Engineering, D.Eng.Sc., 1972
Engineering, mechanical

THE EFFECT OF VARIABLE PROPERTIES ON THE LAMINAR FLOW OF GASES IN CYLINDRICAL TUBES AT LOW WALL TO BULK TEMPERATURE RATIOS

BY

NORMAN ZETHWARD SHILLING

A DISSERTATION

PRESENTED IN PARTIAL FULFILLMENT OF

THE REQUIREMENTS FOR THE DEGREE

OF

DOCTOR OF ENGINEERING SCIENCE IN MECHANICAL ENGINEERING

AT

NEWARK COLLEGE OF ENGINEERING

Newark, New Jersey

1971

APPROVAL OF THESIS

THE EFFECT OF VARIABLE PROPERTIES ON THE LAMINAR FLOW OF

GASES IN CYLINDRICAL TUBES AT LOW WALL TO BULK TEMPERATURE RATIOS

BY

NORMAN ZETHWARD SHILLING

FOR

DEPARTMENT OF MECHANICAL ENGINEERING

NEWARK COLLEGE OF ENGINEERING

BY

FACULTY COMMITTEE

APPROVED: ______________________ CHAIRMAN

____

____

____

____

NEWARK, NEW JERSEY

NOVEMBER, 1971

ABSTRACT

The problem of heat transfer in laminar flow of a gas through a constant diameter cylindrical tube is treated. The gas is cooled by the tube walls held at constant temperature. Two tube inlet conditions are considered: (1) fully developed velocity and uniform temperature profiles (Graetz boundary condition) and (2) uniform velocity and temperature (UTV) profiles. Results of the theoretical and experimental phases of the work are presented.

The theoretical solution is based on the compressible boundary layer equations with varying transport and thermodynamic property terms retained. For the Graetz condition, an existing finite difference solution scheme is modified for improved prediction of gradients at the wall. For the UTV condition, a combined analytical-numerical solution scheme is utilized. Similarity conditions are assumed at the tube entrance continuing to a short distance downstream. The results of this analytic solution are then patched to the numerical finite difference scheme. Improved convergence over the finite difference scheme is thus obtainable.

Numerical calculations of velocity and temperature profiles as well as of friction factors were carried out for air and helium at wall-to-bulk temperature ratios ranging from 0.1 to 0.95 with inlet Mach numbers varying from 0.01 to 0.05.

The results of the calculations are presented in terms of Nusselt number and product of friction factor and Reynolds

number vs. Graetz number. The local Nusselt number is shown to be relatively insensitive to variation in inlet wall-to-bulk temperature ratio, whereas the local friction factor Reynolds number parameter showed some sensitivity to the variation of this ratio.

Empirical equations are given for the Nusselt-Graetz number relationship and the friction factor-Reynolds number and a modified Graetz number relationship (which includes the temperature ratio effect).

To substantiate the theoretical results, a limited experimental investigation was conducted. Local heat fluxes and static pressure drops at several points along a 0.3 in. diameter tube were measured. Data was obtained for air for inlet Reynolds numbers ranging from 815 to 1950 and inlet wall to bulk temperature ratios ranging from 0.4 to 1.0.

Heat transfer data for the Graetz boundary condition and friction factor data for the UTV boundary condition are in substantial agreement with the theoretical results. Close agreement also exists for heat transfer results in the entrance for the UTV boundary condition, but in the downstream region the data falls approximately 30% below the theoretical. Friction factor data for the Graetz condition are substantially less than the theoretical prediction in the entrance. This may be due to a slight discontinuity in tube diameters (about 0.02 in.) between the flow development and cooling sections.

ACKNOWLEDGEMENTS

The author wishes to thank his principal advisor, Dr. Richard C. Progelhof, for his helpful criticisms and suggestions made during this investigation. He also appreciates the interest and encouragement of Dr. Rong Chen and Professor Robert Jacobs while the work was in progress. He is grateful for the constructive criticism offered by Dr. G. Peyser, Professor E.H. Stamper, Dr. P.J. Florio and Dr. William Haberman during the preparation of the manuscript and he is also grateful for the support provided by the Foundation for the Advancement of Graduate Study in Engineering.

Cahit Kitaplioglu aided in the correlation of theoretical results. Special thanks are extended to Anita LaSalle for her encouragement and help in the programming and debugging. Paul Baham and Richard Baseil also provided assistance.

These acknowledgements would not be complete if mention were not made of my dear wife, Eleanor, who in addition to her sacrifice and inexhaustable supply of encouragement also did the typing.

TABLE OF CONTENTS

LIST OF ILLUSTRATIONS

Figure | Page

LIST OF TABLES

Nomenclature

Roman Letter Symbol	Meaning
A_1, A_2	area
A_n^I, A_n^{II}	coefficient in linearized form of momentum and energy difference equations pertaining to radial node n
a	exponent in power law for specific heat, or exponent in wall parameter correlation
B_n^I, B_n^{II}	coefficient in linearized form of momentum or energy difference equations pertaining to radial node n
b	exponent in power law for viscosity, or exponent in wall parameter correlation
C'	coefficient in expression for local friction factor, $2\int \rho u^2 r\,dr/\rho_m u_m^2$
C	coefficient in transformation of axial coordinate in similar boundary layer solution
C_n^I, C_n^{II}	coefficient in linearized form of momentum or energy difference equations pertaining to radial node n
c	exponent in power law for thermal conductivity
c_p	specific heat at constant pressure
c_p^+	dimensionless specific heat
c_v	specific heat at constant volume
D	diameter
D_n^{II}, D_n^I	term in linearized form of momentum or energy difference equations pertaining to radial node n
E	voltage, or sum-squared error

E_n^I, E_n^{II}	coefficient in recursive relationship for axial velocity or enthalpy
e	thermocouple output
F	hypothetical closed form solution for velocity or enthalpy
$F_1(\eta), F_2(\eta)$	right hand sides of momentum and energy similar boundary layer equations
	coefficient of pressure in recursive relationship for axial velocity
F_{2-1}	viewfactor from heating element to tube wall in radiation calibration
f	friction factor based on local wall shear stress
$f_{\Delta p}$	friction factor based on static pressure gradient
f	velocity function, U^+/U_e^+
G	enthalpy function, $H_2^+/H_{2,e}^+$
G_n^I, G_n^{II}	term in recursive relationship for velocity or enthalpy
H	enthalpy
H_1^+	dimensionless enthalpy, $(H-H_o)/c_{p,o}T_o$
H_2^+	dimensionless enthalpy, $(H-H_w)/c_{p,o}T_o$
I	current
k	thermal conductivity
k^+	dimensionless thermal conductivity, k/k_o
K	calorimeter conductance, $q_w''/(T_i-T_o)$
L	length
M	total number of axial steps in finite difference solution

M_o	inlet Mach number
$\dot{M}$	mass flow rate
m	axial node index
N	radial node index at wall
Nu_m	local Nusselt number, $-2r_o q_w''/k_m(T_w-T_m)$
n	radial node index
P	dimensionless pressure defect, $(p_o-p)/\rho_o U_o^2$
Pe	Peclet modulus, $Re_x Pr$
Pr	Prandtl number, $c_p\mu/k$
Pr^+	modified Prandtl number, $c_p^+\mu^+/k^+$
p	static pressure
p^+	dimensionless static pressure, p/p_o
Q_r	radiative heat flux
q_w''	heat flux at tube inner wall
q^+	dimensionless wall heat flux, $r_o q_w''/k_o T_o$
R	gas constant in perfect gas law
R_1	ratio of neglected terms to viscosity variation terms in axial momentum equation
R_2	ratio of neglected terms to specific heat and thermal conductivity variation terms in energy equation
R_3	ratio of axial molecular momentum transfer to axial convective momentum transfer
R_4	ratio of axial molecular heat transfer to axial convective heat transfer
Re_o	inlet Reynolds number, $2r_o U_o \rho_o/\mu_o$
R_o, r_o	tube radius
Re_m	Reynolds number based on local mean properties, $2r_o U_m \rho_m/\mu_m$

r	radial coordinate
r^+	dimensionless radial coordinate, r/r_o
T	temperature
U	axial velocity
U^+	dimensionless axial velocity, U/U_o
$\bar{U}$	representative magnitude of axial velocity variation
$\bar{V}$	radial velocity
V^+	dimensionless radial velocity, $(V/U_o)Re_oPr_o$
V	representative magnitude of radial velocity variation
x	axial coordinate
x^+	dimensionless axial coordinate (modified Graetz parameter), $x/r_oRe_oPr_o$
x_m^+	dimensionless axial coordinate based on local mean properties
y^+	dimensionless distance from tube wall, $1-r^+$
Y	thermodynamic or transport property, or dependent variable

Greek Letter Symbols

β	modified Falkner Skan parameter, $\frac{2\xi}{U_e^+}\frac{dU_e^+}{d\xi}$
Γ	$\prod_{i=1}^{n}(r-r_i)$
γ	ratio of specific heats, c_p/c_v
$\Delta p_x, \Delta p_r$	representative magnitudes of radial and axial pressure variation
$\Delta r^+, \Delta x^+$	dimensionless radial and axial mesh steps
δ, δ^2	radial difference operators
ϵ	small parameter in error expansion for wall derivative of axial velocity

ζ	term in Navier Stokes equations
η	similarity parameter, $\frac{U_e^+}{\sqrt{2\xi}}\int_0^{y^+}\rho^+ dy^+$
θ	temperature ratio, T/T_o
Λ_n	Lagrangian polynomial of degree n-l
λ	term in transformed momentum and energy similarity boundary layer equations, $\mu^+\rho^+/C\rho_e^+\mu_e^+$ or second coefficient of viscosity
μ	absolute viscosity
μ^+	dimensionless viscosity, μ/μ_o
ξ	transformed axial coordinate, $\int_0^{x^+}C\rho_e^+\mu_e^+ dx^+$
ρ	density
ρ^+	dimensionless density, ρ/ρ_o
σ	weighting factor in divided difference derivative representations, or Stefan-Boltzmann constant
τ_w^+	dimensionless wall shear stress, $r_o\tau_w/\mu_o U_o$
τ_w	local wall shear stress, $\mu_w \partial U/\partial r^+ \big\|_{r=r_o}$
$\tau_{w,\Delta p}$	wall shear stress due to static pressure gradient
Φ	dependent variable
ϕ	angle, or dependent variable
Ω	dummy independent variable
ω	absolute uncertainty interval

Subscripts

cp	constant property
e	evaluated at edge of boundary layer
I	isothermal

i	inner, or running index
k	running index
m	mean or bulk
m,n	referring to axial node m, radial node n
o	outer
w	evaluated at wall
x	local
∞	far field

CHAPTER 1. INTRODUCTION

1.1. Objective

It is intended that the present investigation shall give definitive answers to the effect of high rate cooling on the local heat transfer and wall friction parameters for the laminar flow of gases through cylindrical tubes. Two commonly encountered gases - helium and air, are examined in detail. Temperature differences considered may be large enough such that substantial variations in gas transport and thermodynamic properties occur. The tube wall temperature is constant. Initially, radial temperature profiles are uniform and velocity profiles may be either fully developed (parabolic) or uniform at the point where cooling of the gas commences. In particular, it is desired to,

1. Obtain a theoretical prediction of the axial behavior of the developing flow.
2. Develop satisfactory design correlations for the results of the analysis.
3. Test the theoretical analysis by obtaining experimental data under conditions treated in the theoretical analysis.

1.2. Method

For the theoretical analysis, the reduction of the governing equations of motion, continuity and energy to the boundary layer equations is examined. A finite difference algorithm for solution of the combined continuity, energy and (axial) momentum boundary layer equations with property variation has been obtained from Worsoe-Schmidt (ref. 100) and modified for use in the present investigation. Because of the non-convergence of the finite difference approach when a uniform inlet velocity profile is specified, an analytical boundary layer solution is applied at the tube entrance. This solution, which is based on a similarity assumption and which includes property variations, is patched to the finite difference solution at a downstream point. An improved method of evaluating wall parameters is examined. Correlation of the wall parameter results in terms of significant operational parameters is attempted along with criteria as to when property variations can be ignored.

For the experimental portion of the investigation, a cylindrical test section is fabricated and calibrated for the measurement of axial variation of local heat transfer and static pressures for laminar gas flow. Two inlet configurations provide approximately the two general sets of boundary conditions examined in the theoretical portion of the investigation. Experimental data will be used to verify, when possible, the assumptions inherent in the theoretical solution or to point our areas where the analysis may be deficient.

A additional advantage of the combined experimental and theoretical approach is in the practical type of data that is supplied. The idealized boundary conditions treated in the theoretical portion are unattainable in a physical situation. A special effort was made in the design of the apparatus to approach the idealized conditions. Comparison of results with those from the theoretical solution will help to determine if the theoretical results can be applied to physical situations which also do not attain either of the idealized conditions, but are closer to one set than the other. In a crude sense, the derivative or sensitivity of the wall parameters to small deviations in the boundary conditions has been defined in addition to its value at the limiting cases. This type of data is of much greater value to the designer.

1.3. Scope and Reason for the Work

Recently, interest in the effect of variable fluid properties on internal laminar fluid flow has greatly increased. This can be attested to by the large number of investigations, both experimental and analytical, which have been addressed to this problem in the past decade. Advances in technology have extended the range of temperature at which gas flow is utilized from temperatures near the cryogenic range to several thousand degrees. Extreme temperature differences occuring in a gas flow situation can make the available constant property solutions inapplicable for prediction of heat transfer and flow characteristics. The majority of works devoted to prediction of these characteristics when gas properties vary appreciably deal with heating of the gas. Only a small portion is concerned with cooling of the gas. This is surprising since in many applications where extreme heating occurs, extreme cooling is also obtained.

An example of a possibly very important future use of gas in a heat transfer application with extreme temperature differences can be seen in the development of fast breeder reactors. Fast breeder reactors operate at far higher temperatures than conventional reactors but the result is a higher thermodynamic efficiency and reduced thermal pollution. Also, the breeder reactor produces more fissionable material than it consumes. Gas cooling has a distinct advantage (as opposed to liquid cooling) in fast reactors since bubbles or voids cannot form in a gas (ref. 78). A bubble or void might lead to overheating in a localized area which cannot be detected and may result in consequent failure of a fuel pin or rupture of a coolant passage. This type of failure was responsible for the accident at the Enrico Fermi Nuclear Generating Plant in 1967. While turbulent flow conditions would normally be used for the operating mode, laminar flow may exist for periods during shutdown, low power operation or loss of flow accidents. Increasing public concern over the safety of nuclear facilities restricts the margin for design error and demands that the designer have data available for all possible modes of operation.

Modern electronic technology has triumphed in its ability to miniaturize, but the result has been the creation of extremely high power densities in electronic equipment and a subsequent need for cooling. In order to realize the decrease in size, heat exchangers must of necessity also be kept small. Laminar gas flow is important in this application since the maximum ratio of heat transferred to pumping power required is obtained with laminar flow in compact heat exchangers. While the gas would be undergoing heating in the equipment, applications outside the earth's atmosphere would require recirculation, and subsequently, cooling of the gas.

Several high energy rocket propellants have been developed which can be solidified at very low temperatures and made suitable for use in solid fuel rockets. Prior to burning it is necessary that the fuel be raised to melting temperature. It has been proposed that this could be accomplished by passing high temperature gas through passages in the supercooled propellant. Precise control of the supply of molten propellant generated would require an accurate estimate of the heat transfer from the gas.

Recent application of the Brayton cycle in aerospace applications requires recirculation and cooling of the gas. Since flow and heat transfer losses may make up a substantial portion of the energy expended by the working fluid in the cycle, it is important that precise correlations be available for the cooling as well as the heating of the gas. Here again laminar flow becomes attractive because of its efficiency.

1.4. Previous Theoretical Work

Theoretical consideration of heat transfer for a fluid in laminar flow in a cylindrical tube dates back to the first (correct) derivation of the partial differential equation for conservation of energy derived by Poisson (68) in 1835. The first solution to this equation was published fifty years later by Graetz (31) in 1885. Graetz assumed radial symmetry of the velocity and temperature profiles, constant fluid properties and that second order derivatives of the temperature and velocity in the axial direction could be neglected with respect to other terms. In addition, Graetz assumed the following set of boundary condtions which has come to be known as the Graetz condition:

1. At $x = 0$, the tube wall undergoes a step change

from T_o to T_W and remains constant at T_W for $x \geq 0$.

2. For $x \leq 0$, the fluid temperature is uniform at T_O
3. The velocity profile is fully developed (parabolic) at $x = 0$.

In his analysis, Graetz assumed constant fluid properties so that the axial velocity profile is invariant with axial displacement. Also implicit in this last condition is a zero radial velocity component for all x. Upon substitution of the parabolic velocity profile in the energy equation, a linear second order partial differential equation with temperature as the dependent variable is obtained. Graetz obtained an infinite series solution along with the first three eigenfunctions and eigenvalues for the series. Higher order eigenfunctions, eigenvalues and additional solutions for these boundary conditions can be found in papers by Drew (24), Jakob (40), Larkin (53), Lipkis (55) and Sellers, Tribus and Klein (79). The latter authors (79) also obtained a solution for the laminar flow of a gas in a cylindrical tube for the case of uniform energy input by a superposition of constant wall temperature solutions. A more direct approach to the uniform heat addition problem has been presented by Siegel, Sparrow and Hallman (80).

When the axial conduction term in the energy equation, $k\left(\partial^2 T/\partial x^2\right)$ is non-negligible, the energy equation reduces to a form for which the eigenfunctions are no longer orthogonal. To circumvent this problem, Singh (82) obtained expansions of the appropriate eigenfunctions for the case of constant wall temperature in terms of eigenfunctions for an auxiliary equation satisfying identical boundary conditions. For the case of constant heat addition, Hsu (36) showed that the solution for the case with axial conduction can be reduced to the solution for zero axial conduction as a special case. Hsu also derived the solution in the same eigenfunction form as for the case of zero axial conduction-- the only difference being in the magnitude of the eigenfunctions, eigenvalues and coefficients of terms in the infinite series. The results for both of these analyses showed that the effect of axial conduction is negligible for Peclet numbers. Pe (i.e. product of Reynolds number defined in terms of axial displacement (Re_x) and Prandtl number (Pr) greater than 100).

To date, there does not appear to be any closed form analytical solution for the laminar flow of a fluid in a circular tube with simultaneous development of velocity and temperature profiles. Theoretical results presented are based either partially or totally upon numerical techniques. The first of the solutions for these inlet conditions was given by Kays (42). Kays neglected the radial velocity component and assumed constant properties. In this case the axial momentum equation becomes uncoupled from the energy equation and use could be made of a solution for the developing velocity field in a tube previously obtained by Langhaar (52). Langhaar solved the momentum equation by making several linearizing assumptions. Kays integrated the energy equation numerically for Pr = 0.7. He found that there was a significant increase in the Nusselt number over that obtained for a fully developed profile. Ulrichson and Schmidt (92) refined the work of Kays to include the radial component of velocity. Their results indicated a significant decrease in the calculated Nusselt number from Kays' results at points near the entrance. An implicit total finite difference solution to the momentum equation was presented by Hornbeck (34). Fairly large variation was found compared to the velocity profiles by Langhaar. However, good agreement was found to exist between the axial pressure variations.

One of the first analytical attempts to account for the effect of property variations on the flow of a gas was made by Deissler (20) for the case of uniform heat flux. Deissler assumed fully developed velocity and temperature profiles, so that his analysis would apply only in a region far from the entrance. He removed axial dependence from the governing equations by neglecting acceleration terms in the axial direction and assuming 1. zero radial velocity, 2. constant axial gradient of of the bulk gas temperature (uniform heat addition) and

3. that axial variations in fluid properties were negligible with respect to radial variations. Further assuming that the fluid density varied inversely with temperature and that viscosity and thermal conductivity varied as absolute temperature raised to the 0.68 power, Deissler solved the coupled energy and momentum equations simultaneously by an iterative procedure. Although Deissler did not check his results experimentally, the data in several other references indicate that at high wall to bulk temperature ratios the friction factor is significantly underestimated. Sze (87) refined Deissler's analysis by use of actual experimental transport property variations. His results were in substantial agreement with those of Deissler.

A combined experimental and analytical investigation of the laminar flow of carbon dioxide near its critical point was presented by Koppel and Smith (48). The authors essentially linearized the momentum equation by assuming the radial velocity component was negligible and that the product of density and axial velocity at any radial point is independent of the axial coordinate. These results are rather restricted in their applicability to the flow of other gases due to the severe and unique variation of the density and transport properties of CO_2 at its critical point.

Davenport (18) extended Deissler's analysis by including a radial velocity component. In essence, Davenport concluded that the temperature and velocity profiles are never fully developed. In order to test his hypothesis, he derived a set of axially independent energy and momentum equations in which the radial velocity component was left as an arbitrary function subject to the conditions that the radial velocity be zero at the tube wall and centerline, and that at any radial point the outward convective flux cannot exceed the inward conduction heat transfer. By assuming different forms of the radial velocity distributions, Davenport solved the coupled equations by an iterative procedure. His results indicated that the postulated radial velocity was sufficient to account for the experimentally determined variation of the friction factor. The predicted effect on the Nusselt number was less pronounced but depended more heavily on the postulated variation of the radial velocity component.

Worsoe-Schmidt (100) using a finite difference solution with a variable implicitness to the continuity and coupled momentum and energy equations included the effect of variable fluid properties. Specific heat, viscosity and thermal conductivity were assumed to obey power law variations with absolute temperature ratio and the fluid density was assumed to obey the perfect gas law. Although the solution was quite satisfactory for gas heating and a fully developed inlet velocity profile, a single example computed with uniform velocity at the entrance did not converge to the proper constant property solution for the Nusselt number downstream. Worsoe-Schmidt postulated that this was primarily due to large errors in the solution of the momentum and energy equations at points near the tube entrance. He also postulated that either a restrictively small finite difference mesh size or an appropriate analytical boundary layer solution at the entrance would remove this problem. However, for the Graetz boundary condition, the effect of the variable properties on the Nusselt number when based on properties evaluated at the local bulk temperature was rather small and in good agreement with experimental data. The predicted friction factor increased with heating rate, but not as rapidly as the experimentally measured values. Only one example was calculated for gas cooling, and this was for a fully developed inlet velocity profile.

Following Worsoe-Schmidt's example, several finite difference and finite volume solutions for laminar internal flow with variable fluid properties have appeared. A slightly different algorithm for integration of the same set of equations was published a short time later by Deissler and Presler (20), for the case of constant heat addition and uniform velocity and temperature profiles at the tube entrance. Convergence of the wall parameters was obtained in the far downstream region, but provision was not made for inclusion of other boundary conditions. The effect of variable fluid properties here also showed slight effect on the heat transfer results, but marked effect on the shear stress. Since the boundary conditions examined differed from those in Worsoe-Schmidt's analysis, direct comparison of numerical results is not possible.

A recent numerical solution allowing for inclusion of an eddy exchange coefficient for turbulent motion in addition to the molecular terms for transport properties has been published by Bankston and McEligot (6). Sample calculations for laminar flow included a uniform temperature profile at the entrance and varying hydrodynamic entry lengths with the extremes of fully developed and uniform velocity profiles included. Provision was made for specification of arbitrary inlet profiles. The only wall condition provided for was that of specified heat flux, although this may be variable with the axial coordinate. No cases with gas cooling were presented.

Swearingen (86) in his Ph.D thesis presented a finite difference solution for laminar variable property flow between parallel plates along with experimental results for laminar flow heating in a cylindrical tube which will be discussed later. Swearingen, allowing for a radial pressure distribution, included the radial momentum equation in the set of finite difference equations to be solved, although the other usual boundary layer assumptions were invoked. Flow between parallel plates bears several resemblances to flow in cylindrical tubes since: 1. the flow is two-dimensional, 2. the flow is internal, 3. the boundary layer equations apply at some distance from the entrance and 4. thermal and/or velocity boundary layers are present at the wall in the entrance. In Swearingen's case, only results for the case of specified wall heat flux and fully developed inlet velocity profiles were generated. Specification of a constant wall temperature for all cases with compressible flow resulted in oscillations of the wall parameters near the entrance which were large enough to render the solution of little value in this region. Attempts to remove this oscillation by application of an analytical starting solution at the first two axial steps were not successful. Surprisingly, no radial pressure distributions for any cases were presented.

In a finite volume solution also for variable property flow between parallel plates, Schade and McEligot (73) were able to obtain solutions for specified wall temperatures and uniform wall heat flux. The radial momentum equation was neglected. Both uniform and fully developed inlet velocity profiles for heating and cooling of the gas were treated. Step changes in the wall temperature were approximated by increasing the wall temperature over the first twenty axial steps until the desired value was reached. For several cooling cases specified with a fully developed inlet velocity, the pressure was seen to rise with axial distance in the thermal entrance region. For severe cooling and uniform inlet velocity, the pressure drop in the entrance was found to be very small.

Similar finite difference and finite volume numerical methods have been applied to laminar plasma flow. While property variations associated with plasma cooling are indeed extreme, the present study is addressed to laminar flow of gases at subplasma temperatures. Characteristics unique to plasmas limit the relevance of these investigations to the topic under consideration. These characteristics, along with a review of notable literature in this field will be reserved for a later section.

To this date, no comprehensive numerical solutions were found for cooling and for simultaneous development of velocity and temperature profiles with uniform wall temperatures for flow in cylindrical tubes.

1.5. Previous Experimental Investigations

Experimental results for the laminar flow of gases in circular tubes are meager. This is due in part to the low heat transfer rates encountered in laminar flow. Heat losses from the test section are usually large in comparison with the heat transfer to the gas and can be difficult to account for. Of those experiments performed in apparatus designed to minimize free convection effects, the investigations of Kroll (51), Weiland and Lowdermilk (97), Taylor and Kirchgessener (88), Kays and Nicoll (43), Davenport (18), Dalle Donne and Bowditch (17), Taylor (89), Bergman and Koppel (7) and Swearingen (86) are the most notable. The conditions under which the data was taken are presented in Table I along with correlations proposed. Only one of these reports data for gas cooling (43). With one exception, (7), the experimentally measured Nusselt number and friction factor under the conditions of low to moderate heat flux and negligible natural convection effects were in relatively close agreement with the predicted values from the Graetz (31) and the Sellars, Tribus and Klein (79) solutions. Bergman and Koppel report lower heat transfer coefficients for uniform heat flux at low axial velocities than those predicted by the Sellars, Tribus and Klein analysis, and also a Reynolds number dependence which is not predicted in any of the cited references. They postulate that this is due to an increase in the importance of the radial velocity component at low axial velocities. The Reynolds number dependence may be explained by the reduced validity of the usual boundary layer assumptions for low Reynolds numbers (100).

However, when the heat flux becomes relatively large, the experimental results of Davenport, Dalle Donne and

Bowditch, Kays and Nicoll, and Taylor show significant deviation of the friction factor from values predicted from constant property results, whereas the Nusselt numbers for both uniform energy input and uniform surface temperature were found to be in relatively close agreement with the constant property values. Swearingen, while not taking any pressure drop data, found that the difference between his heat transfer results and Worsoe-Schmidt's predictions were within his estimated experimental uncertainty. Swearingen considered this as being a confirmation of the assumptions made in the Worsoe-Schmidt analysis. However, Searingen maintained a flow development section of 100 diameters prior to the test section. It would seem that a more critical test of Worsoe-Schmidt's assumptions could be obtained for simultaneous velocity and temperature profile development where large axial second derivatives would occur in the momentum as well as in the energy equation at points near the tube entrance.

Of these experimental works, only that of Kays and Nicoll deals with gas cooling. Mean, rather than local, Nusselt numbers were measured for air. No friction factor or pressure drop data were obtained. Velocity profiles were essentially fully developed at the point where cooling commenced since Kays used a development section of about 60 diameters. The bulk of the data was found to lie about five per cent below the constant property solution for ratios of the logarithmic mean fluid temperature to wall temperature ranging from approximately 1.0 to 1.8. This deviation was within the estimated experimental uncertainty and Kays postulates that it was due to a fixed error in the measurement of the inlet air temperature. In none of these investigations were detailed measurements made of velocity and temperature profiles.

When gases are heated to temperatures sufficiently high such that the ionization fraction becomes non-negligible, the gas is described as a plasma. Recently a great deal of attention has been devoted to this topic. Plasma heat transfer differentiates itself from that of a non dissociated gas in several ways (3, 26, 27). Radiation heat transfer is added to that by conduction to the wall. In regions where a high cooling rate predominates, a condition of thermal non-equilibrium can exist. Electron temperatures can exceed heavy particle temperatures by several thousand degrees (3). Also, because of appreciable concentration gradients there is a diffusion of electrons to the cool wall where recombination and consequents release of ionization energy can enhance heat transfer-- for this reason, a plasma must be treated as a reacting two component gas.

Table I. Review of Experimental Results

Author	Gas	Reynolds number	Boundary Conditions	$\frac{T_w}{T_m}$	$\frac{L}{D}$	Correlations, Results
Davenport (18)	Helium	200-2200	Q	1.-2.2	128	$Nu=Nu_{cp}$ $\frac{f}{f_{cp}} = (\frac{T_w}{T_m})^{1.35}$
Kays & Nicoll (42)	Air	664-1300 955-1300	Q T	1.-1.9 .56-.85	80 66.7	$Nu=Nu_{cp}$ $Nu=Nu_{cp}$
Dalle Donne & Bowditch (17)	Air Helium	100-2000	Q	1.-1.80	90 180	$Nu=Nu_{cp}$ $\frac{f}{f_{cp}} =(\frac{T_w}{T_m})^{1.67}$ (1/2" D) $\frac{f}{f_{cp}} =(\frac{T_w}{T_m})^{3.33}$ (1/4" D)
Kroll (51)	Air	80-2300	T	1.-1.35	11-98	$Nu_b=1.5(\frac{wc_p}{k_m L})^{0.40}$ $f= \frac{16}{Re_f}$
		Gr> 15 $5< \frac{wc_{p,m}}{k_m} <400$	Q		8-80	$Nu_b=1.47(\frac{wc_p}{k_m L})^{0.46}$ $f= \frac{16}{Re_f}$
Taylor (88)	Helium	370-1300	Q	1.-3.4		$f= \frac{16}{Re_f}$
Bergman & Koppel (7)	Nitrogen	N.A.	Q	1.-1.13	330	Reynolds number dependence
Swearingen (86)	Helium Air	1442-2065	Q	1.-1.9	1.2-97	Confirmation of Results in Ref. 100

Early theoretical treatments of plasma flow suffered from restrictive assumptions made in the formulation of the problem. In 1967, Watson and Pegot (96) published a numerical solution for the combined energy (with Ohm's law), momentum and continuity equations in the arc region of a plasma generator. Of greater relevance here is the excellent finite difference treatment of plasma flow in the arc free region of a circular tube published by Incropera, et al (38,39). Radiation and recombination effects were included in the analysis, but it was not possible to include thermal non-equilibrium and its effect on the thermal conductivity. It was postulated that this was one of the reasons that poor comparison with existing experimental results was found. It was not possible to correlate the heat transfer results in terms of variables which are effective for moderate temperature gas flow. Also, wall parameters were found to be extremely sensitive to the assumed inlet profiles.

Unfortunately, experimental investigations for plasmas suffer from a lack of consistent inlet conditions. For example, in the experimental studies by Johnson, Choksi and Eubank (41) the flow underwent an abrupt expansion immediately after the plasma generator. Also, a spin was imparted to the gas by the plasma generator in this investigation and those of Skrivan and Jaskowski (83) and Wethern and Brodkey (98). In no case was the magnitude of the spin accurately measured or its effect on the heat transfer and flow characteristics isolated. In the experimental study by Cann (10), the constricted arc region was extended so tha a smooth transition into the cooling section was obtained. However, a small but non-negligible stabilizing axial magnetic field was applied in the cooled section with a probable effect on the wall parameters. Due to the rapid deterioration of any plasma condition, the cooling sections in all these studies were relatively short. For example, in the Johnson et al study, the maximum length to diameter ratio was 6.

Additional problems associated with plasma experimentation are the cost and difficulty of measuring temperature and velocity profiles, the difficulty in measuring ionization level, and the lack of experimental data for gas properties at plasma temperatures which make it necessary to resort to purely theoretical correlations (25). In addition, variations in plasma transport properties with temperature may differ substantially from those of the same gases at moderate temperature levels. For example, the variation of the viscosity of argon with temperatures above 20,000 $^{\circ}$K is opposite to that at moderate temperatures (77).

There are a considerable number of papers referenced in the Bibliography which have not been discussed. However, it is believed that the papers discussed present a good picture of the major contributions to the analysis of the laminar flow of a gas in a cylindrical tube.

CHAPTER 2. ANALYTICAL PROBLEM

2.1. Statement of the Problem

We are considering the laminar flow of a non-reacting, non-absorbing, non-dissociated, single component, monatomic thermally perfect gas inside a cylindrical tube. The tube is axially symmetric, there is zero swirl and no body forces (i.e. free convection effects are negligible) and the flow is steady. The thermal conductivity, absolute viscosity and specific heat are considered to be functions of temperature only. Two sets of boundary conditions are to be studied (Fig.1). In the first set, we consider the gas flowing from a point in the tube at $x = -\infty$. For $x < 0$, the wall temperature is constant and equal to the fluid temperature, T_o. Also for $x \leq 0$ the fluid temperature is uniform and the velocity profile is parabolic. At $x = 0$ the wall temperature undergoes a step change from T_o to T_w and remains at T_w for $x > 0$. This set of boundary condition is referred to as the Graetz boundary condition.

In the second set both the velocity and temperature profiles are uniform at $x = 0$. This condition would be approximated by a fluid flowing directly from a reservoir into a tube in the absence of any development section or more closely approached by providing the tube with a bellmouth entrance. With this latter inlet

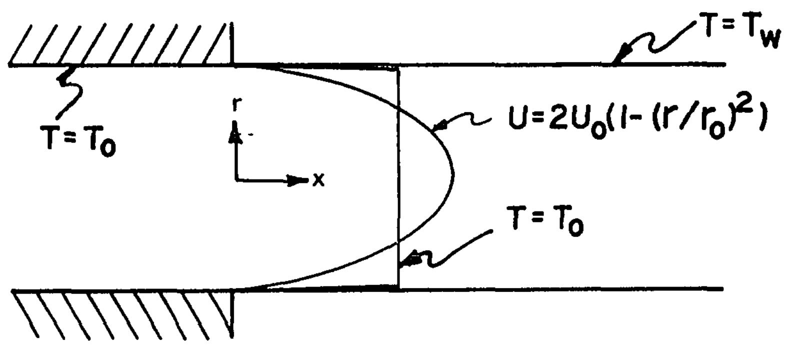

GRAETZ BOUNDARY CONDITION

$X=0$		$U=2U_0(1-(r/r_0)^2)$		$T=T_0$
$X\gtrless 0$	$r=0$	$\partial U/\partial r=0$		$\partial T/\partial r=0$
$X\geq 0$	$r=r_0$	$U=0$	$V=0$	$T=T_W$
$X\leq 0$	$r=r_0$	$U=0$	$V=0$	$T=T_0$

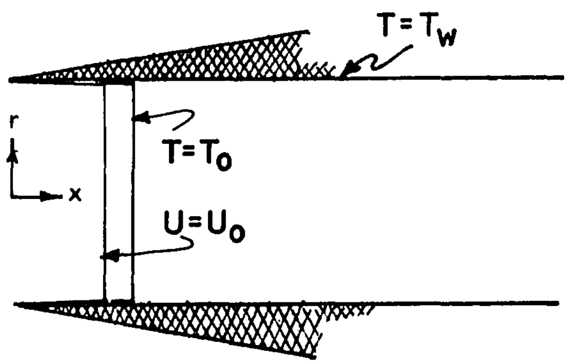

UNIFORM TEMPERATURE AND VELOCITY (UTV)

$X=0$		$U=U_0$		$T=T_0$
$X\gtrless 0$	$r=0$	$\partial U/\partial r=0$		$\partial T/\partial r=0$
$X\geq 0$	$r=r_0$	$U=0$	$V=0$	$T=T_W$
$X<0$		$U=0$	$V=0$	$T=T_0$

FIGURE 1. IDEALIZED BOUNDARY CONDITIONS

condition the set will be referred to as the UTV (Uniform Temperature and Velocity profile) condition.[1] Symmetry of the temperature and velocity profiles and the no slip and impermeability condition at the wall allows us to complete the two sets of boundary conditions which are summarized in Figure 1. Only the case of gas cooling will be considered;

$$T_w/T_o < 1$$

The boundary condition of constant heat removal from the gas was not considered since, unlike the case of gas heating, this is not a physically realizable situation. The analytical problem may now be identified as the determination of the heat transfer and fluid friction at the tube wall for these boundary conditions along with satisfactory methods of correlation of these results.

The differential equations governing the situation are the Navier Stokes, energy and continuity equations. For the cylindrical coordinate system in Figure 1 and incorporating the aforementioned assumptions, we may write these as (37);

radial momentum:

$$\rho\left(V\frac{\partial V}{\partial r}+U\frac{\partial V}{\partial x}\right)=-\frac{\partial P}{\partial r}+\frac{\partial}{\partial r}\left[2\mu\frac{\partial V}{\partial r}+(\zeta-\tfrac{2}{3}\mu)\left[\frac{\partial V}{\partial r}+\frac{V}{r}+\frac{\partial U}{\partial x}\right]\right]$$
$$+\frac{\partial}{\partial x}\left[\mu\left(\frac{\partial V}{\partial x}+\frac{\partial U}{\partial r}\right)\right]+\frac{2\mu}{r}\left[\frac{\partial V}{\partial r}-\frac{V}{r}\right] \qquad (2.1)$$

[1]This set of boundary conditions is sometimes referred to as the simultaneous development case, but this cannot be considered as being sufficiently definitive since strictly speaking, both profiles in the Graetz condition also undergo development.

axial momentum:

$$\rho\left(V\frac{\partial U}{\partial r}+U\frac{\partial U}{\partial x}\right)=-\frac{\partial p}{\partial x}+\frac{\partial}{\partial x}\left[2\mu\frac{\partial U}{\partial x}+(\zeta-\tfrac{2}{3}\mu)\left[\frac{\partial V}{\partial r}+\frac{V}{r}+\frac{\partial U}{\partial x}\right]\right] + \frac{1}{r}\frac{\partial}{\partial r}\left[\mu r\left(\frac{\partial V}{\partial x}+\frac{\partial U}{\partial r}\right)\right] \tag{2.2}$$

energy:

$$U\frac{\partial p}{\partial x}+V\frac{\partial p}{\partial r}+\Phi+\frac{1}{r}\frac{\partial}{\partial r}\left(rk\frac{\partial T}{\partial r}\right)+\frac{\partial}{\partial x}\left(k\frac{\partial T}{\partial x}\right)=\rho\left(V\frac{\partial H}{\partial r}+U\frac{\partial H}{\partial x}\right) \tag{2.3}$$

continuity:

$$\frac{1}{r}\frac{\partial}{\partial r}(r\rho V)+\frac{\partial}{\partial x}(\rho U)=0 \tag{2.4}$$

where Φ= viscous(mechanical) dissipation function

$$=\mu\left[2\left\{\left(\frac{\partial V}{\partial r}\right)^2+\left(\frac{V}{r}\right)^2+\left(\frac{\partial U}{\partial x}\right)^2\right\}+\left(\frac{\partial V}{\partial x}-\frac{\partial U}{\partial r}\right)^2\right]+\lambda\left[\frac{\partial V}{\partial r}+\frac{V}{r}+\frac{\partial U}{\partial x}\right]^2 \tag{2.5}$$

λ= second coefficient of viscosity ($\lambda=-\frac{2}{3}\mu$ for a monatomic gas)

μ= primary coefficient of viscosity

ζ= $\lambda+\frac{2}{3}\mu$ (ζ = 0 for a monatomic gas).

For a thermally perfect gas we may write

$$dH=c_p dT$$

(i.e. the specific heat may be removed from the differential operator). This allows us to write the energy equation solely in terms of enthalpy as the dependent variable;

$$U\frac{\partial p}{\partial x}+V\frac{\partial p}{\partial r}+\Phi+\frac{1}{r}\frac{\partial}{\partial r}r\frac{k}{c_p}\frac{\partial H}{\partial r}+\frac{\partial}{\partial x}\frac{k}{c_p}\frac{\partial H}{\partial x}=\rho\left(V\frac{\partial H}{\partial r}+U\frac{\partial H}{\partial x}\right) \tag{2.6}$$

The equations in this form and generality impose a (presently) nearly unsolvable problem-- both in terms of a closed form or numerical type solution. They form a set of non-linear equations by virtue of the product terms in the dependent variables. The energy equation is coupled to both momentum equations by virtue of its velocity terms, and the momentum equations are likewise coupled to the energy equation by virtue of the density and viscosity terms. The equations are elliptic in character due to the presence of second order derivatives in two spatial directions. The solution for the flow and temperature fields must be made "in toto"--that is, values of the dependent variables must be specified at the exit of the tube as well as at the walls and inlet. As is generally done, the boundary layer assumptions will be invoked which both reduces the number of equations to be solved and changes the classification of the equations.

The rationale underlying the application of the boundary layer assumptions will be reviewed. In certain flow situations, the variation of the velocity and temperature can be much greater in one spatial direction than another. We can identify two such regions in internal tube flow (Fig. 2). In the entrance region where a thin viscous and/or thermal boundary layer are developing at the tube wall, variation of these quantities can be expected to be much greater in a direction normal to the

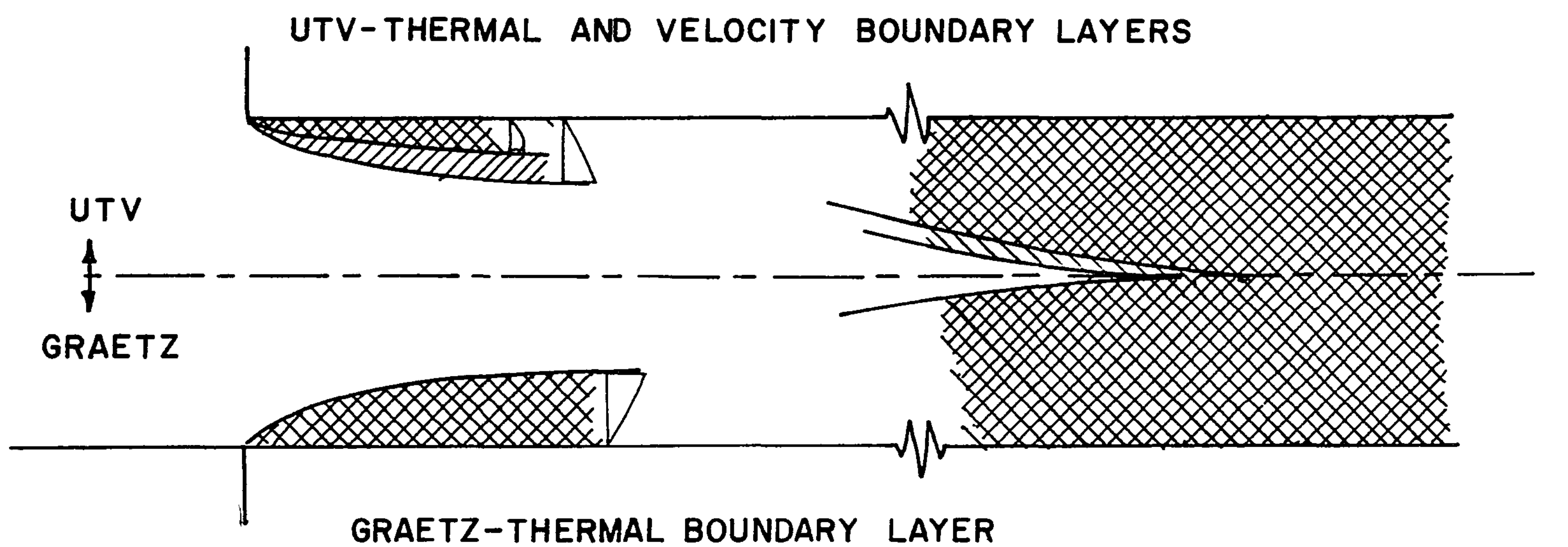

FIGURE 2. BOUNDARY LAYER REGIONS IN INTERNAL TUBE FLOW

flow than in an axial direction. Similar considerations apply downstream of the region where the boundary layers which have been growing along the tube wall have met at the tube centerline. In regions such as these we can apply an approximate order of magnitude analysis. We denote $\sim$ as meaning "of the order of magnitude of" rather than its usual meaning. We then write,

$$\frac{\partial}{\partial r} \sim \frac{1}{r_o} \qquad\qquad \frac{\partial}{\partial x} \sim \frac{1}{x}$$

where r_o is the radius of the tube. In the inlet region of a tube we would use a representative boundary layer thickness as a characteristic dimension rather than r_o. Since for the gases which will be considered the Prandtl numbers are fairly close to unity (i.e. the thermal and velocity boundary layer thickness should be approximately equal), the same characteristic dimension will apply to the energy and momentum equations.

Let ΔP_r = representative magnitude of radial pressure variation

ΔP_x = representative magnitude of axial pres-variation

$\bar{U}$ = representative magnitude of axial velocity

$\bar{V}$ = representative magnitude of radial velocity

$\bar{\rho}$ = representative magnitude of density.

We further denote the operators $\oplus$ and $\ominus$ as being order of magnitude addition and subtraction and to simply mean that the order of magnitude of a sum (or difference) of two terms conncected by the operator is that of the larger term. If both are of the same order of magnitude, then the order of the sum will be the same as for either term. Expanding continuity (2.4) we have

$$\frac{\rho V}{r} + \frac{\partial(\rho V)}{\partial r} + \frac{\partial(\rho U)}{\partial x} = 0 \tag{2.7}$$

Since the first term becomes indeterminate at r = 0, we can apply L'Hospital's rule at the centerline;

$$\left.\frac{V}{r}\right|_{r=0} = \left.\frac{\partial V}{\partial r}\middle/\frac{\partial r}{\partial r}\right|_{r=0} = \left.\frac{\partial V}{\partial r}\right|_{r=0}$$

Due to the crudeness of the analysis, not much will be lost if we use $\overline{V}/r_o$ to represent V/r as well as $\partial V/\partial r$. This will also be extended to the V/r terms which are present in the axial and radial momentum equations. Also, not much will be lost if we treat the density as being constant. Applying an order of magnitude analysis to the continuity equation (2.7) yields

$$\overline{V}/r_o \oplus \overline{V}/r_o \oplus \overline{U}/x = 0 \tag{2.8}$$

or

$$V \sim r_o U/x \tag{2.9}$$

Expanding the axial momentum equation (2.2) by an order of magnitude analysis (for $\zeta = 0$):

$$\overline{V}\frac{\overline{U}}{r_o} \oplus \overline{U}\frac{\overline{U}}{x} \sim -\frac{1}{\rho}\frac{\Delta P_x}{x} \oplus \frac{\mu}{\rho}\frac{1}{x}\left[2\frac{\overline{U}}{x} \ominus \frac{2}{3}\left(\frac{\overline{V}}{r_o} \oplus \frac{\overline{V}}{r_o} \oplus \frac{\overline{U}}{x}\right)\right] \oplus 2\frac{\mu}{\rho}\left[\frac{\overline{V}}{r_o x} \oplus \frac{\overline{U}}{r_o^2}\right] \tag{2.10}$$

Substituting the magnitude of $\overline{V}$ in terms of $\overline{U}$ (1.9)

$$\frac{\overline{U}^2}{x} \oplus \frac{\overline{U}^2}{x} \sim -\frac{1}{\rho}\frac{\Delta P_x}{x} \oplus \frac{\mu}{\rho}\left[2\frac{\overline{U}}{x^2} \ominus \frac{2}{3}\left(\frac{\overline{U}}{x^2} \oplus \frac{\overline{U}}{x^2} \oplus \frac{\overline{U}}{x^2}\right) + \frac{2\mu}{\rho}\left[\frac{\overline{U}}{x^2} \oplus \frac{\overline{U}}{r_o^2}\right]\right. \tag{2.11}$$

The order of magnitude representation of the radial momentum equation (2.1) can be written:

$$\overline{V}\frac{\overline{V}}{r_o} \oplus \overline{U}\frac{\overline{V}}{x} \sim -\frac{1}{\rho}\frac{\Delta P_r}{r_o} \oplus 2\mu\left[\frac{\overline{V}}{r_o^2} \ominus \frac{1}{3}\left(2\frac{\overline{V}}{r_o^2} \oplus \frac{\overline{U}}{x r_o}\right)\right] \oplus \mu\left[\frac{\overline{V}}{r_o x} \oplus \frac{\overline{U}}{r_o x}\right] + 2\frac{\mu}{r_o}\left[\frac{\overline{V}}{r_o} \ominus \frac{\overline{V}}{r_o}\right] \tag{2.12}$$

and substituting the relationship $\overline{V}$,

$$\frac{\overline{U}\,\overline{U}r_o}{x^2} \oplus \frac{\overline{U}\,\overline{U}r_o}{x^2} \sim -\frac{\Delta P_r}{\rho r_o} \oplus 2\mu\left[\frac{\overline{U}}{r_o x} \ominus \frac{1}{3}\left(2\frac{\overline{U}}{r_o x} \oplus \frac{\overline{U}}{x r_o}\right)\right] \oplus \mu\left[\frac{\overline{U}}{x^2} \oplus \frac{\overline{U}}{r_o x}\right] + 2\mu\left[\frac{\overline{U}}{x r_o} \ominus \frac{\overline{U}}{x r_o}\right] \tag{2.13}$$

In the same case that $r_o/x \ll 1$, certain terms become small when compared with others. If these terms are neglected the following equations are obtained;

axial momentum:

$$\frac{\overline{U}^2}{x} \sim -\frac{1}{\rho}\frac{\Delta P_x}{x} \oplus 2\frac{\mu}{\rho}\frac{\overline{U}}{r_o^2} \tag{2.14}$$

radial momentum:

$$\frac{\overline{U}^2}{x}\frac{r_o}{x} \sim -\frac{1}{\rho}\frac{\Delta P_r}{r} \oplus \frac{\mu}{\rho}\frac{\overline{U}}{r_o^2}\frac{r_o}{x} \tag{2.15}$$

It can be seen that both of the terms which could determine the order of magnitude of the term $\frac{-1}{\rho} \Delta P_r / r_o$ differ by a factor r_o/x from similar terms in the axial momentum equation. We can reasonably expect, therefore, that the term representing the radial pressure gradient will differ by a similar factor from the axial pressure gradient. For $r_o/x \ll 1$ we can also reasonably expect that the neglect of the radial pressure variation would not effect the solution greatly. This allows us to discard the radial momentum equation insofar as it provides information about this variation.[2]

In the energy equation, we can use the same type of representation for the variation of the enthalpy. Assuming

$$\frac{\partial H}{\partial r} \sim \frac{\Delta H}{r_o} \qquad \text{and} \qquad \frac{\partial H}{\partial x} \sim \frac{\Delta H}{x}$$

---

[2] From another standpoint, it would seem that more than simplification is gained from this assumption when finite difference or element techniques are used for solution. For compressible laminar flow between parallel plates, Swearingen (82) included the transverse momentum equation by combining the radial and axial momentum equations through elimination of the pressure terms in each. This requires that cross derivatives of the pressure be taken which raises the order of the equation representing momentum transfer from second to third, and for the case of uniform inlet velocity and temperature profiles, introduces a higher order singularity in boundary conditions at x = 0 which must be accomodated by the solution. As noted earlier, in Swearingen's case, large scale oscillations were obtained near the entrance for compressible flow.

where ΔH is a representative magnitude of the enthalpy variation, we obtain after substitution of 2.9 into the energy equation,

$$\bar{U}\frac{\Delta P_x}{x} \oplus \bar{U}\left(\frac{r_o}{x}\right)^2\frac{\Delta P_x}{x} \oplus \Phi \oplus 2\frac{k}{c_p}\frac{\Delta H}{r_o^2} \oplus \frac{k}{c_p}\frac{\Delta H}{r_o^2}\left(\frac{r_o}{x}\right)^2 \sim \bar{\rho}\bar{U}\frac{\Delta H}{x} \oplus \bar{\rho}\bar{U}\frac{\Delta H}{x} \tag{2.16}$$

It can be seen that the second and fifth terms on the left hand side which represent $V\frac{\partial P}{\partial r}$ and $\frac{\partial}{\partial x}\frac{k}{c_p}\frac{\partial T}{\partial x}$ respectively are negligible with respect to the terms derived from $U\frac{\partial P}{\partial x}$ and $\frac{1}{r}\frac{\partial}{\partial r}r\frac{k}{c_p}\frac{\partial H}{\partial r}$. Concerning the dissipation function Φ (2.5), the term $\left(\frac{\partial U}{\partial r}\right)^2$ can be shown to be the controlling term when a boundary layer analysis can be applied. However, inclusion of the additional terms will not affect the results of the simplification that is being developed here-- that is the problem will remain an initial value problem so that the additional terms in the dissipation can be included almost free of charge. Thse terms can become significant in the entrance region for the UTV boundary condition, so discussion will be withheld until Chapter 3 where this boundary condition will be reviewed.

When terms which have been shown to be small are neglected, the usual boundary layer equations are obtained axial momentum:

$$\rho\left(U\frac{\partial U}{\partial x}+V\frac{\partial U}{\partial r}\right)=-\frac{dp}{dx}+\frac{1}{r}\frac{\partial}{\partial r}\left(r\mu\frac{\partial U}{\partial r}\right) \tag{2.17}$$

continuity:

$$\frac{\partial}{\partial x}(\rho U) + \frac{1}{r}\frac{\partial}{\partial r}(r\rho V) = 0 \tag{2.18}$$

energy:

$$\rho\left(U\frac{\partial H}{\partial x} + V\frac{\partial H}{\partial r}\right) = U\frac{dp}{dx} + \frac{1}{r}\frac{\partial}{\partial r} r \frac{k}{c_p}\frac{\partial H}{\partial r} + \Phi \tag{2.19}$$

An additional consideration becomes important before we can fully justify the boundary layer assumptions. If those non-boundary layer terms which we eliminated in our simplification of the governing equations are larger or of the same order of magnitude as the terms which are due solely to property variation, then the solutions should be treated with caution. Those terms due to property variation whose magnitude relative to neglected terms can be calculated are 1.) the ratio of terms that were eliminated from the axial momentum equation to the term due the viscosity variation;

$$R_1 = \left[\frac{\partial}{\partial r}\left(\mu\frac{\partial V}{\partial x}\right) + \frac{4}{3}\frac{\partial}{\partial x}\left(\mu\frac{\partial U}{\partial x}\right) - \frac{2}{3}\frac{\partial}{\partial x}\mu\frac{\partial}{\partial r}(rV)\right] \Big/ \frac{\partial U}{\partial r}\frac{\partial \mu}{\partial r} \tag{2.20}$$

and the ratio of the terms that were eliminated from the energy equation to the term which is due to thermal conductivity and specific heat variation;

$$R_2 = \left[\frac{\partial}{\partial x}\frac{k}{c_p}\frac{\partial H}{\partial x} \Big/ \frac{\partial H}{\partial r}\frac{\partial \frac{k}{c_p}}{\partial r}\right] \tag{2.21}$$

In order to estimate the magnitude of these ratios for verification of our assumptions, we must anticipate the solution of equations 2.17 through 2.19. In figure 3 and 4 these ratios are plotted as a function of distance from the tube entrance for the flow of helium and the UTV boundary condition at $T_w/T_o = 0.1$. This case represents an extreme in terms of both numerators and denominators in 2.20 and 2.21. The derivatives were evaluated by means of radial and axial centered difference operators with dependent variables obtained from a combined analytical finite difference algorithm to be presented herein. It should be noted that we are estimating terms from a solution of equations that neglect them. Along with these ratios are plotted

$$R_3 = \frac{\partial}{\partial x}\mu\frac{\partial U}{\partial x}\Big/\rho U\frac{\partial U}{\partial x} \tag{2.22}$$

which represents the ratio of axial molecular momentum transfer to axial convective momentum transfer, and

$$R_4 = \frac{\partial}{\partial x}\frac{k}{c_p}\frac{\partial H}{\partial x}\Big/\rho U\frac{\partial H}{\partial x} \tag{2.23}$$

which represents the ratio of the axial molecular heat transfer to the axial convective heat transfer. Both numerators again represent terms eliminated from the governing equations. Re_o and Pr_o represent the inlet Reynolds and Prandtl numbers respectively. A feel for the physical significance of these results can be obtained by choosing $Re_oPr_o = 1000$. As a sample case, at $r/r_o = 0.95$

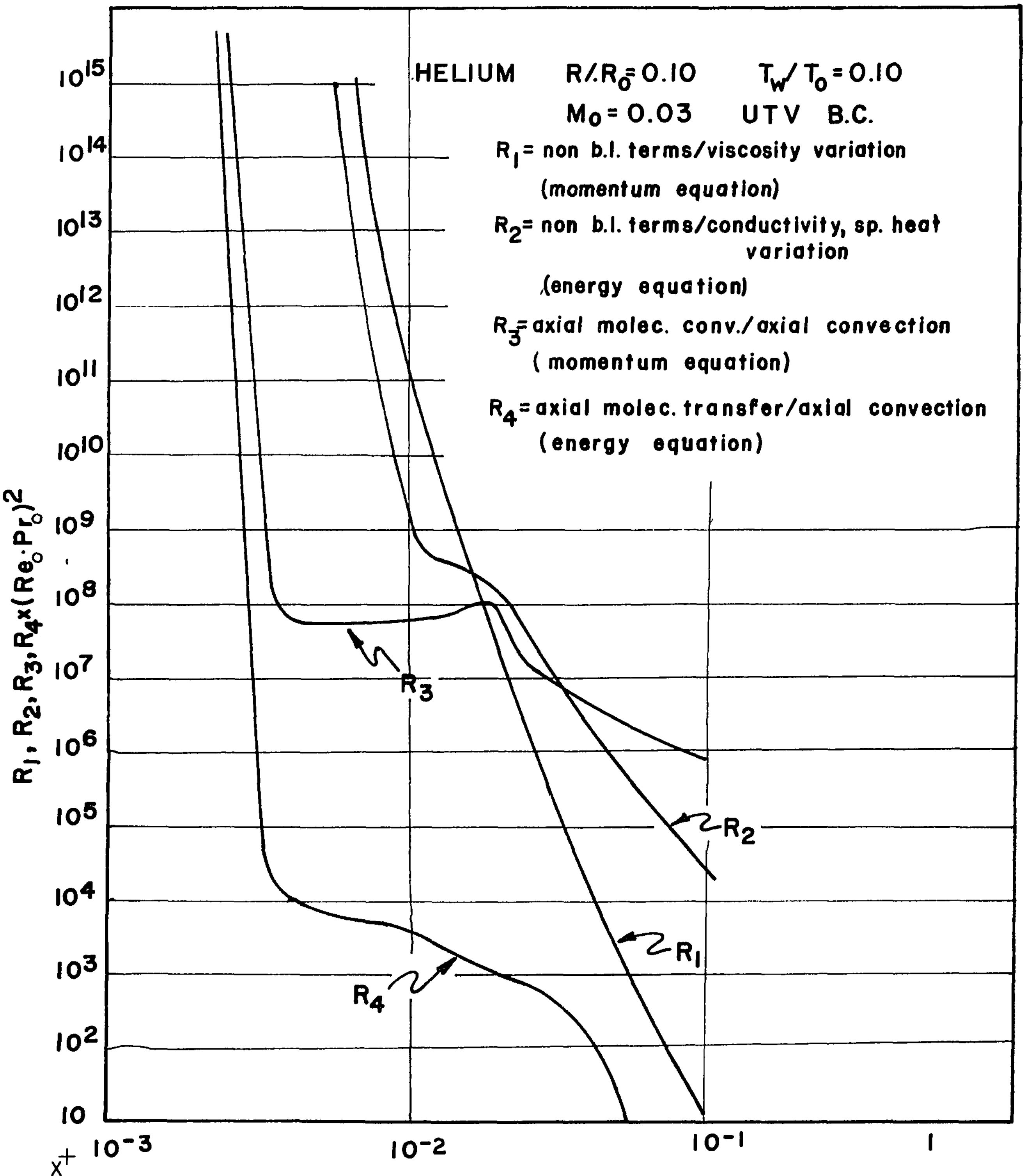

FIGURE 3. RELATIVE MAGNITUDE OF TERMS IN AXIAL MOMENTUM AND ENERGY EQUATIONS. ($x^+ = x/Re_0 Pr_0 r_0$)

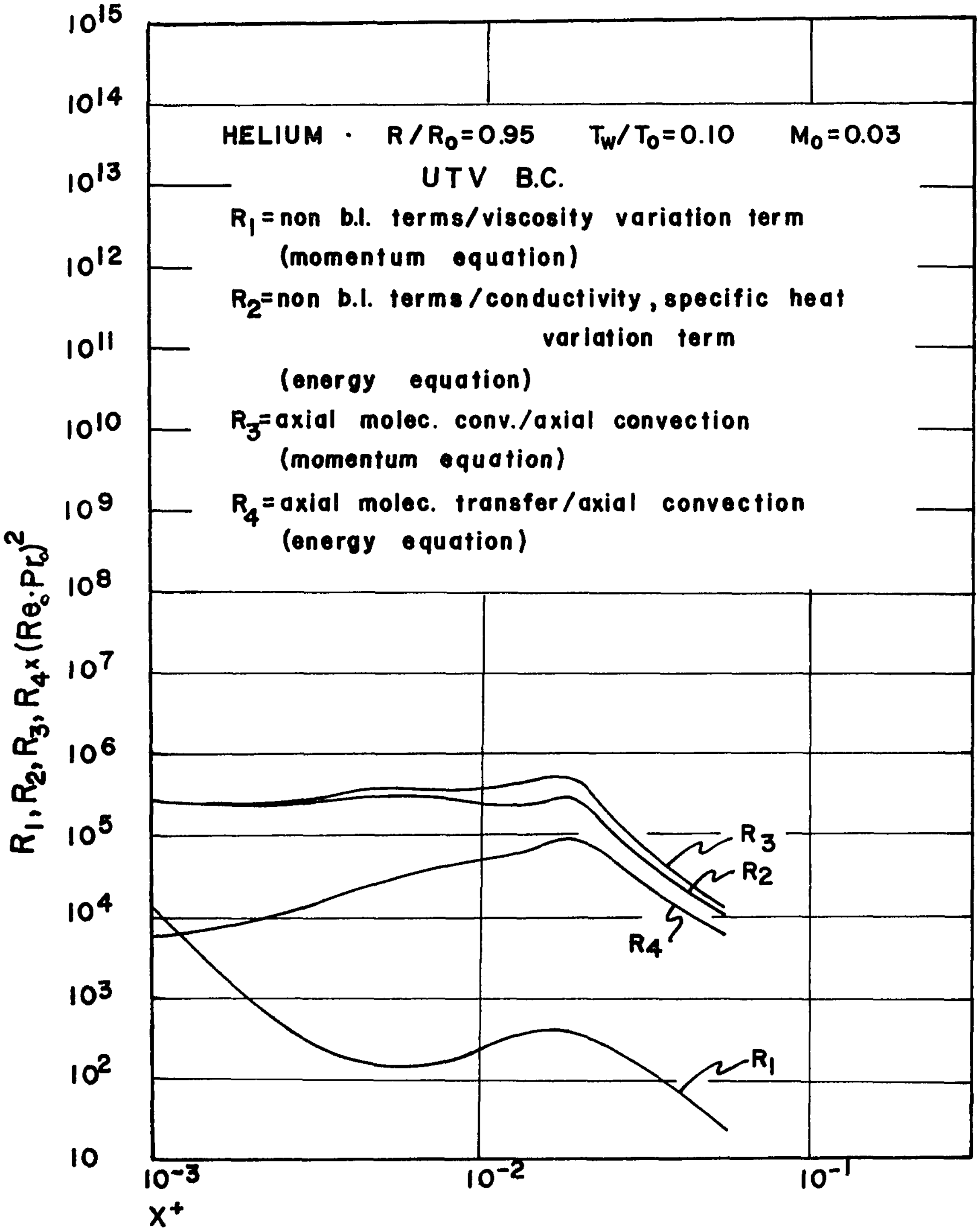

Figure 4. Relative magnitude of terms in axial momentum and energy equations. R/R_0 = 0.95, UTV boundary condition.

it can be seen that all of these ratios are reduced to magnitudes less than 0.10 at ten diameters, whereas for $r/r_o = 0.95$, R_1 does not become less than 1 until 40 diameters downstream and R_3 does not become less than 1 until 50 diameters from the tube entrance. The behavior of R_1 and R_2 is due to the fact that the velocity and temperature profiles remain extremely flat in the central region of the tube for an axial distance which depends upon the severity of the cooling. Radial derivatives in this region will be quite small. It is not easy to determine what represents an unacceptable ratio. Basing our decision upon the ratios of terms in the core flow would lead us to discard the solution almost altogether. However, the absolute magnitude of the derivatives in this region are several orders of magnitude smaller than those occurring in the region near the tube wall and their effect will probably be small. An ultimate quantitative answer will have to wait for a solution to equations 2.1 through 2.4 or for experimental verification. The results for the case shown are not representative of other temperature ratios or boundary conditions.

A finite difference solution to the equations 2.17, 2.18 and 2.19 was published by P.M. Worsoe-Schmidt (100) in his Ph.D dissertation, and his algorithm will be made the basis of the numerical portion of the solution to be presented here. In the next section, the important points of the Worsoe-Schmidt analysis are reviewed.

2.2. The Worsoe-Schmidt Analysis

After Worsoe-Schmidt, we transform the boundary layer equations in terms of the following non-dimensional variables.

Independent variables:

$$x^+ = x/r_o Re_o Pr_o$$

$$r^+ = r/r_o$$

Dependent variables:

$$U^+ = U/U_o$$

$$V^+ = \frac{V}{U_o} Re_o Pr_o$$

$$P = (p_o - p)/\rho_o U_o^2$$

$$p^+ = p/p_o$$

$$\theta = T/T_o$$

where r_o = tube radius

Re_o = inlet Reynolds number $= U_o 2 r_o \rho_o / \mu_o$

Subscript o will otherwise be taken to denote gas properties evaluated at the inlet temperature.

Non-dimensionalized gas properties;

$$c_p^+ = c_p / c_{p,o}$$

$$\mu^+ = \mu/\mu_o$$

$$\rho^+ = \rho/\rho_o$$

The following expressions are assumed to adequately (and most generally) represent the relationships between the properties and thermodynamic quantities for the gases under consideration.

$$c_p^+ = \theta^a \tag{2.24}$$

$$\mu^+ = \theta^b \tag{2.25}$$

$$k^+ = \theta^c \tag{2.26}$$

$$\rho^+ = p^+/\theta \tag{2.27}$$

For air and helium, these assumed power laws are quite good (c.f. Appendix B). We define two non-dimensionalized enthalpies,

$$H_1^+ = \frac{H - H_o}{c_{p,o}T_o} = \int_1^\theta c_p^+ d\theta = \frac{1}{1+a}\left\{\theta^{1+a} - 1\right\} \tag{2.28}$$

$$H_2^+ = \frac{H - H_w}{c_{p,o}T_o} = \int_{\theta_w}^\theta c_p^+ d\theta = \frac{1}{1+a}\left\{\theta^{1+a} - \theta_w^{1+a}\right\} \tag{2.29}$$

Subscript w refers to conditions at the tube wall. The reasons for use of the two definitions of the enthalpy will become clear in Chapter 4. The form in 2.28 is that used throughout the Worsoe-Schmidt analysis. The form 2.29 will become necessary when we consider a similarity boundary layer solution. For the present, we will be using H_1^+, although the form of the energy equation will be unchanged since we have merely changed the zero reference. We also define,

γ_o = ratio of specific heats = $c_{p,o}/c_{v,o}$

M_o = inlet Mach no. = $U_o/\sqrt{\gamma_o R T_o}$

q_w^+ = non-dimensionalized heat flux = $r_o q_w^+/k_o T_o$

With these new quantities, the governing equations become;

$$\rho^+\left(U^+\frac{\partial U^+}{\partial x^+} + V^+\frac{\partial U^+}{\partial r^+}\right) = \frac{dP}{dx^+} + 2\,Pr_o\left[\frac{1}{r^+}\frac{\partial}{\partial r^+}\left(r^+\mu^+\frac{\partial U^+}{\partial r^+}\right)\right] \tag{2.30}$$

$$\frac{\partial}{\partial x^+}(\rho^+U^+) + \frac{1}{r^+}\frac{\partial}{\partial r^+}(r^+V^+\rho^+)=0 \tag{2.31}$$

$$\rho^+\left(U^+\frac{\partial H_1^+}{\partial x^+} + V^+\frac{\partial H_1^+}{\partial r^+}\right) = (1-\gamma_o)M_o^2U^+\frac{dP}{dx^+} + \frac{2}{r^+}\frac{\partial}{\partial r^+}\left(r^+\frac{k^+}{c_p^+}\frac{\partial H_1^+}{\partial r^+}\right)$$
$$+2(\gamma_o-1)M_o^2\mu^+Pr_o\Phi^+ \tag{2.32}$$

where

$$\Phi^+ = \left\{\frac{\partial U^+}{\partial r^+}\right\} + \frac{2}{Re_o Pr_o}\left\{\left(\frac{\partial V^+}{\partial r^+}\right)^2 + \left\{\frac{V^+}{r^+}\right\}^2 - \frac{2}{3}\left[\frac{\partial V^+}{\partial r^+} + \frac{V^+}{r^+}\right]^2\right\} \tag{2.33}$$

The boundary conditions in terms of the non-dimensionalized variables are

$$\underline{\text{at } x^+ = 0} \quad U^+ = 2(1-r^{+2}) \quad \text{or} \quad U^+ = 1 \qquad \theta = 1$$

$$\underline{x^+ < 0 \quad r^+ = 1}$$
$$U^+ = 0 \qquad V^+ = 0 \qquad \theta = 1$$

$$\underline{x^+ \geq 0 \quad r^+ = 1}$$
$$U^+ = 0 \qquad V^+ = 0 \qquad \theta = \theta_w$$

$$\underline{x^+ \lesseqgtr 0 \quad r^+ = 0}$$
$$\frac{\partial U^+}{\partial r^+} = 0 \qquad V^+ = 0 \qquad \frac{\partial \theta}{\partial r^+} = 0$$

The unknowns in these equations are U^+, V^+ and H_1^+ which are function of two space variables x^+ and r^+, and the non-dimensionalized pressure $P(x^+)$ which is a function of only the axial co-ordinate. At first sight, there would seem to be one equation less than that required for solution, since there are only three equations here. Before application of the boundary layer assumptions, the fourth equation was provided by the radial momentum equation. The fourth equation in this case comes from the integrated continuity equation,

$$2\int_0^1 \rho^+ U^+ r^+ dr^+ - 1 = 0 \tag{2.34}$$

which defines the flow as being confined. Integration over the space variable r^+ provides an equation in terms of one variable, x^+. Worsoe Schmidt used a two level finite difference scheme with variable implicitness to generate a marching solution in the axial direction. If the velocity and temperature profiles are known at one axial point, then the profiles at the next step can be obtained with application of appropriate boundary conditions and so on down the tube until the profile development is sufficiently complete. Various discrete radial and axial points in the tube are specified as node points (Fig. 4) where we either know or are solving for values of the dependent variables. We define $\Phi_{m,n}$ as being the value of a dependent variable corresponding to the node m,n whose spatial point in the tube is given as $(m\Delta x^+, n\Delta r^+)$.[3]

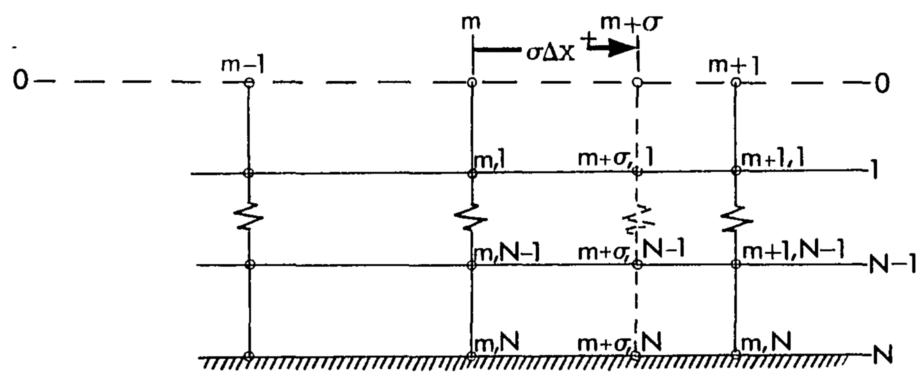

Figure 5. Designation of Mesh Points

[3]This represents a simplification in that the radial and axial mesh steps changed at different points in the tube. If the axial step were Δx_1 for m_1 steps and Δx_2 for m_2 steps, the axial point would be $m_1\Delta x_1+m_2\Delta x_2$.

Although we are solving for the dependent variables at these points, this does not necessitate writing the finite difference representation of the differential equations to apply to these points. In the Worsoe-Schmidt solution, the equations are radially centered at $n\,\Delta r^+$, but if the dependent variables are known at the m'th axial point and we are solving for them at m+1, then the equations are written so as to apply to the point $m+\sigma$, where σ is a constant less than or equal to 1. The reason for doing this, and the significance of σ can be seen in the following analysis. The radial difference operators δ and δ^2 are defined by

$$\delta\,(\Phi_{m,n}) = \Phi_{m,n+1} - \Phi_{m,n} \tag{2.35}$$

$$\delta^2(\Phi_{m,n}) = \Phi_{m,n+1} - 2\Phi_{m,n} + \Phi_{m,n-1} \tag{2.36}$$

By means of Taylor series expansions, the analytical derivatives at the point $m+\sigma, n$ can be related to values of the dependent variables and their derivatives at the axial points m and m+1. After some manipulation, the following relationships can be derived;

$$\frac{\Phi_{m+1,n} - \Phi_{m,n}}{\Delta x^+} = \frac{\partial \Phi}{\partial x^+} + \left[\frac{1}{2}(1-2\sigma)\frac{\partial^2 \Phi}{\partial x^{+2}}\Delta x^+ + \frac{(1-3\sigma+3\sigma^2)}{6}\frac{\partial^3 \Phi}{\partial x^{+3}}\Delta x^{+2} + O(\Delta x^{+3})\right] \tag{2.37}$$

$$\frac{\sigma\delta(\Phi_{m+1,n})+(1-\sigma)\delta(\Phi_{m,n})}{2\Delta r^{+}} = \frac{\partial\Phi}{\partial r^{+}} + \left[\frac{1}{2}\sigma(1-\rho)\frac{\partial^3\Phi}{\partial x^{+2}\partial r^{+}}\Delta x^{+2} + \frac{1}{6}\frac{\partial^3\Phi}{\partial r^{+3}}\Delta r^{+2} + O(\Delta x^{+4}) + O(\Delta r^{+4})\right] \tag{2.38}$$

$$\frac{\sigma\delta^2(\Phi_{m+1,n})+(1-\sigma)\delta^2(\Phi_{m,n})}{\Delta r^{+2}} = \frac{\partial^2\Phi}{\partial r^{+2}} + \left[\frac{1}{2}\sigma(1-\sigma)\frac{\partial^4\Phi}{\partial x^{+2}\partial r^{+2}}\Delta x^{+2} + \frac{1}{12}\frac{\partial^4\Phi}{\partial r^{+4}}\Delta r^{+4} + O(\Delta x^{+4}) + O(\Delta x^{+2}\Delta r^{+2}) + O(\Delta r^{+4})\right] \tag{2.39}$$

where all analytical derivatives apply to the point $(m+\sigma)\Delta x^{+}, n\Delta r^{+}$. The bracketed terms on the right hand sides of these expressions can be considered as representing the error if the difference quotients on the right hand sides are substituted in place of the analytical derivatives in the differential equations. The value of σ can be seen to have a direct influence on the magnitude of these terms, and the value of σ should be chosen with this in mind. Choosing $\sigma = 1/2$ will minimize all the coefficients in which σ appears. This would appear to be an optimum value if it were not for the fact that the solution was found to be unstable in this case. A compromise value of $\sigma = 3/4$ was chosen and was found to yield stable results in all cases. While it is possible that a stable solution could have been chosen closer to 1/2, it is questionable whether it would have been worthwhile to have devoted the time to determing this σ. Similar results were found by Worsoe-Schmidt and are discussed by him (100). It must be remembered that an optimum determined for one set of boundary conditions may not be stable for another set.

The values of the dependent variables at m+1 are evaluated by assuming a linear variation between neighboring axial points;

$$\Phi_{m+\sigma,n} = \sigma \Phi_{m+1,n} + (1-\sigma)\Phi_{m,n} \tag{2.40}$$

In regions where large second and higher order axial derivatives occur, this expression becomes less acceptable. This is in addition to the error incurred by dropping the second derivatives in the original equations. When these representations are substituted into the partial differential equations 2.29, 2.30 and 2.31, a relationship combining $\Phi_{m+1,n}$, $\Phi_{m+1,n+1}$ and $\Phi_{m+1,n-1}$ is obtained at each radial node for $\sigma > 0$. For this case there are 3N +1 simultaneous equations in order to solve for 3N +1 unknowns. For the particular case $\sigma = 0$, we have an expression explicitly in $\Phi_{m+1,n}$ and known quantities at each radial node.

The difference equations obtained will still contain products of the unknown variables. This non-linearity can be neatly eliminated if we allow of linearization by means of iteration. Wherever a product of the same two dependent variables occur, we will substitute the best available value for one of them and then solve the linearized equation for the succeeding value. For example if the first solution at $(m+\sigma)\Delta x^+$ is being performed, the quantity $\Phi_{m,n}\Phi_{m+1,n}$ will be used in place of $\Phi^2_{m+1,n}$ On the next iteration at this point, $\Phi_{m+1,n}$ from the first solution of the linearized equation would be used, and so on until convergence is obtained.

A further linearization allows us to uncouple the equations at each iteration, insofar as products of different dependent variables occur. The details of this linearization depend upon the sequence in which the equations are solved. The energy equation (2.32) is the first equation to be solved at an axial point, so where products of enthalpies and velocities occur, velocities from the previous axial point are used. The integrated continuity equation 2.34 can then be arranged to bring out explicitly P_{m+1} which is contained in $\rho^+_{m+1,n}$. Values of enthalpy from the present solution of the energy equation are used in evaluating the temperature dependent quantities in the momentum equation. One exception to this is the term $\rho^+ U^+$. Generally, ρ^+ and U^+ vary in opposite directions along the tube. Using the new enthalpy and pressure for the evaluation of ρ^+ and the old value of U^+ would roughly give us $\rho^+_{m+1,n} U^+_{m,n}$ which overestimates $\rho^+_{m+1,n} U^+_{m+1,n}$. A better approximation can be obtained by using $\rho^+_{m+1,n} U^+_{m,n}$ until estimates of both $\rho^+_{m+1,n}$ and $U^+_{m+1,n}$ are available.[4] After the energy and momentum equations, the differential form of the continuity equation (2.31) can be used for the evaluation of radial velocities for use on the next iteration or at the next step. Using this procedure reduces the problem to the solving of 3 sets of N linear simultaneous equations plus the total continuity equation.

Considering that upwards of 320 radial mesh divisions were necessary for the solution of the most severe boundary conditions, the solution of this many simultaneous equations would still be prohibitive if it were not for the fact that the coefficient matrices for the dependent variables were of a particularly simple form. After the aforementioned linearizations are made, the general form

---

[4] An extreme example of this type of linearization was used in the theoretical analysis of Koppel and Smith (48) where it was assumed that the product of velocity and density, ρu, at any radius is independent of the axial coordinate.

of the relationships that holds among the velocities and enthalpies can be written as;

$$D_n^I = -A_n^I U_{m+1,n-1}^+ + B_n^I U_{m+1,n}^+ - C_n^I U_{m+1,n+1}^+ - P_{m+1} \qquad (2.41)$$

$$D_n^{II} = -A_n^{II} H_{m+1,n-1}^+ + B_n^{II} H_{m+1,n}^+ - C_n^{II} H_{m+1,n+1}^+ \qquad (2.42)$$

where the coefficients are functions of σ and known values of enthalpies from the previous step and/or the last iteration. For the present the solution for the pressure defect and the radial velocities is skipped. At the centerline, consideration of symmetry allows a relationship to be written among two of the dependent variables:

$$B_o^I U_{m+1,0}^+ - C_o^I U_{m+1,1}^+ - P_{m+1} = D_o^I \qquad (2.43)$$

$$B_o^{II} H_{m+1,o}^+ - C_o^{II} H_{m+1,1}^+ = D_o^{II} \qquad (2.44)$$

Since there is specified wall temperature (and enthalpy) and no slip (zero axial velocity) at the wall, the equations are written at the wall are:

$$-A^{I}_{N-1}U^{+}_{m+1,N-2} + B^{I}_{N-1}U^{+}_{m+1,N-1} - P_{m+1} = D^{I}_{N-1} \qquad (2.45)$$

$$-A^{II}_{N-1}H^{+}_{m+1,N-2} + B^{II}_{N-1}H^{+}_{m+1,N-1} = D^{II}_{N} + C^{II}_{N-1}H^{+}_{m+1,N} \qquad (2.46)$$

where subscript N refers to the node point at the wall. The coefficient matrices for the enthalpy and velocity are of the form:

$$\left|\begin{array}{ll} \mathrm{XX000} & \\ \mathrm{0XXX0} & \\ \mathrm{00XXX} & \\ \quad\ddots & \\ & \mathrm{0XXX0} \\ & \mathrm{00XXX} \\ & \mathrm{000XX} \end{array}\right|$$

which is a matrix of the tri-diagonalized type. Since many of the elements are zero, inversion could be accomplished by means of one of the many available computer inversions, particularly one which makes use of zero checks. However, further simplification can be obtained by assuming that relationships of the form;

$$U^{+}_{m+1,n} = E^{I}_{n}U^{+}_{m+1,n+1} + F_{n}P_{m+1} + G^{I}_{n} \qquad (2.47)$$

$$H^{+}_{m+1,n} = E^{II}_{n}H^{+}_{m+1,n+1} + G^{II}_{n} \qquad (2.48)$$

exist. If such a relationship for $U^+_{m+1,n-1}$ is substituted in terms of $U^+_{m+1,n}$ and $H^+_{m+1,n-1}$ is substituted in terms of $H^+_{m+1,n}$ in equations (2.45) and (2.46) respectively, solution may be made explicitly for $U^+_{m+1,n}$ and $H^+_{m+1,n}$.

$$U^+_{m+1,n} = \frac{C^I_n}{B^I_n - A^I_n E^I_{n-1}} U^+_{m+1,n+1} + \frac{(1+A^I_n F_{n-1})}{B^I_n - A^I_n E^I_{n-1}} P_{m+1} + \frac{D^I_n + A^I_n G^I_{n-1}}{B^I_n - A^I_n E^I_{n-1}} \tag{2.49}$$

$$H^+_{m+1,n} = \frac{C^{II}_n}{B^{II}_n - A^{II}_n E^{II}_{n-1}} H^+_{m+1,n+1} + \frac{D^{II}_n + A^{II}_n G^{II}_{n-1}}{B^{II}_n - A^{II}_n E^{II}_{n-1}} \tag{2.50}$$

where coefficients on the right hand sides can be directly associated with the coefficients in equations (2.47) and (2.48). The following coefficients can be identified;

$$E^I_n = \frac{C^I_n}{B^I_n - A^I_n E^I_{n-1}} \tag{2.51}$$

$$E^{II}_n = \frac{C^{II}_n}{B^{II}_n - A^{II}_n E^{II}_{n-1}} \tag{2.54}$$

$$F^I_n = \frac{1+A^I_n F_{n-1}}{B^I_n - A^I_n E^I_{n-1}} \tag{2.52}$$

$$G^{II}_n = \frac{D^{II}_n + A^{II}_n G^{II}_{n-1}}{B^{II}_n - A^{II}_n E^{II}_{n-1}} \tag{2.55}$$

$$G_n^I = \frac{D_n^I + A_n^I G_{n-1}^I}{B_n^I - A_n^I E_{n-1}^I} \qquad (2.53)$$

where all coefficients in the recursive relationship corresponding to radial node n can be written in terms of the coefficients for radial node n-1 and other known quantities. It can be seen that if the values of these coefficients are known at the tube centerline, then all coefficients can be evaluated successively out to the tube wall. These coefficients are directly available in the momentum and energy difference equations as written for the tube centerline in equations 2.43 and 2.44. The following identities can be made;

$$E_o^I = C_o^I / B_o^I \qquad (2.56)$$

$$F_o^I = 1 / B_o^I \qquad (2.57)$$

$$G_o^I = D_o^I / B_o^I \qquad (2.58)$$

$$E_o^{II} = C_o^{II} / B_o^{II} \qquad (2.59)$$

$$G_o^{II} = C_o^{II} / B_o^{II} \qquad (2.60)$$

Once all the coefficients are known and after applying the boundary conditions at the wall (i.e. - known $U^+_{m+1,N}$ and $H^+(\theta_w)_{m+1,N}$), the enthalpies and axial velocities can be evaluated, this time from the wall succesively out to the tube centerline.

The differential form of the continuity equation provides the radial velocities. Worsoe-Schmidt wrote the difference quotients for this equation so as to apply to the point $m+\sigma, n-1/2$. A new difference operator is defined as

$$\delta'(\Phi_{m,n+\frac{1}{2}}) = \Phi_{m,n} - \Phi_{m,n-1} \tag{2.61}$$

In this case, the quotient representation of the partial differential equation (2.31) contains only two unknown quantities, $V^{+}_{m+1,n-1}$ and $V^{+}_{m+1,n}$ so that an explicit solution may be made for V^{+}.

Returning to the solution for the pressure defect, an integration of the continuity equation consistent with the finite difference scheme was obtained by successive elimination of the radial velocities in the difference representation of the continuity equation. This results in;

$$\frac{1}{8}(\rho^{+}U^{+})_{m+1,o} + \sum_{n=1}^{N-1} n(\rho^{+}U^{+})_{m+1,n} = \frac{1}{8}(\rho^{+}U^{+})_{m,o} + \sum_{n=1}^{N-1} n(\rho^{+}U^{+})_{m,n} \tag{2.62}$$

Extraction of a common term P_{m+1} from the density terms on the left hand side of (2.62) and substitution of the recursive relationships for the axial velocities results in an equation with P_{m+1} as the only unknown. Once this quantity is determined the solution of the momentum equation may proceed since $\frac{dP}{dx^+}$ is known from $(P_{m+1}-P_m)/\Delta x^+$

A note should be mentioned concerning the way in which radial derivatives of the temperature and velocity profiles were obtained at the wall. These quantities are necessary for the calculation of the fluid friction and heat transfer at the wall. Worsoe-Schmidt evaluated these terms by taking the derivative of a third order polynomial in r^+ fitted to the velocities and enthalpies at the 4 radial node points closest to the wall. In terms of the quantities at these nodes;

$$\left.\frac{\partial U^+}{\partial r^+}\right|_w = \frac{1}{6\Delta r^+}(18U^+_{N-1} - 9U^+_{N-2} + 2U^+_{N-3}) \qquad (2.63)$$

$$\left.\frac{\partial H^+}{\partial r^+}\right|_w = \frac{1}{6\Delta r^+}(11H^+_N + 18H^+_{N-1} - 9H^+_{N-2} + 2H^+_{N-3}) \qquad (2.64)$$

where subscript N refers to the node point at the wall. Subscript m is absent since all variables pertain to the same axial point. The term U^+_N is absent from 2.63 since $U^+_N = 0$. The third order insures that inflection points can be acommodated.

The order of solution and basic features of the inversion for equations 2.45 and 2.46 and as described by Worsoe-Schmidt in reference 100 were used without major modification. Those requiring a more detailed review than that presented here should consult that reference.

CHAPTER 3. FINITE DIFFERENCE SOLUTION
THE GRAETZ BOUNDARY CONDITION

3.1. Basic Considerations

The variation with axial distance and inlet wall to bulk temperature ratio of the local Nusselt number $Nu_{,m}$ and friction factor f is sought. In terms of flow quantities and fluid properties, these are defined by;

$$fRe_{,m} = \left[\frac{-\tau_w}{\frac{1}{2}(\rho U)_m U_m}\right]\left[\frac{2r_o U_m \rho_m}{\mu_m}\right] = \frac{-2\tau_w^+}{\mu_m^+ \int_o^1 U^+ r^+ dr^+} \tag{3.1}$$

$$Nu_{,m} = \frac{2r_o h}{k_m} = \frac{-2r_o q_w''}{k_m(T_w - T_m)} = \frac{2q^+}{k_m^+(\theta_w - \theta_m)} \tag{3.2}$$

where subscript m refers to quantities or properties evaluated at the bulk fluid temperature at an axial point. The non-dimensionalized heat transfer and wall shear stress are defined in terms of the temperature and velocity profiles by;

$$\tau_w^+ = -\mu_w^+ \frac{\partial U^+}{\partial r^+}\bigg|_{r^+=1} \tag{3.3}$$

$$q_w^+ = -k^+ \frac{\partial \theta}{\partial r^+}\bigg|_{r^+=1} \tag{3.4}$$

respectively.

Values of the power law exponents a,b,c (2.24, 2.25, 2.26) and γ_0 and Pr_0 were evaluated from published property data for three gases: air, helium and carbon dioxide. (See Appendix B) The transport properties of helium follow the power law almost exactly. While air and CO_2 are not monatomic gases, the transport properties for air can still be fairly represented by the power law. These representations are not very good for CO_2, but this type of variation was assumed to hold true anyway so as to provide a rough idea of the behavior of the gas. This gas is of some interest since its transport properties vary much more severely than the other two gases. Due to this approximation, correlation of the wall parameters for CO_2 was not attempted. The properties and exponents were evaluated from a least squares fit to the tabulated data. The exponents were chosen so as to minimize the sum-squared error for all reference (subscript zero) points chosen in the range of tabulated data. Also, the properties are weak functions of pressure. The data was chosen for a pressure of 1 atmosphere which corresponds closely with the conditions run in the experimental apparatus, although this data should represent the properties quite accurately up to several atmospheres. The data for the three gases is summarized in Table 3.1.

Table 3.1. Transport and Thermodynamic Properties

Gas	a	b	c	Pr_o	γ_o
Air	0.12	0.64	0.71	0.71	1.36
He	0.00	0.69	0.69	0.67	1.67
CO_2	0.29	0.74	1.38	0.71	1.21

Straightforward application of the finite difference program obtained from Worsoe-Schmidt and corresponding to the description given in reference 100 typically resulted in the behavior of $fRe_{,m}$ as shown in Figure 6. Similar behavior was obtained for $Nu_{,m}$. The results are for He at an inlet wall to bulk temperature ratio of 0.10. The parametric curves in each plot correspond to different radial mesh divisions which are indicated on the graphs--also, the discontinuities in each curve correspond to the point where the number of mesh nodes was halved. At first it was suspected that this behavior might be due to a local instability or error in the profiles due to the mesh change, but examination of the profiles directly before and after the change revealed little or no noticeable difference over what could be considered as normal axial development. It should be noted from these plots that the effect of the step change is diminished as the mesh is refined. Also, the change to a coarser mesh in each

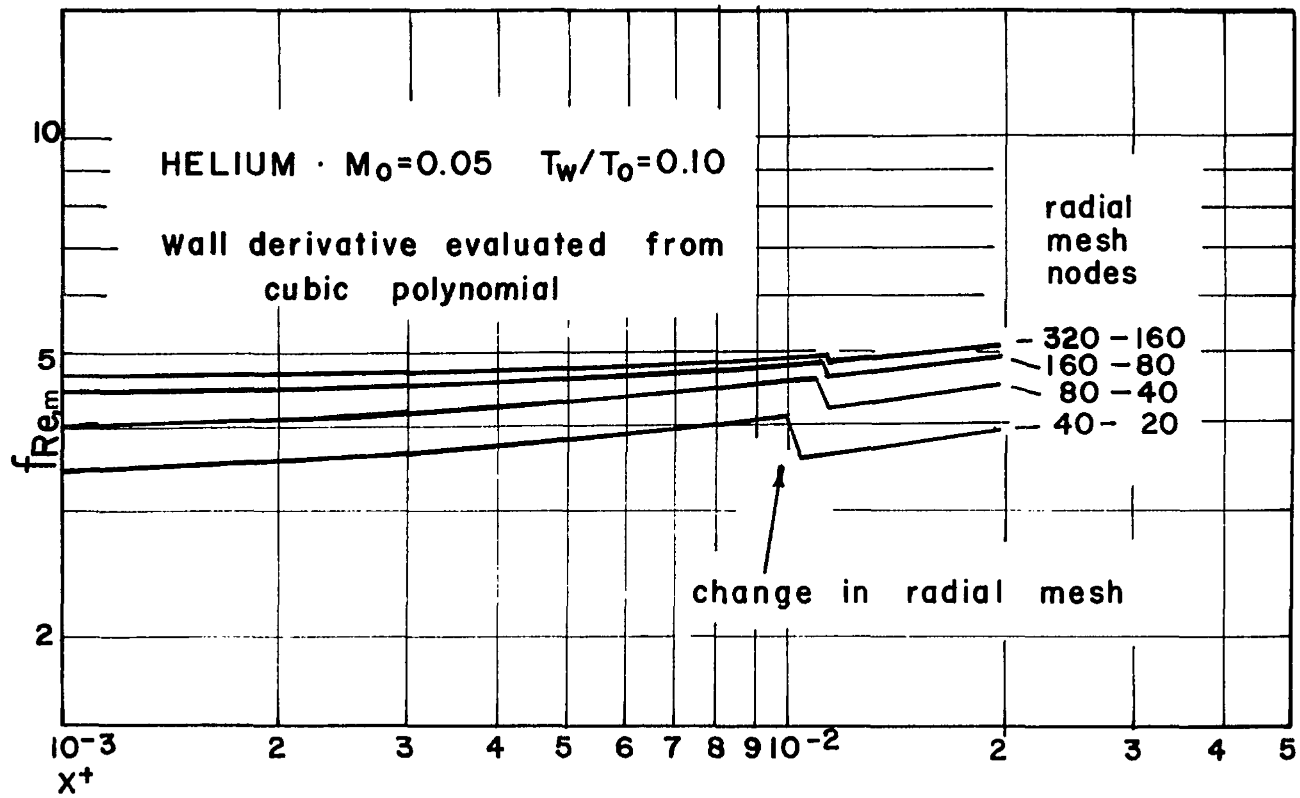

Figure 6. Effect of change of radial mesh size on $fRe,_m$ when evaluated from a cubic polynomial.

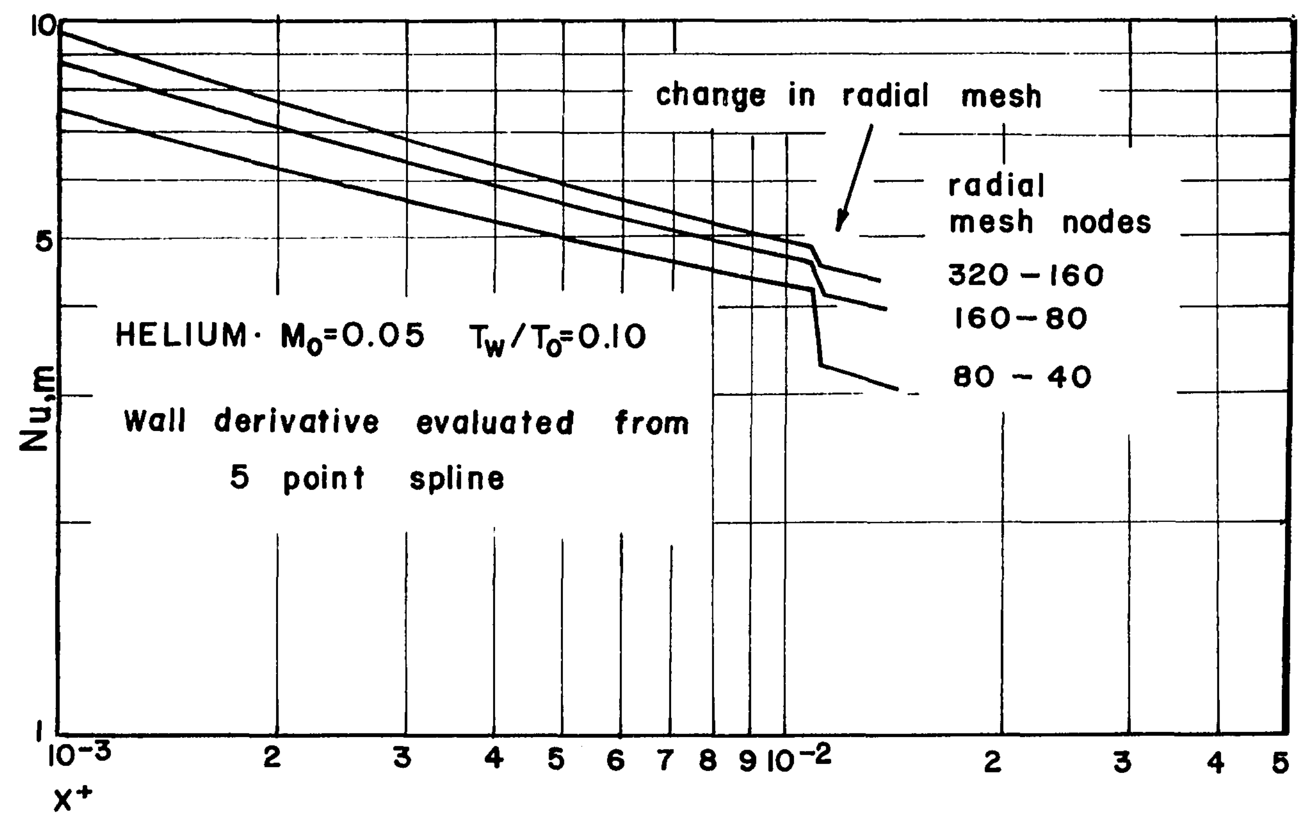

Figure 7. Effect of change of radial mesh size on $Nu,_m$ when evaluated from a 5 point spline.

case yields results that would be obtained if the coarser mesh had been used entirely. For example, the wall parameters after a change from 80 to 40 radial divisions have the same value as the results obtained for 40 radial divisions throughout. This would seem to indicate an invariance of the solution of the governing equations and points to a deficiency in the method of evaluating the wall derivatives.

In an effort to correct this, many types and orders of curvefits (for example-- splines, Chebyshev polynomials, Lagrangian polynomials, ratios of rational polynomials, etc.) were tried in place of the cubic polynomial used by Worsoe-Schmidt and none were found to significantly improve the behavior. For example, values of $Nu_{,m}$ obtained from a 5 point spline for varying radial meshes are shown in Figure 7. The reason for this failure in the cooling case and not in the heating case can be illustrated by examination of the expression for the error incurred when a first derivative is evaluated from taking the derivative of a Lagrangian polynomial of order n-1. The polynomial is fitted at n tabular points of an analytical function F. The true derivative is F'. At a tabular point, we can write the error as (71);

$$\frac{d}{dr^+}(F(r))_{r=r_i} - \left(\frac{d\Lambda_{n-1}}{dr^+}\right)_{r=r_i} = \frac{\Gamma_n}{n!} F^n(r') \qquad (3.5)$$

where n = number of tabular points

n-1 = order of the polynomial fit

$\Gamma_n(r) = \prod_{i=1}^{n-1}(r-r_i)$

$\Lambda_n(r)$ = Lagrangian polynomial of order n-1

r_i = tabular point

r' = a value of the independent variable included in the range spanned by the tabular points

F = hypothetical closed form solution for the velocity or enthalpy profile

Although it is impossible to evaluate r' in this case, maximum values of the higher order derivatives of the temperature and velocity profiles near the tube wall as evaluated from difference quotients are summarized in Table 3.2. These maximum values occur in the region that would be included by polynomials of the degrees indicated for 80 radial mesh points and were evaluated from a solution using 320 radial mesh points for the severest cooling case ($\theta_w = 0.10$) considered here. Magnitudes of the derivatives for the severest heating case considered in the Worsoe-Schmidt analysis ($q_w^+ = 20$) are included for comparison. Since the factor $\frac{\Gamma_n}{n!}$ will be the same for both the heating and cooling cases when the same order polynomial and mesh sizes are used, the errors will be proportioned to $F^n(r')$. Polynomials of degree greater than 5 were not included because of generally poor suitability of high ordered polynomials for the calculation of derivatives.

Both results are for helium with $M_o = 0.03$. It can be seen that the higher ordered derivatives in our case are greater by as much as three orders of magnitude, and are on the average, one degree of magnitude greater. In particular, for the third order polynomial, the applicable derivative of the velocity profile is 35 times greater and for the temperature profile more than 250 times greater for the cooling case.

Table 3.2. High Ordered Profile Derivatives

Heating and Cooling

n	Degree of Fit	Velocity Profile $\left\lvert \frac{\Delta^n}{\Delta r^n}\left(\frac{U}{U_o}\right)_{max}\right\rvert$		Temperature $\left\lvert \frac{\Delta^n}{\Delta r^n}\left(\frac{T}{T_o}\right)_{max}\right\rvert$	
		Cooling	Heating	Cooling	Heating
3	2	0.786×10^{4}	0.332×10^{3}	0.148×10^{6}	0.312x10[illegible]
4	3	0.723×10^{7}	0.211×10^{6}	0.277×10^{8}	0.110x10[illegible]
5	4	0.158×10^{10}	0.133×10^{9}	0.588×10^{10}	0.237x10[illegible]
6	5	0.387×10^{12}	0.731×10^{11}	0.134×10^{13}	0.151x10[illegible]

An independent method of evaluating the shear stress and heat transfer can be obtained if a momentum and energy balance is performed between two axial mesh points. Radial integration of the momentum and energy equations 2.30 and 2,32 results in the following expressions for the average heat transfer q_w^+ and wall shear stress τ_w^+ between two adjacent axial points;

$$\bar{q}_w^+ = \frac{1}{2\Delta x^+}\Big\{ \Big(\int_0^1 \rho^+ U^+ H_1^+ r^+ dr^+\Big)_{m+1} - \Big(\int_0^1 \rho^+ U^+ H_1^+ r^+ dr^+\Big)_m$$

$$+ \frac{1}{2}(\gamma_o - 1) M_o^2 \Big[(P_{m+1} - P_m) \Big[\Big(\int_0^1 U^+ r^+ dr^+\Big)_{m+1} - \Big(\int_0^1 U^+ r^+ dr^+\Big)_m \Big]\Big]$$

$$- (\gamma_o - 1) M_0^2 Pr_o \Big[\Big(\int_0^1 \mu^+ \Big(\frac{\partial U^+}{\partial r^+}\Big)^2 r^+ dr^+\Big)_{m+1}$$

$$+ \Big(\int_0^1 \mu^+ \Big(\frac{\partial U^+}{\partial r^+}\Big)^2 r^+ dr^+\Big)_m \Big] \Delta x^+ \Big\}$$

$$\tau_w^+ = \frac{1}{2 Pr_o \Delta x^+} \Big[\Big(\int_0^1 \rho^+ U^{+2} r^+ dr^+\Big)_{m+1} - \Big(\int_0^1 \rho^+ U^{+2} r^+ dr^+\Big)_m \Big]$$

$$+ \frac{1}{4 Pr_o \Delta x^+} (P_m - P_{m+1})$$

The radial integrations were evaluated by means of Simpson's rule with a resultant error of the order $(\Delta r^+)^5$ which is smaller by a factor $(\Delta r^+)^3$ than that of the finite-difference scheme. Values of the Nusselt number and $fRe_{,m}$ as evaluated from these expressions at one axial point are shown in Figures 8 and 9 respectively as functions of the maximum number of radial mesh points. Wall parameters from the curvefit method are included for comparison. In both cases, variation of the integrated values are quite small, while the curvefit results are asymptotically approaching these values. The error between the curvefit and the true first derivative will decrease with decreasing Δr^+ by virtue of the function $\Gamma_n(r)$ in equation 3.7. However, for the plotted values, a small difference between the two methods would still be present even for infinitesmal Δr^+ since the integrated parameters apply to the point $(m - 1/2)\Delta x^+$ rather than $m\Delta x^+$. At most points though, the value of Δx^+ was sufficiently small with respect to x^+ such that these values could be considered as point values. The results presented herein were plotted with this correction at small x^+.

Two additional considerations arising from this analysis should be noted here. The first deals with convergence checks that Worsoe-Schmidt was able to use. An independent check of how well the solution is satisfying conservation of total momentum and energy in the tube can be obtained by comparison of two sides of the equalities obtained from the double integration of the momentum and

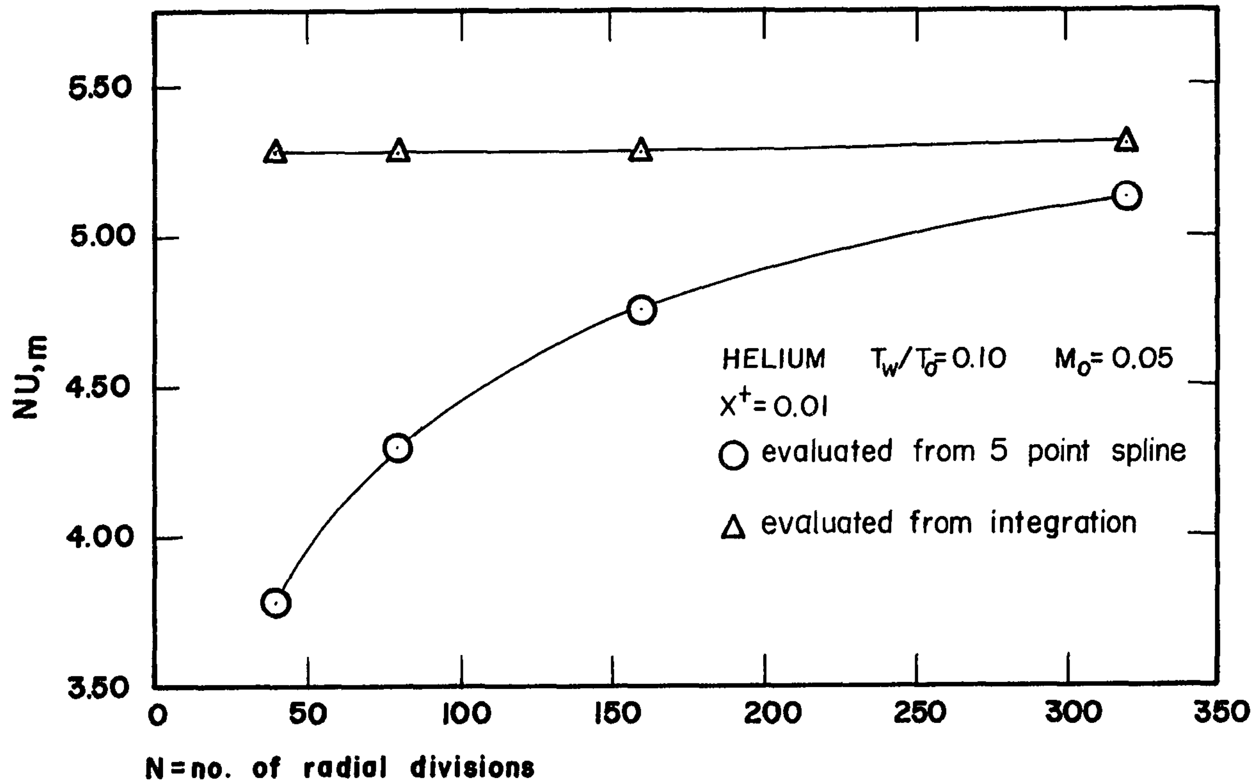

Figure 8. Variation of local Nusselt number with radial mesh size at a fixed axial point. Integrated energy equation and 5 point spline.

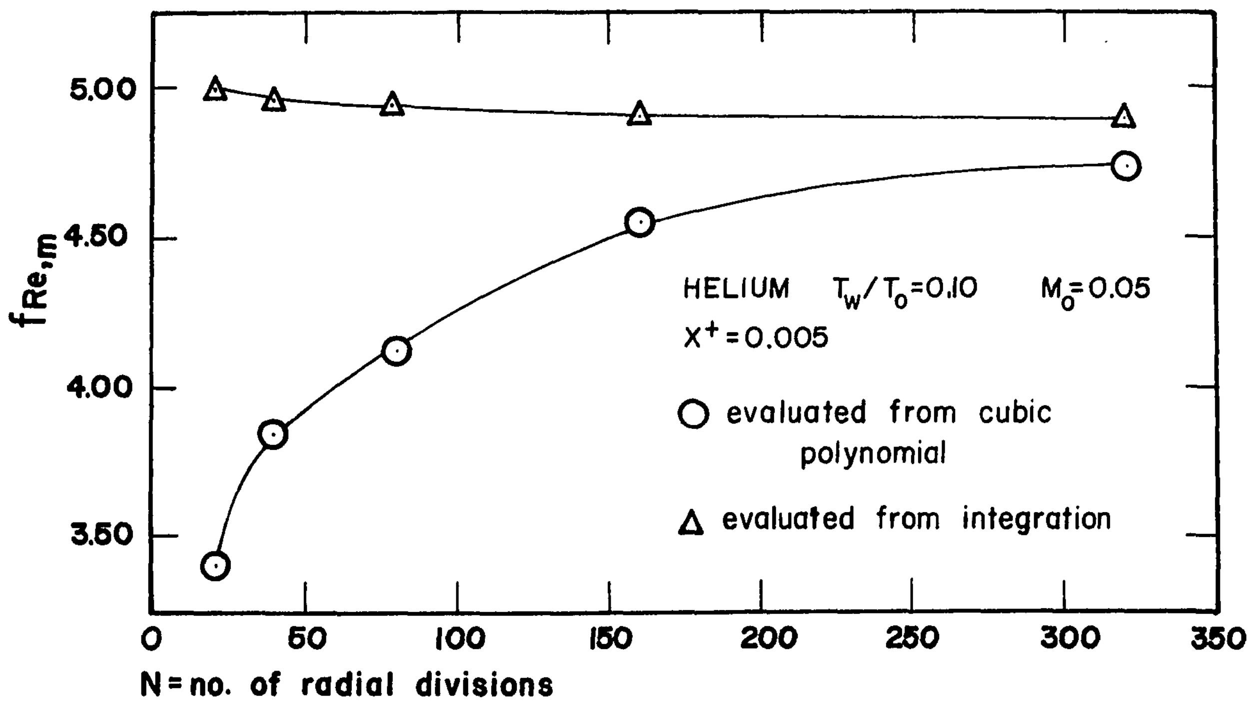

Figure 9. Variation of $fRe,_m$ with radial mesh size at a fixed axial point. Integrated energy equation and cubic polynomial.

energy equations;

Total Momentum:

$$2\left[\left(\int_0^1 \rho^+ U^{+2} r^+ dr^+\right)_{x^+} - \left(\int_0^1 \rho^+ U^{+2} r^+ dr^+\right)_{x^+=0}\right. \tag{3.8}$$

$$= P - 4Pr_0 \int_0^{x^+} \tau_w^+ dx^+$$

Total Energy:

$$2\left(\int_0^1 \rho^+ U^+ H_1^+ r^+ dr^+\right)_{x^+} = 4\int_0^{x^+} q_w^+ dx^+ - 2(\gamma_0 - 1)M_0^2 \Bigg\{ \tag{3.9}$$

$$\int_0^{x^+} \frac{dP}{dx} + \int_0^1 U^+ r^+ dr^+ dx^+ - 2Pr_0 \int_0^{x^+}\int_0^1 \mu^+ \left(\frac{\partial U^+}{\partial r^+}\right)^2 r^+ dr^+ dx^+ \Bigg\}$$

where Worsoe-Schmidt evaluated the τ_w^+ and q_w^+ terms from the curvefit method. Since this method has been shown to be unacceptable in our case, the only independent check remaining is that of the conservation of mass equation;

$$2\int_0^1 \rho^+ U^+ r^+ dr^+ - 1 = 0 \tag{3.10}$$

The conservation of mass is incorporated into the solution on a local basis (2.62) so that equation 3.10 represents a measure of the drift of the solution. It is also likely that large errors in 3.10 would reflect large errors in the overall conservation of axial momentum. In addition, a good indication of how well the solution is progressing can be provided by observing whether the wall parameters converge to their correct asymptotic values in the downstream region and how the solution in the developing region behaves with varying mesh size and σ . These latter methods were used quite liberally throughout the generation of results.

Wall parameters obtained from equations 3.6 and 3.7 are shown plotted as a function of x^+ in Figures 10 and 11 for air and helium respectively and Figures 12 and 13 for carbon dioxide. The parametric curves correspond to different inlet wall to bulk temperature ratios which range from sum 0.90 to 0.1.[5] The same results for air are plotted in Figure 14 as a function of the non-dimensionalized axial co-ordinate x_m^+ based on local rather than inlet conditions.

No clear advantage of one representation over the other exists. While the parameters converge to their asymptotic values more rapidly when plotted against x_m^+, the effect of wall to bulk temperature ratio is augmented on $Nu_{,m}$. No improvement or degradation of the product $fRe_{,m}$ occurs in the entrance since these curves are very

---

[5]It was not possible to evaluate the fully isothermal Nusselt number since the term $\theta_w - \theta_m$ becomes zero in the denominator of equation 3.2. Also, small absolute errors in the solution for the temperature profile would result in large errors in $\theta_w - \theta_m$ if θ_w were specified as, say 0.99.

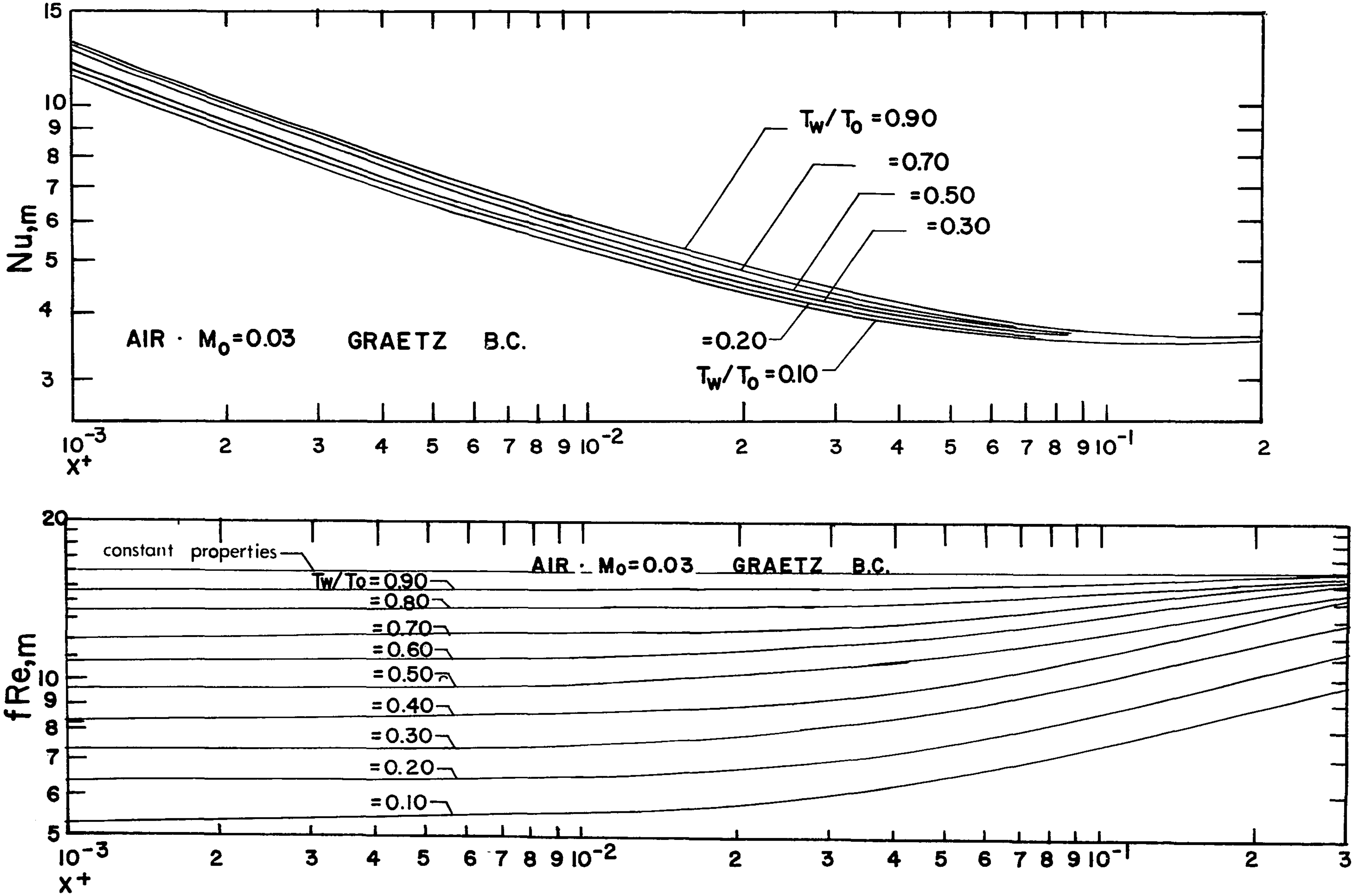

Figure 10. Axial variation of $fRe_{,m}$ and $Nu_{,m}$ for air. Graetz boundary condition, $M_o = 0.03$

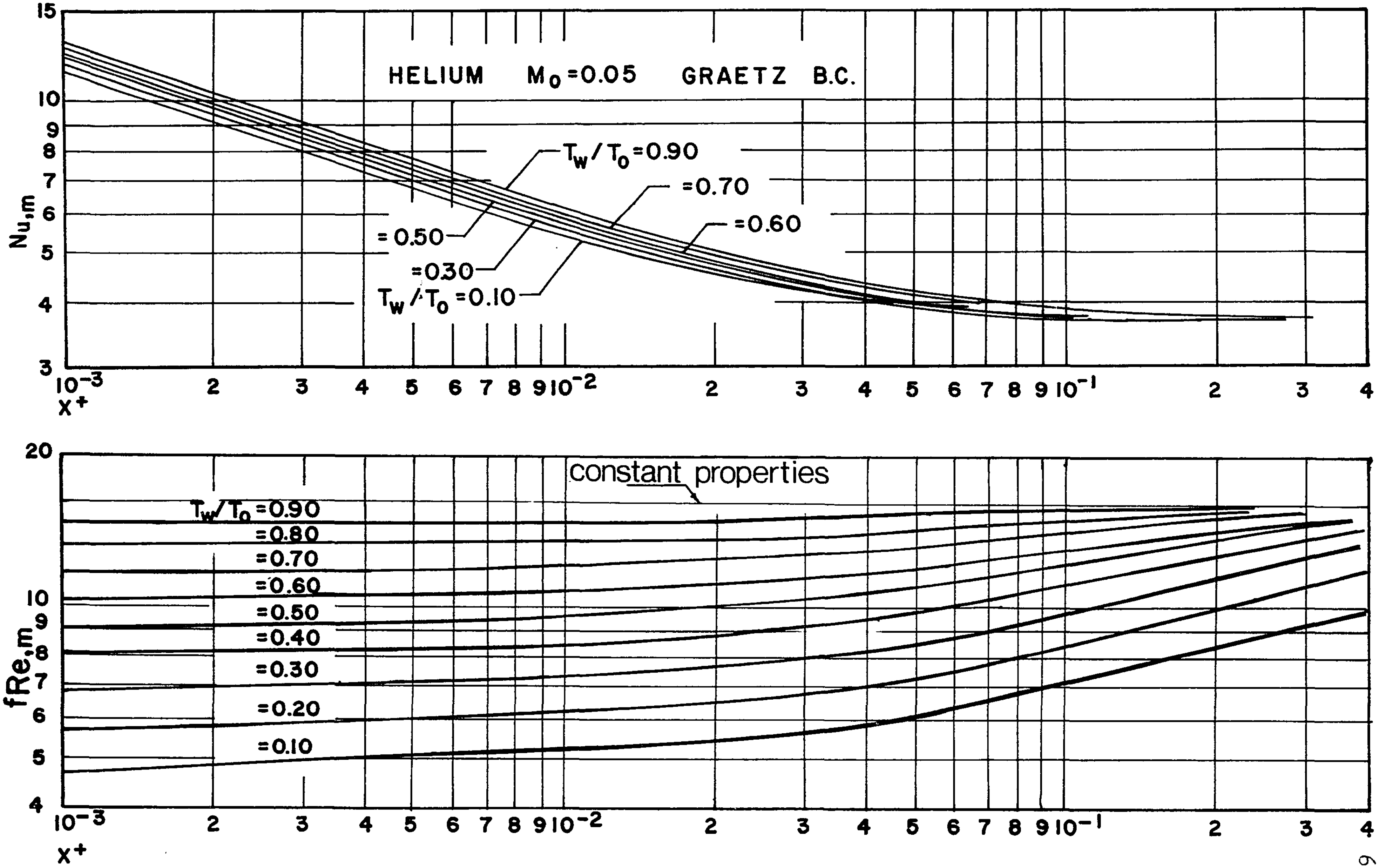

Figure 11. Axial variation of $fRe_{,m}$ and $Nu_{,m}$ for Helium. Graetz boundary condition, $M_0 = 0.05$

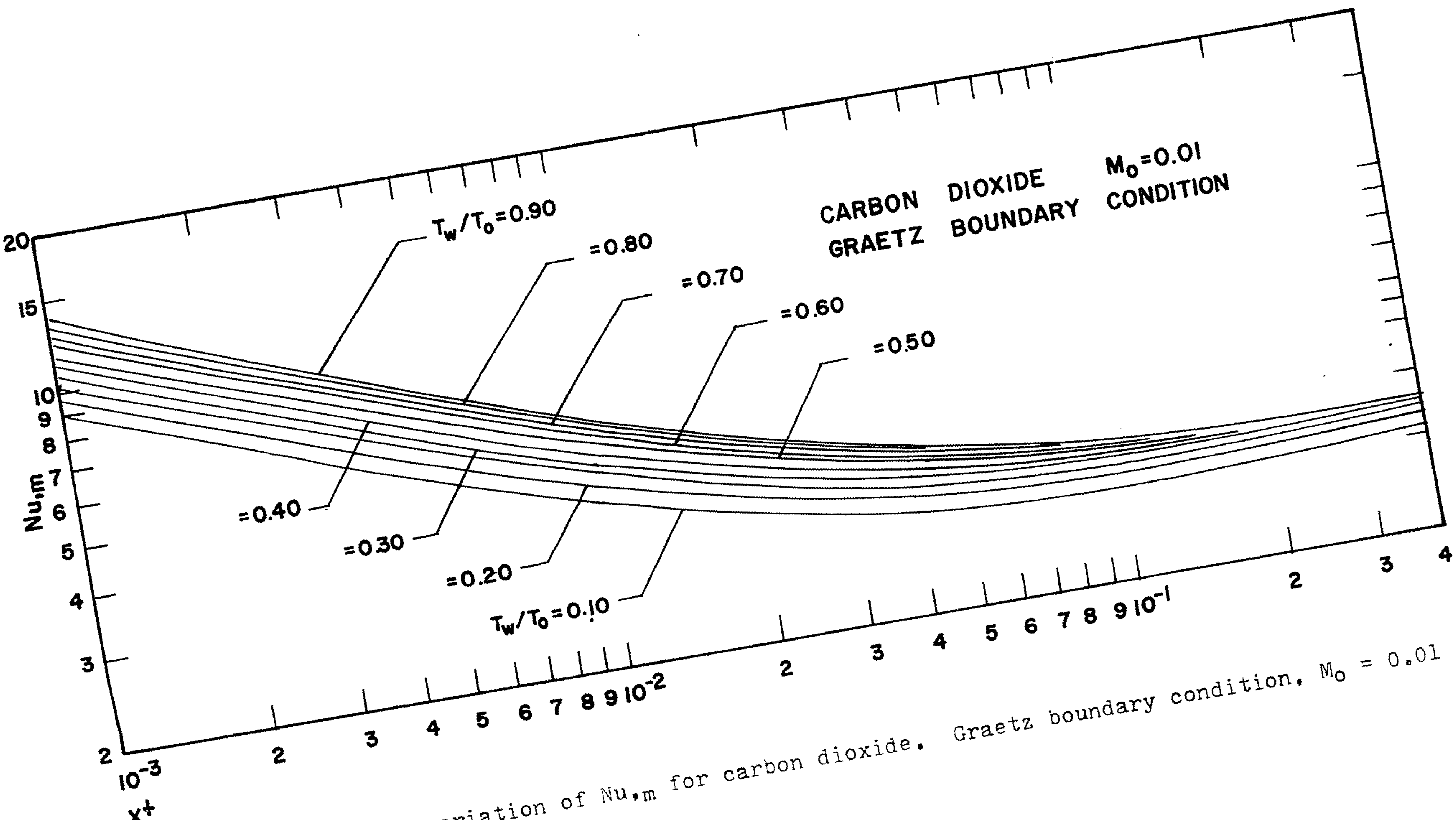

Figure 12. Axial variation of Nu,m for carbon dioxide. Graetz boundary condition, M_o = 0.01

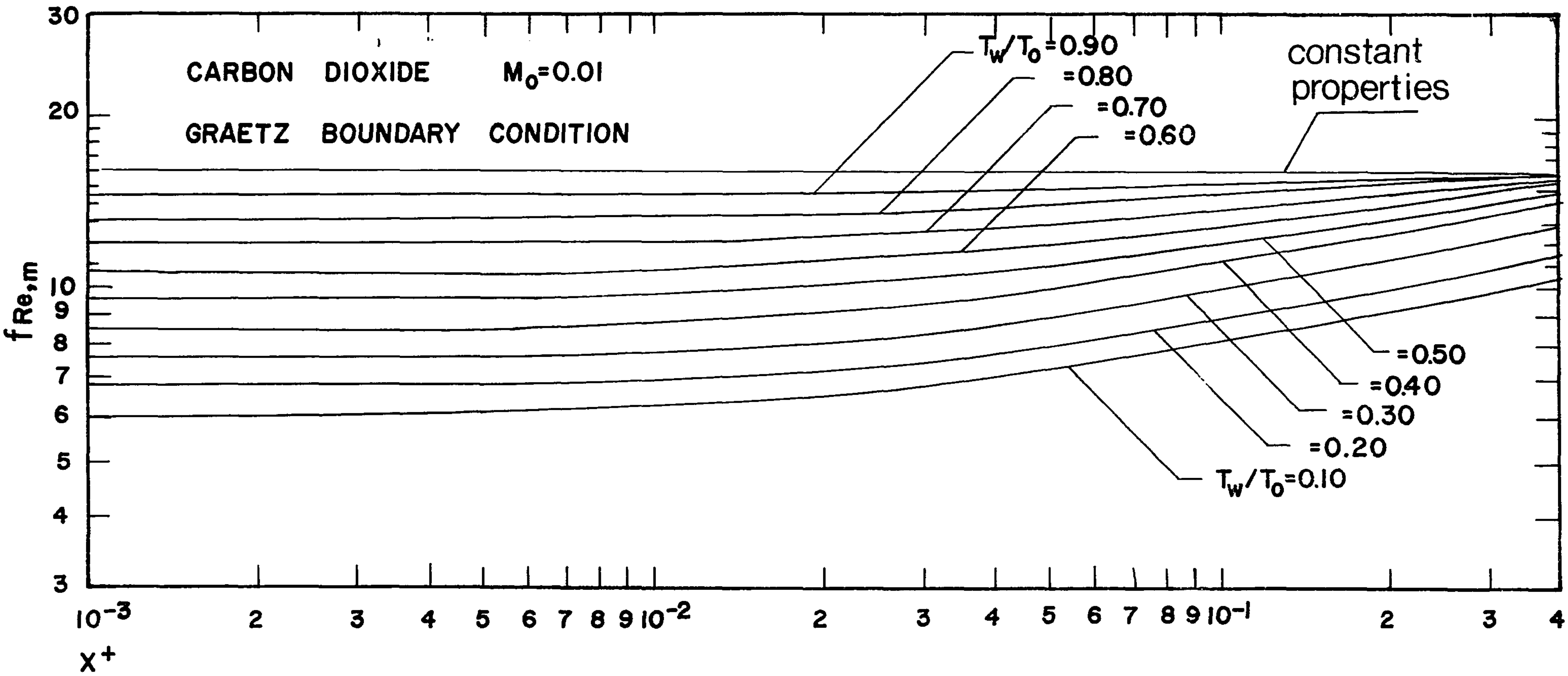

Figure 13. Axial variation of $fRe_{,m}$ for carbon dioxide. Graetz boundary condition, M_o = 0.01

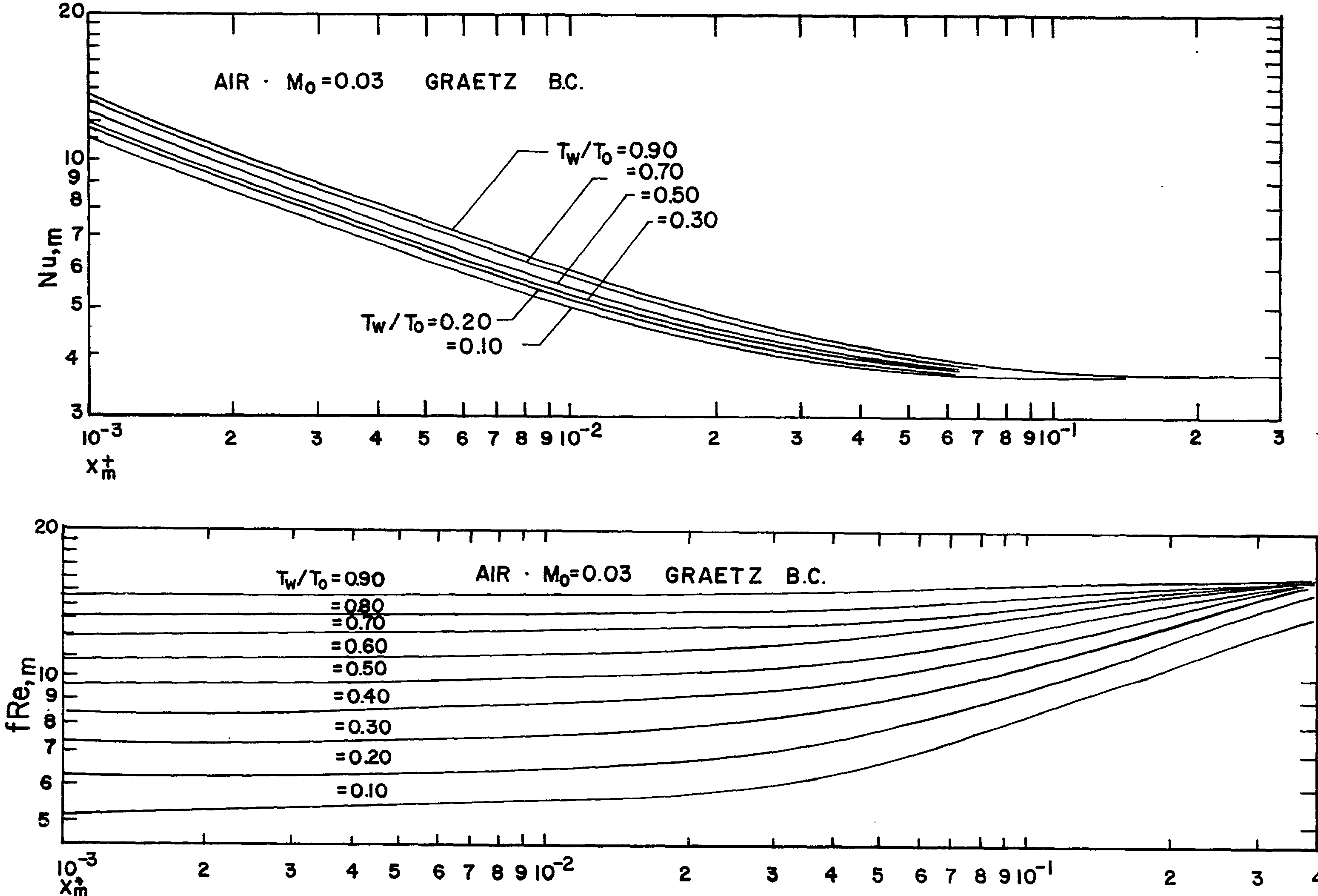

Figure 14. Local Nusselt number and fRe_m versus X_m^+ for air. Graetz boundary condition $M_o = 0.03$

nearly horizontal-- relative axial displacement does not affect the vertical spacing. When plotted as a function of x^+, $Nu,_m$ shows surprisingly little variation with respect to the inlet wall to bulk temperature ratio. For example, the maximum decrease in this quantity resulting from an almost ten fold decrease in the temperature ratio is on the order of 14% for air and helium and 33% for CO_2. The Nusselt number reaches the fully developed value more rapidly with reduced θ_w. A simple linear variation with inlet wall to bulk temperature ratio will describe the theoretical Nusselt number behavior to within 5%.

$$Nu,_m = (3.67 + Ax^{+B} e^{-\beta x^+})(1 - C(\frac{T_o}{T_w} - 1)) \qquad (3.11)$$

$$0.001 \leq x^+ \leq 0.35$$

$$Nu,_m = 3.67 \qquad x^+ > 0.35 \qquad (3.12)$$

where for air, $A = 0.198 \quad B = -0.584 \quad C = 0.13$

He $\quad A = 0.201 \quad B = -0.584 \quad C = 0.15$ $\qquad \beta = -20.8$

The variation of the friction factor is more pronounced and required a different type of correlation. If the product $fRe,_m$ is plotted as a function of local wall to mean temperature ratio, Figures 15 for helium and 16 for air result. The different curves correspond to different

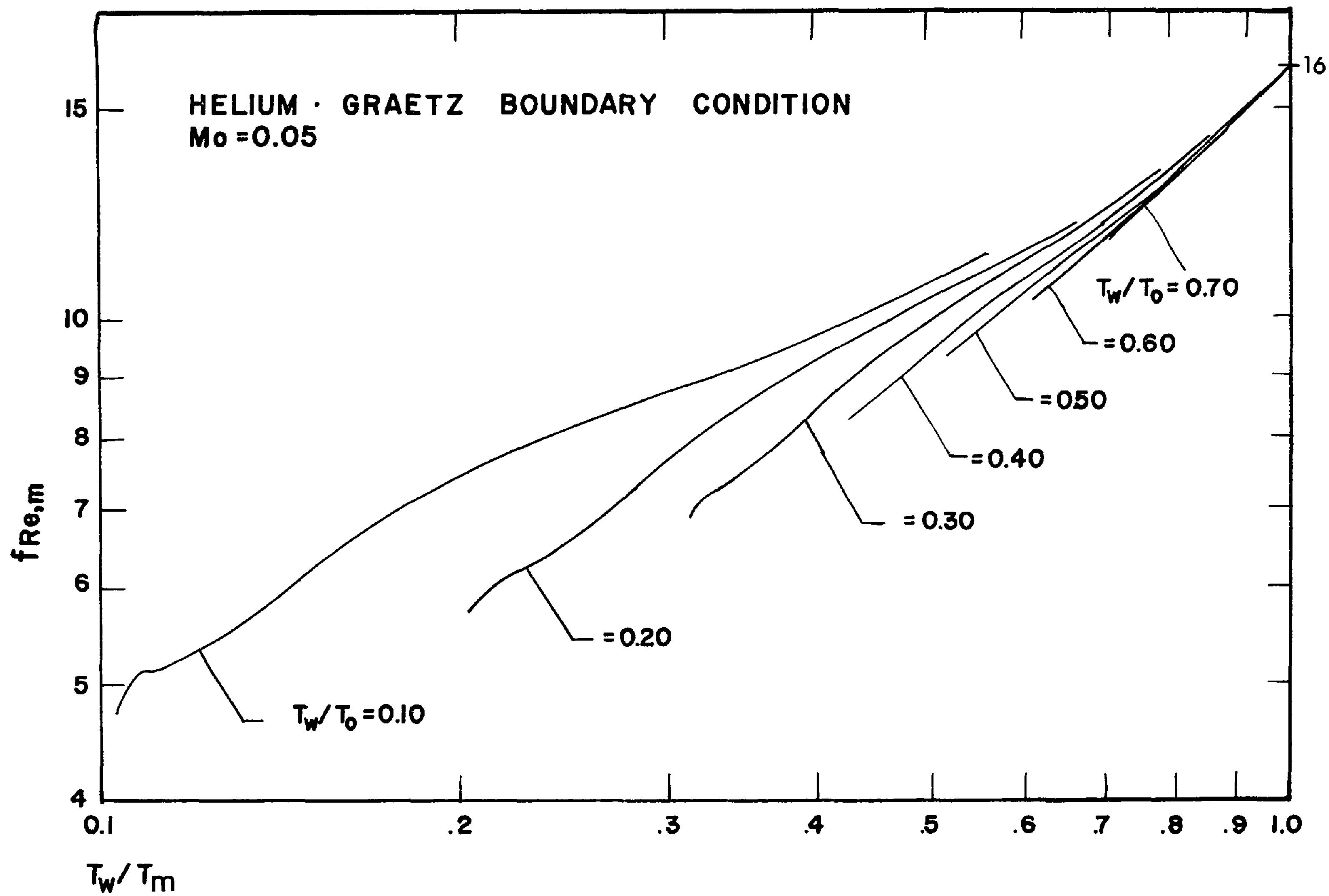

Figure 15. $fRe,_m$ versus T_w/T_m. Helium, Graetz boundary condition, M_o = 0.05

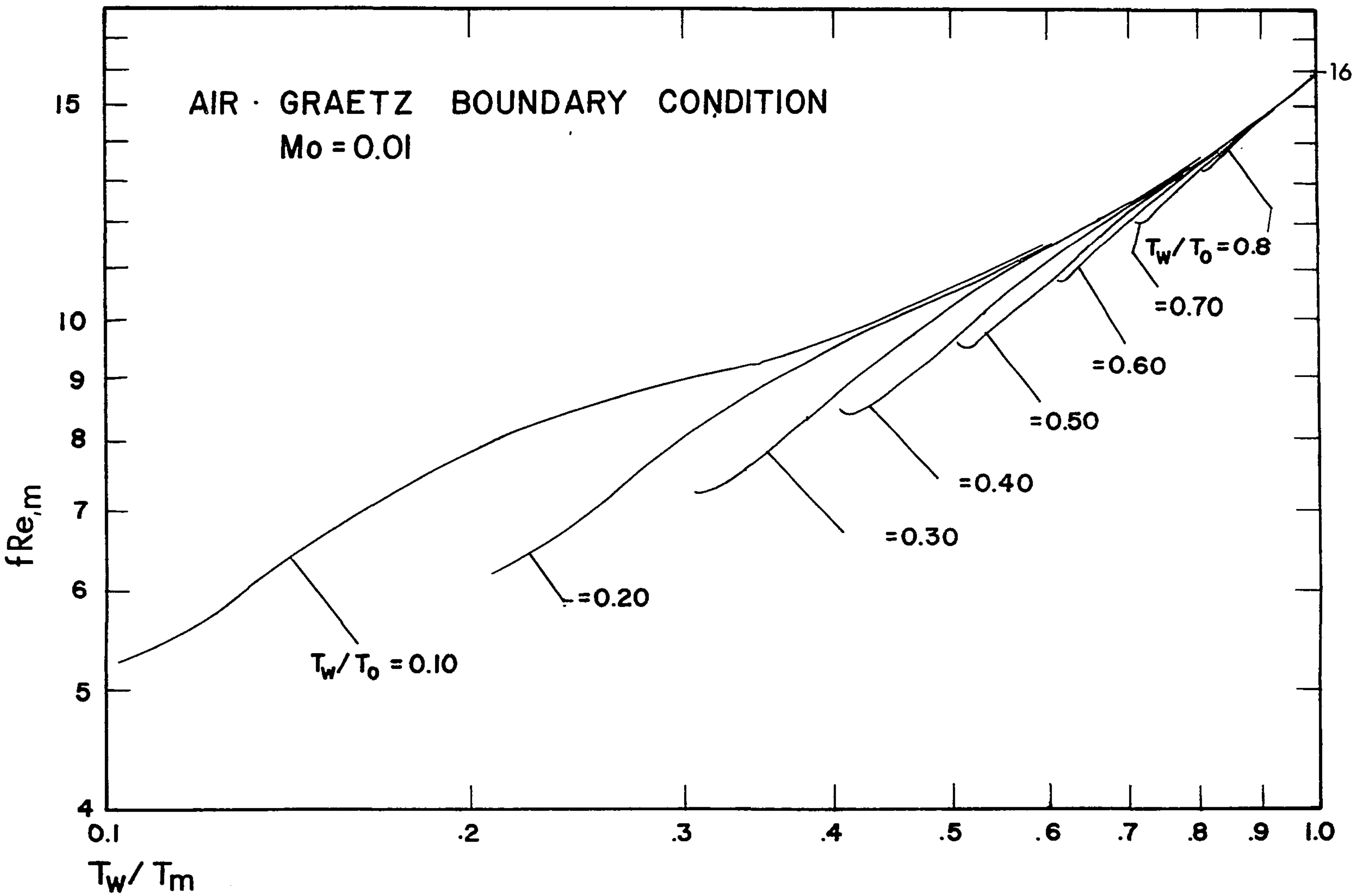

Figure 16. $fRe_{,m}$ versus T_w/T_m. Air, Graetz boundary condition, M_o = 0.01

inlet wall to bulk temperature ratios and were approximated by straight line segments passing through $fRe,_m=16.0$ at $T_w/T_m=1.0$. The slopes of these lines were determined by a least squares criterion for nearly equally spaced T_w/T_m. These straight line approximations would seem to be fairly good with the exception of $T_w/T_o=0.10$. The significance of the slope a of these log-log plots is defined in the equation;

$$fRe,_m=16\left(\frac{T_w}{T_m}\right)^a \qquad (3.13)$$

In Figure 17, a for each gas is plotted against T_w/T_o on log-log paper and a correlation of the form

$$a = b\left(\frac{T_w}{T_o}\right)^c \qquad (3.14)$$

is excellent. The values of b and c were also chosen by a least squares criterion. The final form of the friction factor correlations are,
for air,

$$fRe,_m=16\left(\frac{T_w}{T_m}\right)^a \qquad a = 0.904\left(\frac{T_w}{T_o}\right)^{0.257} \qquad (3.15)$$

and for helium

$$a = 0.957\left(\frac{T_w}{T_o}\right)^{0.251} \qquad (3.16)$$

In the range $0.001 \leq x^+ \leq 0.5$. These correlations will

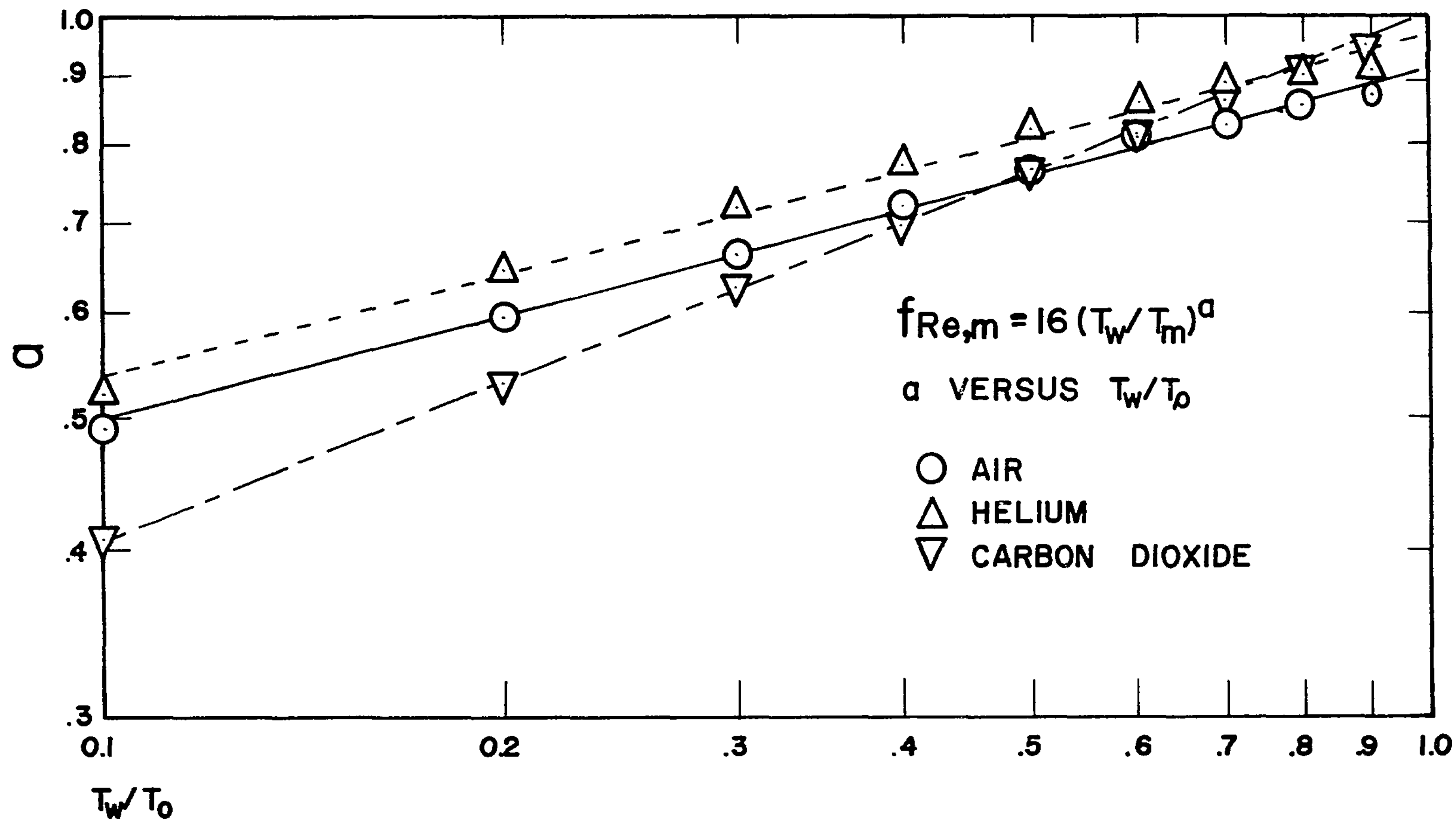

Figure 17. Exponent in $fRe_{,m}$ correlation versus T_W/T_o for air, helium and carbon dioxide. Graetz boundary condition.

describe the theoretical results within 9% for $T_w/T_o = 0.10$ and within 5% for $T_w/T_o \geq 0.20$. The initial curvature at the beginning of each of the curves in Figure 15 is probably due to starting errors in the finite difference solution.

The axial development of the axial velocity non-dimensionalized with respect to the local mean velocity and the reduced temperature, T_{red}, where

$$T_{red} = (T-T_w)/(T_m-T_w) \tag{3.17}$$

is shown in Figure 18 for air at inlet wall to bulk temperature ratios of 0.10 and 0.90. Radial velocity V^+ development for the same cases are shown in Figure 19. The physical reason for the observed behavior of the wall parameters can be seen from these figures. For example, the radial derivative of this reduced temperature,

$$\frac{\partial T_{red}}{\partial r^+} = \frac{\partial}{\partial r^+}\left(\frac{T_w - T}{T_w - T_m}\right) = -\frac{\partial \theta}{\partial r^+} \Big/ (T_w - T_m) \tag{3.18}$$

is a term in the expression for $Nu_{,m}$

$$Nu_{,m} = \left(\frac{2k_w}{k_m}\right)\frac{\partial T_{red}}{\partial r^+} \tag{3.19}$$

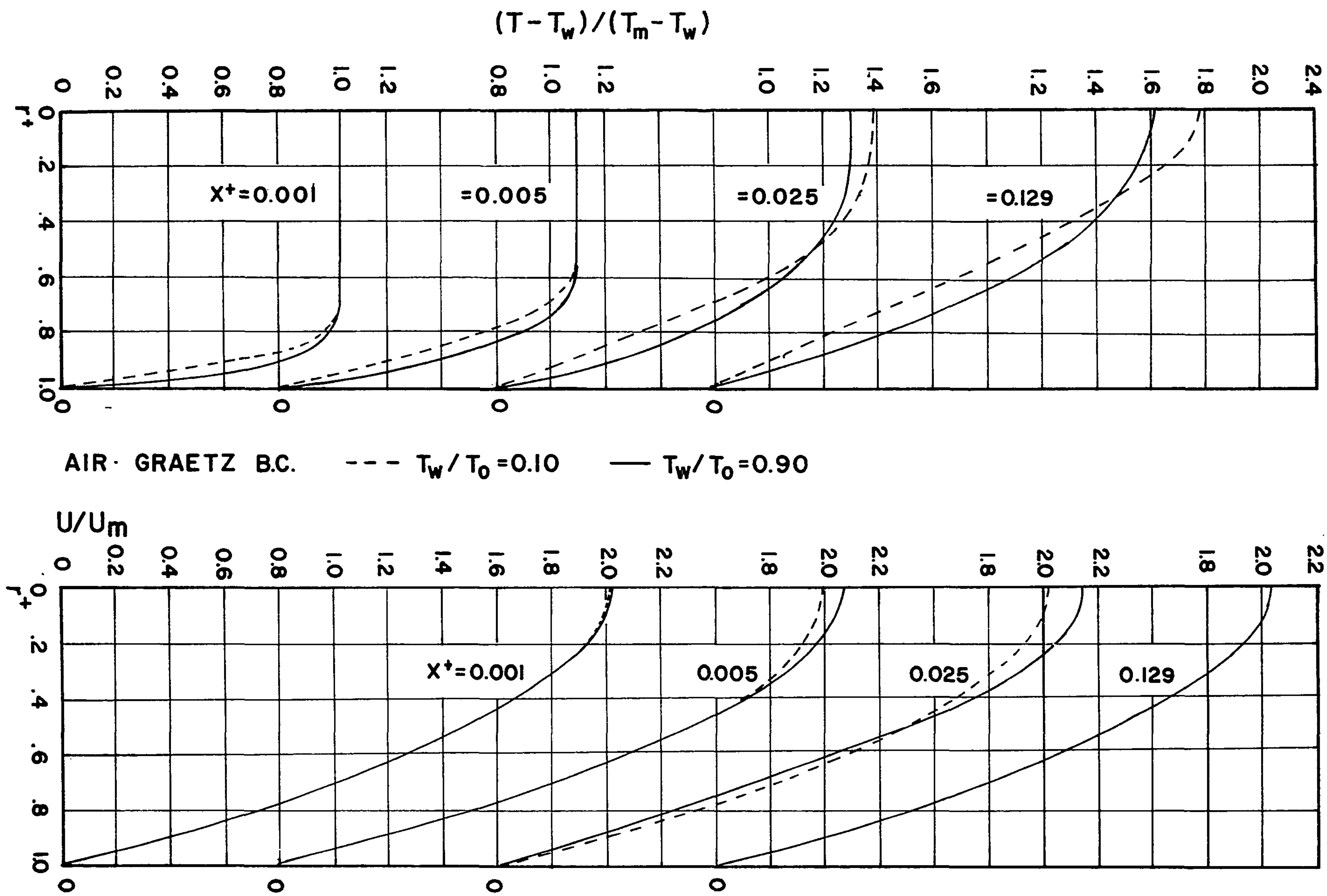

Figure 18. Axial development of reduced temperature and velocity profiles for two wall to inlet temperature ratios. Air, Graetz boundary condition.

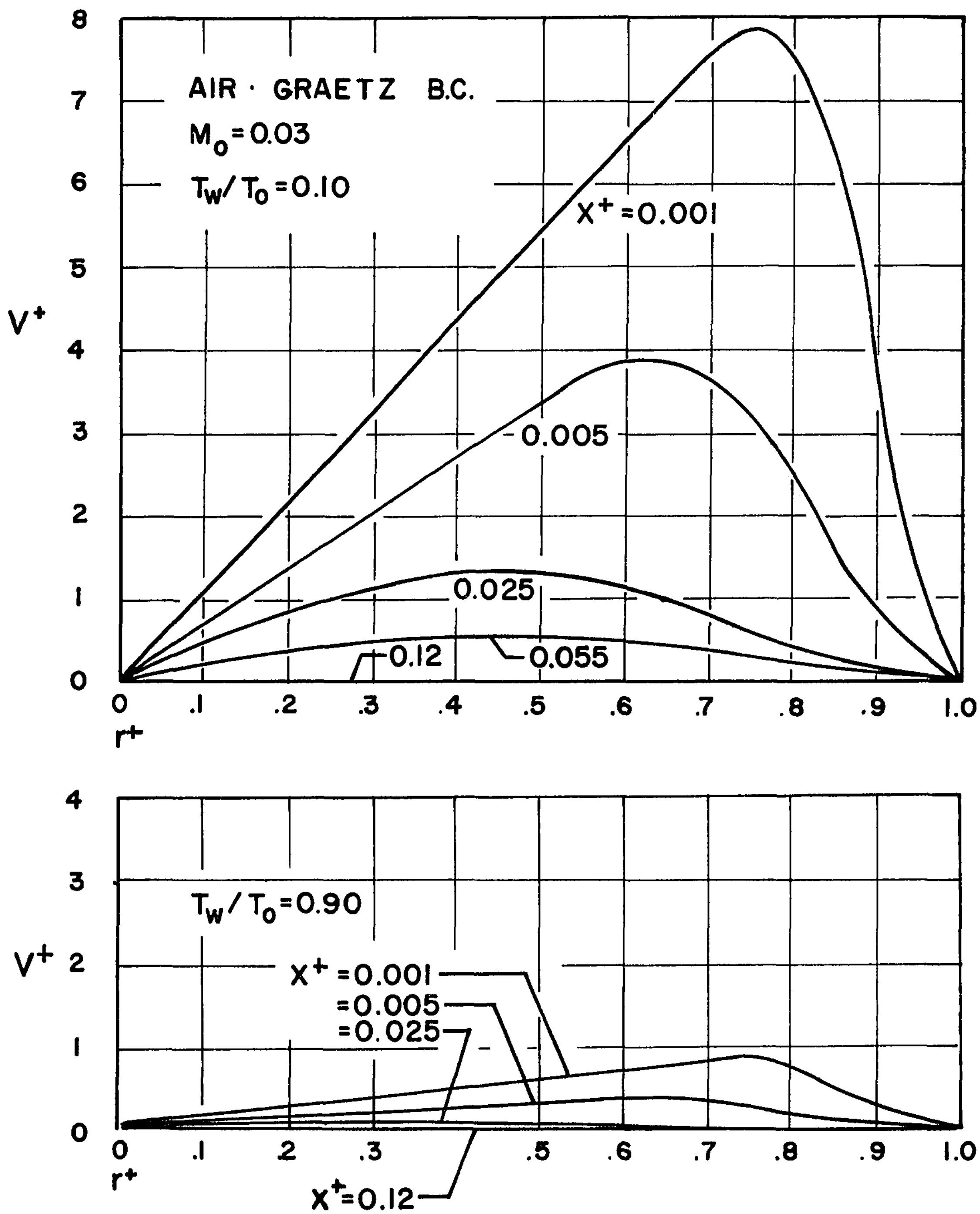

Figure 19. Dimensionless radial velocity profiles for developing flow of air at two wall to inlet temperature ratios. Graetz boundary condition.

As the wall to bulk inlet temperature ratio is reduced, the magnitude of the radial velocity increases in an outward direction along with a convected energy. The increasing density of the gas at the wall tends to augment the heat transfer, while the reduced thermal conductivity at the wall tends to decrease it. The temperature profiles are seen to remain flatter for a further axial distance with decreasing θ_w along with a corresponding increase in the magnitude of $\frac{\partial T_{red}}{\partial r^+}$ which tends to offset the decrease in thermal conductivity. On the other hand, the slope of the non-dimensionalized velocity U/U_m is relatively insensitive to changes in θ_w.
The product $fRe,_m$ may be written as,

$$fRe,_m = \frac{4\mu_w}{\mu_m}\frac{\partial(U/U_m)}{\partial r^+} \tag{3.20}$$

where since $\partial(U/U_m)/\partial r^+$ shows little change, the controlling factor will be the term μ_w/μ_m. For example, at small x^+ we have $T_w/T_m \approx T_w/T_o$. On this basis, for $\theta_w = 0.10$, $fRe,_m$ should differ by a factor approximately equal to;

$$\frac{\mu_w}{\mu_m} = \left(\frac{T_w}{T_m}\right)^b \approx \left(\frac{T_w}{T_o}\right)^b = (0.10)^{0.69} = 0.21$$

from the isothermal product $fRe_{,m}$ for helium. In the actual case, this factor is approximately equal to 0.28 at $x^+ = 0.001$ and becomes less than this and closer to the above value for axial displacements less than this. However, wall parameters obtained in the region before this occur only after a few axial steps and should be treated with a great deal of caution. For all inlet wall to bulk temperature ratios, a region of increasing static pressure occurred in the entrance-- the magnitude of the rise and the extent of the region depended on the magnitude of the temperature ratio. Where a step change in the wall temperature occurs, the axial derivative of the bulk fluid temperature and the fluid bulk density will be infinite. The deceleration of the flow in the entrance will be of sufficient magnitude to overcome the static pressure drop due to wall friction. This will be discussed further in Chapter 5. The Mach numbers that were specified for the results presented (0.05 for helium and 0.03 for air) may be considered as being on the high side for laminar flow, although the effect of halving these values was found to have a negligible influence on the results.

CHAPTER 4

UNIFORM TEMPERATURE AND VELOCITY PROFILE BOUNDARY CONDITIONS ANALYTICAL SOLUTION

4.1. Background

Typical results obtained from the finite difference solution when the boundary condition of uniform inlet velocity and temperature profile is specified are shown by the dotted line in Figure 20 for helium at an inlet wall to bulk temperature ratio of 0.95. Mesh sizes and points where changes occur are indicated. The solution has not converged to yield the correct asymptotic value of Nu_m while not enough is known to determine if the friction factor is correct. Due to the coupling of the momentum to the energy equation, it is quite likely that error exists. For the case $\theta_w = 0.95$, small absolute errors in the temperature profile due both to computational truncation in the computer and truncation of the terms in the derivative representations 2.37, 2.38 and 2.39 would result in large errors in the evaluation of $\theta_w - \theta_m$ and Nu_m. However, divergent results in the downstream region for wall to bulk temperature ratios down to 0.10 were obtained. Absolute errors in the temperature profile would have to be an order of magnitude greater to affect the results for $\theta_w = 0.10$. This would seem to rule out computational truncation as being responsible in this

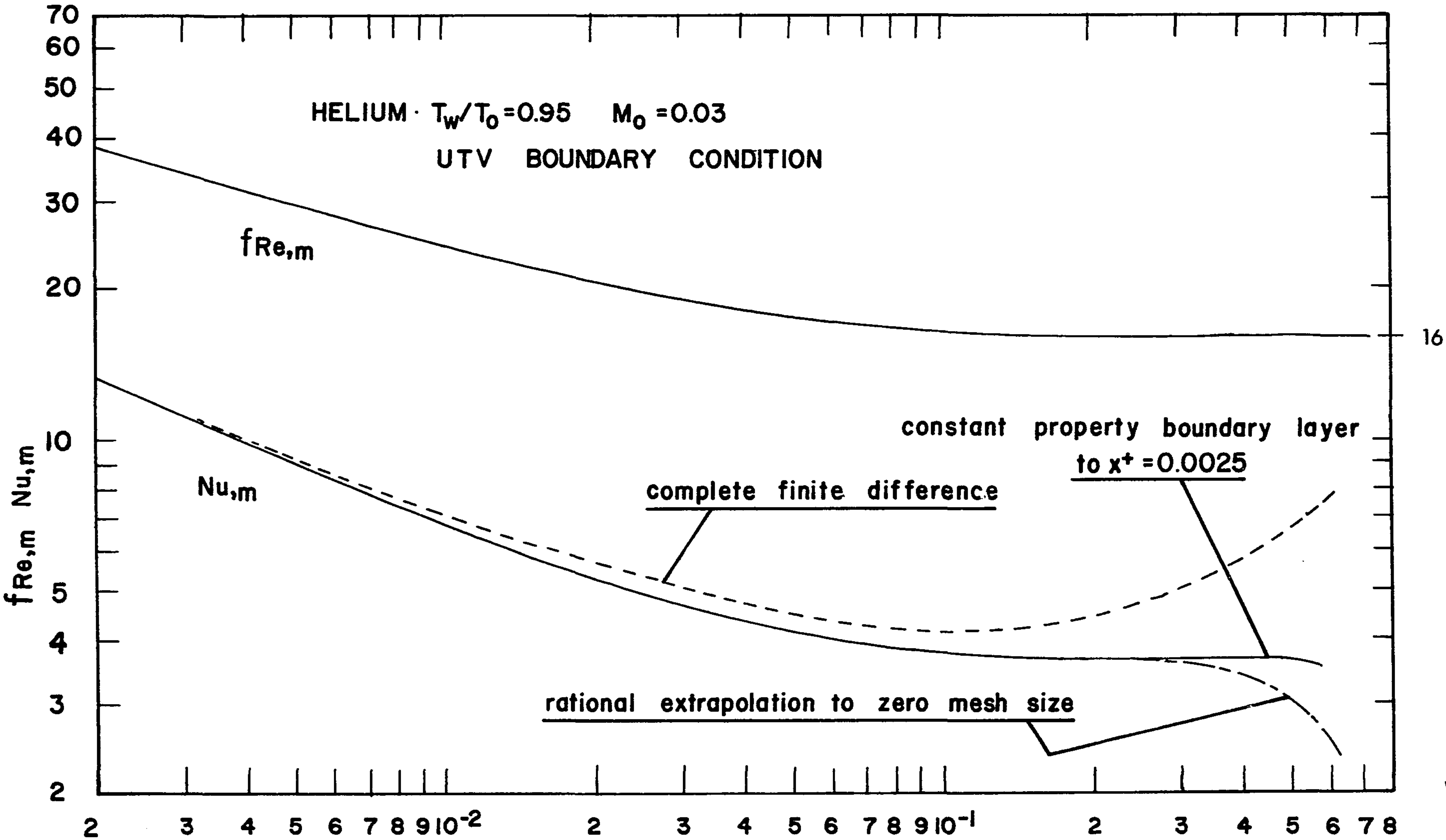

Figure 20. Axial variation of $Nu_{,m}$ and $fRe_{,m}$ for UTV boundary condition. Helium, T_w/T_o = 0.95, M_o = 0.03

case, since this error will probably remain of the same order of magnitude for both temperature ratios since for the same mesh size, the number of computations will stay roughly the same. The increased severity of the cooling will result in larger magnitudes of the higher order derivatives and increased magnitudes for the error terms in equations 2.37, 2.38 and 2.39. This could be the cause of the error. For a case Worsoe-Schmidt ran with uniform temperature and velocity and constant heat addition, $Nu_{,m}$ converged to the wrong asymptotic value. He conjectured that this was due to large errors incurred in the solution of the energy and momentum equations at the tube entrance. Several cases run here with different mesh sizes showed that in general, refinement of the mesh in the entrance region improved the downstream results, whereas refinement of the downstream mesh had little or no effect. Little change was noted from varying σ or use of double precision arithmetic. These would seem to support Worsoe-Schmidt's conjecture. While improvement was noted, results were still unacceptable even using 320 radial mesh points and Δx^+ as small as 1.0×10^{-5} near the entrance ($X^+ \leq 0.001$).

4.2. Choice of Method of Solution

Two methods of resolving this difficulty were considered; 1.) by improvement and continued use of a completely finite difference solution or 2.) by use of an analytical boundary layer solution in the tube entrance. There are many methods by which the numerical solution could be improved. For example, the program could have been rewritten so that it would check its own convergence and choose its own mesh size to achieve convergence, and/or a variable radial mesh which would allow a much finer radial step to be used near the wall where the variables are undergoing far more variation than in the center region of the tube. In order to test the suitability of the completely finite difference scheme, a technique was used which is often applied in the numerical solution of ordinary differential equations (71). As an illustration, consider an ordinary differential equation of the form;

$$\frac{dY}{dx} = F(x,y) \qquad Y(x_o)=Y_o \qquad (4.1)$$

which we are integrating from x_o to x_e using a numerical scheme-- for example, a Runge-Kutta method. If we obtain values of $Y(x_e)$ from use of three different step sizes for the variable x, we can plot the value of $Y(x_e)$ versus step size Δx (Figure 21a). If our numerical scheme is stable and consistent with the differential equation, we would expect that a better estimate of $Y(x_e)$ (i.e. closer to the exact solution of the differential equation) could be obtained by fitting a curve through these values at x_e and extrapolating to Y_e for zero step size. For a

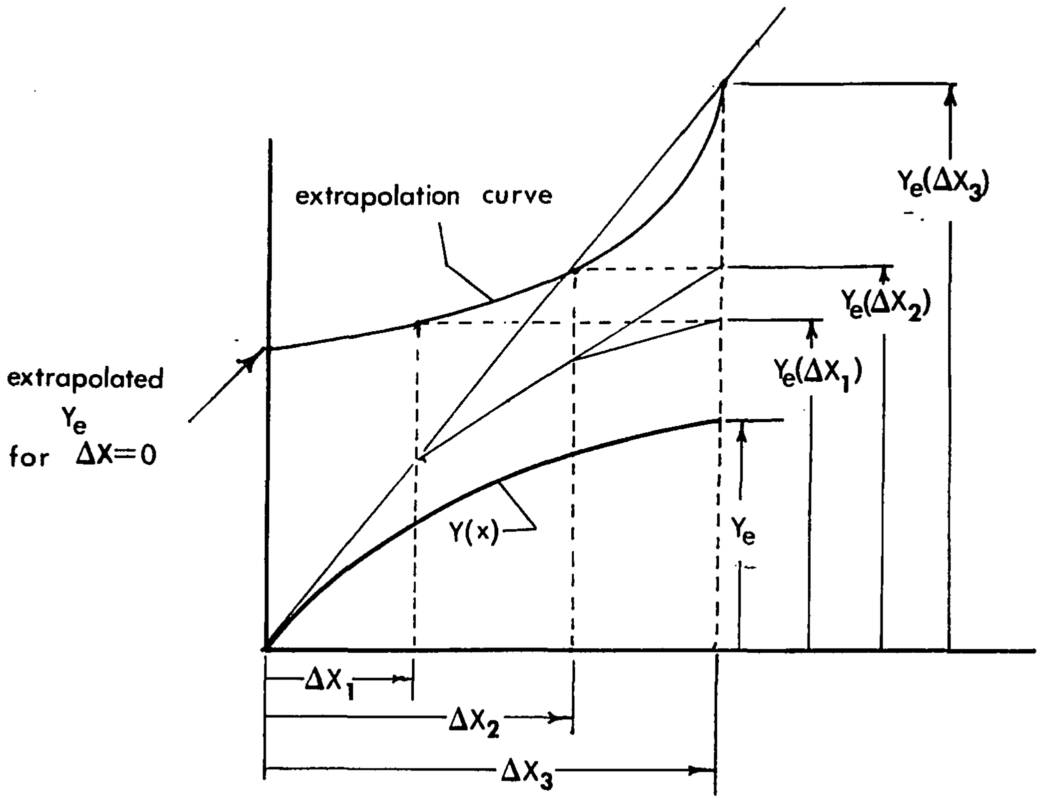

Figure 21. a. One dimensional extrapolation of finite difference solution to zero mesh size.

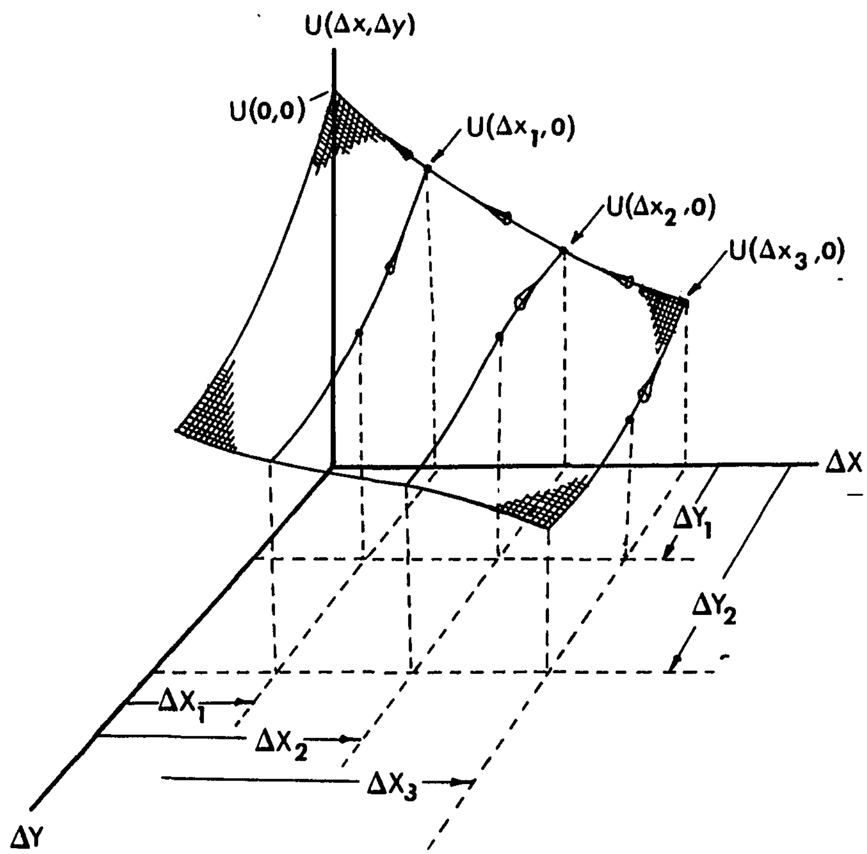

Figure 21. b. Two dimensional extrapolation of finite difference solution to zero mesh size.

function of two variables, say $U(x,y)$, the value of $U(x_e,y_e)$ for different step sizes in x and y would define a surface (Figure 21b) and an estimate of the value $U(x,r)$ corresponding to $\Delta x=0$, $\Delta r=0$ would be obtained by extrapolating the surface to a line in the $\Delta y=0$ plane, then extrapolating the line to $\Delta x=0$. For the case considered here, a relation of the form

$$\Phi_{m,n} = \Phi_{o_{m,n}}(1+A'_{m,n}\Delta x^{+2}+B'_{m,n}\Delta x^{+4}+\ldots)(1+A''_{m,n}\Delta r^{+2}+B''_{m,n}\Delta r^{+4}+\ldots) \qquad (4.2)$$

was assumed to exist. $\Phi_{m,n}$ is the value of the dependent variable (temperature or velocity) obtained at the node m,n by use of step sizes Δx^+ and Δr^+ in the numerical solution, $\Phi_{o_{m,n}}$ represents the value that would be obtained for zero step sizes and $A'_{m,n}$, $B'_{m,n}$, $A''_{m,n}$ and $B''_{m,n}$ are constants which must be determined for each node. In the actual implementation of this equation to solve for $\Phi_{o_{m,n}}$, the series in Δx^+ and Δr^+ were truncated after three terms. The constants were determined for all the radial nodes at the axial point $x^+=0.001$ by running 5 separate solutions to this point for the same boundary conditions, but with varying Δx^+ and Δr^+, (the finest mesh used was $\Delta x^+=10^{-5}$ with 320 radial nodes). This allowed solution for the values of the radial and axial velocity, the enthalpy profiles and the pressure defect that correspond to a mesh much finer than the smallest actually used. These refined profiles were reinserted into the finite difference program and the solution continued in a normal manner. Double precision arithmetic and ten iterations at each axial step for the complete set of equations 2.30, 2.31, 2.32 up to $x^+ = 0.20$ were used. The results are shown in Figure 20 for $\theta_w = 0.95$. Similar improvement was found for $\theta_w = 0.10$, but in both cases, complete convergence was not obtained. Differences between the extrapolated profiles and those from the finest mesh size used were surprisingly small and occurred in the second decimal place.

The method of using an analytical boundary solution was evaluated by applying the Blasius solution for the growth of a thermal and velocity boundary layer with zero pressure gradient and constant properties. The velocity and temperature fields are assumed to undergo a normal boundary layer growth at the tube wall. Outside of this boundary layer lies a potential flow field with uniform temperature and velocity. After determination of a similarity parameter for use in the Blasius solution consistent with the non-dimensionalized form of the boundary layer equations, the axial velocity in the core, U_e^+, and the pressure defect, $(p_o-p)/\rho_o U_o^2$ were evaluated at any axial point by solving the total momentum and continuity equations.

The axial velocity profile development as obtained from this solution is compared with that of Hornbeck (35) for the isothermal case in Figure 22. For small x^+, the comparison is very good. The profiles obtained from this method were patched to the numerical solution at several axial points. A wide range of axial points was found for which convergence in the downstream region was significantly improved. Results for this method applied at $x^+ = 0.00025$ and $\theta_w = 0.95$ are shown plotted in Figure 20 along with those from the rational extrapolation method. On the basis of these results, it was decided to proceed with an improved analytical boundary layer solution at the entrance.

The application of the constant property boundary layer growth for $\theta_w = 0.10$ seemed to result in a significant overestimate of $Nu_{,m}$ at the entrance (with respect to the completely numerical solution) for an extended distance after a patch to the finite difference solution. Properties in the boundary layer solution were evaluated at a film temperature midway between the wall and inlet bulk temperatures. It should be noted that the wall parameter results at the entrance obtained from the finite difference solution were found to be insensitive to mesh size. This lends confidence to the finite difference results as being correct there and indicates that Blasius

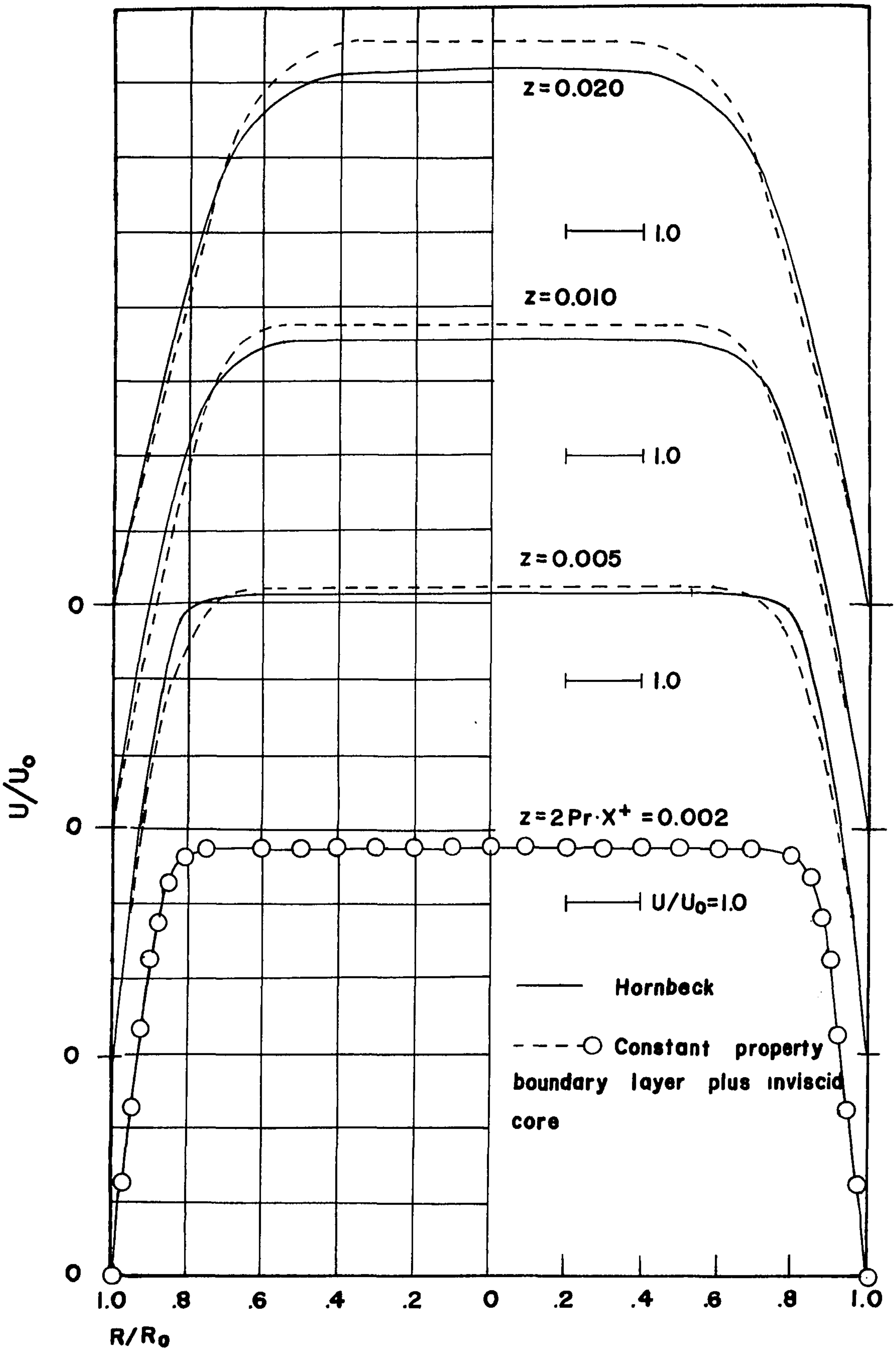

Figure 22. Comparison of axial velocity development from simplified analysis with that from Hornbeck.

profiles are not suitable for the non-isothermal case.

An analytical boundary layer solution which includes property variation and pressure gradient is described in the next section.

4.3. Similarity Solution-- Compressible Variable Property Boundary Layer Growth with Pressure Gradient for Tube Flow

A solution for the thermal and velocity boundary layer growth at the wall in the entrance of a cylindrical tube is sought along with a method of coupling this solution to the internal flow. Similarity methods have been shown to yield satisfactory results for may situations even where the requirements for similarity are not satisfied exactly (23, 85). More will be said about these requirements after the transformation of the boundary layer equations in terms of the similarity parameter.

At points where the boundary layer thickness is small with respect to the tube radius, (i.e. $\delta/r_o << 1$), the boundary layer behaves as though it were developing on a flat plate. When an order of magnitude analysis is applied to the boundary layer equations in cylindrical co-ordinates, certain terms can be shown to be negligible. When they are neglected the following non-dimensional equations obtain;

Momentum;

$$\rho^+\left(U^+\frac{\partial U^+}{\partial x^+} + V^-\frac{\partial U^+}{\partial y^+}\right) = \frac{dP}{dx^+} + 2Pr_o\frac{\partial}{\partial y^+}\left(\mu^+\frac{\partial U^+}{\partial y^+}\right) \qquad (4.3)$$

Continuity

$$\frac{\partial}{\partial x^+}(\rho^+U^+) + \frac{\partial}{\partial y^+}(\rho^+V^+) = 0 \qquad (4.4)$$

Energy;

$$\rho^+\left(U^+\frac{\partial H_2^+}{\partial x^+} + V^-\frac{\partial H_2^+}{\partial y^+}\right) = \frac{\partial}{\partial y^+}\left(\frac{k^+}{c_p^+}\frac{\partial H_2^+}{\partial y^+}\right)$$

$$-(\gamma_o-1)M_o^2\left[U^+\frac{dP}{dx^+}-2Pr_o\,\mu^+\left(\frac{\partial U^+}{\partial y^+}\right)^2\right]$$

where the non-dimensionalized variables are the same as in equations 2.30, 2.31 and 2.32 with the exception of

$$H_2^+ = (H - H_w)/c_{p,o}T_o \qquad (4.6)$$

and

$$y^+ = 1 - r^+ \qquad (4.7)$$

where y^+ represents the distance measured in a positive sense away from the wall. The transverse velocity maintains the usual boundary layer convention of being positive in a direction away from the wall. The transverse velocity is related to the radial velocity by $V^- = -V^+$.

We transform to the following non-dimensionalized independent variables after Dewey and Forbes (23):

$$\xi = \int_0^{x^+} \rho_e^+ \mu_e^+ U_e^+ dx^+ \qquad (4.8)$$

$$\eta = \frac{U_e^+}{\sqrt{2\xi}} \int_0^{y^+} \rho^+ dy^+ \qquad (4.9)$$

where subscript e refers to conditions at the edge of the boundary layer or in the central core flow. η is the similarity parameter. We assume that at any point x^+;

$$U^+/U_e^+ = U/U_e = f'(\eta)$$

$$H_2^+/H_{2,e}^+ = G(\eta)$$

where $f(\eta)$ and $G(\eta)$ are functions of η only. The differential continuity equation 4.4 can be eliminated by solving for V^- in terms of f and G. After the required transformations are made (c.f. Appendix I), the following differential equations are obtained;

Momentum:

$$2Pr_o(\lambda f''(\eta))' + f(\eta)\, f''(\eta) = \beta(f'^2(\eta) - \frac{\rho_e}{\rho}) \qquad (4.10)$$

Energy:

$$2\left(\frac{\lambda G'(\eta)}{Pr^{+}}\right)' + G'(\eta)f(\eta) = (\gamma_o-1)M_o^2 \frac{U_e^{+2}}{H_e^{+}}\left(\frac{\rho_e}{\rho}\beta f'(\eta) - 2Pr_o\lambda f''^2\right) \quad (4.11)$$

where $\lambda = \rho\mu/\rho_e\mu_e$ (4.12)

β = modified Falkner-Skan parameter $= \frac{2\xi}{U_e^{+}}\frac{dU_e^{+}}{d\xi}$ (4.13)

the boundary conditions to be satisfied are

at $\eta = 0$ $f'(\eta) = 0$ $G(\eta) = 0$

and at $\eta = \infty$, $f'(\eta) = 1$ $G(\eta) = 1$

The equations in this form represent a pair of coupled, non-linear ordinary differential equations. In addition they are of the two point boundary value type rather than an initial value problem. The terms in these equations which provide coupling to the internal flow are β in the momentum equation and U_e^{+2} and β in the energy equation.

It should be noted that an attempt was made to use the Probstein-Elliott-Levy-Lees Transformation where it is assumed that

$$U/U_e^{+} = f'(\eta,\xi)$$

and

$$H^{+}/H_e^{+} = G(\eta,\xi)$$

The prime still represents differentiation with respect to η. The differential equations which result will contain derivatives in both the η and ξ directions, but are treated as differential equations in η only. The ξ derivatives are written as axial centered difference operators in terms of the unknown dependent variables and their values on the previous step. This allows a stronger coupling to conditions outside the boundary layer, or for example, to an axial variation of the wall temperature. The problem came with representation of the profiles at the previous step for evaluation of the axial derivatives. The values of the dependent variables there are known at specified and equal η intervals, while the integration procedure at the new step solves the equations and requires evaluation of the non η-derivative terms at intermediate steps which are determined by the convergence of the equations and are not known beforehand. At the edge of the boundary layer, all terms in the differential equations become extremely small. Evidently, small error or inflections in the interpolation schemes used were sufficient to give the integration routine a great deal of difficulty in this region and the routine often would report non-convergence at large values of η. When convergence could be obtained, little difference was seen in the profile from a test solution where the ξ dependence in f and G was removed so the variation terms were removed altogether.

The assumption that the profiles are similar with respect to η is satisfied exactly if these differential equations are functions of η only. This requirement places the following restriction on some of the terms;

$$\lambda = \lambda(\eta) \tag{4.14}$$

$$\beta\left(f'^2 - \frac{\rho_e}{\rho}\right) = F_1(\eta) \tag{4.15}$$

$$(\gamma_o - 1) M_o^2 \left(\frac{U_e^{+2}}{H_e^+}\right)\left(\frac{\rho_e}{\rho}\beta f' - 2Pr_o \lambda f''\right) = F_2(\eta) \tag{4.16}$$

Since the static pressure is assumed constant across the boundary layer,

$$\lambda = \left(\frac{T_e}{T}\right)\left(\frac{T}{T_e}\right)^b \tag{4.17}$$

In the central core, we will have $T_e = T_o$ and using equation 2.29 we have

$$\frac{T}{T_e} = \frac{T}{T_o} = \theta = \left(G(1-\theta_w^{a+1}) + \theta_w^{a+1}\right)^{1/a+1} \tag{4.18}$$

and

$$\lambda = \left(\theta_w^{a+1} + (1-\theta_w^{a+1})G\right)^{a-1/a+1} \tag{4.19}$$

where $G=G(\eta)$ is the only dependent variable present so that equation 4.14 is satisfied exactly. Clearly, equations 4.15 and 4.16 cannot be satisfied exactly, but we note that in the entrance region, it can be shown by using a constant property boundary layer solution in conjunction with the total continuity equation, that β behaves approximately as $\sqrt{\xi}$ and is equal to zero at $x^+ = 0$. Since we are applying this solution only for small x^+, β will always be small. The addition of variable properties is not expected to change these results significantly. In fact for the cooling case, the increased density at the wall results in a reduced velocity boundary layer displacement thickness and correspondingly, a reduced $dU_e^+/d\xi$ and β since the flow to the core is reduced. Our requirements are then met more closely in the cooling than in the heating case. At small x^+, expression 4.15 should be approximately equal to zero. For laminar flow, the Mach numbers considered are in the range 0.01 to 0.05 so that the multiplication factor M_o^2 is very small (0.0001 to 0.0025). Also, the magnitude of U_e^{+2}/H_e^+ does not differ significantly from 1 in the region under consideration. It is important to note that for some types of equations, the inclusion of a small term can change the solution entirely, for example, if the terms govern the order of the equation. This is not the case here. It would be extremely difficult to give a definitive answer as to the error that is incurred by the assumption that at least local similarity is satisfied. However, in an analysis of the incompressible momentum equation with an external pressure gradient, Dewey and Gross (23) by using an approach based on the work of Mecksyn were able to show that the derivative of the velocity at the wall $f''(0)$ from a solution assuming local similarity can be written in terms of the exact solution of the equation $f_o''(0)$ by,

$$f''(0) = f_o''(0)\left[1 - 0.053\epsilon + O(\epsilon^2) + \ldots\right] \tag{4.20}$$

where prime again denotes differentiation with respect to η. The small parameter ϵ is defined by

$$\epsilon(\beta) = 2\xi \frac{d\beta}{d\xi} = 2\xi \frac{d}{d\xi} \frac{2\xi}{U_e^+} \frac{dU_e^+}{d\xi} \tag{4.21}$$

which measures the departure of the solutions from complete similarity. Expanding ϵ and noting that $dU_e^+/d\xi \sim \frac{1}{\sqrt{\xi}}$ in the tube entrance, we obtain

$$\epsilon(\beta) \sim 2\left(\beta - \beta^2 + \frac{\xi^2}{U_e^+} \frac{d^2U_e^+}{d\xi^2}\right) = 0 \quad \text{at } \xi = 0 \tag{4.22}$$

This means that relaxation effects due to increasing or decreasing β will be zero at the entrance and can be expected to remain small for small x^+. This adds further confidence to the use of this method for the present problem.

4.4. Integration Procedure

The program for the integration of equations 4.10 and 4.11 was written so that an available algorithm for the integration of ordinary differential equations of the initial value type could be used (15). Reduction of these equations to initial value problems and the coupling to the internal flow is described in this section. It is assumed initially that the correct U_e^+ and β are known at the axial point where the boundary layer profiles are being determined. For the solution at the first point, $x^+ = 0$ ($\xi = 0$), the exact values are known to be;

$$\beta = 0 \qquad U_e^+ = 1 \tag{4.23}$$

The integration is started by specifying the known values $f'(0) = 0$, $G(0) = 0$, guessing initial values of $f''(0)$ and $G'(0)$ and integrating the equations to a relatively large value of the independent variable η_e where the boundary layer growth is considered to be essentially complete. For the Blasius solution and for the variable property cases, the solutions were within 0.01% of fully developed for $\eta = 7.0$. At $\eta = 7$, a check was made on the quantities $f'(\eta_e)-1$ and $G(\eta_e)-1$. If these were both less than 0.0001 in absolute magnitude, then the values of $f''(0)$ and $G'(0)$ were considered as the correct values for the specified U_e^+ and β and solution could be transferred to determination of new values of β and U_e^+ (Figure 23). If not, each of the initial guesses $f''(0)$ and $G'(0)$ were perturbed-- the magnitude of the perturbation dependent on how many previous times solution had been attempted for β and U_e^+ at this axial point. For example, on the first solution, initial guesses for $f''(0)$ and $G'(0)$ are made from the Blasius solution. On the next guess, $f'(0)$ is perturbed by an absolute amount 0.01, and on the third guess, $G'(0)$ and $f'(0)$ are both perturbed by 0.01 from their initial values. We can solve for the terms in the matrix

$$\begin{vmatrix} \dfrac{\partial G(\eta_e)}{\partial f''(0)} & \dfrac{\partial G(\eta_e)}{\partial G'(0)} \\[2ex] \dfrac{\partial f'(\eta_e)}{\partial f''(0)} & \dfrac{\partial f'(\eta_e)}{\partial G'(0)} \end{vmatrix} \approx \begin{vmatrix} \dfrac{\Delta G(\eta_e)}{\Delta f''(0)} & \dfrac{\Delta G(\eta_e)}{\Delta G'(0)} \\[2ex] \dfrac{\Delta f'(\eta_e)}{\Delta f''(0)} & \dfrac{\Delta f'(\eta_e)}{\Delta G'(0)} \end{vmatrix} \qquad (4.24)$$

and, on a linear basis, can solve for the $\Delta f''(0)$ and $\Delta G'(0)$ which will make the dependent variables assume their correct free stream magnitudes. In matrix form,

$$\begin{vmatrix} \dfrac{\partial G(\eta_e)}{\partial f''(0)} & \dfrac{\partial G(\eta_e)}{\partial G'(0)} \\[2ex] \dfrac{\partial f'(\eta_e)}{\partial f''(0)} & \dfrac{\partial f'(\eta_e)}{\partial G'(0)} \end{vmatrix} \begin{vmatrix} \Delta f''(0) \\[2ex] \Delta G'(0) \end{vmatrix} = \begin{vmatrix} 1.0 - G(\eta_e) \\[2ex] 1.0 - f'(\eta_e) \end{vmatrix} \qquad (4.25)$$

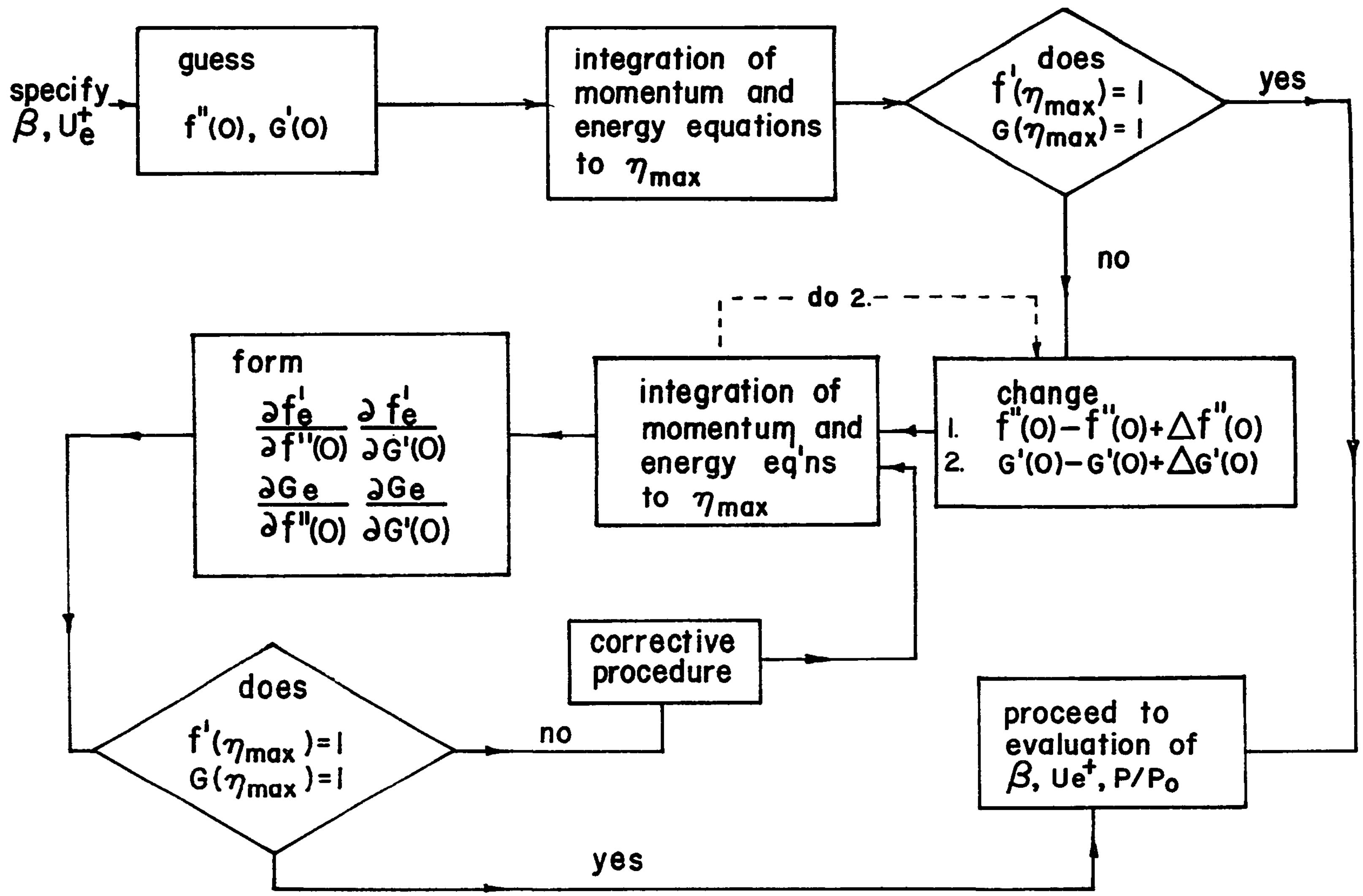

Figure 23. Flow diagram for solution of similarity boundary layer equations.

The pair of initial values G'(0) and f"(0) from the last trio of initial values which provided the best free stream values for G and are designated the base solutions onto which f"(0) and G'(0) will be added in order to form the next coefficient matrix. A flow chart of this procedure is shown in Figure 24.

After the correct boundary values have been chosen and the profiles obtained for a given β and U_e^+, control is returned to the part of the program which will calculate a new β and U_e^+ corresponding to these profiles (Figure 24). The new value of U_e^+ and static pressure must be determined by applying total conservation of momentum;

$$2\left[\int_0^1 \rho^+ U^{+2} r^+ dr^+ - \left(\int_0^1 \rho^+ U^{+2} r^+ dr^+\right)_{x^+=0}\right] - P + 4Pr_o \int_0^{x^+} \tau_w^+ dx^+ = 0 \tag{4.26}$$

and conservation of mass (2.34). We denote y_e^+ as that value of displacement corresponding to , or;

$$y_e^+ = \frac{\sqrt{2\xi}}{U_e^+}\int_0^{\eta_e}\frac{d\eta}{\rho^+} = \frac{\sqrt{2\xi}}{U_e^+}\frac{p_o}{p}\int_0^{\eta_e}\theta d\eta$$
$$= \frac{p_o}{p}\frac{\sqrt{2\xi}}{U_e^+}\int_0^{\eta_e}\left[(1-\theta_w^{a+1})G+\theta_w^{a+1}\right]^{1/a+1} d\eta \tag{4.27}$$

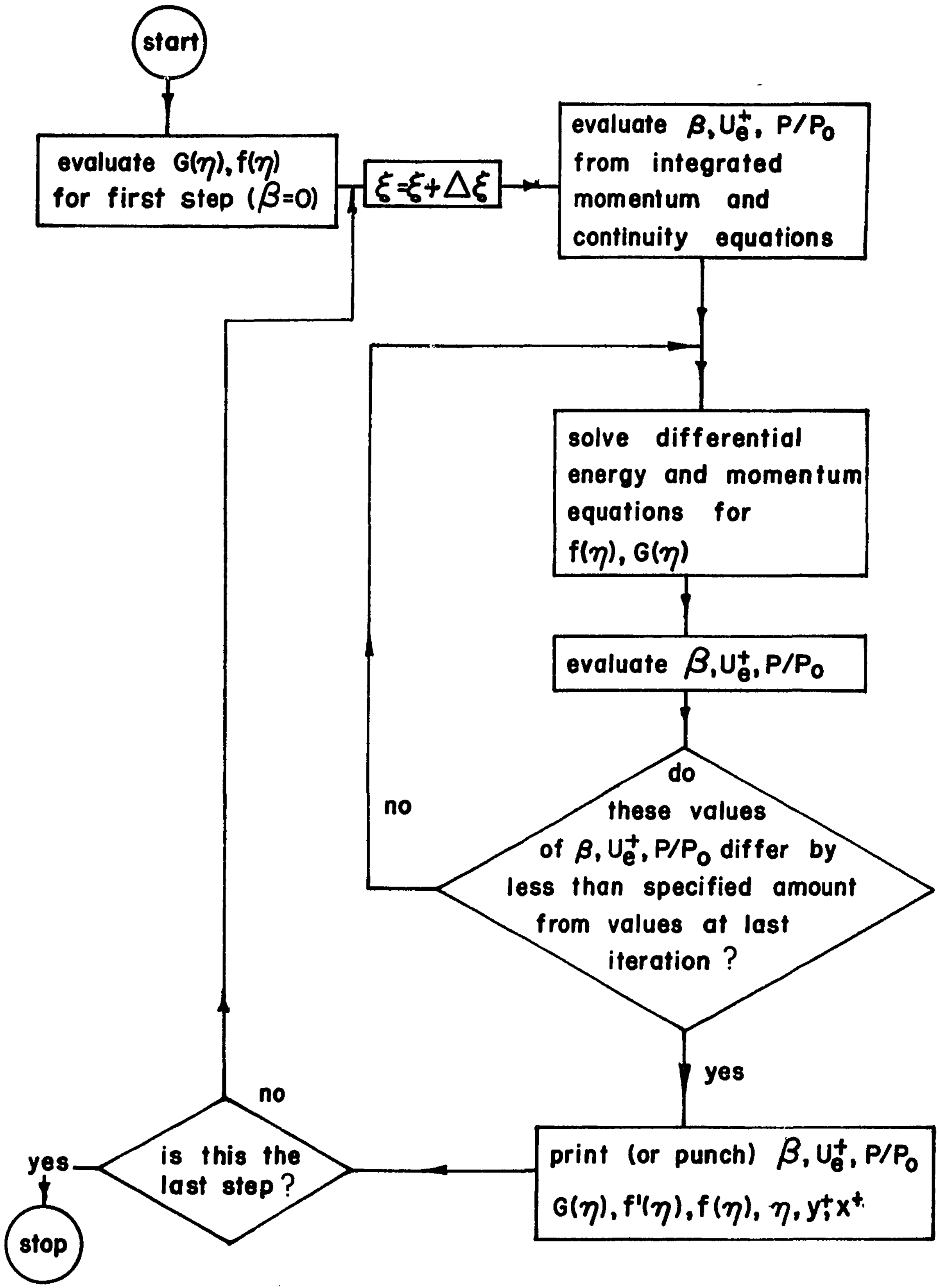

Figure 24. Flow diagram for coupling of boundary layer development to internal tube flow.

In the radial integrations, the following values of the dependent variables were used;

$$r^+=0 \quad \text{to} \quad r^+=1-y_e^+ \qquad U^+ = U_e^+$$

$$r^+=1-y_e^+ \quad \text{to} \quad r^+=1 \qquad U^+=U_e^+ f' \qquad \theta = \left[(1-\theta_w)^{a+1} G+\theta_w^{a+1}\right]^{1/a+1}$$

The wall shear stress is given by

$$\tau_w^+ = \frac{\mu_w^+ \rho_w^+ U_e^{+2} f''(0)}{\sqrt{2\xi}} \tag{4.28}$$

The following equations are obtained from 2.34 and 4.26;

Total continuity;

$$\left(\frac{p}{p_o} U_e^+\right)^2 + \left(\frac{p}{p_o} U_e^+\right)\left(2\sqrt{2\xi}\left[f(\eta_e) - \int_0^{\eta_e} \theta d\eta\right] - 1\right) + 2\xi\left[\left(\int_0^{\eta_e} \theta d\eta\right)^2 - 2\int_0^{\eta_e} f' \int_0^{\eta} \theta(\Omega) d\Omega \, d\eta\right] = 0 \tag{4.29}$$

Total momentum;

$$\left(\frac{p}{p_o}\right)^2 - \left(\frac{p}{p_o}\right)(1+\gamma_o M_o^2) + \left(\frac{p}{p_o} U_e^+\right)\gamma_o M_o^2\left[2\sqrt{2\xi}\left(\int_0^{\eta_e}\left[f'^2 - \theta\right] d\eta\right) + \frac{p}{p_o} U_e^+\right]$$
$$+ \gamma_o M_o^2\left[2\xi\left\{\left(\int_0^{\eta_e} \theta d\eta\right)^2 - 2\int_0^{\eta_e} f'^2 \int_0^{\eta} \theta(\Omega) d\Omega \, d\eta\right\}\right.$$
$$\left. + 4 \mathrm{Pr}_o \frac{\mu_w \rho_w}{\mu_e \rho_e} \frac{p}{p_o} \int_0^{\xi} \frac{U_e^+}{\sqrt{2\xi}} f''(0) d\xi\right] = 0 \tag{4.30}$$

Once the correct wall parameters were determined at a given axial step, an additional integration of the equations 4.10 and 4.11 was performed with evaluation of the dependent variables at equal η intervals. This was so that all radial integrations could be carried out by Simpson's rule. The analytical solution was applied in a stepwise manner at equally spaced intervals $\Delta\xi$. Once a solution was complete at an axial point, the independent axial variable was incremented by $\Delta\xi$ and the values of the profile dependent terms in equations 4.29 and 4.30 were approximated on this first solution at $\xi+\Delta\xi$ by their values from the previous axial point. This allowed for an initial estimate of β and U_e^+ and control would be returned to the integration procedure. On proceeding iterations, new values for these terms would be used. The last integral in the equation was linearized by applying a modified midpoint rule.

$$\int_0^{\xi} \frac{U_e^+}{\sqrt{2\xi}} f''(0)\, d\xi = \int_0^{\xi-\Delta\xi} \frac{U_e^+}{\sqrt{2\xi}} f''(0)\, d\xi$$

$$+ \left(\frac{f''(0)\big|_{\xi-\Delta\xi} + f''(0)\big|_{\xi}}{2} \right) \left(\frac{U_e^+\big|_{\xi-\Delta\xi} + U_e^+\big|_{\xi}}{2} \right) \left(\sqrt{2\xi} - \sqrt{2(\xi-\Delta\xi)} \right) \tag{4.31}$$

We note that the continuity equation is a quadratic in the product of unknowns $\frac{p}{p_o} U_e^+$ for which solution may be made directly. The momentum equation is a quadratic both in p/p_o and $p/p_o U_e^+$ and solution for the former unknown may be made directly after determination of $p/p_o U_e^+$. The unknown U_e^+ can then be determined.

The parameter β (4.13) was evaluated at each axial point by use of local ξ and U_e^+ and using

$$\frac{dU_e^+}{d\xi} = \frac{U_e^+\Big|_{\xi} - U_e^+\Big|_{\xi-\Delta\xi}}{\Delta\xi} \tag{4.32}$$

for the derivative term. Solution could have been made for this quantity directly at ξ by taking the ξ–derivatives of equations 4.29 and 4.30 and solving the non-linear simultaneous equations in $dU_e^+/d\xi$ and $d(p/p_o)/d\xi$ which result, but it is questionable whether this approach would be worth the effort. In the entrance region, the higher order derivatives will be rapidly decreasing in magnitude with axial distance. Consider the evaluation of the first axial derivative by use of this difference quotient (2.37). The coefficients of the higher order derivatives in the error term are monotonically increasing with σ for $\sigma > 1/2$. At the same time, the decrease in the magnitude of the derivatives with increasing σ (increasing x^+) will partially offset this so that the minimum error will occur at a point in-between $(m+\sigma)\Delta x^+$ and $(m+1)\Delta x^+$. After several axial steps, the relative difference in $(m+\sigma)\Delta x^+$ and $(m+1)\Delta x^+$ will be negligible. Also, 4.32 is consistent with the way axial derivatives were evaluated in the finite difference solution.

Convergence on the two iteration levels was considered complete at an axial point when successive values of the parameter β differed by less than 0.1% and successive values of U_e^+ and p/p_0 differed by less than 0.00005 in absolute magnitude. The program was coded in Fortran IV and run on the RCA Spectra 70 computer at the college. Integration of equations 4.10 and 4.11 took about 8 seconds and, on the average, 4 such solutions were needed for convergence of $G'(0)$ and $f''(0)$. Approximately 3 or 4 of these converged solutions were needed to complete iteration for β, U_e^+ and p/p_0 so that a total of about 1.5 minutes was needed for each axial step. The axial increment used for all patching solutions was $\Delta\xi = 5\text{x}10^{-5}$. No change in the free stream value of U_e^+ was found for the axial step. Also, changing the value of η_e from 7 to 14 resulted in a change in absolute value of U_e^+ of less than 10^{-5} at the same axial displacement.

Comparison of the boundary layer profiles generated from this solution was made, when possible, with published boundary layer data. For the constant property case with zero pressure gradient, agreement was found to be perfect within the 5 decimal place accuracy for the enthalpy and velocity profiles of the Blasius solution presented in Schlichting(75). Also, no difference was found between present results for Pr = 1, $T_W/T_O = 0.20$ and the results of Reshotko and Cohen (72) for $\beta = 0$.

The joining of this analytical solution to the finite difference solution was made in a two step patch at $\xi = 0.00025$ and $\xi = 0.00030$. These particular points were chosen because previously the best downstream behavior was obtained when the Blasius solution was patched to the finite difference solution in this region. At $\xi = 0.00025$, complete radial and axial velocity and enthalpy profiles along with p/p_O generated by the similarity solution were inserted as initial values into the Worsoe-Schmidt program.

It can be shown that the function f is related to the Cartesian stream function ψ by

$$\psi = 2\xi f \tag{4.33}$$

and the radial velocity in terms of the stream function is,

$$V^- = -\frac{1}{\rho^+}\frac{\partial \psi}{\partial x^+} = \frac{\rho_e}{\rho}\mu_e^+ U_e^+ \sqrt{2\xi}\left[\frac{f}{2\xi} - \frac{\eta}{U_e^+}\frac{dU_e^+}{d\xi} - \eta\frac{U_e^+}{2\xi}\right] \tag{4.34}$$

This was the expression used to evaluate the transverse velocity in the boundary layer. Outside of the boundary layer, the radial velocity is obtained from integration of the continuity equation from the centerline out to a radius r^+;

$$V^+ = -\frac{1}{\rho^+ r^+}\int_0^{r^+} r^+ \frac{\partial}{\partial x^+}(\rho^+ U^+)\,dr^+ \qquad (4.35)$$

Since in the core flow, $\rho_e^+ U_e^+ = F(x^+)$ only, $\frac{\partial}{\partial x^+}(\rho_e^+ U_e^+)$ is a function of x^+ only in the region from $r^+=0$ to $1-y_e^+$ where y_e^+ denotes the edge of the velocity boundary layer;

$$V^+ = \frac{-r^+}{2\rho_e}\frac{\partial}{\partial x^+}(\rho_e U_e^+) = -\frac{r^+}{2}\frac{p_o}{p}\frac{\partial}{\partial x^+}\left(\frac{p}{p_o}U_e^+\right) \qquad (4.36)$$

The radial velocity is seen to be a linear function of the radius. The axial derivative was evaluated by the difference quotient 4.32. Once the profiles were patched, the finite difference program was allowed to generate all profiles for the next axial step. However, at this step the axial velocities and enthalpies were re-entered from the analytical entrance solution to begin the solution at the following step. Radial velocities from the finite difference solution were retained. This was done in order to help smooth the patch. The solution for all proceeding steps continued in a normal manner. The effect of the patch on the velocity boundary layer development can be seen in Figure 22 where the velocity boundary layer as developed by the finite difference solution after a typical patch is shown compared with the solution from further independent development of the similarity solution. The difference is quite small and it would seem to indicate that the two solutions are at least compatable. A listing of the computer program used for the entrance region solution is given in Appendix F.

4.5. Results

The largest descrepancy between the present entrance solution and the finite difference solution can be seen in the variation of the static pressure with axial distance. In Figure 26, the non-dimensionalized pressure defect is shown for He at $\theta_w = 0.1$ from the similar boundary layer growth and for two finite difference solutions-- one being the results from the rational extrapolation procedure noted earlier. The most obvious difference is in the difference in signs of the static pressure drop. The present analytical solution predicts a pressure rise in the entrance due to deceleration from the severe cooling. However, note that if the finite difference solutions are visually extrapolated to $x^+ = 0$, a non zero pressure defect is the result. This is not physically possible.

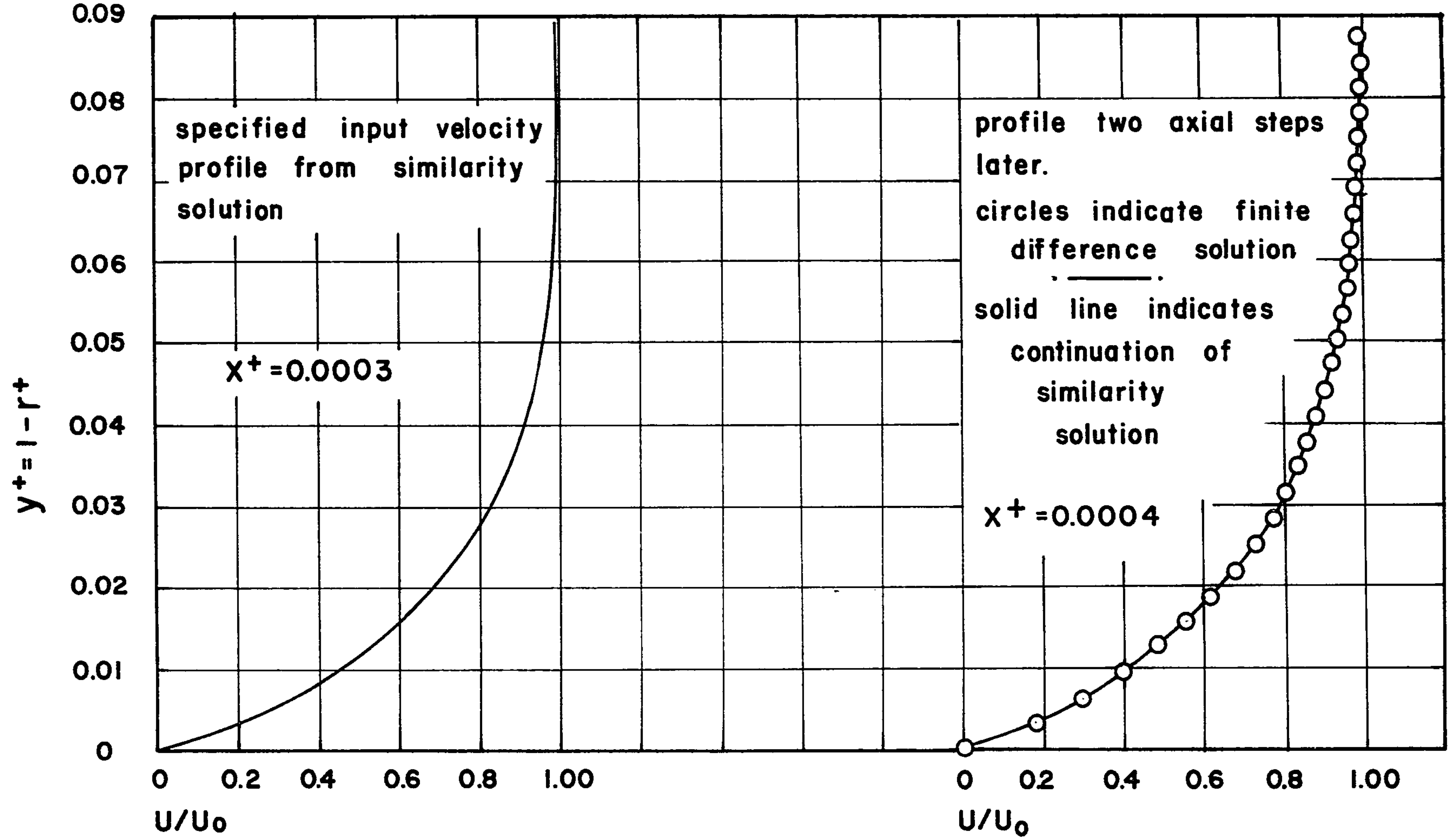

Figure 25. Comparison of velocity boundary layers before and after patch to finite difference solution.

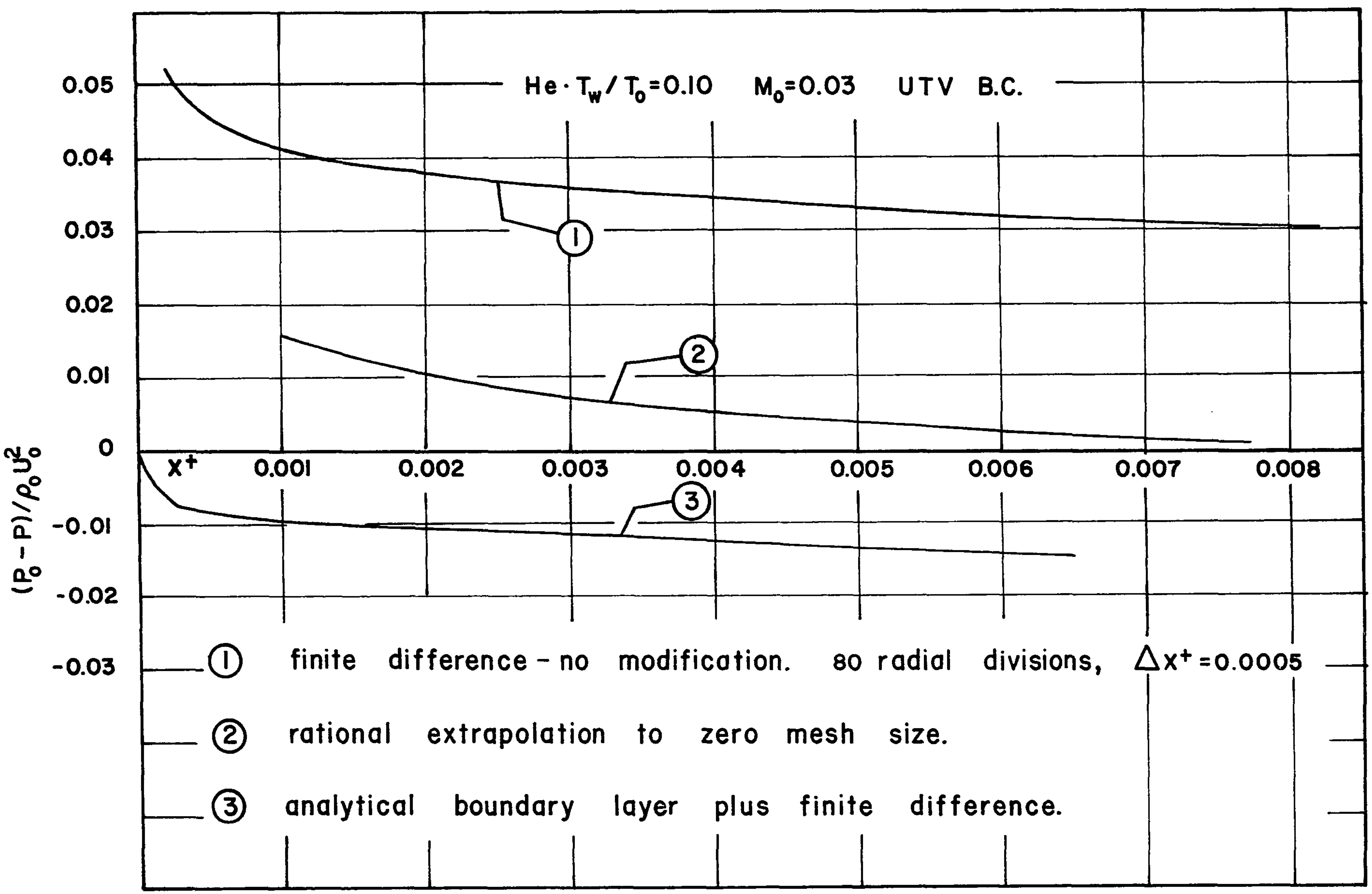

Figure 26. Axial variation of dimensionless pressure defect for patched and complete finite difference solution. Air, UTV boundary condition, M_o = 0.03

It should be noted that refinement of the mesh was found to reduce this pressure defect and displace it closer to the results from the similarity solution. The finite difference program normally begins the iterations at the second step by using a pressure defect calculated on the basis of a constant property boundary layer growth. This implies a static pressure drop for all cases. Changing the magnitude and sign of this initial guess was found to make no difference in the final pressure defect obtained after several iterations at the first step. It should be noted that the shape of the curves from both solutions are the same. Very little difference was found in the wall parameters $Nu_{,m}$ and $fRe_{,m}$ near the entrance for all solutions. The closest agreement was obtained from the rational extrapolation procedure. This would also lend confidence to the present results. Perhaps it is not without merit to reiterate that all we are actually doing is providing a better solution to the set of equations 2.30 - 2.32. The question is still open as to the applicability of these equations in the entrance region.

Downstream convergence was improved considerably by this method, although absolute convergence (i.e. stability of the wall parameters to infinite x^+) was not obtained. In all cases, the asymptotic Nusselt number was attained first and stayed at this value until the friction factor differed by only a few percent from its fully developed value. Downstream results from this method are compared with those from the finite difference method in Figure 27 for He at $T_W/T_O = 0.50$. Roughly the same mesh sizes were used in the patching solution and in the completely finite difference solution. The same magnitude of deviation indicated by the horizontal line is developed in the solution with the analytical boundary layer growth at an axial point which is more than twice as far downstream than the completely numerical method. Comparison of the axial variation of $\theta_w - \theta_m$ and q_w^+ for the two showed that the error in $\overline{Nu}_{,m}$ is about equally divided between these two quantities and is not due solely to the error in either quantity. For example, if a large error in the local heat flux is responsible, then the problem could be indentified as a local one. Since we can reasonably expect that $Nu_{,m}$ will remain constant once it has reached the fully developed value, continuation of the solution might be made by specifying as a boundary condition that $Nu_{,m} = 3.67$ and evaluating a heat flux on this basis. An error in the wall to bulk temperature ratio represents an accumulation of small errors whose presence and origin are hard to detect and correct.

Wall parameters for the flow of helium and air are shown plotted versus x^+ in Figures 28 and 29 respectively.

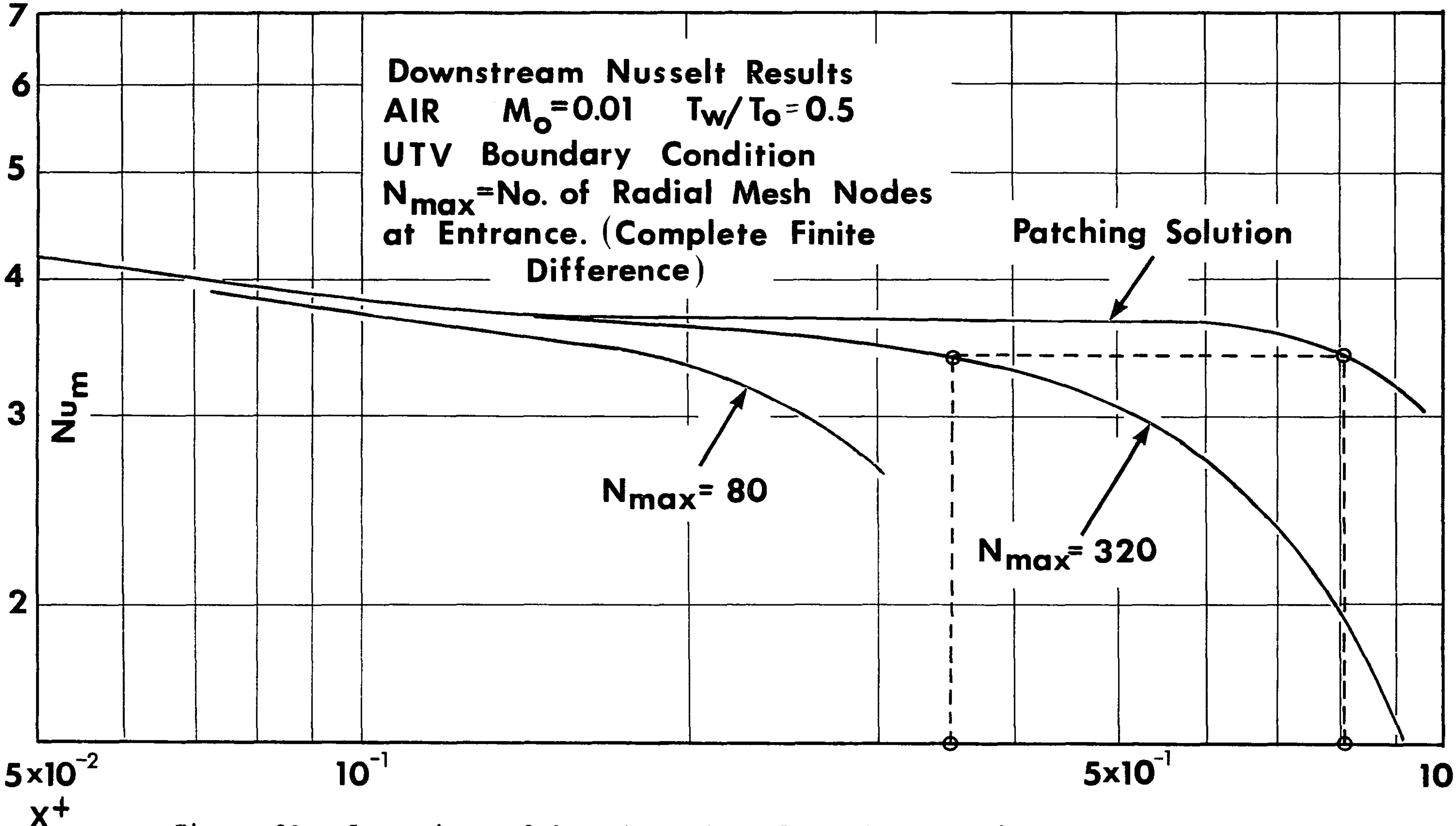

Figure 27. Comparison of downstream Nusselt number bahavior from patched and complete finite difference solutions. Air, UTV boundary condition, T_w/T_o = 0.5

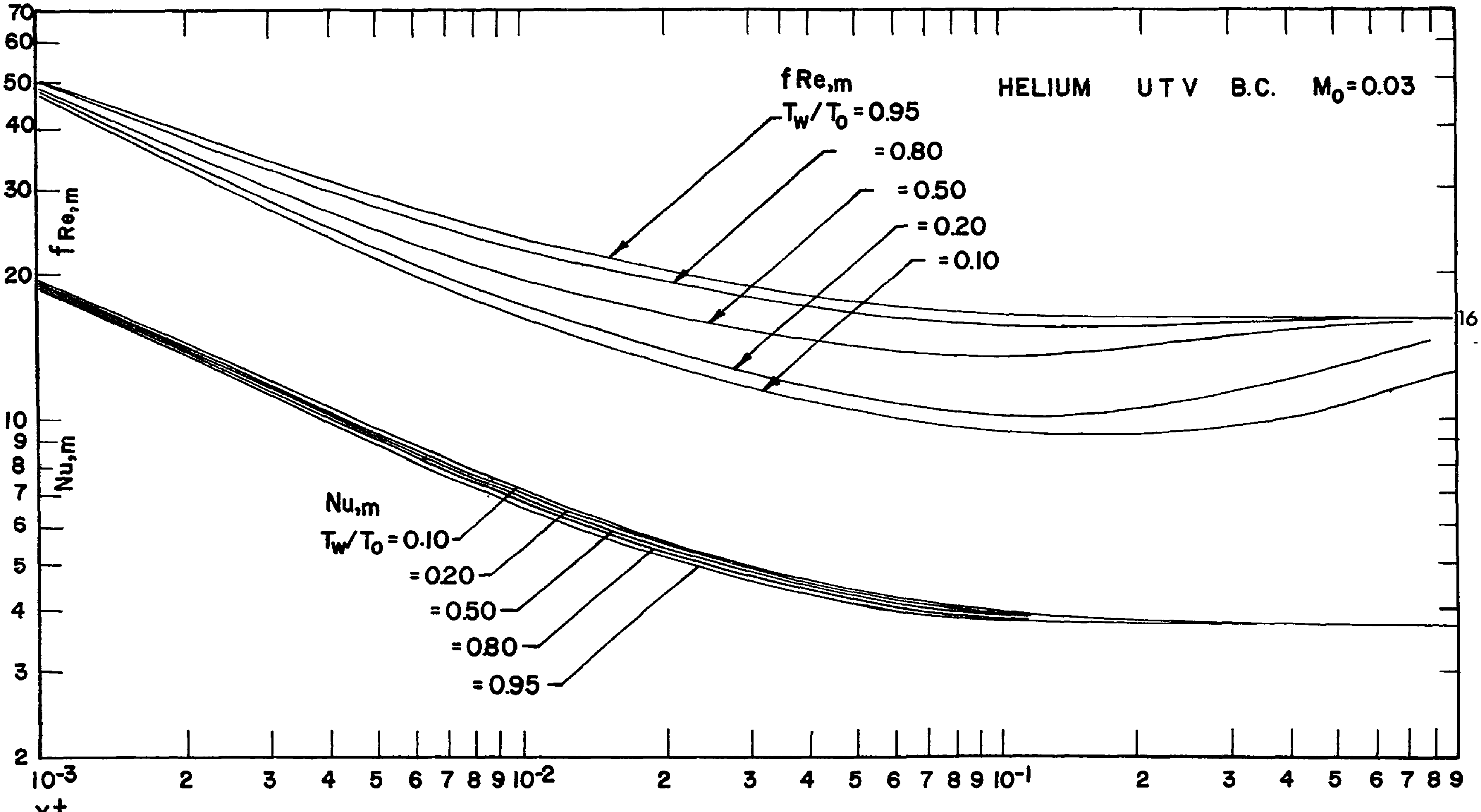

Figure 28. Axial variation of $fRe_{,m}$ and $Nu_{,m}$ for Helium at several wall to inlet temperature ratios. UTV boundary condition, M_o = 0.03

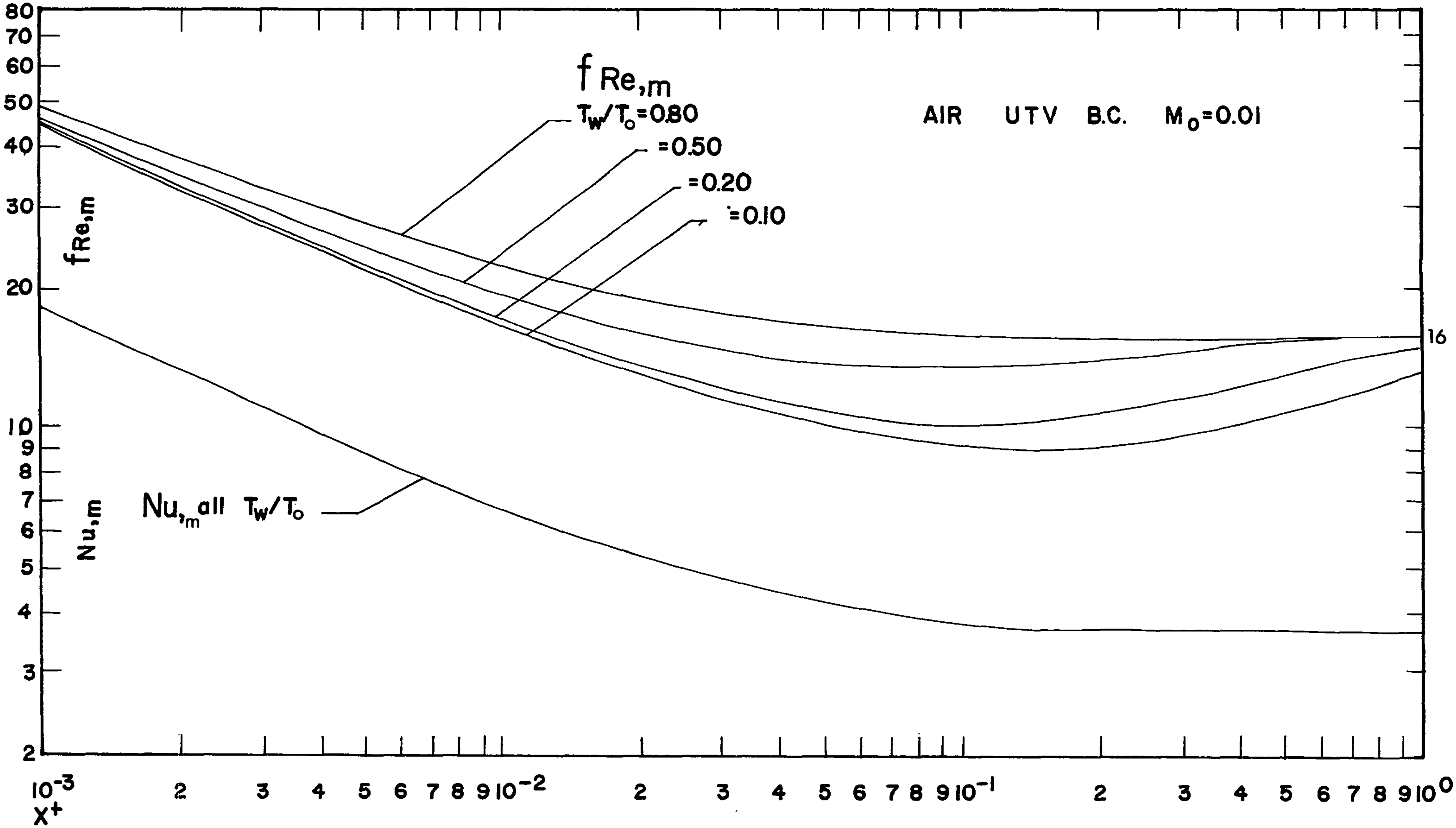

Figure 29. Axial variation of $fRe_{,m}$ and $Nu_{,m}$ for air at several wall to inlet temperature ratios. UTV boundary condition, M_o = 0.01

The Nusselt number is almost completely insensitive to the temperature ratio. This is not completely surprising since the flow in the entrance of the tube is of a boundary layer character and results from variable property external boundary layer solutions for gases (72,23) have shown little change with severe cooling. Here, for helium $Nu_{,m}$ actually exhibits a slight increase with increased cooling. The variation of the product $fRe_{,m}$ with θ_w is large in comparison with that of $Nu_{,m}$, but still rather small in an absolute sense. For example, a tenfold decrease in the inlet wall to bulk temperature ratio results in less than a 50% decrease in $fRe_{,m}$. The friction factor variation is nearly identical for the two gases. The extremely slow convergence of this parameter for the case of $\theta_w = 0.1$ should be noted. For example, for both gases, $fRe_{,m}$ still differs from its fully developed value by 25% at $x^+ = 0.85$. To translate this to physical terms, consider the flow of He at $Re_o = 1000$. Then $x^+ = 0.85$ corresponds to an axial displacement of more than 300 diameters. For the Graetz condition and this same temperature ratio, this magnitude of deviation from the isothermal $fRe_{,m}$ corresponds to approximately half this displacement. Data for the isothermal case for $Nu_{,m}$ and $Pr_o = 0.70$ is also plotted from references 43, 57 and 93 in Figure 30. Present results fall midway between the results of Manohar and Ulrichson and Schmitz.

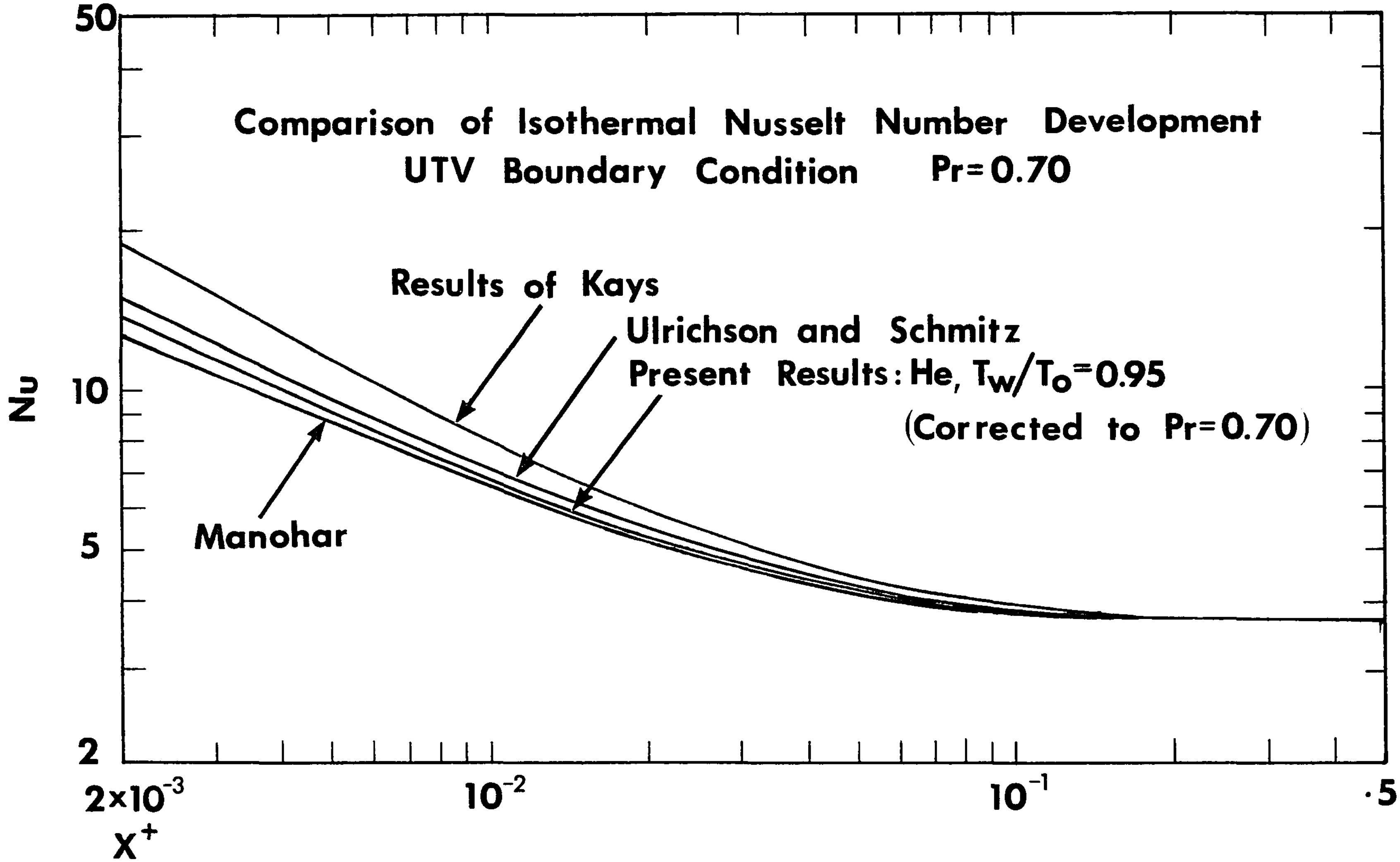

Figure 30. Comparison of Isothermal Nusselt number development from other investigations.

In Figure 31, the centerline axial velocity development from this solution is compared with that from Hornbeck (35). Since, for reasons given previously, it was not possible to run the fully isothermal case here, the case of $\theta_w = 0.95$ was used for comparison. Agreement here is excellent.

Representative axial velocity and temperature profiles are shown in Figure 32 for $\theta_w = 0.10$ and 0.50 and radial velcity profiles in Figure 33 for $\theta_w = 0.10$ and 0.95 and the flow of helium. With the exception of helium, where for the case shown of $\theta_w = 0.10$ an outward radial velocity existed for a short distance from the entrance, the displacement of gas in the velocity boundary layer is responsible for an inward radial velocity. For gas cooling, an outward radial velocity would bring gas at a higher temperature from the core towards the wall. The result is a flatter temperature profile and an increased magnitude of temperature gradient and heat transfer at the wall. In an incompressible UTV case, the inward radial velocity profile reverses this effect, and in a sense, effectively 'insulates' the wall. When compressibility and cooling are introduced, the magnitude of this inward velocity is reduced. Qualitatively, the heat transfer is augmented for the reasons previously stated and the net effect is to partially offset the decrease in the thermal conductivity ratio at the wall,

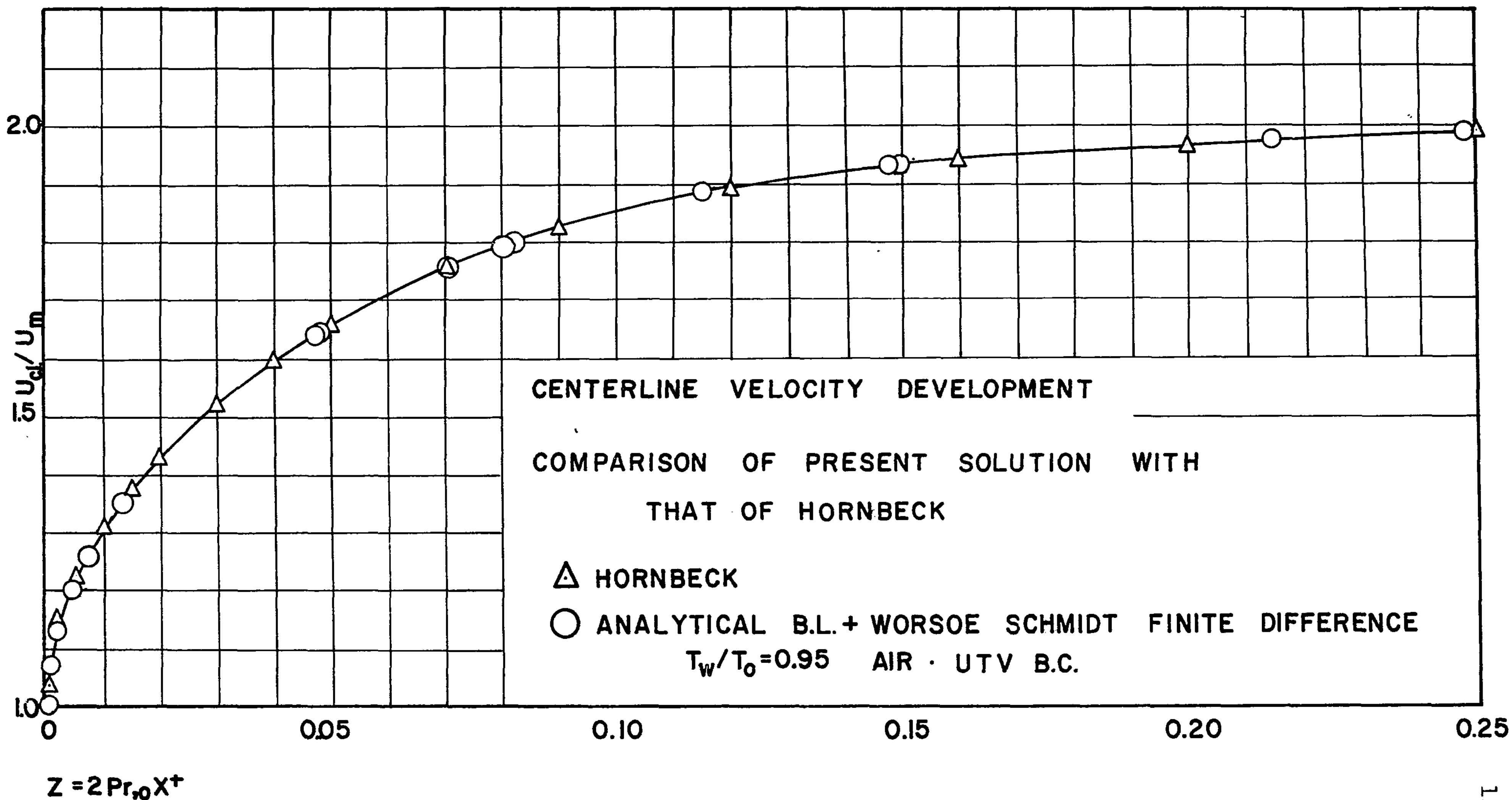

Figure 31. Development of centerline axial velocity from patching solution compared with results of Hornbeck. UTV boundary condition

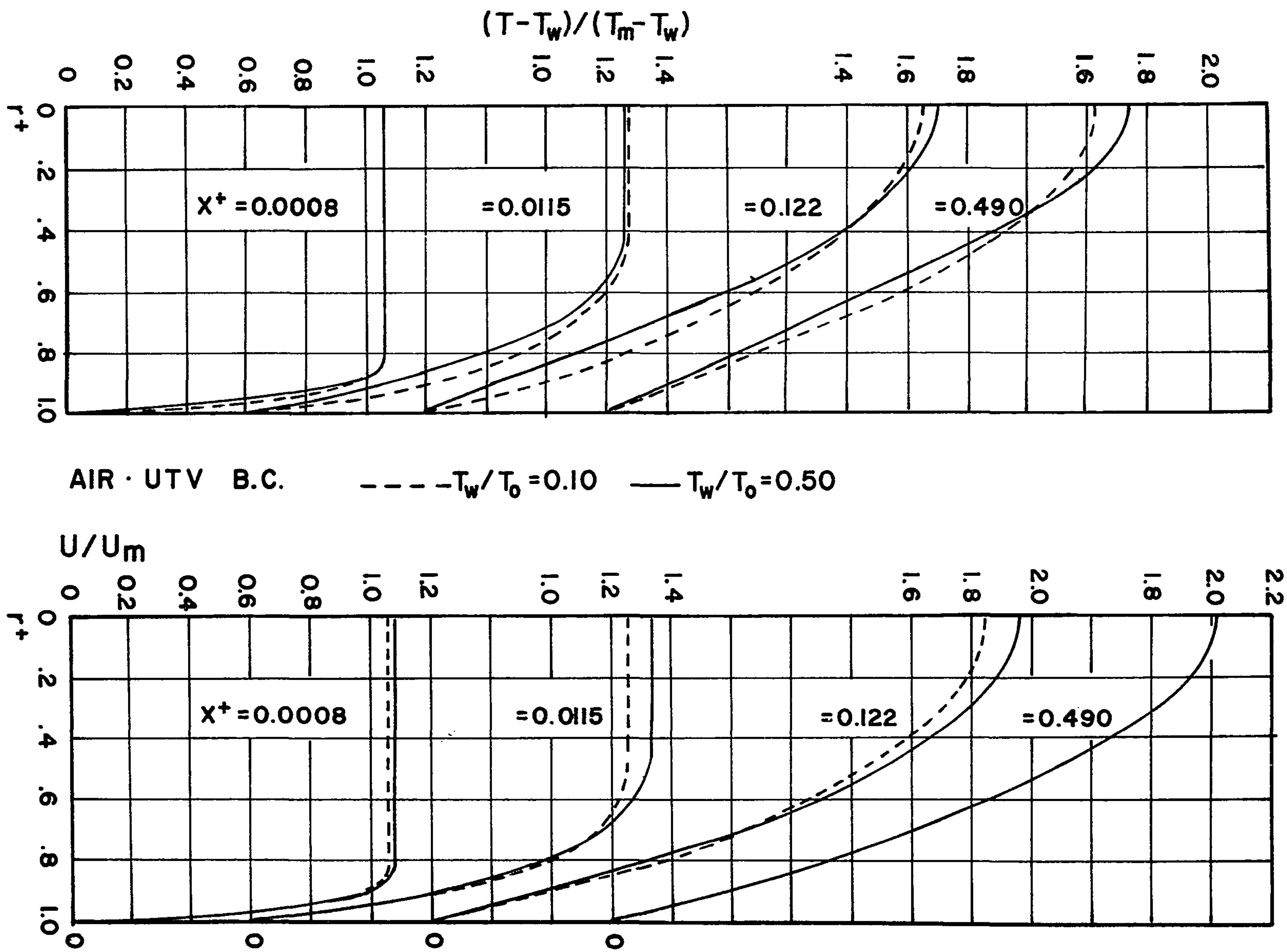

Figure 32. Axial development of reduced temperature and axial velocity profiles for air at two inlet temperature ratios. UTV boundary condition

Figure 33.

Dimensionless radial velocity profiles for developing flow of helium at two inlet temperature ratios. UTV boundary condition, $M_o = 0.03$

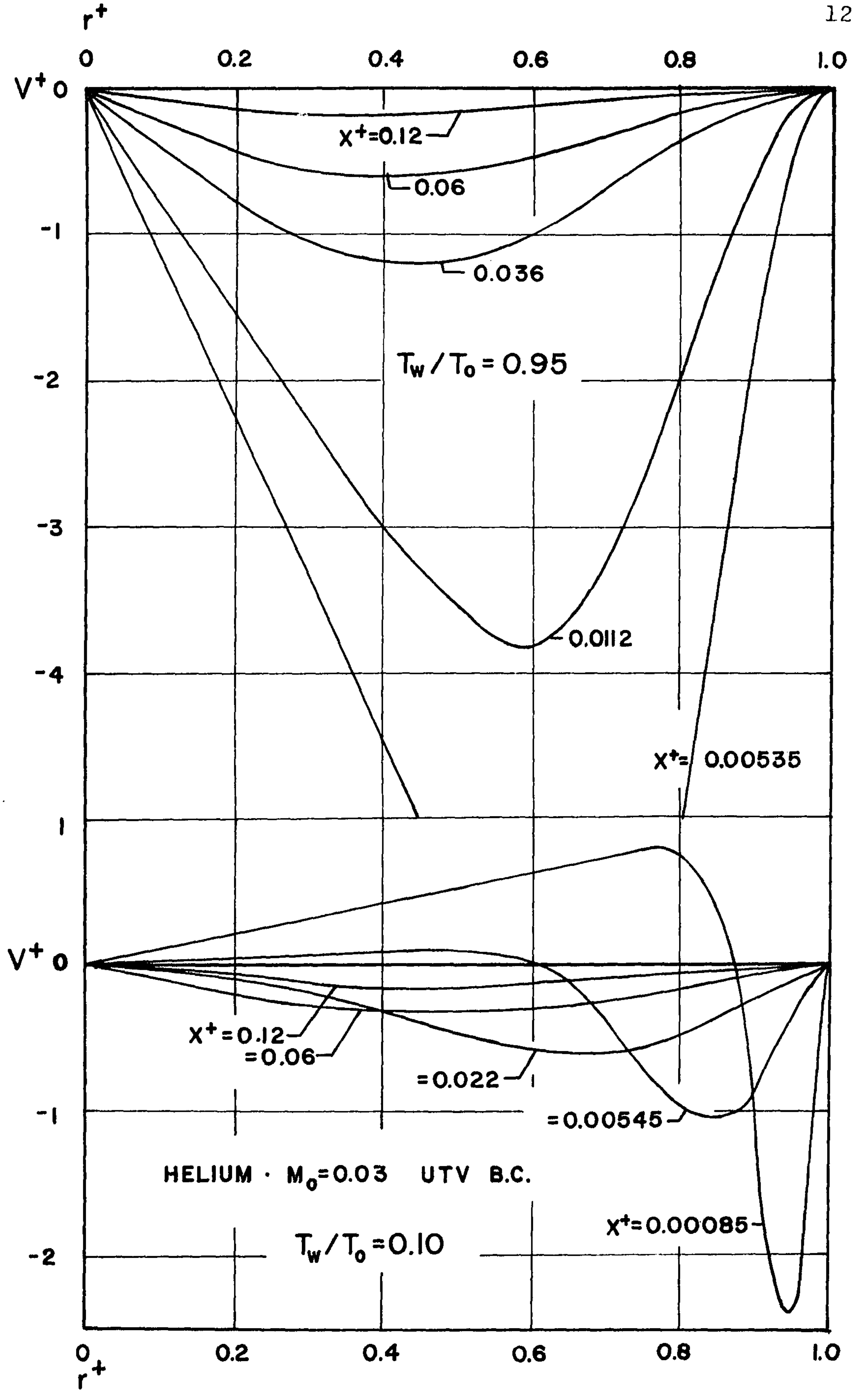
r+
0
0.2
0.4
0.6
0.8
1.0
V+ 0
-1
-2
-3
-4
1
V+ 0
-1
-2
X+=0.12
0.06
0.036
Tw / To = 0.95
0.0112
X+= 0.00535
X+=0.12
=0.06
=0.022
=0.00545
HELIUM · Mo=0.03 UTV B.C.
Tw / To =0.10
X+=0.00085
0
0.2
0.4
0.6
0.8
1.0
r+

k_w/k_m (3.21). This is probably the primary reason for the insensitivity of $Nu_{,m}$ to temperature ratio.

Near the center of the tube, the axial velocity profiles show the most variation with wall to bulk temperature ratio (Figure 31). As is the case with the temperature profile, cooling flattens the profile. It is difficult to argue through the reasons why this behavior is present since there are many possibly cancelling effects. For example, as cooling is increased the static pressure drop along the tube is increased. The density near the wall is increased which in the absence of a radial velocity tends to decrease the axial velocity and its gradient at the wall. The magnitude of the outward radial velocity component and the viscosity ratio at the wall μ_w/μ_m are also all decreased. For the examples shown, at $x^+ = 0.490$ the velocity profiles have essentially reached the fully developed state, while the product $fRe_{,m}$ still differs from its fully developed value by more than 50%-- this difference must be attributable to the factor μ_w/μ_m again. If the velocity profile development is plotted as a function of x_m^+ instead of x^+ (Figure 34), the fully developed state is reached more quickly. Also the distortion of the profiles with x_m^+ is reduced when presented on this basis. Using x_m^+ for the representation of $fRe_{,m}$ and $Nu_{,m}$ is questionable. Even though convergence of these quantities

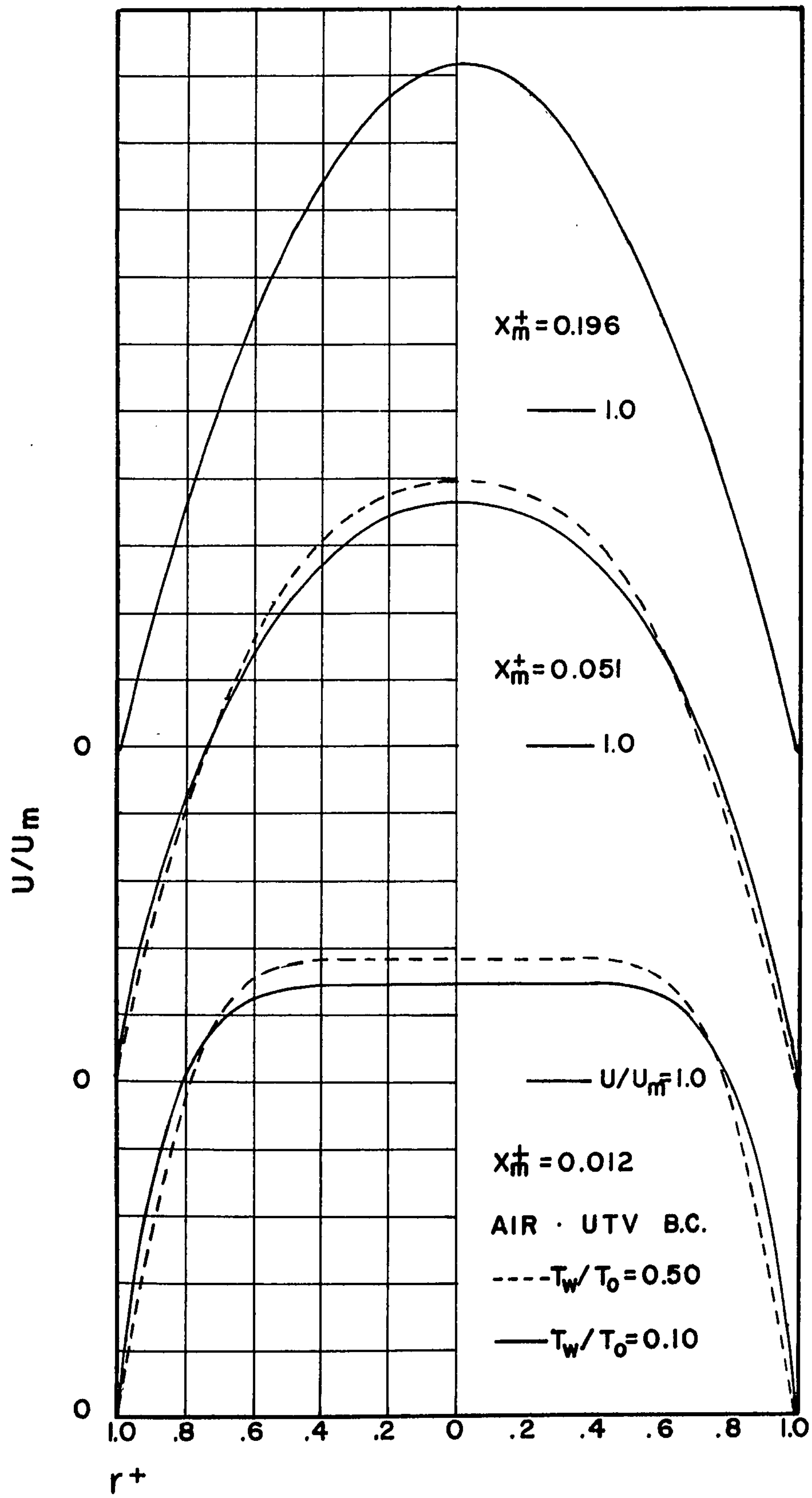

Figure 34. Reduced axial velocity development with X_m^+

is also quicker. The displacement of the curves with respect to each other at points intermediate between the entrance and fully developed regime would be increased. Also, the excellent correlation of $Nu_{,m}$ with x^+ for all T_w/T_o should not be sacrificed.

For $Nu_{,m}$, a single correlation for all inlet wall to bulk temperature ratios is recommended (maximum error 3%),

$$Nu_{,m} = 3.67 + 0.246 x^{+^{-0.592}} e^{-20.6x^+} \qquad 0.001 \le x^+ \le 0.50 \tag{4.37}$$

$$Nu_{,m} = 3.67 \qquad x^+ > 0.50 \tag{4.38}$$

for both helium and air. For the local friction factor, the following correlation is proposed;

$$1 - (fRe_{,m})/(fRe)_I = \left[1.067(1-\theta_w)x^{+^{-0.576}}\right] e^{-\beta x^+} \qquad x^+ > 0.002 \tag{4.39}$$

where

$$\beta = 7.70\,\theta_w^{0.675} \tag{4.40}$$

The coefficients were determined from a least squares multiple regression analysis. The quantity $(fRe)_I$ represents the isothermal quantity whose variation with axial distance is well represented by,

$$(fRe)_I = 16.0 + 0.694 x^{+^{-0.576}} e^{-22.9x^+} \tag{4.41}$$

for both gases in the range $x^+ > 0.001$. An attempt was made to isolate the effect temperature ratio has on the friction factor by plotting the ratio $(fRe_{,m})/(fRe)_I$ at the same axial (x^+) points as a function of local wall to mean temperature ratio. This is shown in Figure 35 for air and shows that for developing flow, correlation is not possible on this basis.

4.6. Dissipation Function

The form of the dissipation function used in the Worsoe-Schmidt analysis was,

$$\Phi^+ = \mu^+ \left(\frac{\partial U^+}{\partial r^+}\right)^2 \tag{4.42}$$

However, in the assumed core flow for the UTV boundary condition $\partial U^+/\partial r^+$ was assumed to be zero for the similarity inlet solution and in the finite difference solution, this term was found to be extremely small in in the core. Since for an acceleration or deceleration of the mass flow in the core, the continuity equation predicts a non-zero radial velocity in the core even when $\partial U^+/\partial r^+ = 0.$, a re-examination of the complete dissipation function showed that for the UTV boundary condition the form

$$\Phi^+ = \mu^+ \left[\left(\frac{\partial U^+}{\partial r^+}\right)^2 + \frac{2}{(Re_o Pr_o)^2} \left\{\left(\frac{V^+}{r^+}\right)^2 + \left(\frac{\partial V^+}{\partial r^+}\right)^2 - \frac{2}{3}\left(\frac{\partial V^+}{\partial r^+} + \frac{V^+}{r^+}\right)^2\right\}\right] \tag{4.43}$$

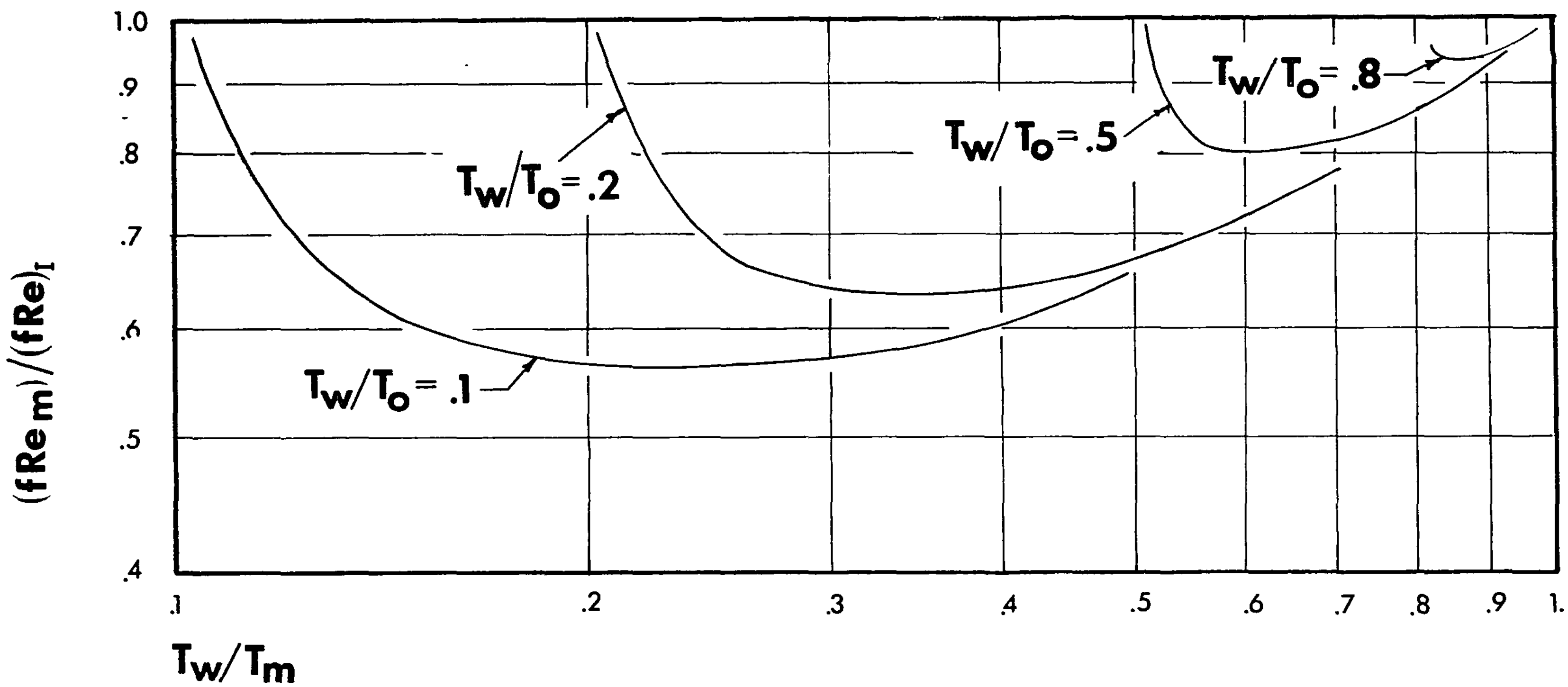

Figure 35. $(fRe_{,m})/(fRe)_I$ versus T_w/T_m. Air, UTV boundary condition.

should be used. For the isothermal UTV condition, the term $\partial V^+/\partial r^+$ can be shown to be larger by a factor r_o/δ than the term $\partial U^+/\partial x^+$ at the entrance. Examination of these terms from the numerical solution showed that the axial derivative could still be neglected when property variations were present. At the tube centerline ($r^+ = 0$) application of L'Hospital's rule and symmetry yields:

$$\frac{4\mu^+}{3(Re_o Pr_o)^2}\left(\frac{\partial V^+}{\partial r^+}\right)^2 = \Phi^+ \tag{4.44}$$

This dissipation function is operating over a fairly long axial distance in the core and the integrated effect on the temperature profile and the wall parameters may be non-negligible. An interesting point in the inclusion of the factor $Re_o Pr_o$ which requires the specification of the Reynolds number when the additional terms are included. Generally, Reynolds number dependence is a characteristic of non-boundary layer flow. For example, inclusion of axial second derivatives also requires specification of Re_o. The initial value nature of the problem is not changed by the inclusion of these terms. The variation of $Nu_{,m}$ for helium at $\theta_w = 0.90$ is shown in Figure 36 for several inlet Reynolds numbers. For $Re_o >$ 100, the change in $Nu_{,m}$ is negligible. While Reynolds

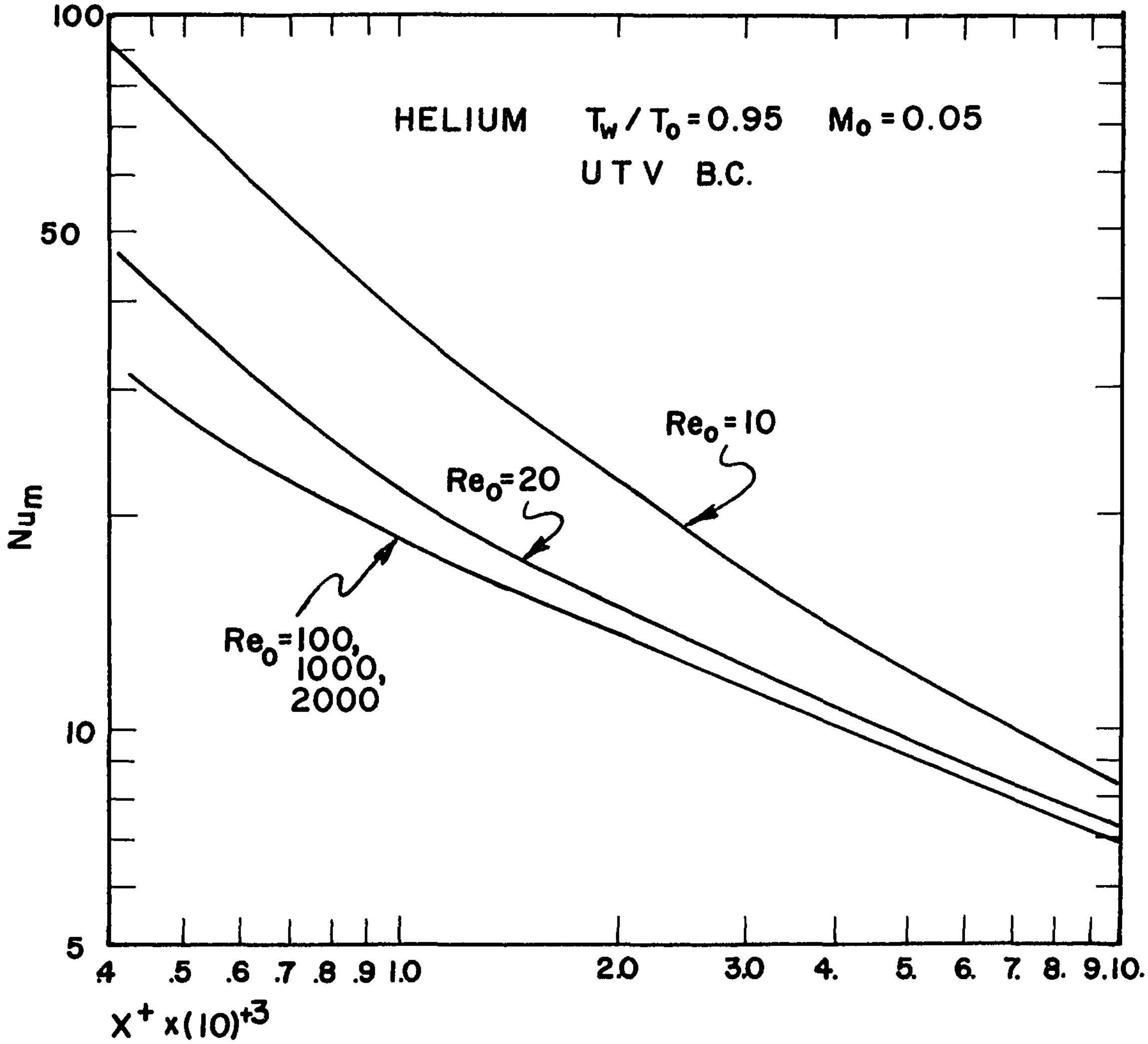

FIGURE 36. EFFECT OF ADDITIONAL TERMS IN DISSIPATION FUNCTION Φ ON HEAT TRANSFER.

numbers lower than this are not of any practical importance, solutions are presented for Reynolds numbers less than this for the sake of completeness. For Reynolds numbers of this magnitude, the second order axial terms would probably be of such magnitude as to make these results of academic interest only. The effect will be reduced for lower wall to bulk temperature ratios due to 1.) the decrease in the magnitude of the radial velocity component and 2.) the increasing magnitude of boundary layer terms relative to these terms, so that it was not necessary to test further cases. It is interesting to note that the effect of the new dissipation function is felt immediately in the entrance. This indicates that the increased magnitude of $Nu_{,m}$ is probably due to the dissipation in the boundary layer at or near the wall rather than in the core. Local viscous energy generation at the wall would raise the gas temperature near the wall. Perhaps it would be more applicable to define a convective heat transfer coefficient using a wall to local film temperature difference. Such a film temperature could be defined, for example, by using the bulk temperature in the thermal boundary layer rather than across the whole tube. The effective "film" to wall temperature difference is increased by a greater factor than the ordinary wall to bulk temperature difference.

CHAPTER 5. EXPERIMENTAL INVESTIGATION

5.1. Introduction

In this chapter the procedure and apparatus used to obtain experimental data for gas cooling with the sets of boundary conditions examined in the theoretical portion of the investigation is described.

5.2. Experimental Apparatus

The apparatus was designed to measure the local heat transfer and static pressure at several axial points along a constant temperature cylindrical tube for cooling of a gas with severe transverse temperature gradients. The flow diagram is shown in Figure 37. Air supplied from a reciprocating air compressor flows into supply plenum, through a filter, scrubber and regulator and into a settling tank. The flow than passes through a resistively heated inconel tube into a mixing plenum where its temperature and pressure are measured before passing into a development section mounted directly before the test section. The gas temperature is measured in a mixing plenum mounted directly after the cooling section. It then passes through a constant temperature bath after which its temperature is measured. Finally the flow is metered by a laminar flow meter and vented to atmosphere.

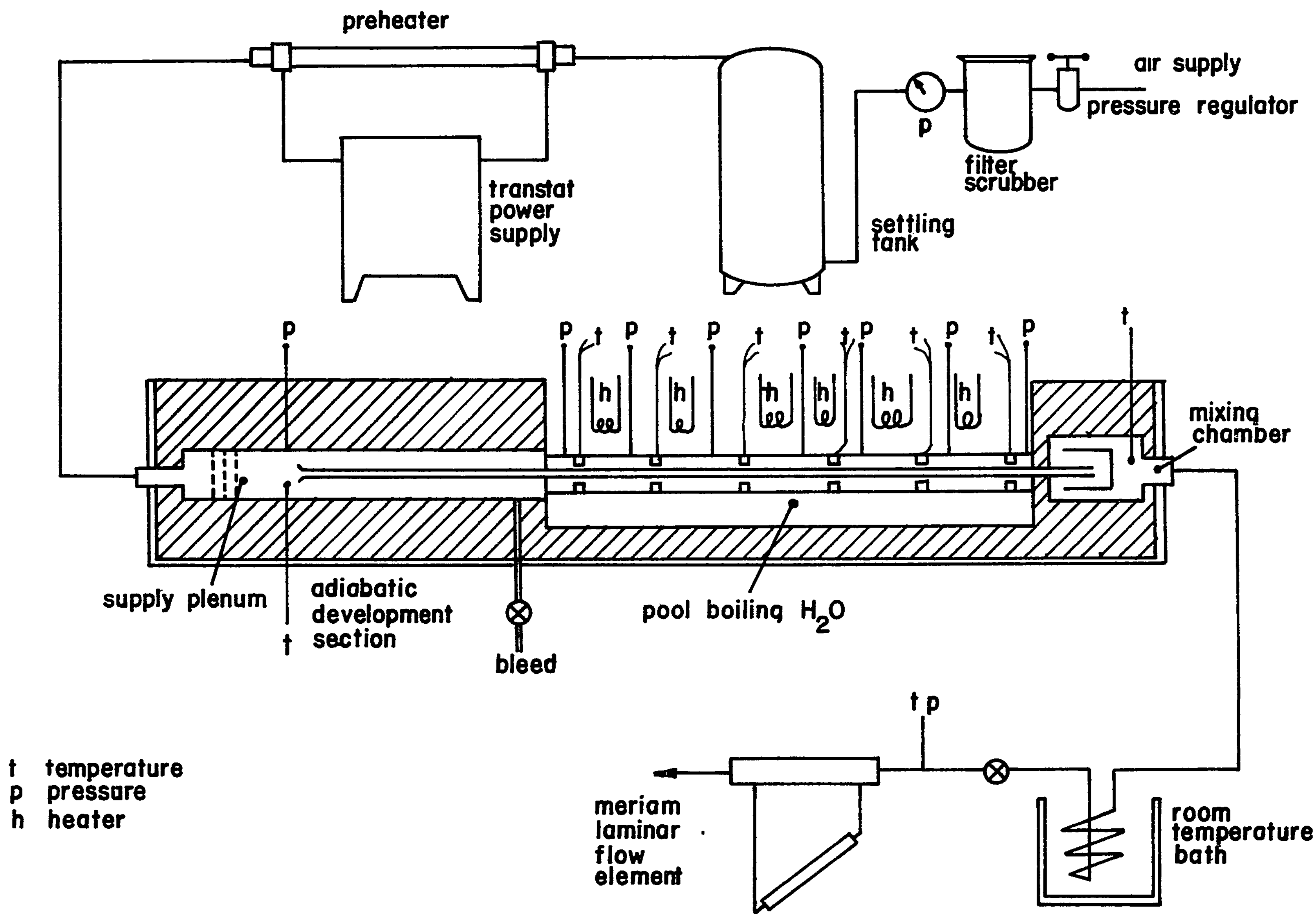

Figure 37. Schematic diagram of experimental apparatus

A. Air Supply

A Worthington two stage air compressor was connected into the supply line. The gas was initially dried in a water jacketed condensor after the high pressure cylinder in the compressor. The compressor ran continuously during each test. Primary regulation of the supply plenum pressure was accomplished by varying the bleed flow from the supply plenum. This method provided an extremely steady flow. The pressure was maintained in the plenum at approximately 90 psig.

A King Model 2260-1 filter fitted with a King Model 9326 polisher cartridge was mounted in line directly before a Denver-Harris model 1603-C two stage pressure regulator.

B. Preheater

The preheater consisted of a 1/8"D x 0.020" wall x 5' inconel tube mounted in a steel cylinder loosely packed with MgO powder and externally insulated with magnesite sheath (Figure 38). Power is supplied from a Transtat catalog no. 29145 single phase voltage regulator through specially fabricated taps mounted at opposite ends of the inconel tube. The preheater was electrically insulated from the test section by a special flange fabricated from 316 S.S. and a Cermacast pottable ceramic. The power input to the tube was measured with a Weston voltmeter-ammeter combination. Maximum exit gas temperatures obtained were on the order of 1800 F.

C. Development Section

Two flow development sections were used. The first provided a fully developed velocity and uniform temperature profile to the test section and is shown in a photograph in Figure 39 and schematic in Figure 40. The entering gas temperature was measured by a chromel-alumel thermocouple mounted downstream of a pair of mixing baffles. The thermocouple was fitted with a cylindrical stainless steel radiation shield so that it effectively "saw" only the center portion of these baffles and the development tube centered in the downstream region. The flow divided into a portion which flowed through an isolated central tube leading into the cooling section and a portion which flowed in an annulus surrounding this tube. This flow was vented to the atmosphere through a needle valve. The annular flow served as insulation to assure that the flow development was adiabatic. The length to diameter ratio of the section was well over 100. For the second development section, the annular section was removed from the plenum. A bellmouth entrance was used to provide nearly uniform velocity and temperature profiles to the test section. The inlet bulk temperature of the gas was measureed by bleeding air from the supply

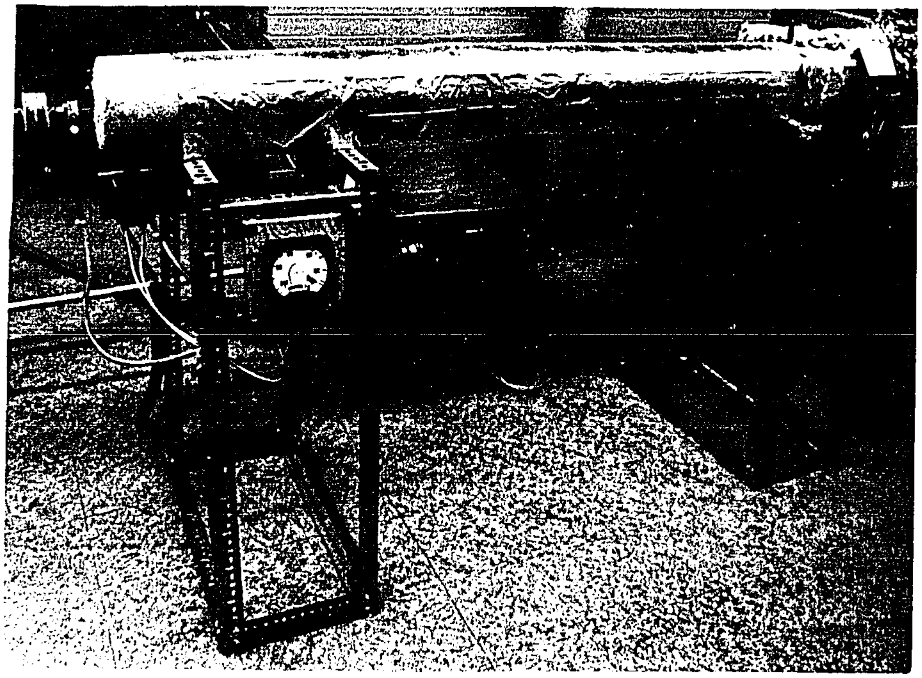

Figure 38. Photograph of preheater

Figure 39. Photograph of adiabatic development section

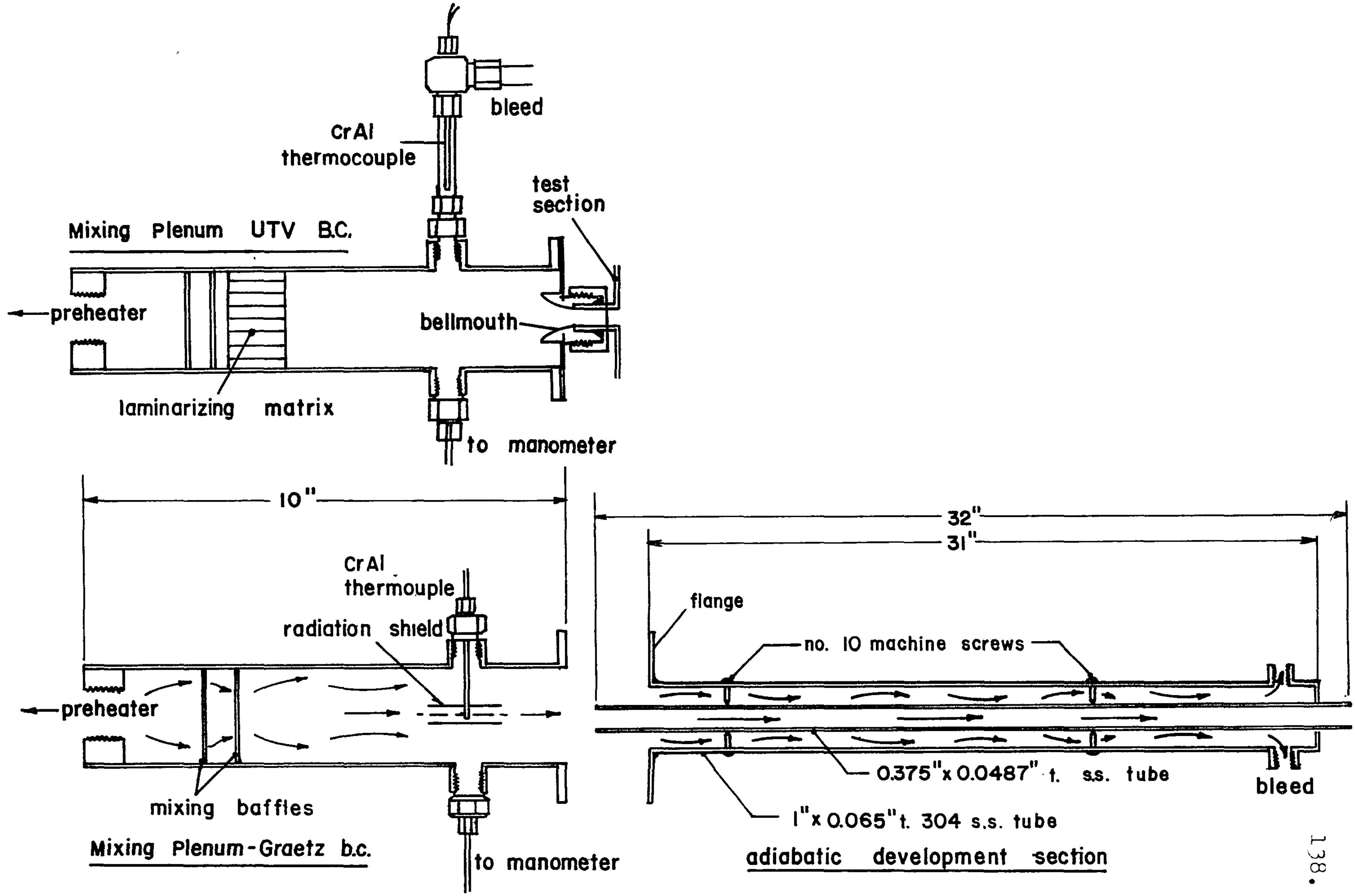

Figure 40. Schematic of inlet development section apparatus

plenum around a long stem 1/16 inch diameter chromel alumel thermocouple (Figure 40). Pressure in the plenum was measured by a Meriam 40 inch air-over-mercury manometer. Magnesite sheath of approximately 1-1/2 inch thickness was bonded to both development sections with a refractory cement. Several inches of exterior fiberglass insulation was added. All tube and thermocouple fittings used were Gyrolok 316 stainless.

D. Exit Mixing Section

A schematic of this apparatus and a photograph showing the section mounted in its insulating case are shown in Figure 41. After passing through the test section, the gas flows through a short length of tube in which several mixing baffles are mounted and over a long stem, small diameter Cu-Con thermocouple probe. This air then flows back in an annulus around the tube to serve as an insulator and then passes over the rear of the thermocouple stem so the conduction losses are reduced. This mixing portion was mounted in a box filled with several inches of MgO powder and vermiculite insulation. The entire apparatus was then covered with fiberglass insulation.

E. Metering

Prior to metering, the gas passes through several turns of 1/4 inch D copper tubing immersed in a room

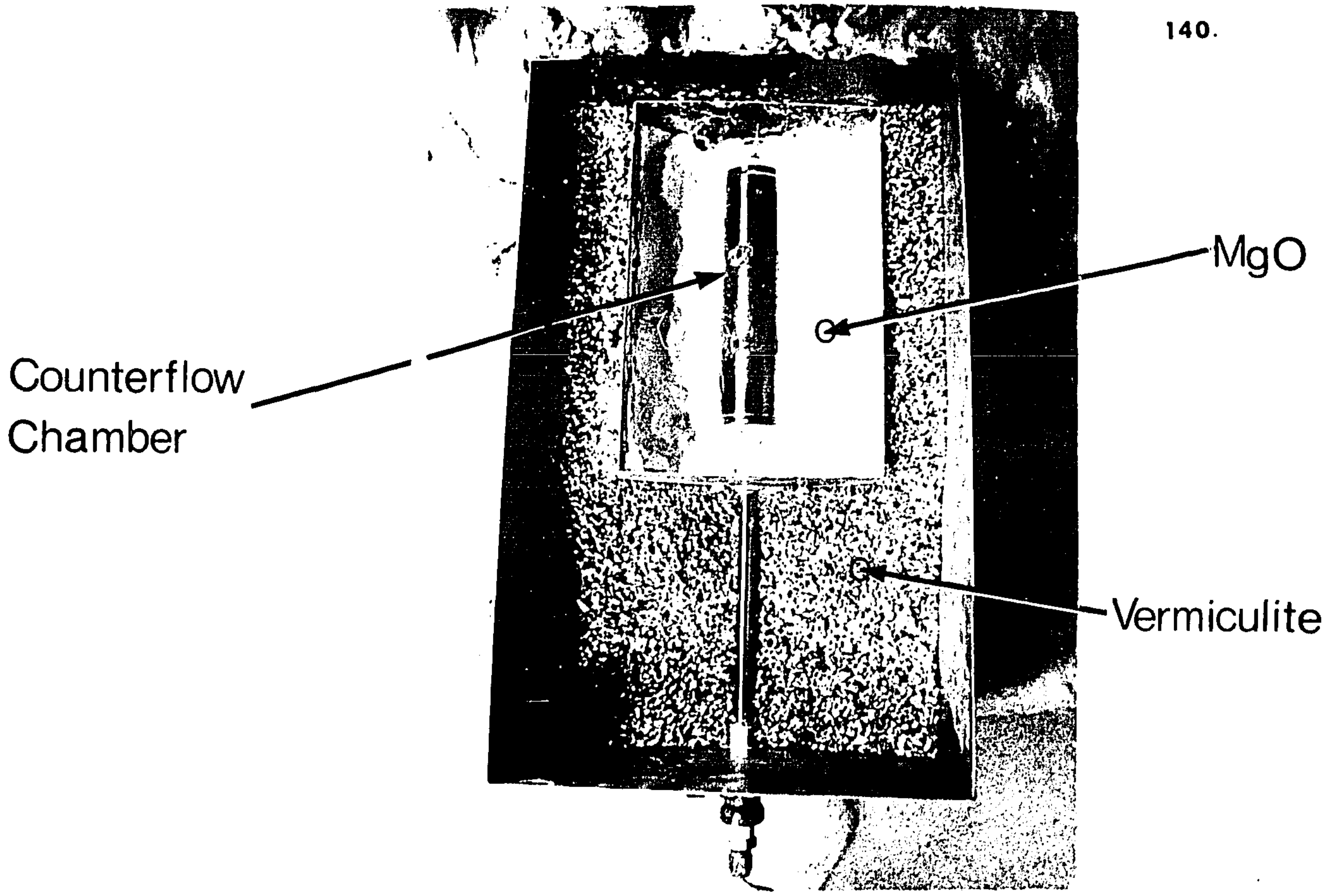

Photograph: Mixing Section

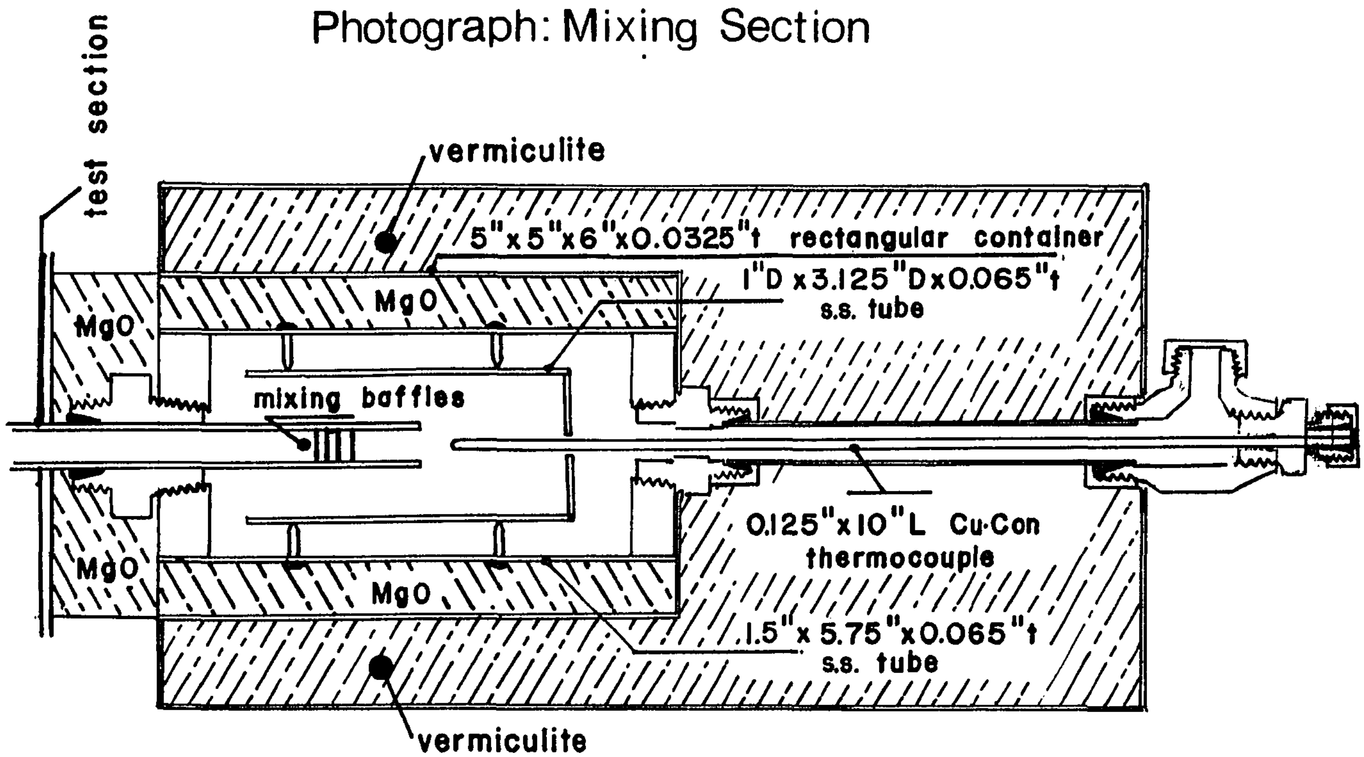

Figure 41. Schematic and photograph of exit mixing plenum

temperature water bath. This insures that the temperature correction term for the flowmeter will be small. The flow rate is measured with a Meriam model 50 MW 20-1 factory calibrated laminar flow element which provides a linear differential pressure output with air flow rates up to 8 S.C.F.M. The output pressure is measured by a Teltrue type A micromanometer with a resolution as low as 0.001 inch H_2O. Gas temperature at the flowmeter was measured by a long stem Cu-Con thermocouple mounted so that the junction was inside the flowmeter and the gas flow was along the stem.

F. Flow Control

The flow through the test section is controlled by three needle valves. One is mounted in line between the test section and flowmeter, one is upstream of the preheater and one is mounted on the bleed line from the development section. The bleed flow rate was maintained at a much larger value than the flow through the test section. This was done so that changes in this latter flow rate through the test section made by adjusting the downstream valve would make only small relative changes in the total flow rate through the preheater. Since the power input to the preheater was not normally changed during a test series for a fixed inlet temperature, this procedure assured a fairly steady output temperature.

G. Test Section

The test section is a 1" O.D. x 0.294" I.D. 304 stainless steel tube. Pressure taps made from 1/16 D x 0.006 inch wall stainless tubes are brazed into the tube at 7 axial points. Actual entry into the inner tube is made by 0.040 inch diameter holes in the tube wall. Six heat flux calorimeters are clamped to the tube at 6 axial points where grooves are turned into the section. Axial locations of the pressure taps and calorimeters are given in Table 5.1.

Table 5.1. Test Section Dimensions

A. Axial location of pressure taps (in.)

1.250	6.550	16.150	25.749	35.349	44.949	50.248

(0.981 in. additional with bellmouth)

B. Axial location of calorimeters (to center of each)

1.730	11.330	20.930	30.529	40.129	49.728

The calorimeters consist of 304 S.S. semi-circle sections 0.380 inch I.D. x 1.000 inch O.D. x 0.500 inch width fabricated from the same tube stock as the test section. Thermocouple holes 0.030 inch D x 0.250 inch deep are drilled into each section at radii of 0.250 inch and 0.437 inch. Teflon insulated 36 gage Cu-Con thermocouples made from thermocouple wire supplied by Thermo Electric Company are mounted in the holes which are packed with a high conductivity GE silicone grease. The thermocouples are mounted in matched pairs formed by cutting the wire and welding leads directly on either side of the cut. This insures that each pair of thermocouples will have leads of essentially the same composition since thermocouple wire may vary even from the same spool. The thermocouples are soldered with a 60-30 resin solder.

A 1/16 inch thick balsa facing is bonded with epoxy to the face of each calorimeter (see photograph, Figure 43). The thermocouple leads are epoxied into grooves cut into this facing such that thermocouple conduction error is reduced and the leads are protected from abrasion. The calorimeters are pressed against the test section by means of simple clamps fabricated from 1/8 inch t 304 S.S. sheet stock. Contact resistance between the calorimeters and the test section was reduced by liberal application of silicone grease to all contact surfaces prior to mounting.

The test section is immersed in a bath of H_2O which is maintained at a pool boiling condition by approximately 12 immersion heaters.[6] The test section plus constant

---

[6] Inital attempts at using liquid N_2 as the boiling medium were unsuccessful due to the difficulty of maintaining a good thermal bond of the calorimeters to the test section at extremely low temperature.

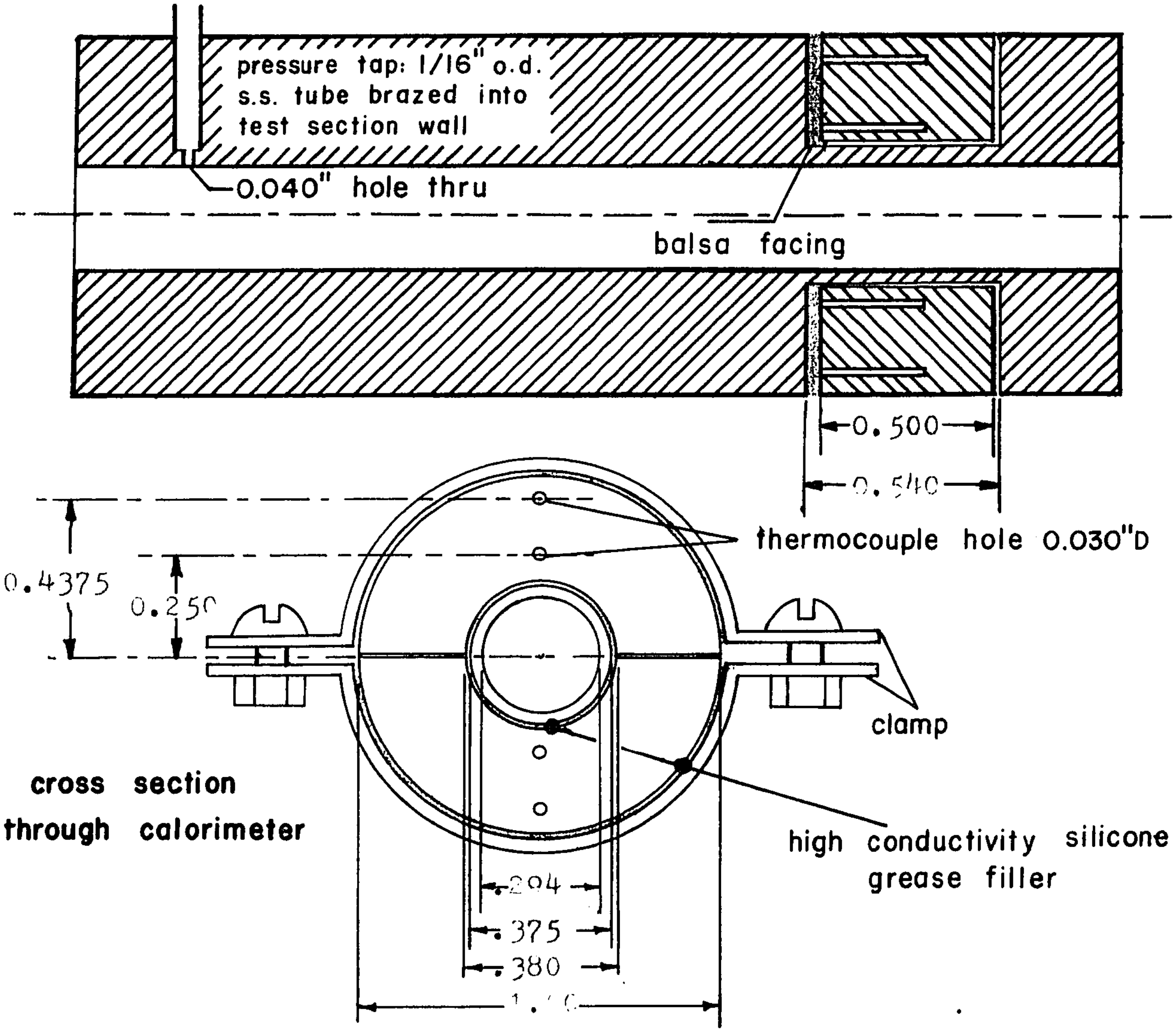

Figure 42. Test Section Pressure Tap and Calorimeter - Detail

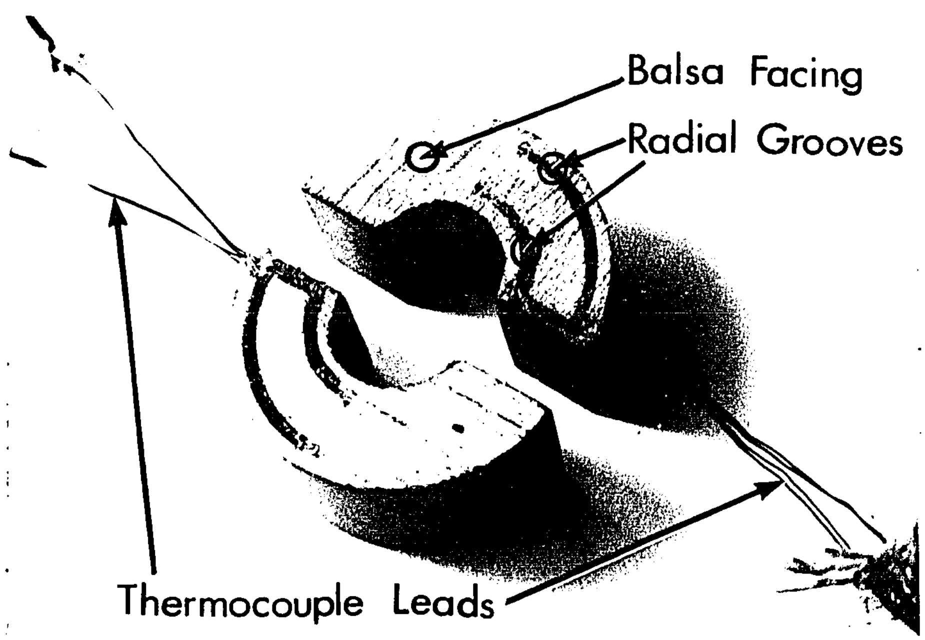

Figure 43. Heat flux calorimeter pair – photograph

temperature bath is mounted in a large rectangular vermiculite filled box. Maximum values of the ratio Gr/Re^2 obtained in the test section were on the order of 2.5×10^{-3} so that free convection effects are expected to be negligible (50,63). Gr is the Grashof number calculated on the basis of maximum wall to gas temperature difference, tube diameter and using gas properties evaluated at temperatures midway between wall and maximum gas temperature.

Provision was made for measurement of the static pressure drop between any pair of pressure taps by means of a pair of pressure switching banks. Pressure drops were measured by a Teltrue type A. micromanometer.

The thermocouple outputs are measured on a recently calibrated Leeds and Northrup type K3 potentiometer and type 9834 null detector. External reference junctions for the thermocouples were placed in an ice bath. Absolute rather than differentail EMFs from the calorimeter thermocouples are measured because most of the measuring junctions were grounded to the test section.

Where possible, electrostatic shielding is applied to thermocouple leads. External thermocouple leads are glass on teflon insulated. Leakage currents are minimized through extension of the internal guard circuit of the potentiometer to its power supply and standard cell. These are mounted on a capacitor formed from sheets of polymethyl methacrylate and aluminum. This was necessary due to the high humidity in the laboratory from the boiling off of the H_2O in the test section bath. Ground loops are eliminated by use of a 0.01 microfarad mica capacitor inserted between the potentiometer and earth ground.

5.3. Calibration

A series of calibrations performed on portions of the apparatus are described in this section.

A. Calibration of the Heat Flux Calorimeters

An analysis of the possible error in using a one dimensional heat conduction equation to evaluate calorimeter conductances is presented in Appendix C. This result necessitates a calibration of the calorimeters. The calibration was performed on the calorimeters after mounting on the test section by applying a known heat flux to the inside wall of the test section and measuring the corresponding ΔT across the calorimeters. The inside wall of the test section was coated with several layers of a flat black refractory enamel in order that the absorptivity of the wall would be uniform. A 1/8 in. D thin walled stainless steel tube whose surface was uniformly roughened on a lathe with a #500 grit emery cloth was mounted along the centerline of the test section. Figure 44 is a photograph of the calibration setup. Thin ceramic spacers were mounted at points midway between successive calorimeters in order to insure centering of the wire. An analysis of the error introduced by these spacers is presented in Appendix D and is shown to be negligible. In order to eliminate sag at high temperatures, a tension was applied to the wire by a spring mounted in a vacuum chamber at the end of the test section. Power leads and voltage taps were introduced into the chamber containing the tensioning spring by means of Conax sealing glands. Power was provided by a Variac model W20MT3 autotransformer and was measured with a Weston 0-25 volt range voltmeter and 0-30 amp range precision ammeter. The system was evacuated by a mechanical vacuum pump and pressure was measured with a Scientific Glass no. 1-759 tilting type McLeod gaga. Pressure in the test section was maintained at a maximum of approximately 0.02mm Hg in order to minimize conduction and convection heat transfer.

The test was performed with boiling H_2O in the test section bath. Tare thermocouple readings with zero power to the heating tube were subtracted from readings in the power-on test to correct for possible spurious heat losses. The conductances as determined from this procedure are shown plotted as a function of axial position in Figure 45. Error limits with respect to the

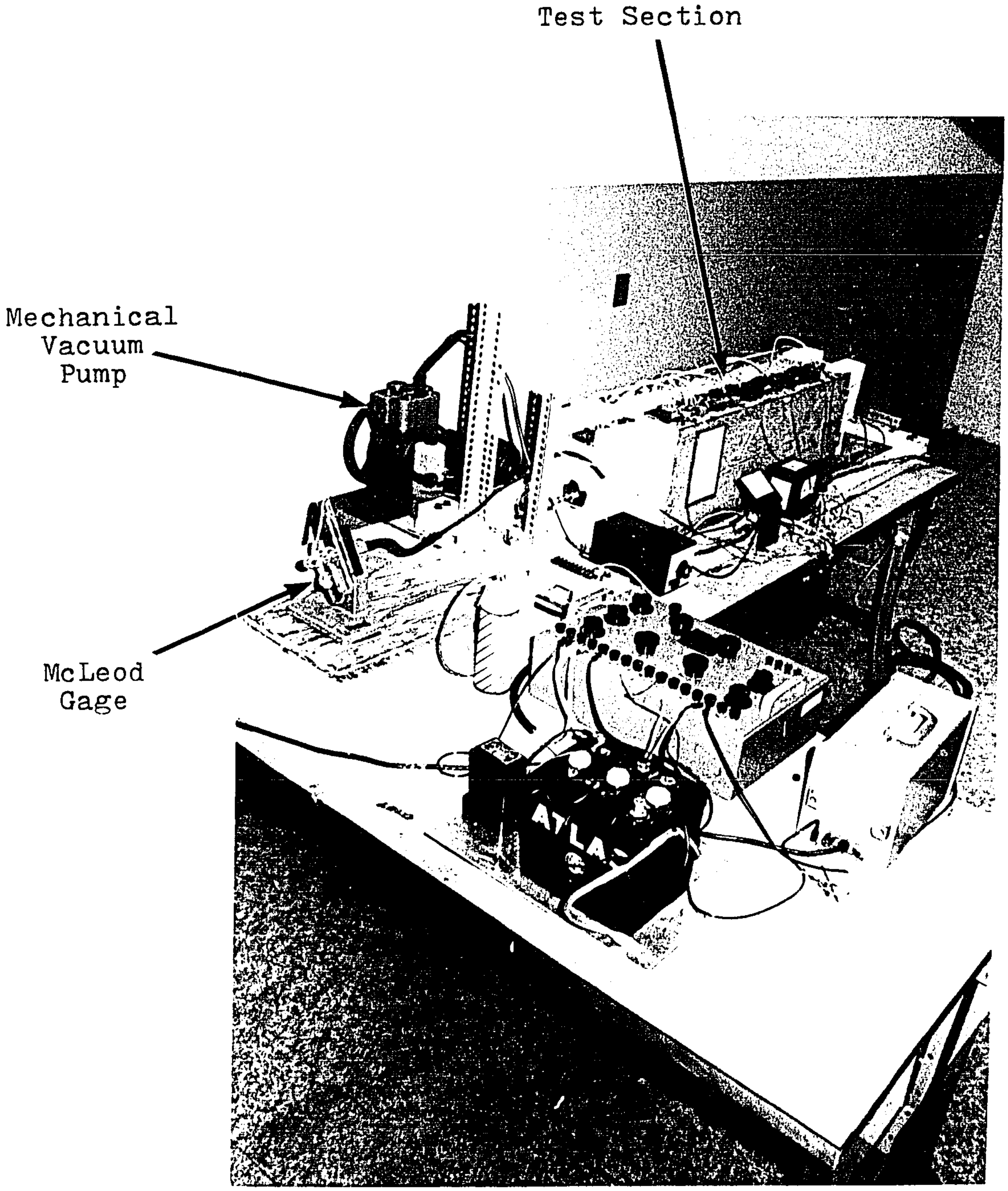

Figure 44. Photograph of test section and apparatus for radiation calibration

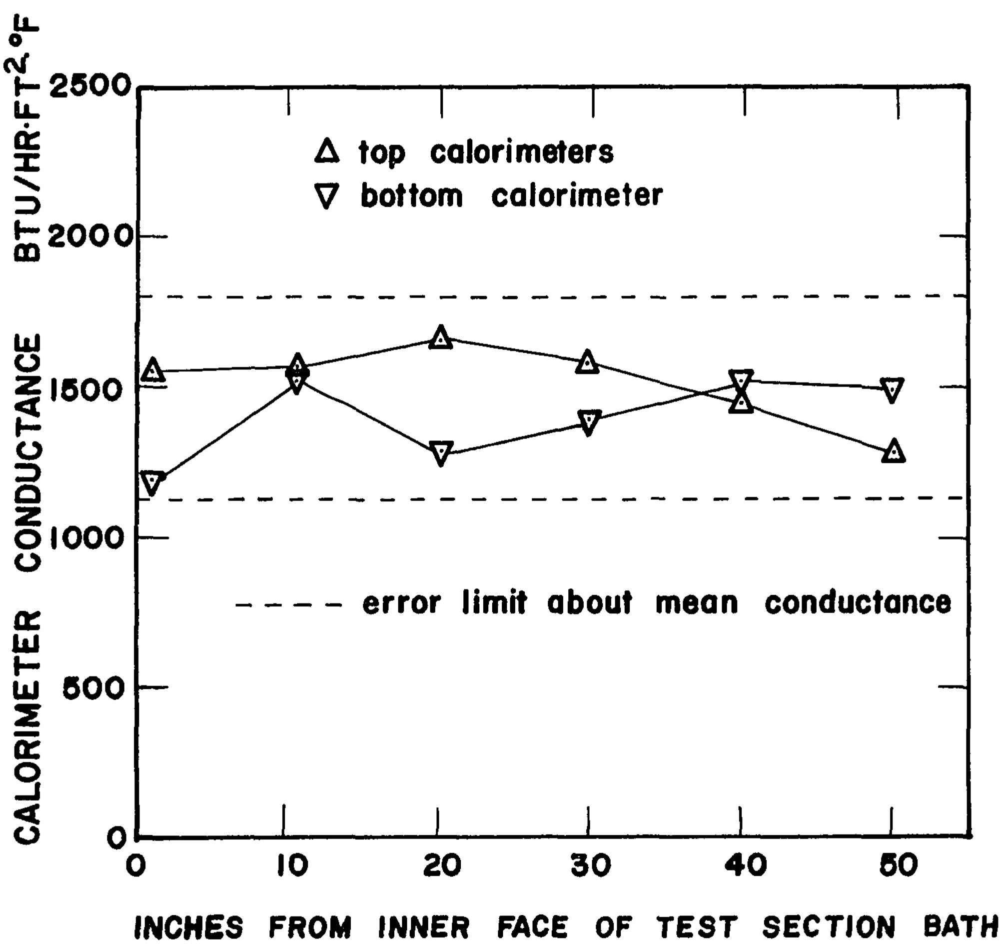

Figure 45. Axial variation of calorimeter conductance.

mean value of all the conductances (Appendix C) are shown plotted as horizontal lines. All conductances are seen to lie within these limits.

B. Calibration of Thermocouples

The copper-constantan reference junction was obtained from Conax Corporation with a factory calibration in accordance with ASTM procedure E220-64 against a National Bureau of Standards calibrated Platinum versus Platinum-Rhodium thermocouple. The deviation at 32 °F was 0.00 °F. This thermocouple was used for calibration of the flow-meter and exit bulk temperature measuring thermocouples. The deviations were too small (<0.25 °F) to make a noticeable difference in the results. No calibration was necessary for the test section thermocouples.

C. Adiabatic Development Section

Velocity profiles were measured at the exit of the adiabatic development section which was used for generation of fully developed velocity profiles. This measurement was taken for two reasons. 1.) Since the velocity profile development in the section will depend on $L/(DRe_o)$ where L/D is the length to diameter ratio of the development section, it was necessary to find the maximum Reynolds number for which the flow could be treated as fully developed and 2.) it could be used for a check on the flowmeter. During the test all bleed valves on the development section were closed and the flowmeter was mounted upstream of the section.

A total pressure probe was fabricated from 0.020 inch O.D. x 0.010 inch I.D. 316 stainless steel hypodermic needle stock. The probe was mounted on a microscope vernier control stage and output was measured on a type A micromanometer (see photograph, Figure 46). The control stage was set for a traverse across a diameter of the tube by means of a cylindrical brass plug which fit into the end of the test section. A 0.022 inch wide rectangular groove was cut into the plug. The probe was moved into this groove and the microscope stage adjusted until a traverse could be made by moving one of the verniers without touching the sides of the channel. An electrical circuit was set up with the probe connected to one side of a battery and the test section and plug connected to the other polarity. An ammeter was placed in the circuit so that when contact of the probe and plug occurred, the ammeter would give a non-zero reading. Static pressure at the exit was assumed equal to atmospheric. Corrections for measurements near the tube wall as describe in reference 95 were applied. The data showed a flattening of the profile at the centerline occuring at approximately Re_o = 1800. A third order polynomial identically satisfying the zero slip condition at the wall was fitted to the data

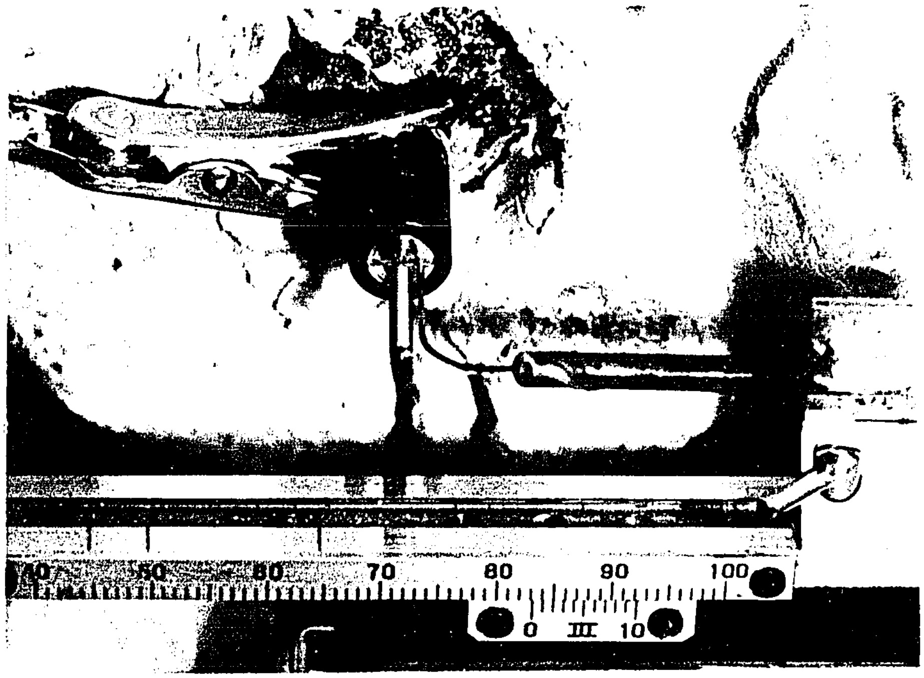

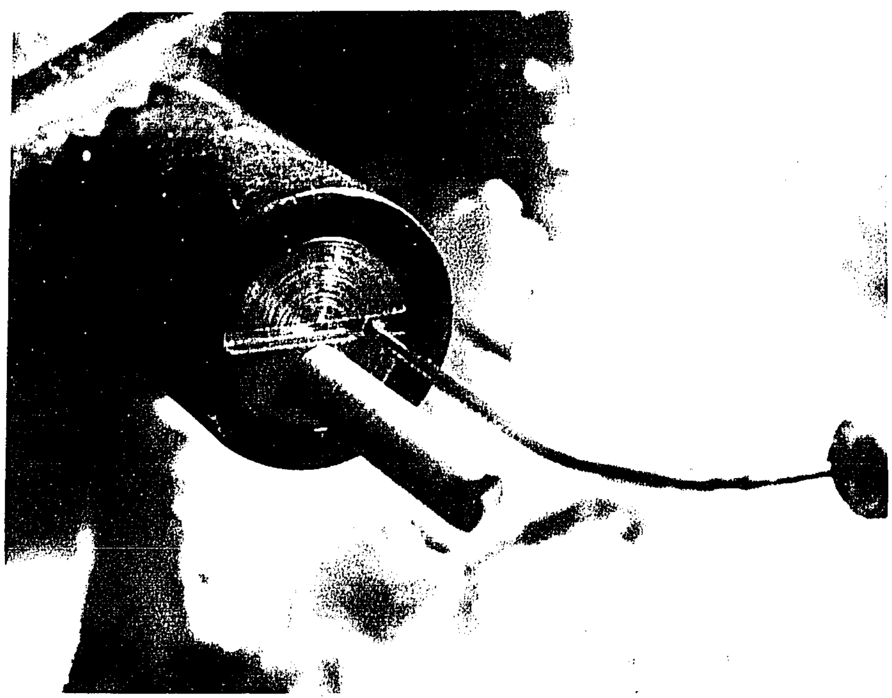

Figure 46. Velocity profile measuring apparatus
Microscope stage and plug

at Re_o = 1585 by a least squares criterion (Figure 47) and inserted as an initial velocity profile along with a uniform temperature profile in the finite difference solution. The effect on $Nu_{,m}$ and $fRe_{,m}$ was neglible. No difference was seen in $fRe_{,m}$ at $x^+ = 0.001$ while $Nu_{,m}$ was about 1% higher than that in the idealized case. Also, an itegration of this prófile yielded a mass flow rate within 3% of that indicated by the Meriam flowmeter. This agreement is excellent considering that velocity measurements near the tube wall have the least accuracy and a greater weight in a flow rate calculation than points near the center of the tube.

A second calibration was performed after the plenum and development section were run for several hours at 1800 F. This was done so that any incipient change in the calibration of the chromel alumel thermocouple in the mixing section of the development section would be triggered. The bulk temperature measuring chamber described in section 5.2. was fitted with a chromel-alumel thermocouple and fitted onto the end of the development section. The flowmeter was mounted downstream of the chamber. For a Reynolds number of 1500 with the bleed open, the exit temperature was correlated with the output from the upstream thermocouple. The final exit temperature correlation with upstream thermocouple output is shown in Figure 48 which includes a correlation after a two point

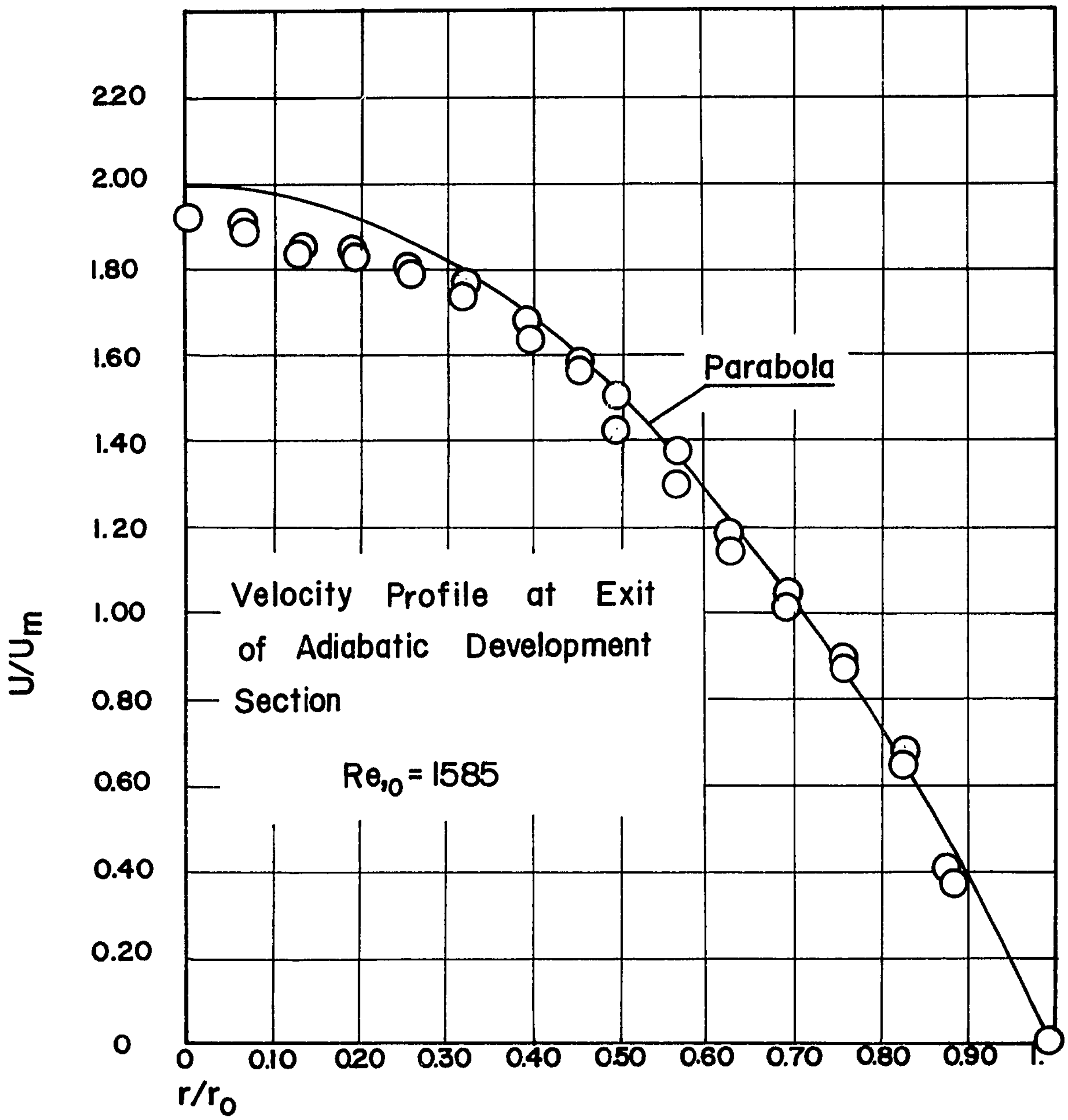

Figure 47. Exit velocity profile from adiabatic development section.

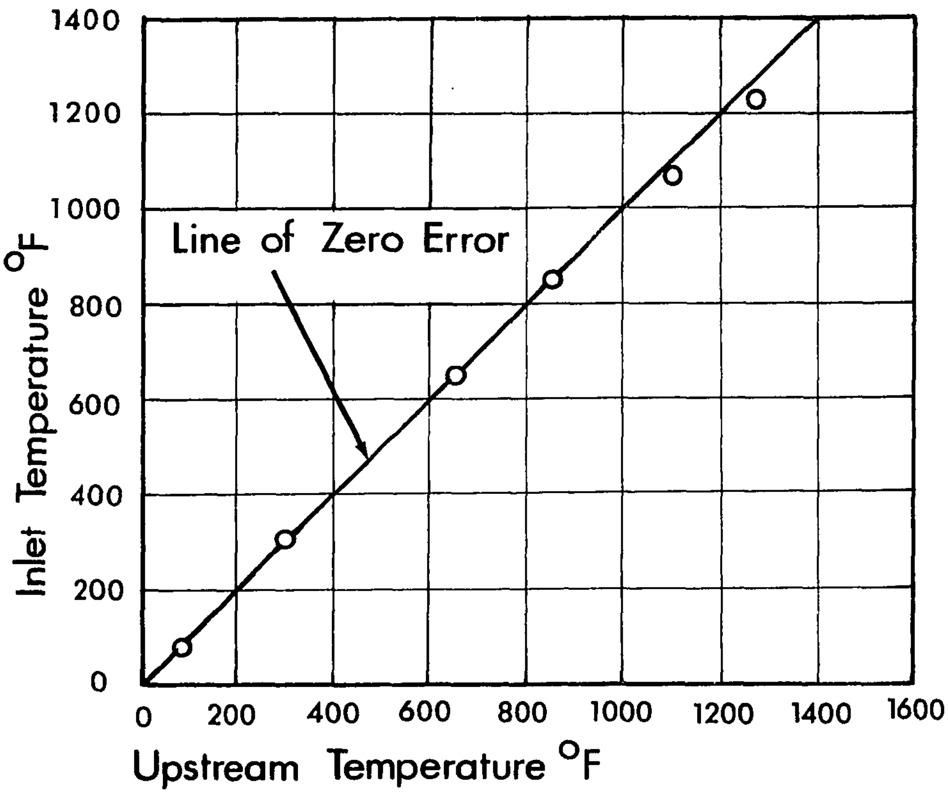

Figure 48. Calibration of adiabatic development section.

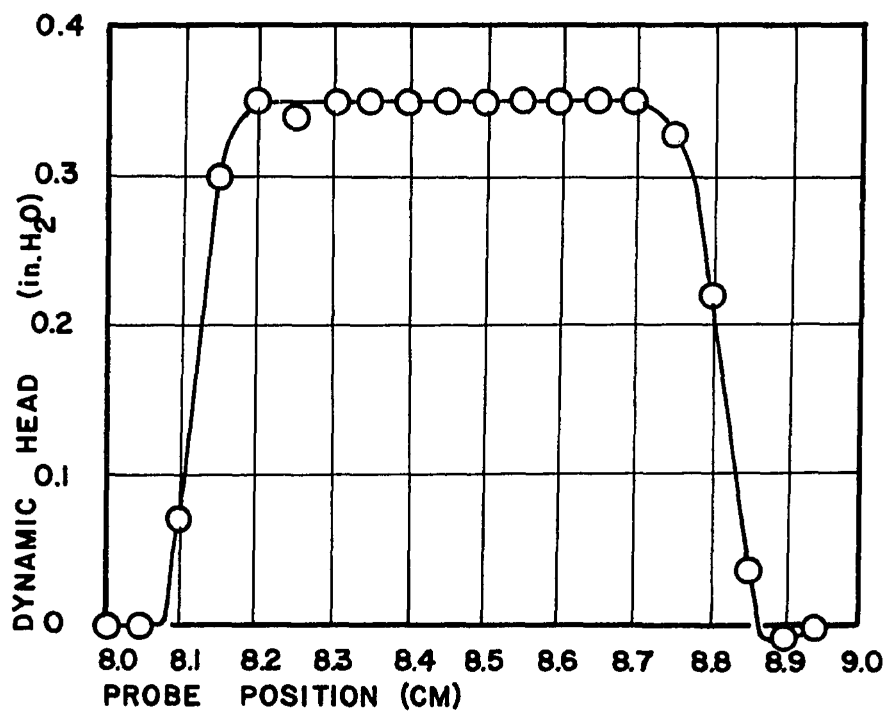

Figure 49. Velocity profile from bellmouth used in UTV development section.

calibration at 32 °F and 212 °F of the chromel-alumel thermocouple used in the bulk temperature measuring device. This curve was used in the data reduction program for correction of the upstream thermocouple output.

D. Mixing Section and Bellmouth

The velocity profiles from several bellmouths with slightly varying geometry were measured with the total pressure probe apparatus described in the previous section. The bellmouth giving the most uniform velocity profile (Figure 49) was mounted in the mixing supply plenum for the portion of the experiment dealing with the UTV boundary condition. Output of the chromel-alumel thermocouple mounted in the bleed flow was monitored as a function of its depth of immersion in the bleed flow to determine the depth at which conduction error becomes negligible.

5.4. Leak Tests

Prior to the beginning of the two test series, the test section was pressurized to 35 psig and all connections were covered with a soap solution. This pressure was well in excess of the maximum pressure (20 psig.) used during the actual testing. Tygon plastic tubing was used throughout and G.E. RTV silicone sealant was used at all plastic-metal tube connections.

5.5 Adiabatic Pressure Drop and Friction Factor

With the adiabatic development section in place, two sets of pressure drop data were taken at $\theta_w = 1.0$ for the entering gas and test section both at room temperature and 212 °F. The non-dimensionalized pressure defect is plotted as a function of $x^+ - x_o^+$ along with the theoretical constant property pressure defect which, due to the low experimental Mach numbers, should correspond to the experimental data. x_o^+ is the position of the first pressure tap measured from the point where cooling was assumed to commence (Figure 50). Pressure drops are taken with respect to the first tap. The second tap is reading low and yields an average friction factor between the first two taps which is almost 10% low. No burrs were evident at the second tap. Other friction factors agreed to within 5% of fully developed.

With the UTV development section in place, low Reynolds number friction factors calculated on the basis of a least squares fit to the pressure drop from pressure taps 5 and 6 are shown in Figure 51. Since these taps are so far downstream ($\sim$ 100 diameters), the fully developed friction factor should be present. This is borne out by the excellent agreement in Figure 51. In addition to serving as a check on individual taps, the adiabatic friction factor is important in another respect.

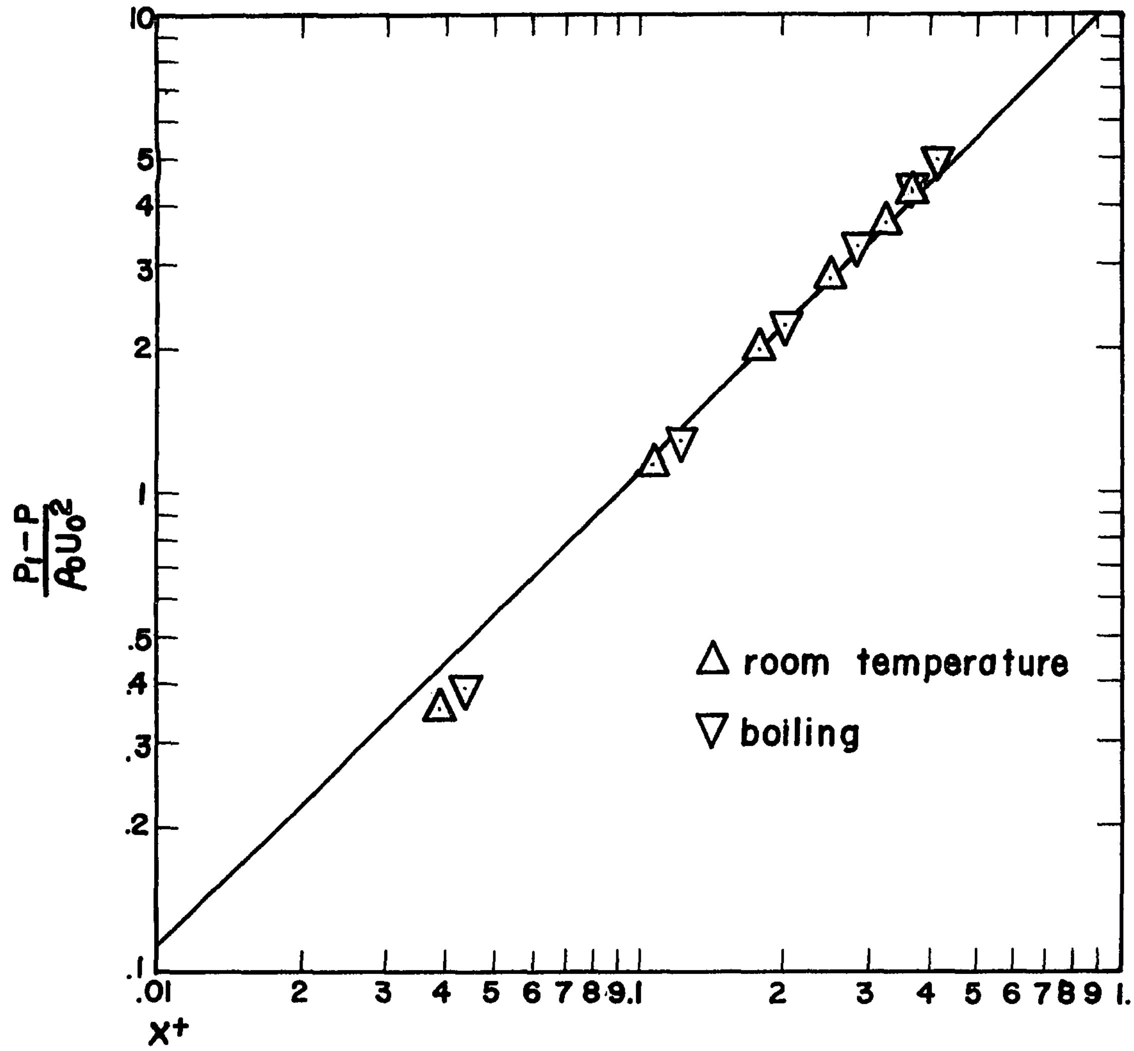

Figure 50. Isothermal dimensionless pressure drop along test section with adiabatic development section in place.

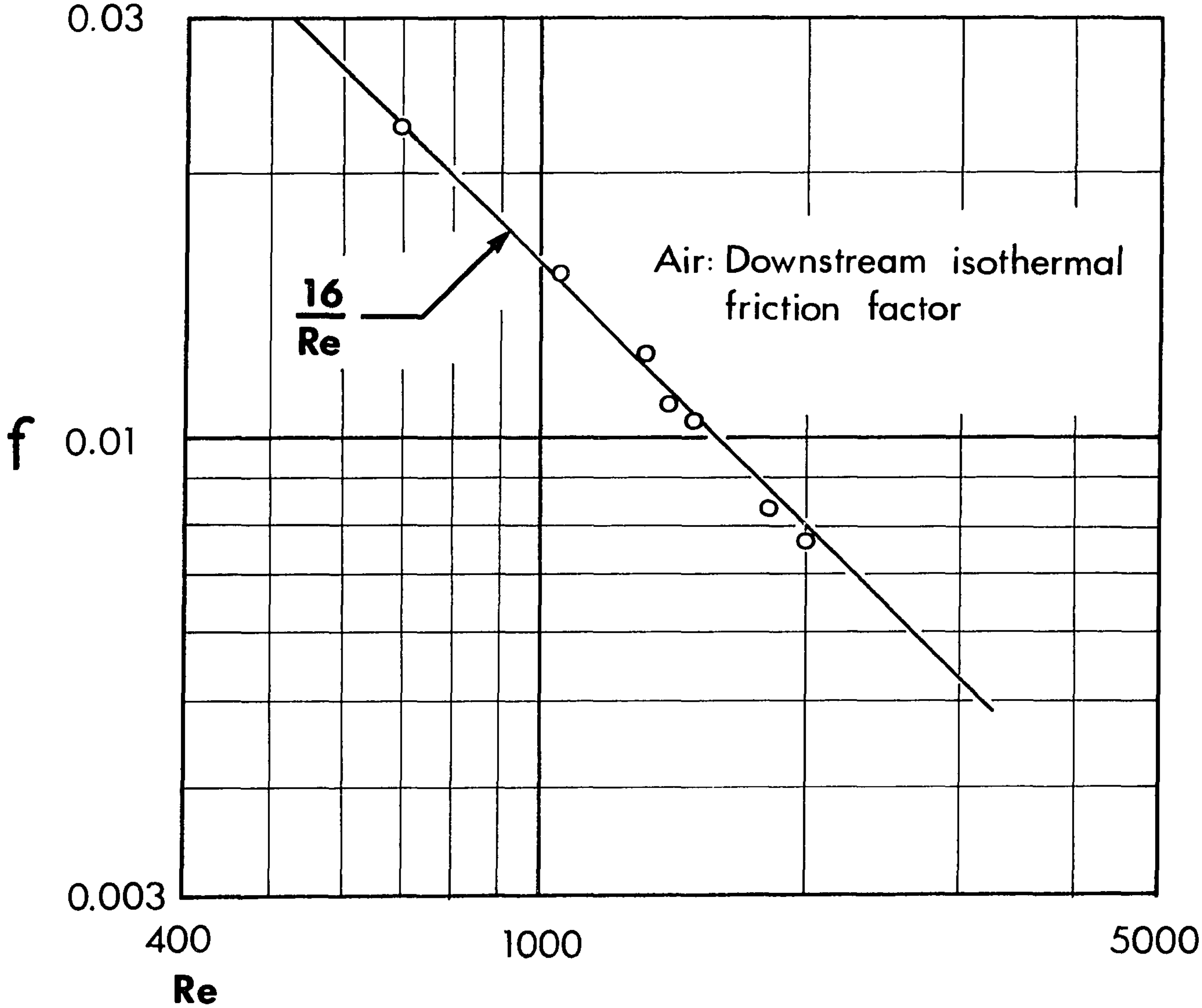

Figure 51. Friction factor in downstream region with UTV development section in place.

Since in a plot of f versus Re, the tube diameter effectively enters the reduction calculation in the fifth power, errors in the measurement of this diameter will be evident here.

5.6. Repeatability Test

In order to determine what effect the arrangement of the immersion heaters in the constant temperature bath have, two additional tests were performed with a re-arranged immersion heater configuration for the UTV b.c. for $\theta_w = 0.50$. (tests #50 and 51). No apparent effect was found on either the heat transfer or the friction factor results.

5.7. Wall Temperature Uniformity

The axial wall temperature drop between the first and last calorimeter was, in the worst case, approximately 15°F. The local axial wall temperature gradients are estimated to be approximately two orders of magnitude less than the radial gradients.

5.8. Experimental Procedure

Prior to the beginning of each set of test runs at a given inlet wall to bulk temperature ratio, the bleed flow from the development section was opened, the valve downstream of the test section was closed and the supply pressure adjusted to 60 psig. The power level to the preheater was adjusted in accordance with a bulk temperature power level curve that had been obtained from a previous test series. About 7 hours of operation in this state was necessary for elimination of all thermal transients in the development section. Zero points on the flowmeter and pressure drop micromanometers were set. The integrity of the lines from the pressure taps and the pressure switching banks were checked by seeing that the micromanometer zero was maintained for pressure measurements between several pairs of taps in the pressurized zero flow condition. Also at the no flow condition, power was supplied to the immersion heaters and the constant temperature bath was brought up to and held at the pool boiling condition for approximately a half an hour. This allowed a complete set of tare thermocouple readings to be taken. This data was used as a correction for the readings with gas heat transfer for that day.

The valve downstream of the test section was set for the maximum inlet Reynolds number to be run and about 45 minutes was allowed before data was taken. Boiloff from the pool was replaced by boiling water from a separate heater and tank in the laboratory. The following data was taken;

1. Static pressure drops. With the adiabatic

development section in place, the pressure drop between the first and 6 succeeding pressure taps were taken. With the bellmouth inlet, pressure drops were recorded between the inlet plenum and 2nd taps, the first and second tap, and then between the second and 5 succeeding taps. This series was made necessary by fluctuation in the plenum pressure that were not present in the downstream regions of the tube. These fluctuations were dampened by insertion of a laminarizing element in the plenum and the insertion of a large volume in the line from the inlet pressure tap so than an integrated pressure difference was measured rather an instantaneous value.

2. Thermocouple outputs from both thermocouples in each of the twelve calorimeters, the upstream and exit mixing chamber and the flowmeter.
3. Pressure in the inlet plenum, atmospheric and supply pressure.

A typical data sheet is shown in Figure 52. At the end of a test series which usually included 5 or 6 mass flow rates, the downstream valve was closed and an additional set of zero gas flow thermocouple readings was taken. The purpose of this second set of tare readings was to detect any abnormal thermocouple output rather than to

Figure 52. Facsimile of original data sheet.

Variable Property Gasflow Test # 11
Date 4/12/71
V(in) volts 22.0
I(in) amps 31.0
Supply Pressure (lbf/in^2) 68.0
Atmospheric Pressure (in. hg) 30.20

Tare Thermocouple Readings - Boiling, zero flow

Cal.	Station	Output(mv)	Cal.	Station	Output(mv)
1	1	SEE TEST #4 - 4/12/71	7	13	SEE TEST #4 - 4/12/71
	2			14	
2	3		8	15	
	4			16	
3	5		9	17	
	6			18	
4	7		10	19	
	8			20	
5	9		11	21	
	10			22	
6	11		12	23	
	12			24	

Flow Test

Differential Pressure - Flowmeter (in. H_2O) 0.400
Flowmeter Temperature Cu-Con (mv) 0.5760
Bulk Temperature Cu-Con (mv) 4.8980
P_1 (in. hg.) Left 3.60 Right 3.70
Upstream Temperature Cr-Al (mv) 13.942

Static Pressure Drop (in. H_2O) --BLUE MANOMETER FLUID

P_1-P_2	-0.015 (AVE.)	P_1-P_5	0.118
P_1-P_3	0.011	P_1-P_6	0.175
P_1-P_4	0.053	P_1-P_7	0.210

Thermocouple Output

Cal.	Station	Output(mv)	Cal.	Station	Output(mv)
1	1	4.2530	7	13	4.3034
	2	4.2567		14	?-DEAD-
2	3	4.2421	8	15	4.3037
	4	4.2416		16	4.3184 (SPURIOUS)
3	5	4.2509	9	17	4.3199
	6	4.2417		18	4.3423
4	7	4.2552	10	19	4.3274
	8	4.2587		20	4.3421
5	9	4.2250	11	21	4.3366
	10	4.3148		22	4.4252
6	11	4.2894	12	23	4.3318
	12	4.2413		24	4.4126

Taken by M. Shilling 4/12/71

serve as a tare reading.

5.9. Data Reduction Program

A computer program written in Fortran IV was used in the reduction of all the data. It contained provisions so that data from both inlet sections could be treated. A listing of the program in included in Appendix G along with a list of significant I/O and intermediate variables. Many descriptive comment cards are distributed throughout the listing. The program initially prints out all input data for an echo check. Complete input and reduced data for all tests are included in Appendix H. Third degree polynomial least squares fits were used to represent various calibrations and property variations. Coefficients for these fits are initially read in as punched data. Gas properties were taken from reference 32. A two section fit to the Cu-Con thermocouple tables in reference 62 was used for better accuracy. Also, the x/D ratios at which the pressure taps and calorimeters are located are read in as initial data. Since the test section is maintained at a uniform temperature, no thermal expansion corrections to the non-dimensionalized displacements are necessary. Initially, the program converts and corrects the inlet and flowmeter gas temperatures, calculates a corrected mass flow rate and uses the expression

$$Re_o = 4\mathring{M}/\pi D\mu_o \qquad (5.1)$$

for the inlet Reynolds number where $\mathring{M}$ is the mass flow rate (lb_m/min). The inlet air density (assuming zero radial pressure variation) is calculated from the perfact gas law using the corrected inlet bulk temperature. For the tests using the adiabatic development section, the first pressure tap on the cooling section was used as the reference for the pressure drops. Friction factor data is measured from the point where cooling was assumed to commence. Since the pressure drop from the beginning of the adiabatic development section to the cooling section will be on the order of 0.5 in. of H_2O, the error in the density will be small from assuming the absolute pressure is equal to the inlet plenum pressure (about 20 psig). The inlet velocity,

$$U_o = 4M/\pi D^2 \rho_o \tag{5.2}$$

and Prandtl number Pr_o are calculated. An additional word should be mentioned concerning the precise points where the cooling and flow development were assumed to start. The initial point of temperature profile development was essentially the same for the two inlet sections. Modified 316 S.S. Gyrolok 3/8 inch to 1/4 inch tube fittings were used to connect the test and development sections. For the adiabatic development section, cooling was assumed to begin at the end of a small lip on the cooling section on which the ferrules for the connecting tube fitting clamped. Little was known about the type of thermal contact present, so for the UTV development section, a high conductivity epoxy was used to seal all fitting components. For this case, cooling was assumed to begin midway between the downstream face of the mixing plenum and the outside face of the test section bath. For both development sections the connection was insulated with MgO powder. Actually, the tube wall temperature will decrease along the connection from nearly inlet bulk temperature to 212 °F near the face of the cooling section. The difference in starting the cooling midway or at the lip is quite small, amounting to only a few percent difference in the location of the first calorimeter and pressure tap and almost indistinguishable in the graphs presented herein. However, the measured velocity profile for the bellmouth (Figure 45) shows that a finite velocity boundary layer thickness has developed at the end of the bellmouth. The point where the velocity field development begins was therefore taken upstream of this. In order to make this point correspond to a physical point on the test section, displacements of the pressure taps are measured from the upstream tip of the bellmouth.[6] The effect of

[6]A detailed measurement of the profile with a boundary layer probe might have allowed solving for an equivalent point from which a constant property layer would have reached the same displacement thickness. However, the difference between this approach and the present is not expected to be large.

this displacement for the pressure drop data for a UTV test run is shown in Figure 53.

A. Heat Transfer Data Reduction

The emf difference across each calorimeter is calculated and the tare emf difference is subtracted to leave the differential emf due only to heat transfer from the gas. The output from the thermocouple at the inner radius of each calorimeter is converted to a temperature (deg. F) and the tube wall temperature used in the Nusselt number is calculated from the one dimensional heat conduction equation in cylindrical co-ordinates;

$$T_w = T_i + \frac{(TT_i - TT_o)}{26.0} \frac{\ln(r_i/0.147)}{\ln(r_o/r_i)} \quad \text{(deg.F)} \qquad (5.3)$$

Subscript o refers to the mean radius at which the outer thermocouple is located and i refers to the inner thermocouple. The factor 26.0 represents the thermoelectric power of a Cu-Con thermocouple with reference junction at 32 °F and measuring junction at 212 °F obtained by a visual fit to plotted data in reference (62). TT refers to thermocouple output (mv) and 0.147 represents the inside radius of the test section (in.).

Provision is included in the program for the elimination of calorimeters whose thermocouples were giving spurious output. In such a case, this is noted on the data sheet. The position of the bad calorimeters were read into the data reduction program. If the response of only one of the pair of calorimeters at each axial position is poor, then the unit heat flux and wall temperature for that point are calculated solely from the good half. When both calorimeters are inoperative, the axial point is skipped altogether. This is usually indicated by a negative or obviously incorrect heat flux in the reduced data. During the testing for the Graetz b.c., the response of thermocouples in both calorimeters at the third axial location from the entrance were consistently spurious. Testing of these thermocouples showed that those giving poor response were not grounded to the test section. Although great care was taken in the composition of the electrical measuring system, this is undoubtably the cause of the trouble. An ungrounded thermocouple at the second axial position intermittently gave spurious output. A filter improved response somewhat for the UTV tests.

An important factor in the reduction of the heat transfer and friction data is the method by which the bulk gas temperature is evaluated at any axial point. For the case of gas heating, the usual experimental facility consists of a resistively heated tube for which the local rate of heat transfer to the gas at every point along the tube can be calculated fairly well once allowance is made for losses. In the present case, we are provided with the local heat transfer rates at discrete axial points rather than as a continuous function. The method of fitting a function $q_w^+(x^+)$ to the heat transfer data for each run was used. The curve may then be integrated to any axial point to obtain the net heat lost up to that point. This was applied for many assumed forms of $q_w^+(x^+)$. Candidate functions examined were those that could attain large magnitudes at the entrance with a rapid decay. Downstream the function had to approach zero asymptotically. Typical functions tested were combinations of exponentials and powers of x^+ with exponents less than 1. No function was found to be satisfactory for the data at all axial points. There are several problems associated with this method. With the exception of the first calorimeter location, the local heat transfer coefficients were found to be extremely sensitive to the form of the assumed function with the sensitivity increasing at the downstream calorimeter locations. Also, since the bulk temperature and hence the heat transfer coefficients at downstream positions depend upon the results from the upstream calorimeters, there will be an integration of errors. This can lead to a great relative error in the wall to bulk temperature difference when this latter quantity becomes small. This problem is magnified in some cases due to the absence of readings from the third calorimeter and the low differential outputs in the downstream region. An uncertainty analysis is presented in Appendix F which shows that the uncertainty in $Nu_{,m}$ at the second calorimeter is already of the order of 13%.

The test section was designed with a length to diameter ratio far in excess of that required for the laminar heat transfer tests. This was done so that tests could be performed at a later time over an adequate range of axial displacements for flow in the transition and turbulent regime[7]. It is possible, however, by varying the inlet Reynolds number to obtain a range of the modified Graetz parameter x^+ sufficient for comparison with the theoretical results. Values of x^+ obtained at the second calorimeter can be made to extend well into the theoretical fully developed region. Emphasis was therefore placed on the reduction of data from the first two calorimeters.

---

[7]For turbulent heat transfer, the problem of experimental uncertainty is somewhat reduced due to the high heat transfer rates which can be maintained further downstream. The high mass flow rates insure a much larger wall to bulk temperature difference and a lower drop in gas bulk temperature at a given displacement. In the experimental study by Brim (9) in an apparatus similar to that used here, but for turbulent flow, these problems were not as acute.

The bulk temperatures were finally evaluated by the integration of an analytical function fitted to the heat flux only at the first two calorimeters. A further restriction placed on the function was that this integrated flux should yield the bulk exit temperature as measured in the exit mixing chamber. It was required that the variation of the heat flux should closely approach the shape of the theoretical variation. Most important, it was necessary that when the function was fitted to theoretical values of the heat flux and bulk temperature for both boundary conditions, the theoretical $Nu_{,m}$ could be retrieved. This is important past the second calorimeter for evaluation of the local friction factor based on total wall shear stress. The fitting of the bulk temperature insures that the tail of the heat flux curve will not shoot off unbounded. Between the second and fifth calorimeters, the wall to bulk temperature differ ence is only on the order of 100 °F. Large relative errors in this difference make up only small errors in the absolute temperature level. The function which best satisfied these criteria out of nearly one hundred forms tested was;

$$q_w'' = F(x) = \frac{A}{\left(\frac{x}{D}\right)^{.45}} + \frac{B}{\left(\frac{x}{D}\right)^{.39}} + \frac{C}{\left(\frac{x}{D}\right)^{.25}} \qquad (5.4)$$

where the three constant A, B, and C are determined from

$$q_w''\Big|_{x=x_1} = F(x_1)$$

$$q_w''\Big|_{x=x_2} = F(x_2)$$

and

$$\mathring{M}\int_{T_o}^{T_{exit}} c_p dT = \pi\int_0^L q_w'' d(x/D)$$

where x_1, x_2 are the axial displacements of the first and second calorimeters respectively.

T_{exit} = exit gas temperature from downstream mixing plenum

L = total length of the test section

The specific heat was represented by a cubic polynomial in temperature.

$$c_p(T) = A(8) + B(8)T + C(8)T^2 + D(8)T^3$$

The bulk temperature $T_{m,x}$ at any x is evaluated from,[8]

$$M\int_{T_o}^{T_{m,x}} c_p(T)dT = A(8)T + \frac{B(8)T^2}{2} + \frac{C(8)T^3}{3} + \frac{D(8)T^4}{4}\Bigg|_{T_o}^{T_{m,x}} \tag{5.5}$$

$$= \pi\int_0^x F(x)d(x/D)$$

[8] For laminar flow the kinetic energy term $\rho_o U_o^2/2g_c J$ can be shown to be negligible.

This equation was solved for $T_{m,x}$(°K) by an iteration process in the computer program which stopped when successive values of T_{mx} differed by less than 1/4 deg. K. Next, the local heat transfer coefficient is calculated from

$$h = q''_w/(T_{m,x} - T_{w,x})$$

and the Nusselt number

$$Nu_m = hD/k_m$$

where k_m = thermal conductivity evaluated at bulk temperature $= 0.01395(A(7)+B(7)T_{m,x} + C(7)T_{m,x}^2 + D(7)T_{m,x}^3)$

Tw_x = wall temperature evaluated from equation 5.3

and the non-dimensionalized heat flux from

$$q_w^+ = q''_w r_o/k_o T_o$$

where To = inlet temperature (deg. R)

k_o = thermal conductivity (BTU/hr ft F)

Also, the local modified Graetz parameter at each calorimeter was evaluated from

$$x_m^+ = x^+ \left(\frac{c_{p,o}}{c_{p,m}}\right)\left(\frac{k_m}{k_o}\right) \tag{5.6}$$

The heat flux fit (5.4) was also used in the reduction of the friction factor and pressure drop data.

With the adiabatic development section in place, the dimensionless pressure drop is;

$$P = (p_o - p)/\rho_o U_o^2 \tag{5.7}$$

where p_o refers to the static pressure at the first tap location. Dimensionless displacements x^+ are measured with respect to this point. For the UTV boundary condition, the dimensionless pressure defect calculated is

$$P = (p_o - p - \tfrac{1}{2}\rho_o U_o^2)/\rho_o U_o^2 \qquad (5.8)$$

and, as mentioned previously, x^+ is measured from the forward tip of the bellmouth. The reference pressure p_o is the supply plenum static pressure. The term $\frac{1}{2}\rho_o U_o^2$ in the numerator of (5.8) is included to account for the acceleration of the gas from zero velocity in the supply plenum to U_o at the end of the bellmouth where the transition into the test section is completed.[9] Two types

[9] An attempt was made to determine the initial pressure drop experimentally since, due to velocity profile distortion in the bellmouth, the pressure drop may differ from $1/2(\rho_o U_o^2)$. It is assumed that this initial pressure drop can be written as $K\rho_o U_o^2$ where K is a constant which is a function of the bellmouth geometry. The pressure drop actually measured is $p_o' - p - K\rho_o U_o^2$ where $p_o' - p$ is the viscous parasitic pressure loss from the point where the bellmouth joins the section to the first pressure tap. It can be expected that the term $(p_o' - p)/\rho_o U_o^2$ will decrease with increasing Reynolds number. For large Reynolds numbers, the governing term will be K and if the total non-dimensionalized pressure drop is plotted as a function of x^+, it should approach K for small x^+ (high Re_o). For several isothermal high Reynolds number runs, the dimensionless pressure did seem to be approaching 1/2, but at a very slow rate. Large pressure fluctuations in the inlet plenum for high flow rates limited the maximum Reynolds number for which this test could be run.

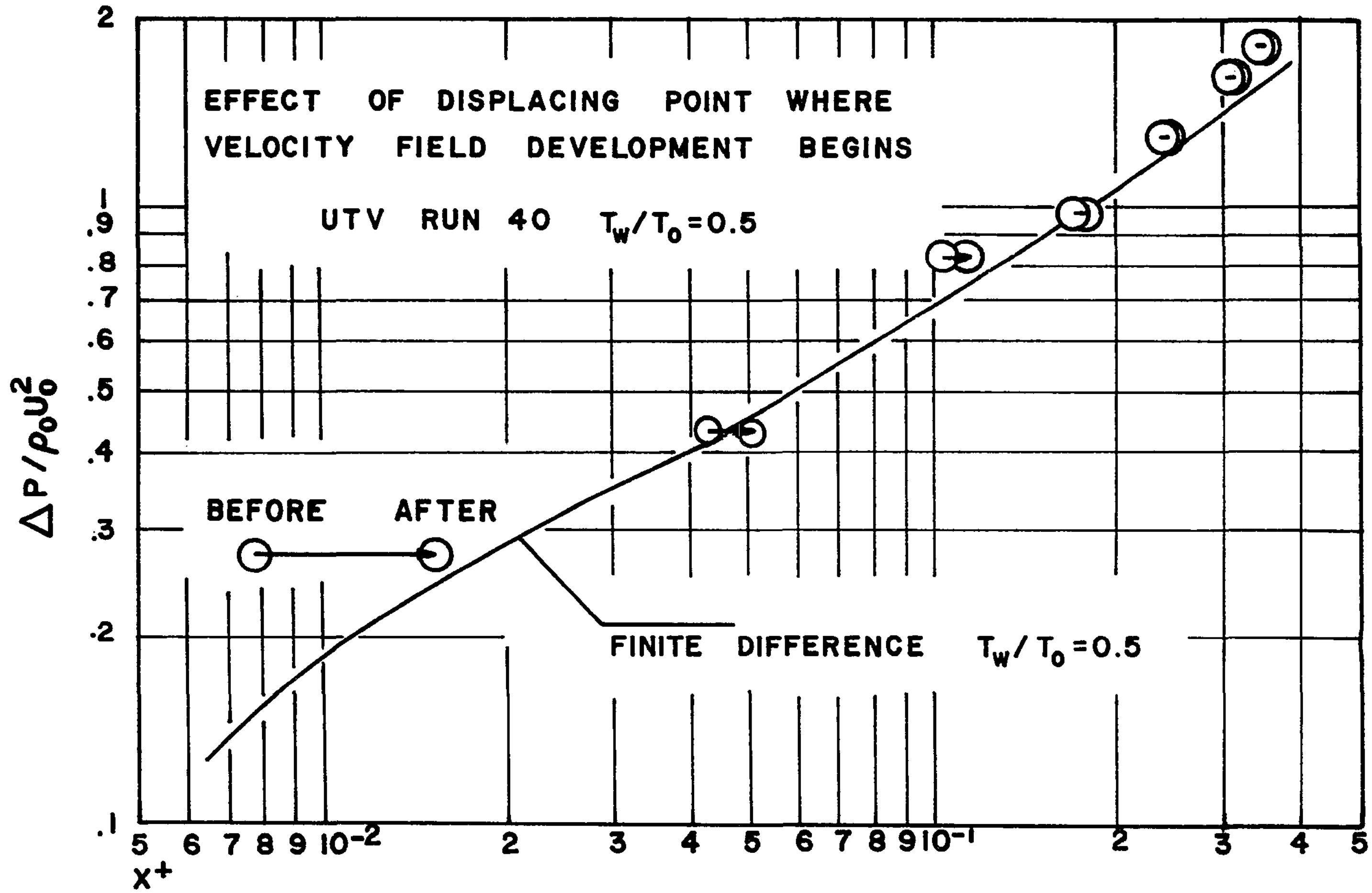

Figure 53. Effect on dimensionless pressure drop of displacing point at which flow development commences. UTV boundary condition.

of manometer fluids (specific gravities 0.826 and 0.797) were used during the experiment and an index JJ is included in the data reduction program to indicate which is used. The micromanomters were scaled to read directly in inches of H_2O when blue manometer fluid (s.g. 0.797) was used.

In addition to the dimensionless pressure drop, two types of local friction factor are calculated. The first is based on the portion of the total wall shear stress due to the static pressure drop only;

$$\tau_{w,\Delta p} = -\frac{r_o}{2}\frac{dp}{dx} \tag{5.9}$$

A corresponding friction factor $f_{,\Delta p}$ is defined in terms of the dimensionless pressure gradient by

$$f_{,\Delta p} = \frac{\tau_{w,\Delta p}}{\frac{1}{2}\rho_m U_m^2} = r_o \frac{\rho_m}{\rho_o}\frac{d}{dx}\left(\frac{p_o - p}{\rho_o U_o^2}\right) \tag{5.10}$$

and in terms of our non-dimensionalized variables.

$$f_{,\Delta p} Re_{,m} = \frac{1}{Pr_o}\left(\frac{dP}{dx^+}\right)\frac{\rho_m^+}{\mu_m^+} \tag{5.11}$$

The total wall shear stress is given by

$$\tau_w = \frac{-r_o}{2}\frac{d}{dx}+\left(p + C'\frac{G^2}{\rho_m g_c}\right) \tag{5.12}$$

and a local friction factor based on total wall shear stress by

$$f = \tau_w / \tfrac{1}{2}\rho_m U_m^2 = r_o \frac{\rho_m d}{\rho_o dx^+}\left(p - C' \frac{\rho_o}{\rho_m}\right) \qquad (5.13)$$

where G is the mean mass velocity which is a constant along the tube. The coefficient C' is defined by,

$$C' \equiv 2\int_0^1 \rho U^2 r^+ dr^+ / \rho_m U_m^2 \qquad (5.14)$$

and is a measure of the non-uniformity of the velocity profile. For a uniform profile, $C' = 1$ and for a parabolic profile $C' = 4/3$. A value of C' less than $4/3$ indicates a flattened profile. Since the experimental profiles will be undergoing development, C' is a function of x^+ and should be kept within the differential operator in equations 5.12 and 5.13. The actual value of C is known only at the entrance and approximately in the downstream regions-- it is not known at intermediate points. In the entrance for the fully developed inlet velocity, this momentum change due to profile development comprises a substantial portion of the total friction factor. For the UTV bondition, it is less important. For present purposes, C' was assumed constant at $4/3$ for the parabolic velocity profile since it will begin at this value and reapproach it in the downstream region.

For the UTV case, the actual C' will begin at 1 and also asymptotically approach 4/3. A value of $C' = 7/6$ which is midway between these limits was used in the data reduction.

In order to evaluate the derivative terms in 5.11 and 5.13, a third order least squares polynomial was fitted to the terms in the parenthesis at the pressure tap locations and differentiated. The bulk properties were evaluated at bulk temperatures obtained by using the same curvefit used in the heat transfer calculations. All densities correspond to inlet static pressure and local bulk temperature. Even though this approach would allow plotting of the friction factors as continuous functions of x^+, they are calculated and printed out only at the pressure tap locations. It is felt that this better reflects the experimental nature of the data.

Experimental inlet Mach numbers ranged from 0.009 to 0.023 which are somewhat less than that treated in the theoretical analysis(i.e. $M_o = 0.03$). For cooling, the Mach number based on the mean axial velocity will decrease along the tube. For example, for $T_w/T_o = 0.5$, the Mach number downstream of the thermal development region will be reduced by approximately 30% from its initial value. Compressibility effects were shown to be small in the theoretical analysis and are expected to have little effect on the experimental results.

CHAPTER 6. EXPERIMENTAL RESULTS

6.1. Graetz Boundary Condition

For both boundary conditions, heat transfer and pressure drop data for air was obtained for inlet wall to bulk temperature ratios of 0.6, 0.5 and 0.4 and pressure drop data only for the additional isothermal cases. For the Graetz boundary condition, the non-dimensionalized pressure defect P is shown plotted against x^+ in Figures 54, 55 and 56 along with the same quantity from the finite difference solution. This defect was considered as the best quantity for comparison for three reasons. 1.) The experimental defect requires the least amount of computational reduction. 2.) There is minimal dependence on additional experimental or inferred quantities such as the heat transfer and bulk temperature. 3.) The defect, rather than the wall shear stress, would be the most significant parameter to a designer. Similar to the friction factor, for laminar flow it is a function solely of x^+ for a given gas and θ_o, and hence, maintains the same generality.

In these plots one immediately notes that there is a pressure rise in the entrance for both the experimental and theoretical results. The reason is that when the gas undergoes cooling, the resulting increase in bulk density causes a net deceleration of the flow. If the

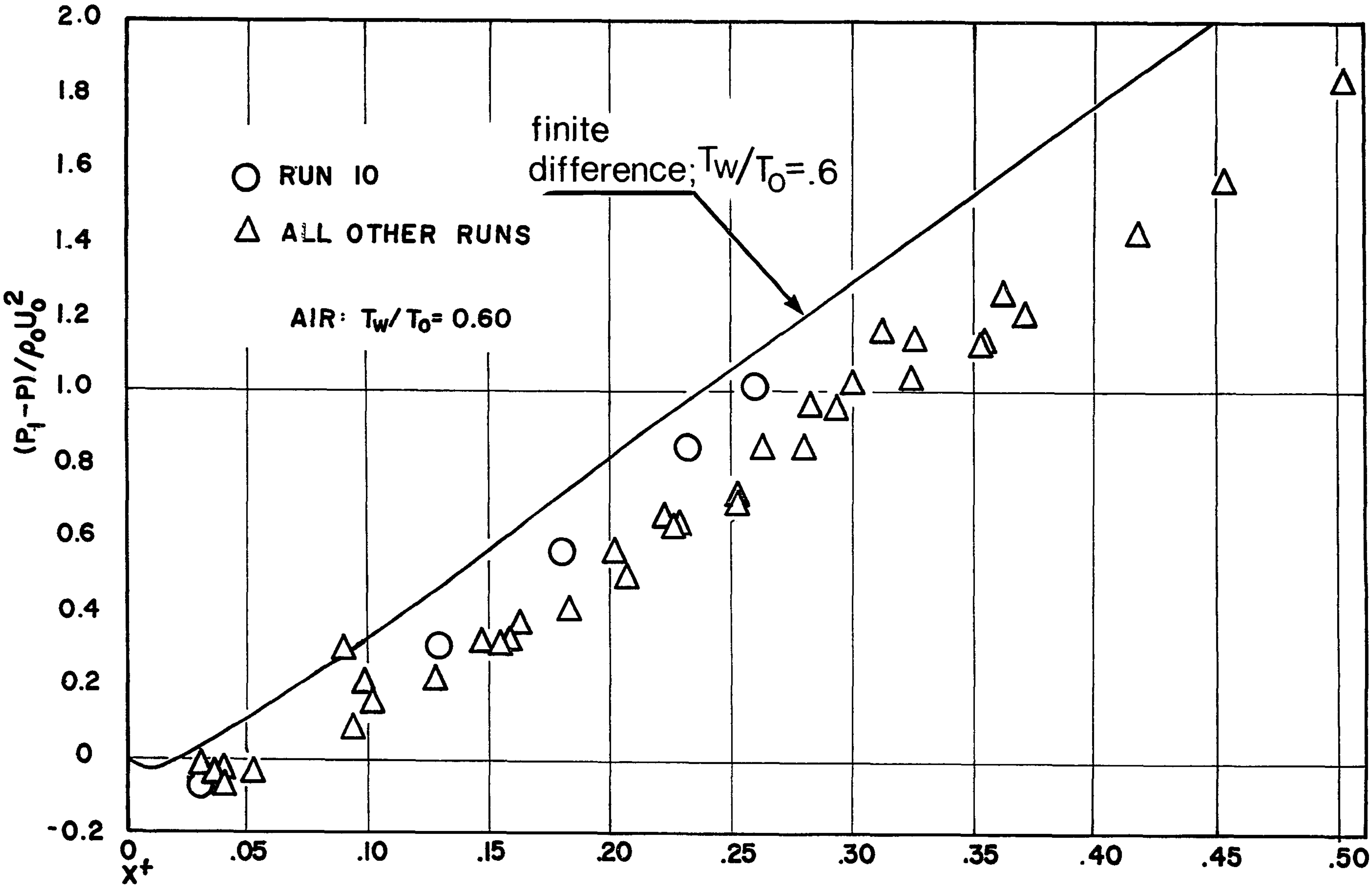

Figure 54. Experimental dimensionless pressure defect versus X^+. Air, Graetz boundary condition, $T_w/T_o = 0.60$

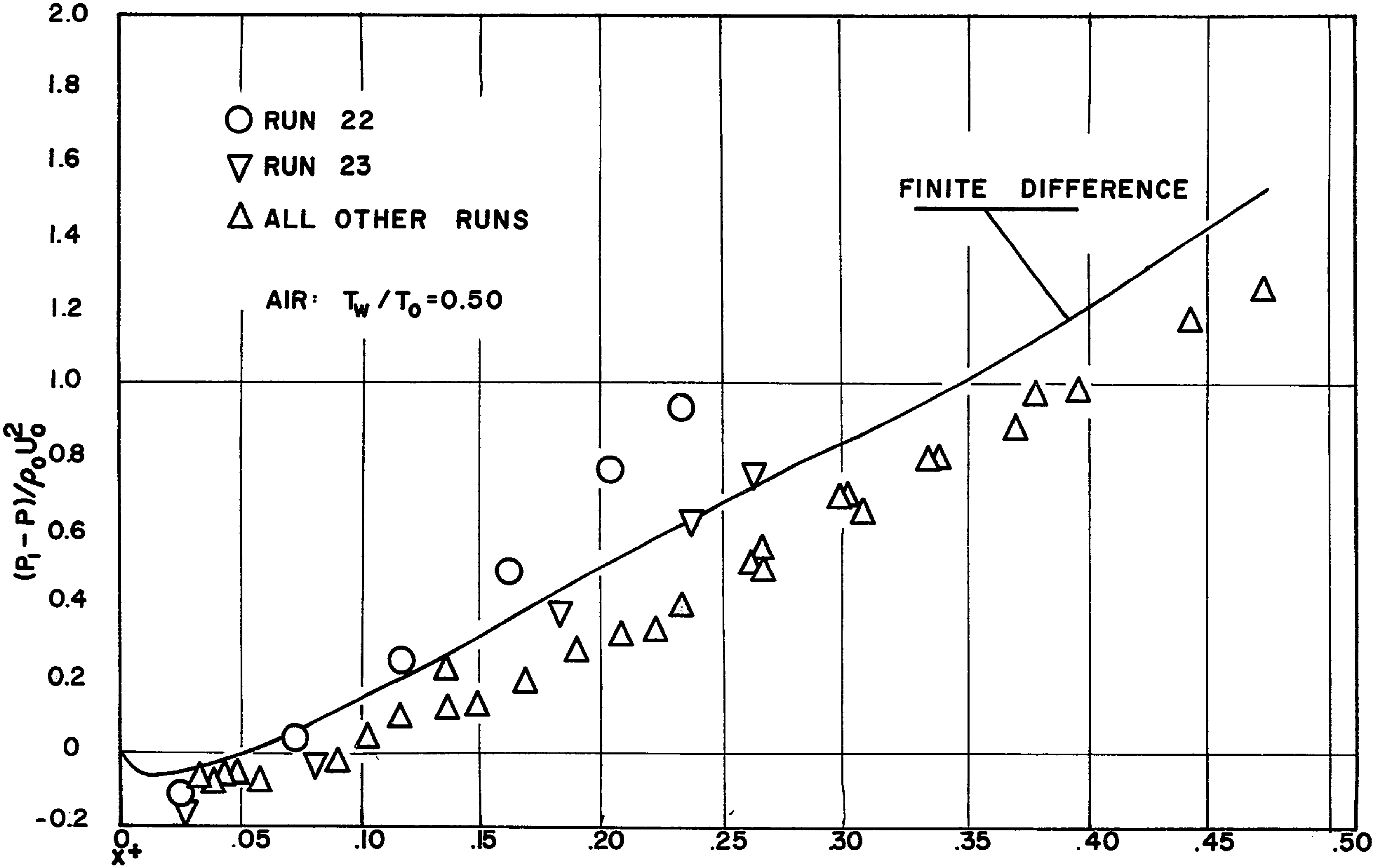

Figure 55. Experimental dimensionless pressure defect versus X^+. Air, Graetz boundary condition, $T_W/T_0 = 0.5$

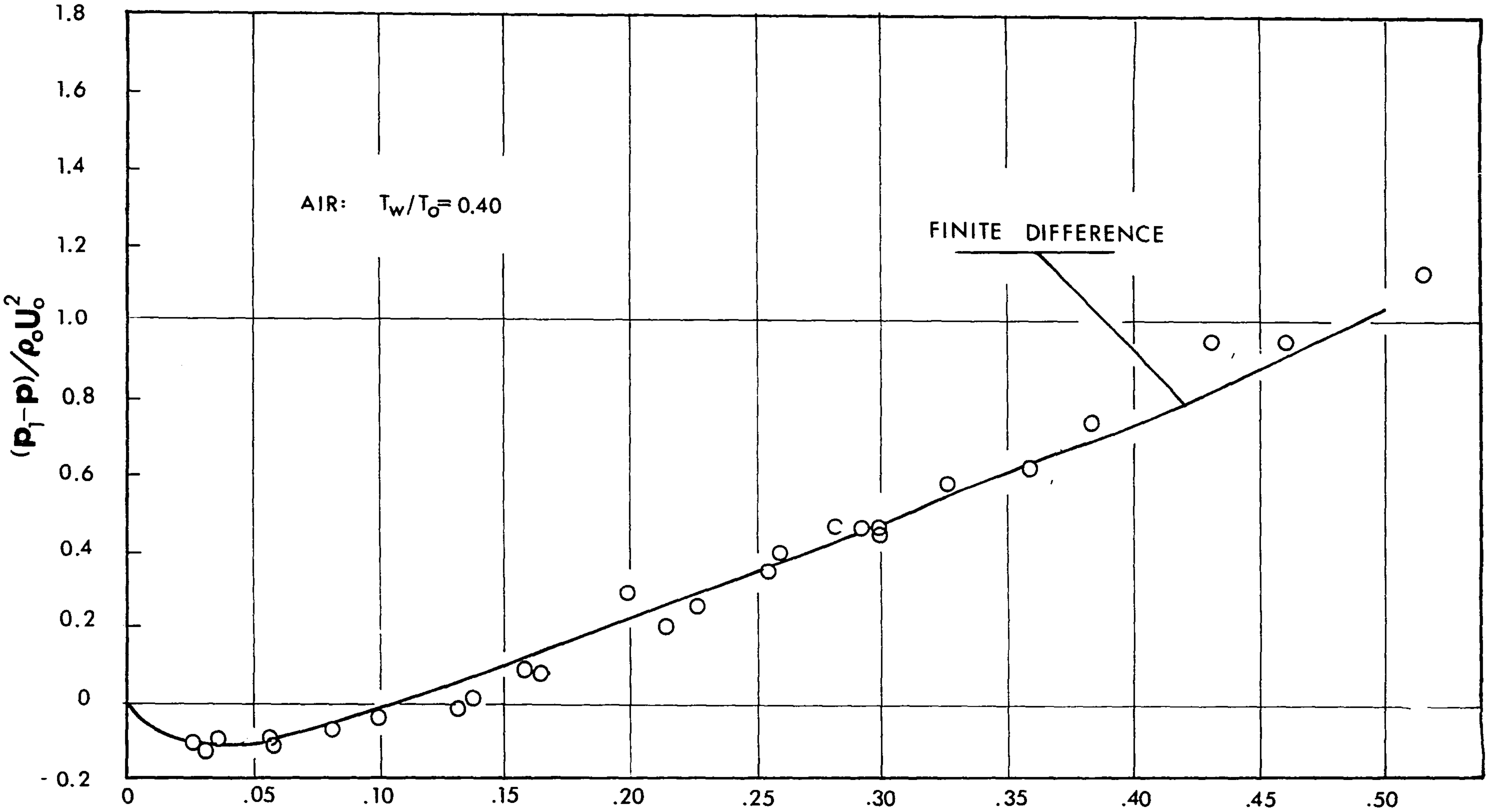

Figure 56. Experimental dimensionless pressure drop, Graetz boundary condition,

$T_w/T_o = 0.40$

cooling is severe enough, the deceleration pressure rise can be great enough to offset the frictional pressure drop. The experimental results show a pressure rise greater in magnitude and extending over a further displacement than the theory predicts. The pressure rise at the entrance has profound effect on the character of the flow. Separate curves diverging from the bulk of the data are shown in Figure 54 and 55 for some of the higher Reynolds number tests. Similar divergent data corresponding to high Reynolds number tests for the other wall to bulk temperature ratios was obtained. It should be noted that for gas cooling, the Reynolds number increases with axial distance. Although the data shown is for an inlet Reynolds number less than 2000, this magnitude will be exceeded at some point. All the results for several Re_o are seen to plot on single curves and no Reynolds number dependence is present. Evidently, the divergence of the pressure defect for the higher Reynolds number is the result of a transition to the turbulent regime. It is not possible to determine the precise point at which transition was triggered. It is interesting to note that the comparison between the theoretical and the experimental results improve as wall to inlet bulk temperature ratio decreases. The friction factor for these same tests for $T_W/T_O = 0.50$ and 0.40 are shown in Figure 57 and 58. The experimental $fRe_{,m}$ is

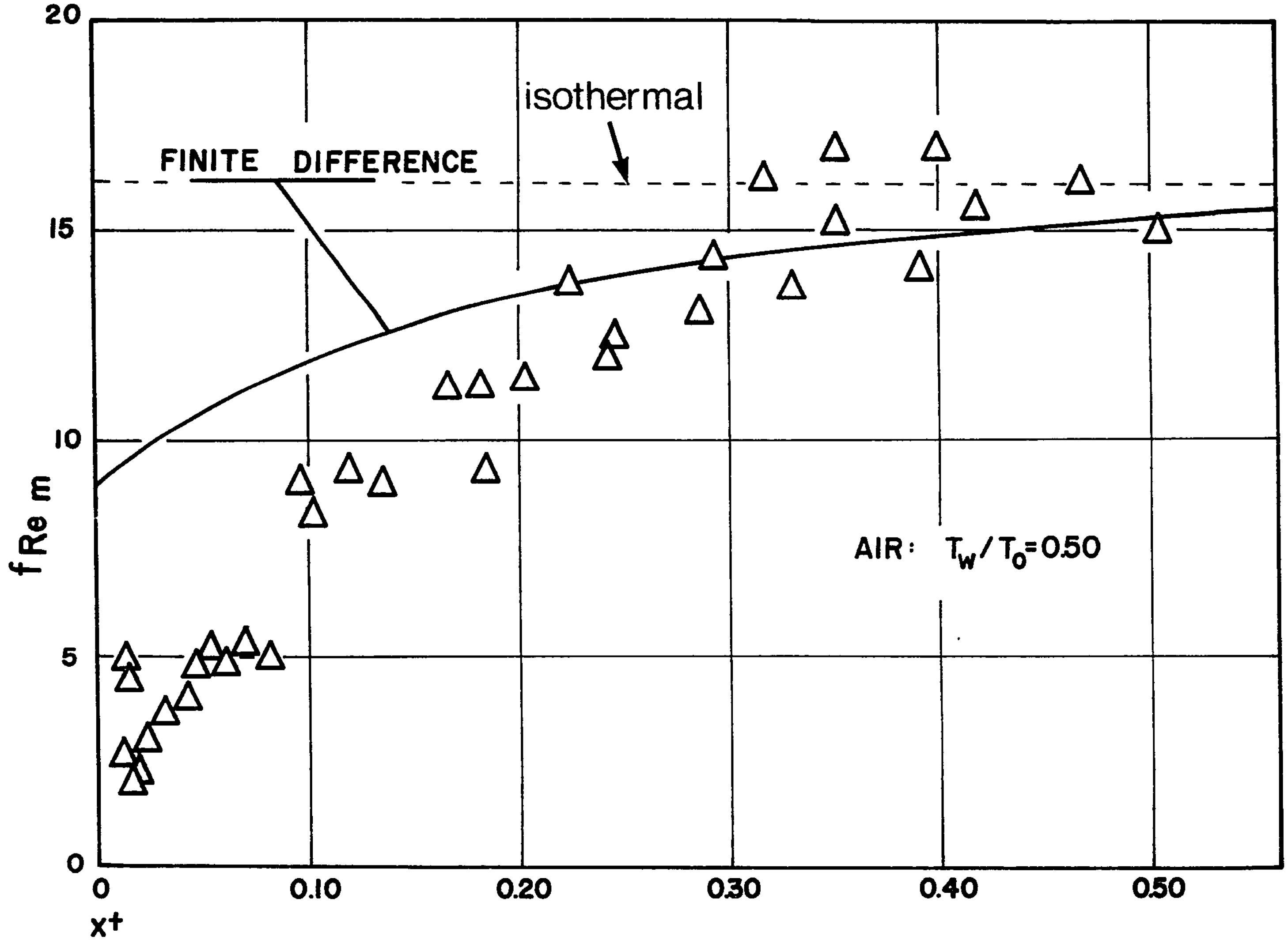

Figure 57. Experimental fRe_m versus x^+: Air, Graetz boundary condition, $T_W/T_O = 0.50$

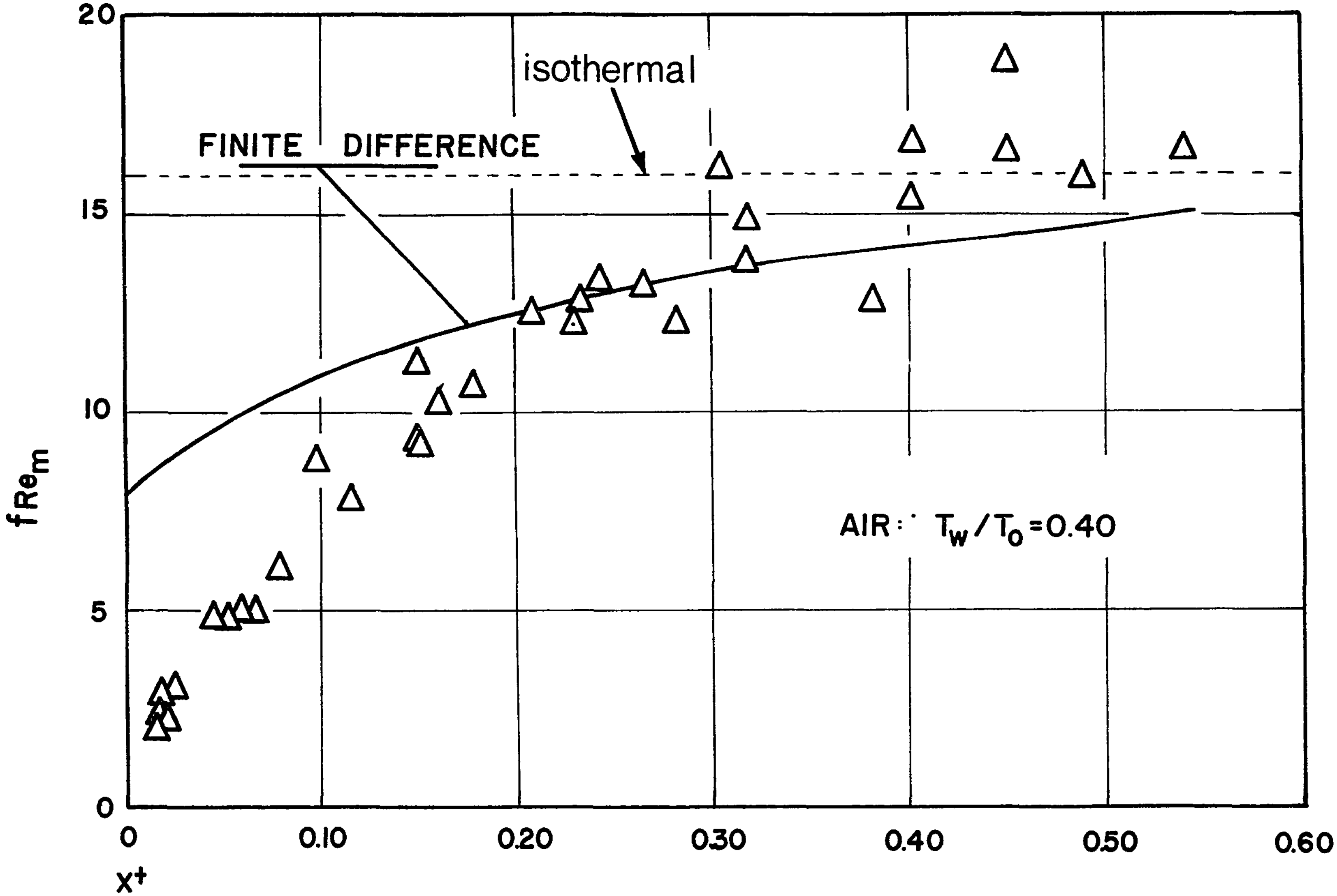

Figure 58. Experimental fRe_m versus x^+. Air, Graetz boundary condition, $T_w/T_o = 0.40$

much smaller in the entrance and increases at a much greater rate than the theoretical results for all temperature ratios. The fully developed $fRe_{,m}$ is reached more quickly than the theoretical in each case. Of necessity, the adiabatic development section was designed so as to be 0.009" smaller in diameter than the test section at room temperature. For the higher inlet temperatures, the adiabatic section will be at a higher temperature and will grow due to thermal expansion, so the transition between the two sections will become smoother. The increasing static pressure may have a profound effect in the presence of such a discontinuity. Another possible reason for this behavior may be the factor C' in equation 5.13 which may be underestimated by choosing C' = 4/3. This is not however, considered a probable reason since the theoretical velocity profiles for the Graetz condition show a distinct flattening with decreasing θ_w. This results in a value of C' closer to 1. Also, the pressure tap at the entrance is reading a static pressure along the wall. In a region of severe cooling and possible non-neglibible radial pressure gradient, this pressure may not be representative of the mean pressure existing across the radius. Since the radial velocity will be in a radially outward direction, we can reasonably expect that the static pressure will decrease from the centerline to the wall. If this is the case, then the pressure measured at the wall is underestimated so that pressure drops along the tube would also be underestimated and the magnitude of the pressure rise overestimated. Use of the mean pressure would tend to move the experimental and theoretical pressure drop and friction factor closer to each other.

The local Nusselt number data from the first two calorimeters are shown in Figure 59 for $\theta_w = 0.40$, 0.50 and 0.60 along with theoretical results for $\theta_w = 0.40$ and 0.60. Agreement is good, although the experimental results show more sensitivity to inlet temperature ratio. Also, the variation with x^+ is greater than the theoretical. This can be explained in terms of the configuration of the test section. There was a short, insulated section between the annular section of the development section and the cooling section. In the absence of heat transfer from the gas in this section, a linear temperature gradient could be expected. With gas flowing in the section, the average temperature of the section would probably increase. If the point at which cooling is assumed to commence is taken as the centroid of the temperature-displacement curve, this point would move downstream. This displacement would increase with higher flow rates and Reynolds numbers. In terms of the experimental results shown in Figure 59, the data

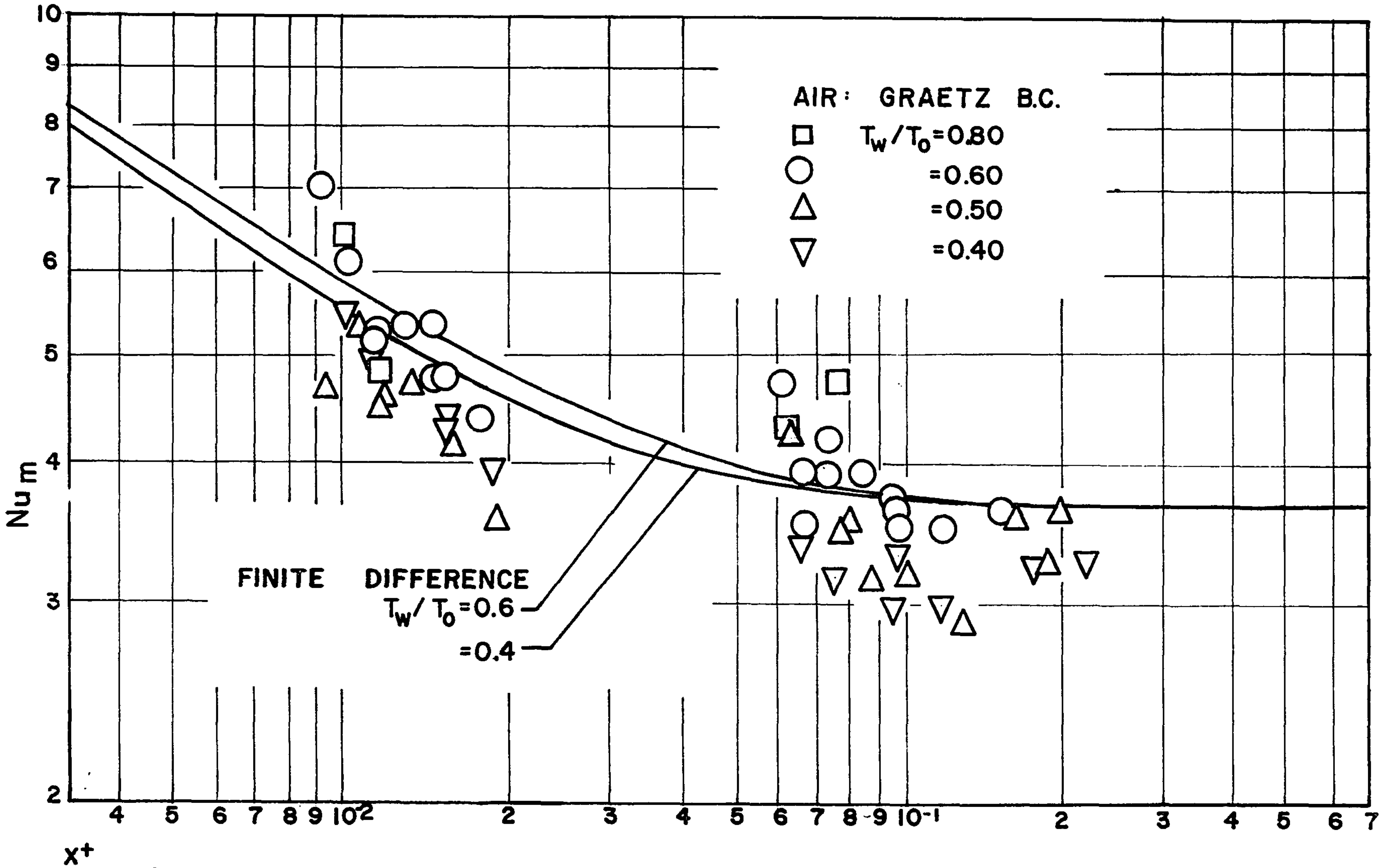

Figure 59. Experimental local $Nu_{,m}$ versus X^+. Graetz boundary condition.

points at the left side of each of the two data clusters correspond to higher Reynolds numbers than the other points. The displacement of these points from the point of cooling is reduced, so that these points should be displaced to the left. Since the abscissa is logarithmic, points in the left cluster will be affected more than those in the right hand cluster. The 'floating' point at which cooling starts will affect the results since the integration of the heat flux curve used to determine the bulk temperature begins at a fixed point.

The indeterminateness of the bulk temperature is not present in the comparison of theoretical and experimental dimensionless heat flux in Figure 60 for $\theta_w = 0.5$ and 0.6 and in Figure 61 for $\theta_w = 0.40$. Agreement is excellent with the exception of some low experimental points from the second calorimeter in Figure 62. Output was rather spurious from this calorimeter during this test series, but the data is included for completeness. These results would seem to indicate that the spread of the data for $Nu_{,m}$ may be due to the bulk temperature calculation.

6.2. UTV Boundary Condition

Non-dimensionalized pressure defect data for the UTV boundary condition is plotted in Figure 63 for $\theta_w = 0.60$, 0.50 and 0.40 along with theoretical results for $\theta_w = 0.50$.

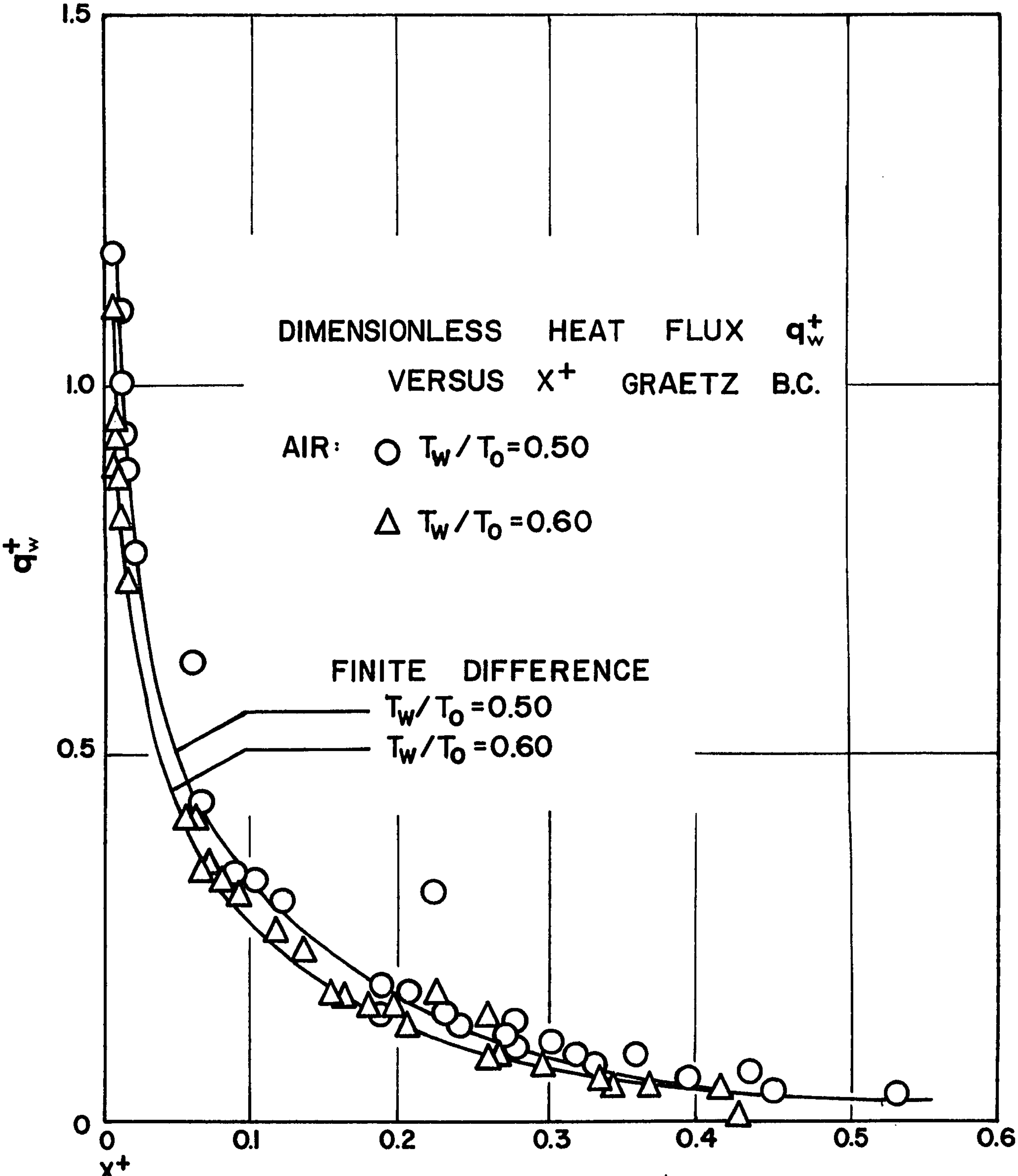

Figure 60. Experimental q_w^+ versus X^+ for air. Graetz boundary condition. T_W/T_O = 0.6, 0.5

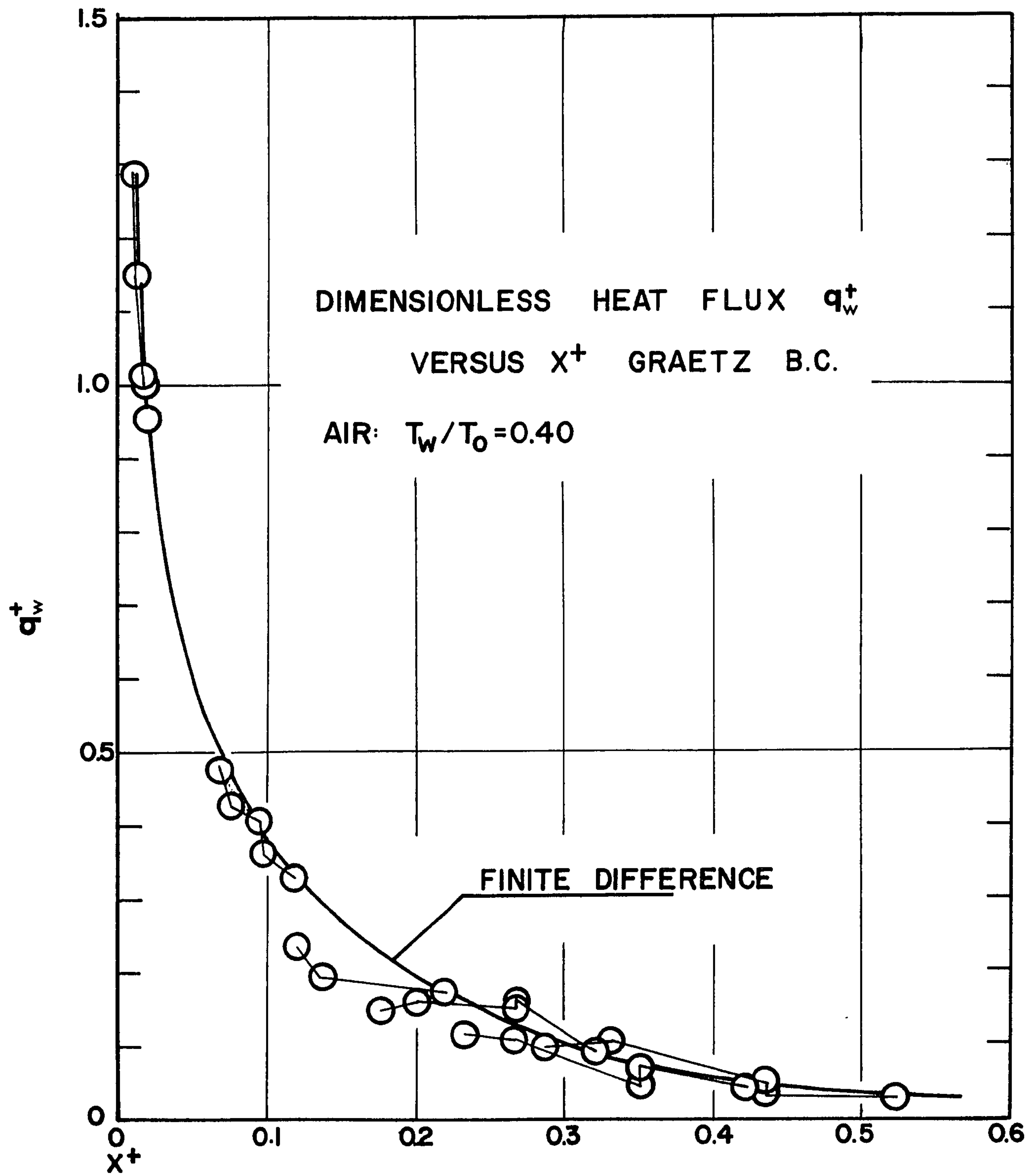

Figure 61. Experimental q_w^+ versus X^+ for air. Graetz boundary condition, $T_w/T_o = 0.40$

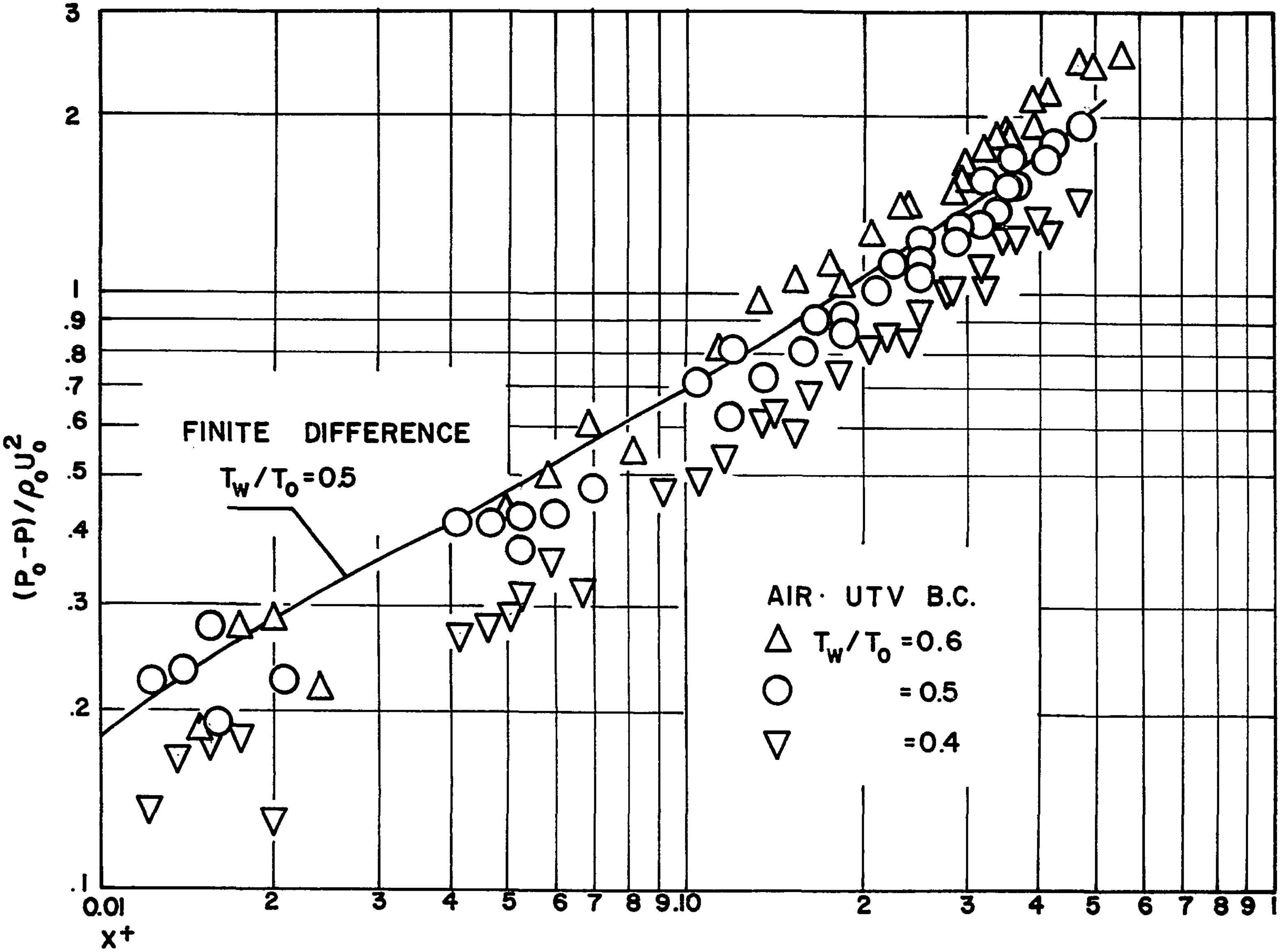

Figure 62. Experimental dimensionless pressure defect versus X^+ for air. UTV boundary condition. T_w/T_o 0.6, 0.5, 0.4.

The experimental results for $\theta_w = 0.50$ lie approximately 8% below the theoretical. It should be noted that for the UTV inlet geometry, the pressure drop is measured from the plenum. At the first pressure tap, it is possible that a radial pressure gradient exists. In this case, the deceleration of the flow at the wall and the inward radial velocity at the wall is indicative of a static pressure which decreases from wall to centerline. This means that the first pressure tap would be reading relatively high. Using the mean pressure across the section would result in a higher pressure drop from the plenum to the first tap. Although the situation at the first tap is reversed from what it was in the Graetz boundary condition, use of a mean pressure would again move the experimental results closer to the theoretical.

Friction factor results are shown in Figure 63. Theoretical results are for $\theta_w = 0.50$ are included for comparison. Agreement is very good. It should be noted that the use of a mean or lower pressure at the first tap would tend to raise the friction factor slightly at the first pressure tap ($x^+ < 0.022$) and lower the data at $x^+ \sim 0.05$. This would make the comparison even better. In the downstream region ($x^+ > 0.2$) the effect of temperature ratio is small, but somewhat greater than the theory predicts. This may be partially due to

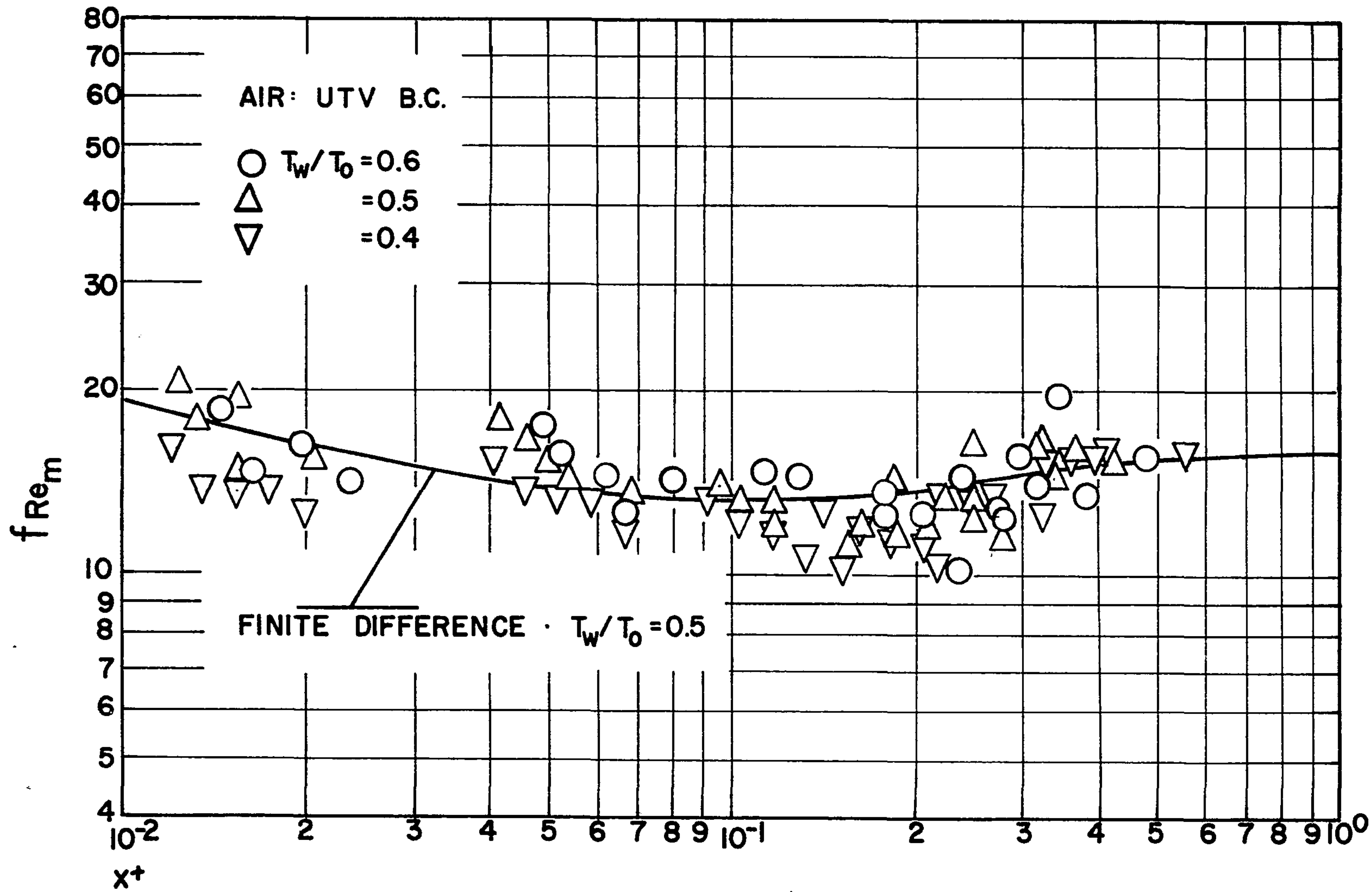

Figure 63. Experimental $fRe_{,m}$ versus X^+ for air. UTV boundary condition.

T_W/T_O = 0.6, 0.5, 0.4.

use of a value of C' (1 1/6) in equation 5.13 which is lower than the actual values in this region. Further downstream, the axial variation of density will be so small that the correct asymptotic value of $fRe_{,m}$ would still be reached. It should be noted that friction factor data at the last pressure tap (#7) was not included in the results. Values of the friction factor at this tap for the isothermal flow tests were found to be about 20% high. Similar results were obtained at this tap during the cold flow tests. Since this tap is so far downstream, it is highly unlikely that the actual $fRe_{,m}$ at this point differs by more than a few percent from 16.0.

Local $Nu_{,m}$ is shown in Figure 64. The exaggerated variation with x^+ of the data in each cluster is probably due to the variation of wall temperature in the transition from the plenum to the test section. The darkened data points are for run #44 and the uncertainty interval for this run is indicated. This was discussed in section 5.1. A more direct comparison of theoretical and experimental data is included in the axial variation of plotted in Figure 65 for all the experimental UTV data. Again, for run #44, data points are darkened and the uncertainty interval is shown. The data falls a maximum of approximately 35% below the theoretical. Data from the third calorimeter from the entrance (which was

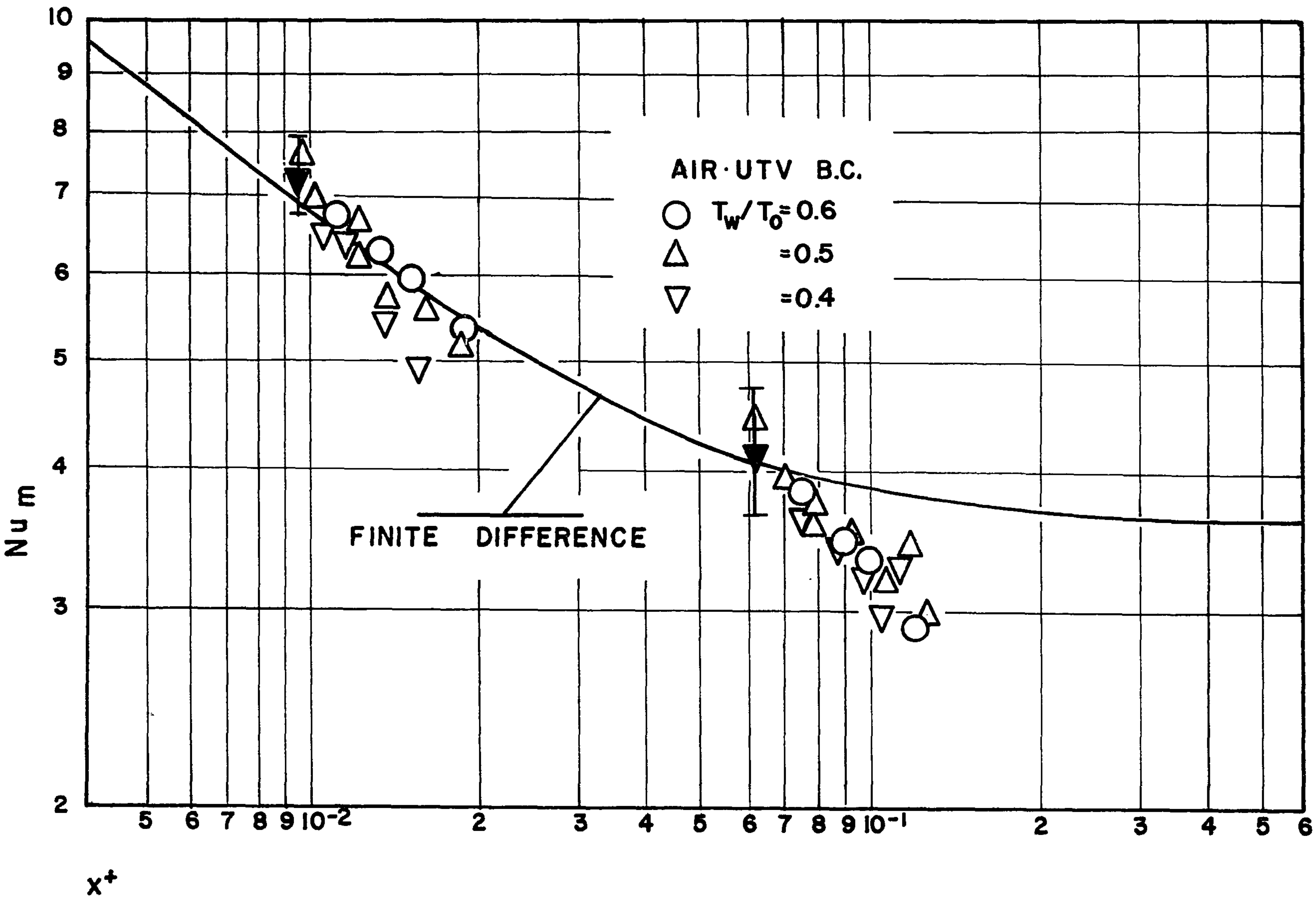

Figure 64. Experimental $Nu_{,m}$ versus X^+ for air. UTV boundary condition, T_w/T_o = 0.6, 0.5, 0.4.

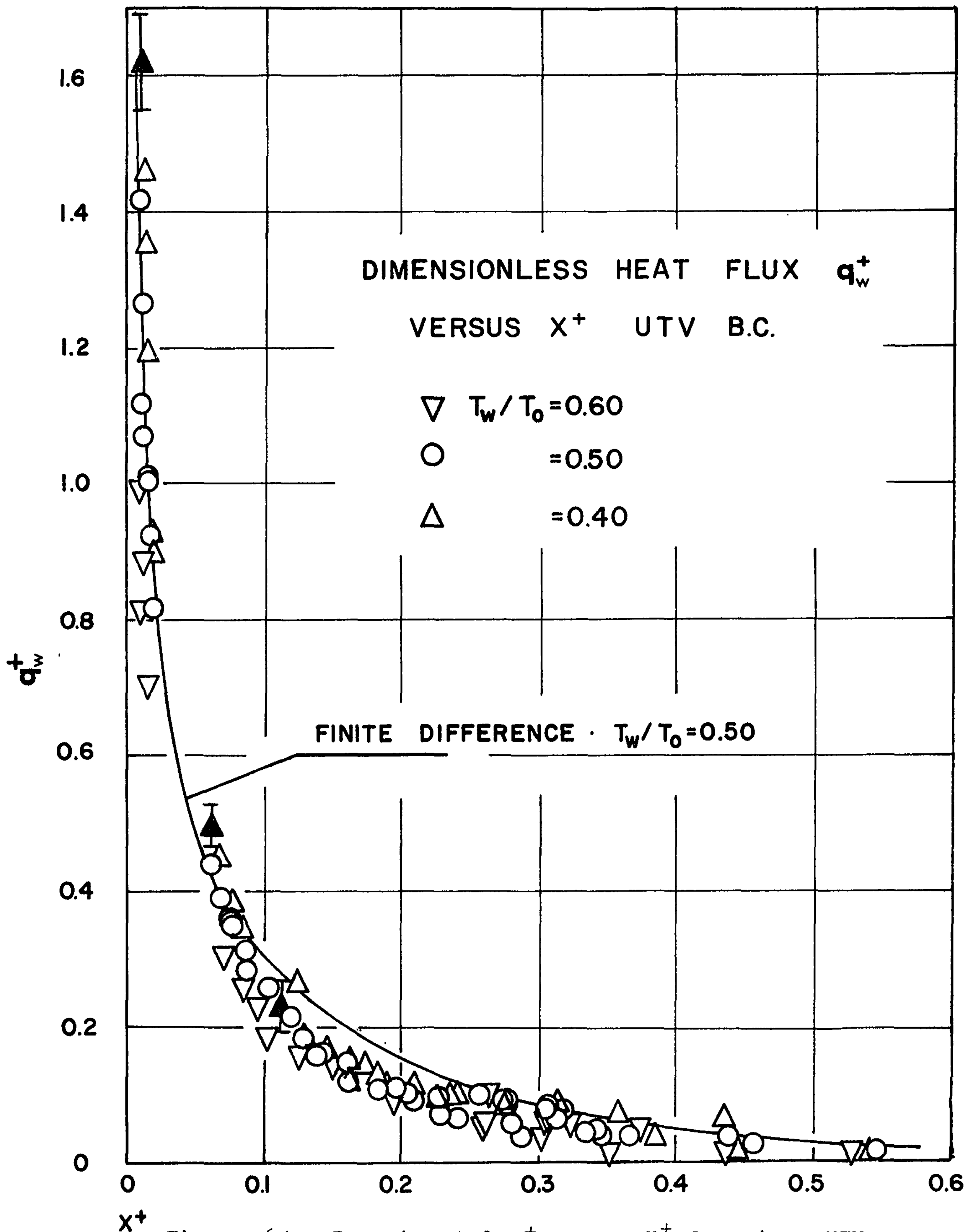

Figure 65. Experimental q_w^+ versus X^+ for air. UTV boundary condition. T_W/T_O = 0.6, 0.5, 0.4

not operative during most of the testing for the Graetz b.c.) was relatively low for those tests in which it was operative. It is hard to argue that this difference is due to an error in one calorimeter (for example-- a low calibration of the conductance of the third calorimeter) since the transition of data between neighboring calorimeters is continuous and the data is consistently lower. Also, the good results obtained from the calorimeters for the Graetz b.c. would add confidence to the calibration.

CHAPTER 7. SUMMARY AND CONCLUSIONS

7.1. Summary

The results of a combined experimental and analytical investigation of heat transfer and flow characteristics for the laminar flow of gases in cylindrical tubes at low wall to bulk temperature ratios has been presented. For the theoretical analysis, gas transport and thermodynamic properties were treated as variable. It was possible to modify an existing finite difference solution to the boundary layer equations with property variation terms for use in cooling cases. For the case when inlet temperature and velocity profiles were uniform, the conditions for similar thermal and velocity variable property boundary layers to exist at the tube wall were found to be closely obtained for small distances from the tube entrance. An entrance region solution based on the similarity assumption was patched to the finite difference solution and downstream convergence of the wall parameters from the finite difference solution was seen to be significantly improved. This improvement is believed due to reduced error in maintaining net conservation of energy in the presence of initial singularities in both the thermal and velocity boundary conditions. Wall friction and heat transfer results obtained for air and helium can be best discussed in four categories.

7.2. Conclusions

7.2.1. Heat Transfer (Graetz Boundary Condition)

Theoretical heat transfer results as expressed in the axial variation of the Nusselt number for fully developed inlet velocity profiles were found to be relatively insensitive to temperature ratio. Experimental Nusselt number and dimensionless heat flux, q_w^+ data for air supports this conclusion. Maximum variation of the theoretical Nu_m from the isothermal Nu_m occurring at an inlet wall to bulk temperature ratio of 0.10 was found to be a decrease of approximately 13% for air and 15% for helium. The theoretical axial variation of Nu_m can be correlated within ± 5% by the following equations:

<u>for air</u>: $(0.001 \leq x^+ < 0.35)$

$$Nu_m = (3.67 + 0.198x^{+^{-.584}} e^{-20.8x^+})\ (1-0.13(\theta_w-1))$$

<u>for helium</u>: $(0.001 \leq x^+ < 0.35)$

$$Nu_m = (3.67 + 0.201x^{+^{-.584}} e^{-20.8x^+})(1-0.15(\theta_w-1))$$

<u>for both gases</u>: $(x^+ > 0.35)$

$$Nu_m = 3.67$$

7.2.2. Friction Factor (Graetz Boundary Condition)

Friction factors for fully developed inlet velocity profiles are affected more severely by temperature ratio, but the experimental and theoretical results are not in agreement as to the degree of this variation. Experimental friction factors and pressure drops were significantly lower in the entrance than the theoretical. This may have been due to several factors. A pressure rise in the entrance in the presence of a discontinuity in the tube diameter may have changed the character of the flow in this region. The theoretical variation of the total friction factor is well represented by the following equation:

$$fRe_m = 16\left(\frac{T_w}{T_m}\right)^a \quad \text{where} \quad \begin{array}{l} \text{for air:} \\ \text{for helium:} \end{array} \begin{cases} a=0.904(T_w/T_o)^{.257} \\ a=0.957(T_w/T_o)^{.251} \end{cases}$$

This correlation is offered with the reservation that it does not represent the experimental variation.

7.2.3. Heat Transfer (UTV Boundary Condition)

For the UTV boundary condition, the theoretical Nusselt number, Nu_m, was found to be almost totally insensitive to cooling throughour the flow development region. Constant property correlations for friction factor are recommended. In the entrance region this behavior could have been predicted, at least on a qualitative basis, by variable property external boundary layer results for cooling (23). Entrance effects predominate throughout the thermal development region and correlation in terms of local significant temperature ratios was not possible. The experimental heat transfer data confirmed these results in the entrance region where experimental uncertainties were smallest, but in the mid and downstream region, experimental values of the local heat flux were found to be about 30% below the predicted. The difference is not within the estimated uncertainty and the consistency of the data is difficult to explain. A single correlation applies to the theoretical variation of Nu_m for helium and air at all wall to bulk temperature ratios:

$$Nu_m = 3.67 + 0.246x^{+^{-.592}} e^{-20.6x^+} \qquad (0.001 \leq x^+ < 0.5)$$

$$Nu_m = 3.67 \qquad (x^+ \geq 0.5)$$

This is offered with the reservation that it does not represent the downstream experimental data well.

7.2.4. Friction Factor (UTV Boundary Condition)

Again, the small variation of the friction factor with temperature ratio at the entrance could have been predicted from variable property external boundary layer results. However, the axial pressure gradient has a greater weight in the momentum equation than on the energy equation. This gradient was found to be strongly effected by temperature ratio along with a greater sensitivity of the flow characteristics to temperature ratio. The flow development region was found to be substantially lengthened with extreme cooling. Maximum decrease of the friction factor-Reynolds product for air and helium was approximately 45%. Excellent agreement between theoretical and experimental pressure drop and friction factor variation was obtained for the UTV boundary condition. The theoretical friction factor results for air and helium are well correlated by:

$$1-(fRe_m)/(fRe)_I = 1.067(1-\theta_w)x^{+\frac{1}{4}}\, e^{-\beta x^+} \qquad (x^+>0.001)$$

where $\beta = 7.70\theta_w^{0.675}$

and $(fRe)_I$ = isothermal friction factor-Reynolds number product, $(fRe)_I = 16.0 + 0.694x^{+^{-.576}}\, e^{-22.9x^+}$

In general, for both boundary conditions, friction factor and flow characteristics for both gases were found to be much more sensitive to temperature ratio than heat transfer results. In an absolute sense, variation of all theoretical wall parameters were found to be relatively insensitive to temperature ratio when the severity of the cooling is considered. The modified Graetz parameter based on inlet properties was deemed a better independent variable for representation of the results than x_m^+ which is based on local properties evaluated at the mean temperature.

REFERENCES

1. Atkins, G.T., Some Special Cases of Laminar Flow Heat Transfer, Preprint 57a, A.I.Ch.E., 1965

2. Back, Lloyd H., Effects of Surface Cooling and Heating on Structure of Low Speed, Laminar Boundary Layer Gas Flows with Constant Free Stream Velocity, Technical Report 32-1301, Jet Propulsion Laboratory, Pasadena, 1968

3. Bahadori, M.N. and Soo, M., "Non Equilibrium Transport Phenomenon of Partially Ionized Argon," Int. Jour. of Heat and Mass Transfer, Vol. 9, 1966

4. Bankston, C.A. and McEligot, "Calculation of Heat Transfer to Gases with Varying Properties in the Entry Region of Circular Ducts," Int. Jour. of Heat and Mass Transfer, Vol. 13, No. 2, 1970

5. Bankston, C.A. and D.M. McEligot, Calculation of Heat Transfer to Gases Flowing in a Circular Tube with Arbitrary Wall Heat Flux Distributions, Report LA-4154, Los Alamos Scientific Laboratory, 1969

6. Bankston, C.A. and D.M. McEligot, A Numerical Method for Solving the Boundary Layer Equations for Gas Flow with Transfer and Property Variations, Report LA-4149, Los Alamos Scientific Laboratory, 1969

7. Bergman, P.D. and L.B. Koppel, "Uniform Flux Heat Transfer to a Gas in Laminar Forced Convection in a Circular Tube," A.I.Ch.E., Vol. 12, No. 4, 1966

8. Bradley, D. and A.G. Entwistle, "Developed Laminar Flow Heat Transfer from Air for Variable Physical Properties," Int. Jour. of Heat and Mass Transfer, Vol. 8, 1965

9. Brim, Larry Hyde, Turbulent Heat Transfer in a Circular Tube at High Bulk to Wall Temperature Ratio: An Experimental Study, Ph.D. Thesis, Institute for Plasma Research, Stanford University, 1969

10. Cann, G.L., Energy Transfer Processes in a Partially Ionized Gas, GALCIT Memo No. 61, Gugenheim Aeronautical Laboratory, California Institute of Technology, June 1961

11. Cebeci, T. and A.O. Smith, A Finite Difference Method for Calculating Laminar and Turbulent Boundary Layers, A.S.M.E. Paper No. 70-WA/HT-34, 1970

12. Cholette, S., See Ref. 30

13. Crane, P.C. and P.A. Fox, "Desub - Integration of a First Order System of Ordinary Differential Equations," Numerical Mathematics Computer Library 1, Vol. 2, Issue 1, Bell Telephone Laboratories, 1969

14. Crane, P.C. and P.A. Fox, "A Comparative Study of Computer Programs for Integrating Differential Equations," Numerical Mathematics Computer Programs - Library 1, Vol. 2, Issue 2, Bell Telephone Laboratories, 1969

15. Christiansen E.B. and H.E. Lemmon, "Entrance Region Flow," A.I.Ch.E., Vol. 11 No. 6, 1965

16. Codegone, C., "The Air Convection Coefficients in Pipes from 400 to 70 700 C," Proc. of the General Discussion on Heat Transfer, Inst. of Mech. Engrs., 1951

17. Dalle Done, M. and F.H. Bowditch, "High Temperature Heat Transfer, Nuclear Engr., Vol. 8, 1963

18. Davenport, M., The Effect of Transverse Temperature Gradients on the Heat Transfer and Friction for Laminar Flow of Gases, Ph.D. Thesis, Department of Mechanical Engineering, Stanford University, 1962

19. Davenport, M.E. and G. Leppert, "The Effect of Transverse Temperature Gradients of the Heat Transfer and Friction for Laminar Flow of Gases," Trans. A.S.M.E., Jour. of Heat Transfer, Ser. C, Vol. 87, 1965

20. Deissler, R.G., Analytical Investigation of Fully Developed Laminar Flow in Tubes with Heat Transfer with Fluid Properties Variable Along the Radius, NACA TN 2410

21. Deissler, R.G. and A.L. Loeffler, Jr., "Heat Transfer and Friction for Fluids Flowing Over Surfaces at High Temperatures and High Velocities," Trans. A.S.M.E., Jour. of Heat Transfer, Ser. C., Vol. 81, 1959

22. Deissler, R.G. and A.F. Presler, "Analysis of Developing Laminar Flow and Heat Transfer in a Tube for a Gas with Variable Properties," Proc. of the Third International Heat Transfer Conference, Vol. 1, 1966

23. Dewey, C.F. Jr. and J.F. Gross, "Exact Solutions of the Laminar Boundary Layer Equations," Advances in Heat Transfer (Hartnett, J.P. and T.F. Irvine -eds.), Vol. 4, 1967

24. Drew, T.B., "Mathematical Attacks on Forced Convection Problems," Amer. Inst. of Chem. Engrg., Vol. 26, 1931

25. Eckert, E.R.G. and E. Pfender, "Advances in Plasma Heat Transfer," Advances in Heat Transfer (Hartnett, J.P. and T.F. Irvine -eds.), Vol. 4, 1967

26. Emmons, H.W., "Recent Developments in Plasma Heat Transfer," Mod. Dev. in Heat Transfer (W. Idele -ed.), Academic Press, 1963

27. Emmons, H.W., "Plasma Heat Transfer," Proc. of the Annual Meeting of the A.S.M.E., (Clark, J.A. -ed.) Pergamon, 1963

28. Gambill, W.R., "An Evaluation of Recent Correlations for High Flux Heat Transfer," Chemical Engineering, Aug. 1967

29. Gorton, C.W., K.R. Purdy, and C.J. Bell, "Non-Isothermal Velocity Profiles," A.I.Ch.E. Journal, Vol. 9, No. 1, 1963

30. Goryainov, L.A., V.A. Beilin, and V.A. Pavlenko, "Determination of the Reynolds Number in Heat Transfer Relations," Progress in Heat Transfer, (Konakov, P.K. -ed.), Consultant Bureau, New York, 1966

31. Graetz, L., "Uber die Wärmeleitungsfähigkeit von Flussigkeiten," Anneler d. Physik, Vol. 25, 1885

32. Hilsenrath, J., C.W. Beckett, W.S. Benedict, L. Fano, H.J. Hoge, J.F. Masi, R.L. Nuttall, Y.S. Touloukian, and H.W. Woolley, Tables of Thermal Properties of Gases, National Bureau of Standards, Circular 564, 1955

33. Hirschfelder, J.O., C.F. Curtiss and R.B. Bird, Molecular Theory of Gases and Liquids, Wiley, New York, 1954

34. Hornbeck, R.W., An All Numerical Method for Heat Transfer in the Inlet of a Tube, A.S.M.E. Preprint 65-WA/HT-36, 1965

35. Hornbeck, R.W., "Laminar Flow in the Entrance Region of a Pipe," Appl. Sci. Res., Vol. 13, 1964

36. Hsu, C., "An Exact Mathematical Solution for Entrance Region Laminar Heat Transfer with Axial Conduction," Appl. Sci. Res., Vol. 17, 1967

37. Hughes, W.F. and E.W. Gaylord, Basic Equations of Engineering Science, McGraw Hill, New York, 1964

38. Incropera, F.P., N.W. Bower and R.L. Kingsburg, Numerical Studies of Internal Equilibrium Flows of Plasmas, A.S.M.E. Paper 69-WA/HT-55, 1969

39. Incropera, F.P. and G. Leppert, "Laminar Flow Heat Transfer from an Argon Plasma in a Circular Tube," Int. Jour. of Heat and Mass Transfer, Vol. 10, 1967

40. Jakob, M., Heat Transfer, John Wiley, 1959

41. Johnson, J.R., N.M. Choksi, and P.T. Eubank, "Entrance Heat Transfer from a Plasma Stream in a Circular Tube," IEEC Process Design and Development, 7, 1968

42. Kays, W.M., "Numerical Solutions for Laminar Flow Heat Transfer in Circular Tubes," Trans. A.S.M.E., Vol. 77, 1955

43. Kays, W.M. and W.B. Nicoll, "Laminar Flow Heat Transfer to a Gas with Large Temperature Differences," Trans. A.S.M.E., Jour. of Heat Transfer, Ser. C., Vol. 85, 1963

44. Kays, W.M., Convective Heat and Mass Transfer, McGraw Hill, 1958

45. Kettleborough, C.F., Poiseuille Flow with Variable Fluid Properties, A.S.M.E. Paper No. 66-WA/Fe-22, 1966

46. Kline, S.J. and McClintok, "Describing Uncertainties in Single Sample Experiments," Mechanical Engineering, Jan., 1953

47. Knudson, J.G. and D.L. Katz, Fluid Dynamics and Heat Transfer, McGraw Hill, 1958

48. Koppel, L.B. and J.M. Smith, "Laminar Flow Heat Transfer for Variable Physical Properties," Trans. A.S.M.E. Jour. of Heat Transfer, Ser. C, Vol. 84, 1962

49. Kreith, F., Radiation Heat Transfer for Spacecraft and Solar Power Plant Design, International Textbook, Scranton, 1967

50. Kreith, F., Principles of Heat Transfer, International Textbook, Scranton, 1965

51. Kroll, C.L., Heat Transfer and Pressure Prop. for Air Flowing in Small Tubes, ScD Thesis, MIT, 1951

52. Langhaar, H.L., "Steady Flow in the Transition Length of a Straight Tube," Trans. A.S.M.E., Vol. 64, 1942

53. Larkin, B.K., "High Order Eigenfunctions of the Graetz Problem," A.I.Ch.E. Journal, Vol. 7, No. 3, 1961

54. Lick, Wilbert J. and H.W. Emmons, Transport Properties of Helium from 200 to 50,000 K, Cambridge, Harvard University Press, 1965

55. Lipkis, R.P., Heat Transfer to an Incompressible Fluid in Laminar Motion, M.S. Thesis, University of California, Los Angeles, 1954

56. Magee, P.M., The Effect of Large Temperature Gradients on Turbulent Flow of Gases in the Thermal Entrance Region of Tubes, Ph.D. Thesis, Department of Mechanical Engineering, Stanford University, 1965

57. Manohar, R., "Analysis of Laminar Flow Heat Transfer in the Entrance Region of Circular Tubes," Int. Jour. of Heat and Mass Transfer, Vol. 12, No. 1, 1970

58. McAdams, W.H., Heat Transmission, McGraw-Hill, New York, 1954

59. McEligot, D.M., Effect of Large Temperature Gradients on Turbulent Flow of Gases in the Downstream Region of Tubes, Ph.D. Thesis, Department of Mechanical Engineering, Stanford University, 1963

60. McEligot, D.M., P.M. Magee and G. Leppert, "Effect of Large Temperature Gradients on Convective Heat Transfer: The Downstream Region," Trans. of ASME, Jour. of Heat Transfer, Ser. C., Vol. 87, 1965

61. Mori, Y., K. Futagami, S. Tokuda and M. Nakamura, "Forced Convection Heat Transfer in Uniformly Heated Horizontal Tubes," Int. Jour. of Heat and Mass Transfer, Vol. 9, 1966

62. National Bureau of Standards, Reference Tables for Thermocouples, Circular 561, 1955

63. Newell, P.H. and A.E. Bergles, "Analysis of Combined Free and Forced Convection for Fully Developed Laminar Flow in Horizontal Tubes," Trans. ASME, Jour. of Heat Transfer, C, 92, 1970

64. Perkins, H.C. and P. Worsoe-Schmidt, "Turbulent Heat and Momentum Transfer for Gases in Circular Tubes at Wall to Bulk Temperature Ratios to Seven," Int. Jour. of Heat and Mass Transfer, Vol. 8, 1965

65. Petukhov, B.S., V.V. Kirillov, and V.N. Maidanik, "Heat Transfer Experimental Research for Turbulent Gas Flow in Pipes at High Temperature Difference between Wall and Bulk Fluid Temperature," Proc. of the Third International Heat Transfer Conference, Vol. 1, 1966

66. Pigford, R.L., "Non-Isothermal Flow and Heat Transfer Inside Vertical Tubes," Chem. Engrg. Prog. Symp., No. 17 Vol. 51, 1955

67. Pinkel, R.L., "A Summary of NACA Research on Heat Transfer and Friction for Air Flowing Through Tubes with Large Temperature Differences," Trans. ASME, Vol. 76, 1954

68. Poisson, S.D., Theorie Mathematique de la Chaleur , Bachilier, Paris, 1835

69. Poots, G. and M.H. Rogers, "Laminar Flow between Parallel Flat Plates, with Heat Transfer, of Water with Variable Physical Properties," Inst. Jour. of Heat and Mass Transfer, Vol. 8, 1965

70. Poppendick, H.F., "Heating and Cooling Solutions for Viscous Liquid Flow in Pipes," Heat Transfer, Thermodynamics and Education, Pergamon, (Johnson, H.A. -ed.), 1955

71. Ralston, A., A First Course in Numerical Analysis, McGraw Hill, 1965

72. Reshotko, E. and C.B. Cohen, Similar Solutions for the Compressible Laminar Boundary Layer with Heat Transfer and Pressure Gradient, NACA Rep. 1294, 1956

73. Rosenberg, D.E. and J.D. Hellums, "Flow Development and Heat Transfer in Variable Viscosity Fluids," I. & E.C. Fundamentals, Vol. 4, No. 4, 1965

74. Schade, K.W. and D.M. McEligot, "Cartesian Graetz Problems with Air and Property Variations," Int. Jour. of Heat and Mass Transfer, Vol. 14, 1971

75. Scheele, G.F. and T.J. Hanratty, "Effect of Natural Convection Instabilities on Rates of Heat Transfer at Low Reynolds Numbers," A.I.Ch.E. Journal, Vol. 9, No. 2, 1963

76. Schenk, H., Theories of Engineering Experimentation, McGraw Hill, New York, 1961

77. Schmidt, P.S. and G. Leppert, Heat Transfer from Plasma in Tube Flow, ASME Paper 69-WA/HT-54, 1970

78. Seaborg, G.T. and J.L. Bloom, "Fast Breeder Reactors," Scientific American, Vol. 223, No. 5, 1970

79. Sellars, J.R., M. Tribes and J.S. Klein, "Heat Transfer to Laminar Flow in a Round Tube or Flat Conduit - The Graetz Problem Extended," Trans. ASME, Vol. 78, 1956

80. Siegel, R., E.M. Sparrow and T.M. Hallman, "Steady Laminar Heat Transfer in a Circular Tube with Prescribed Heat Flux," Appl. Sci. Res., A7, 1958

81. Siegwarth, D.P., R.D. Mikesell, T.C. Readal, T.J. Hanratty, "Effect of Secondary Flow on the Temperature Field and Primary Flow in a Heated Horizontal Tube," Int. Jour. of Heat and Mass Transfer, Vol. 12, 1969

82. Singh, S.N., "Heat Transfer by Laminar Flow in Cylindrical Tube," Appl. Sci. Res., 1958

83. Skrivan, T.F. and W. Von Jaskowsky, "Heat Transfer from Plasmas to Water Cooled Tubes," I. & E.C. Process Design and Development 4, 1965

84. Slaby, J.G., W.L. Maag and B.L. Siegel, Laminar and Turbulent Hydrogen Heat Transfer and Friction Coefficients over Parallel Plates at 5000 R, NASA TN D-2435, 1964

85. Smith, A.M.O., "Rapid Laminar Boundary Layer Calculations by Piecewise Application of Similar Solutions," Jour. of Aerospace Science, 23, 1956

86. Swearingen, T.B., Internal Laminar Heat Transfer to a Gas with Temperature Dependent Properties, Ph.D. Thesis, Engineering Experiment Station, Arizona University, Tucson, 1969

87. Sze, B.C., The Effect of Temperature Dependent Properties on Heat Transfer in Circular Tubes, Ph.D. Thesis, Stanford University, 1957

88. Taylor, M.F. and T. A. Kirchgessener, Measurements of Heat Transfer and Friction Coefficients for Helium Flowing in a Tube at Surface to Temperatures up to 5900 F, NASA TN-D-133, 1959

89. Taylor, M.F., Experimental Local Heat Transfer Data for Precooled Hydrogen and Helium at Surface Temperatures up to 5300 R, NASA TN-D-2595, 1965

90. Taylor, M.F., "A Method of Correlating Local and Average Friction Coefficients for both Laminar and Turbulent Flow of Gases through a Smooth Tube with Surface to Fluid Bulk Temperature Ratios from 0.35 to 7.35," Int. Jour. of Heat and Mass Transfer, Vol. 10, 1967

91. Taylor, M.F., A Method of Correlating Local and Average Friction Coefficients for both Laminar and Turbulent Flow of Gases through a Smooth Tube with Surface to Fluid Bulk Temperature Ratios from 0.35 to 7.35, NASA, TR-R267, 1967

92. Tyagi, V.P., "Heat Transfer and Skin Friction in a Channel: Laminar Flow with Variable Physical Properties," Int. Jour. of Heat and Mass Transfer, Vol. 8, 1965

93. Ulrichson, D.L. and R.A. Schmitz, "Laminar Flow Heat Transfer in the Entrance Regions of Circular Tubes," Int. Jour. Heat and Mass Transfer, Vol. 8, 1965

94. Vines, R.G., "Measurement of Thermal Conductivity of Gases at High Temperatures," Trans. ASME, Jour. of Heat Transfer, Ser. C, Vol. 82, 1960

95. Volluz, R.J., "Wind Tunnel Instrumentation and Operation," Handbook of Supersonic Aerodynamics, Section 20 NAVORD Report 1488, Vol. 6, 1961

96. Watson, V.R. and E.B. Pegot, Numerical Calculations for the Characteristics of a Gas Flowing through a Constricted Arc, NASA TN-D-4042, 1967

97. Weiland, W.F. and W.H. Lowdermilk, Measurement of Heat Transfer and Friction Coefficients for Air Flow in a Tube Length-Diameter Ratio of 15 at High Surface Temperature, NACA RM E-53E04, 1953

98. Wethern, R.J. and R.S. Brodskey, "Heat and Momentum Transfer in Laminar Flow: Helium at Plasma Temperatures," A.I.Ch.E. Journal, Vol. 9, No. 1, 1963

99. Woff, H., "Heating and Cooling Air and Carbon Dioxide in the Thermal Entrance Region of a Circular Duct with Large Gas to Wall Temperature Differences, Trans. ASME, Journal of Heat Transfer, Sec. C, Vol. 81, 1959

100. Worsoe-Schmidt, P.M., Finite Difference Solution for Laminar Flow of Gas in a Tube at High Heating Rate, Ph.D. Thesis, Department of Mechanical Engineering, Stanford University, 1965

101. Worsoe-Schmidt, P.M., "Heat Transfer and Friction for Laminar Flow of Helium and Carbon Dioxide in a Circular Tube at High Heating Rate", Int. Jour. of Heat and Mass Transfer, Vol. 9, 1966

102. Worsoe-Schmidt, P.M., Personal Communication, March 7, 1969

103. Yang, K., "Laminar Forced Convection of Liquids in Tubes with Variable Viscosity," Trans. ASME, Journal of Heat Transfer, Ser. C., Vol. 84, 1962

104. Zellnik, H.E. and S.W. Churchill, "Convective Heat Transfer from High Temperature Air Inside a Tube," A.I.Ch.E., Vol.4, No. 1, 1958

Appendix A

Variable Property and Non-Boundary Layer Terms

When the full momentum and energy equations 2.2 and 2.3 are non-dimensionalized with the same variables that were used to non-dimensionalize the boundary layer equations in Chapter 2, the following forms result;

Axial momentum:

$$\rho^+\left(U^+\frac{\partial U^+}{\partial x^+}+V^+\frac{\partial U^+}{\partial r^+}\right)=-\frac{P_o}{\rho_o U_o^2}\frac{\partial P}{\partial x^+}+2Pr_o\mu^+\frac{\partial^2 U^+}{\partial r^{+2}}+2Pr_o\left[\frac{\partial U}{\partial r^+}\frac{\partial \mu^+}{\partial r^+}+\frac{1}{(Re_oPr_o)^2}\left\{\frac{\partial}{\partial r^+}\mu^+\frac{\partial V}{\partial x^+}\right.\right.$$

$$\left.\left.+\frac{4}{3}\frac{\partial}{\partial x^+}\mu^+\frac{\partial U^+}{\partial x^+}-\frac{2}{3r^+}\frac{\partial}{\partial x^+}\mu^+\frac{\partial(r^+V^+)}{\partial r^+}\right\}\right]$$

Energy equation;

$$\rho^+\left(U^+\frac{\partial H_1^+}{\partial x^+}+V^+\frac{\partial H_1^+}{\partial r^+}\right)=(1-\gamma_o)M_o^2U^+\frac{\partial P}{\partial x^+}+\frac{2}{(Re_oPr_o)^2}\frac{\partial}{\partial x^+}\frac{k^+}{c_p^+}\frac{\partial H_1^+}{\partial x^+}+\frac{2}{r^+}\frac{\partial}{\partial r^+}r^+\frac{k^+}{c_p^+}\frac{\partial H_1^+}{\partial r^+}$$

$$+2(\gamma_o-1)M_o^2Pr_o\mu^+\Phi^+$$

where Φ^+ = mechanical dissipation function

$$=\left[\left(\frac{\partial U}{\partial r^+}\right)^2+\frac{2}{(Re_oPr_o)^2}\left\{\left(\frac{\partial V^+}{\partial r^+}\right)^2+\left(\frac{V}{r^+}\right)^2-\frac{2}{3}\left(\frac{\partial V^+}{\partial r^+}+\frac{V}{r^+}\right)^2\right\}\right]$$

We note that as the Reynolds number decreases, the importance of the dissipation function as usually defined $\left(\frac{\partial U^+}{\partial r^+}\right)^2$ will decrease in relation to the other terms in the function, However, if the decrease in Reynolds number is due to a decrease in the mass flow rate, the decrease in M_o^2 will offset this rise. The term which is retained in the momentum boundary layer equation and can be identified as being due to property variation (excepting the density) is

$$2 Pr_o \frac{\partial u^+}{\partial r^+}\frac{\partial \mu^+}{\partial r^+}$$

The ratio of the non-boundary layer terms to this is,

$$R_1 = \frac{\frac{\partial}{\partial r^+}\mu^+\frac{\partial v^+}{\partial x^+} + \frac{4}{3}\frac{\partial}{\partial x^+}\mu^+\frac{\partial u^+}{\partial x^+} - \frac{2}{3}\frac{\mu^+}{r^+}\frac{\partial (r^+v^+)}{\partial r^+}}{(Re_o Pr_o)^2 \frac{\partial \mu^+}{\partial r^+}\frac{\partial u^+}{\partial r^+}}$$

Using the power law representation for viscosity!

$$\mu^+ = \theta^b$$

This becomes

$$R_1 = \frac{b\theta^{b-1}\frac{\partial \theta}{\partial r^+}\frac{\partial v^+}{\partial x^+} + \theta^b\frac{\partial^2 v^+}{\partial r^+\partial x^+} + \frac{4}{3}\left(b\theta^{b-1}\frac{\partial \theta}{\partial x^+}\frac{\partial u^+}{\partial x^+} + \theta^b\frac{\partial^2 u^+}{\partial x^{+2}}\right) - \frac{2}{3}\mu^+\frac{\partial (r^+v^+)}{\partial r^+}}{(Re_o Pr_o)^2 b\theta^{b-1}\frac{\partial \theta}{\partial r^+}\frac{\partial u^+}{\partial r^+}}$$

Similarly, expanding the ratio of the non-boundary layer terms in the energy equation to the property variation terms (neglecting the dissipation function),

$$R_2 = \frac{\frac{\partial}{\partial x^+}\frac{k^+}{c_p}\frac{\partial H_1^+}{\partial x^+}}{(Re_o Pr_o)^2\left(\frac{\partial H_1^+}{\partial r^+}\frac{\partial (k^+/c_p)}{\partial r^+}\right)} = \frac{1}{(Re_o Pr_o)^2}\;\frac{\left((c-a)\frac{\partial \theta}{\partial x^+}\frac{\partial H_1^+}{\partial x^+} + \theta\frac{\partial^2 H_1^+}{\partial x^+}\right)}{(c-a)\frac{\partial \theta}{\partial r^+}\frac{\partial H_1^+}{\partial r^+}}$$

The ratio of molecular to convective axial momentum transfer is

$$R_3 = \frac{2 Pr_o}{(Re_o Pr_o)^2}\;\frac{\frac{\partial}{\partial x^+}\left(\mu^+\frac{\partial u^+}{\partial x^+}\right)}{\rho^+u^+\frac{\partial u^+}{\partial x^+}} = \frac{2\left(b\theta^{b-1}\frac{\partial \theta}{\partial x^+}\frac{\partial u^+}{\partial x^+} + \theta^b\frac{\partial^2 u^+}{\partial x^{+2}}\right)}{(Re_o Pr_o)^2\rho^+u^+\frac{\partial u^+}{\partial x^+}}$$

and the ratio of molecular conduction to axial convective heat transfer is;

$$R_4 = \frac{2}{(Re_o Pr_o)^2}\;\frac{\frac{\partial}{\partial x^+}\left(\frac{k^+}{c_p}\frac{\partial H_1^+}{\partial x^+}\right)}{\rho^+u^+\frac{\partial H_1^+}{\partial x^+}}$$

The radial and axial derivatives were evaluated by using central difference operators and values of dependent variables from the finite difference solution with $\Delta x^+ = 10^{-4}$ and $\Delta r^+ = 1/320$.

Appendix B

Gas Thermodynamic and Transport Properties

Data was drawn from several sources in the evaluation of transport and thermodynamic properties for air, helium and CO_2. The exponents in the power law representation with temperature were chosen so as to minimize the least square error for all reference points (subscript zero) in the desired ranges. In a usual least squares fit to N tabulated values of a property Y, the quantity

$$E=\sum_{i=1}^{n}\left(\frac{Y_i}{Y_o}-\left(\frac{T_i}{T_o}\right)^{exp}\right)^2$$

would be minimized by appropriate choice of exp. Subscript 0 quantities are reference values. However, in the present investigation the quantity which was minimized in most instances was

$$E=\sum_{k=1}^{n}\left\{\sum_{i=1}^{n}\left(\frac{Y_i}{Y_k}-\left(\frac{T_i}{T_k}\right)^{exp}\right)^2\right\}$$

which means that the exponent is also an optimum with respect to all reference points in the tabulated range. An exponent chosen by such a criterion will differ somewhat from that chosen by a ordinary least squares fit or a visual fit to plotted data. Properties which did not require the use of a reference quantity, namely Pr_o and γ_o were chosen by an ordinary least squares criterion. In several cases data from more than one source is plotted in order to extend the temperature range or to serve as a confirmation of data from the prime source. Graphical plots of the data are given in Figures 66,67 and 68 for helium, air and CO_2 respectively. The correlations used in the theoetical portion of the investigation are represented by solid lines.

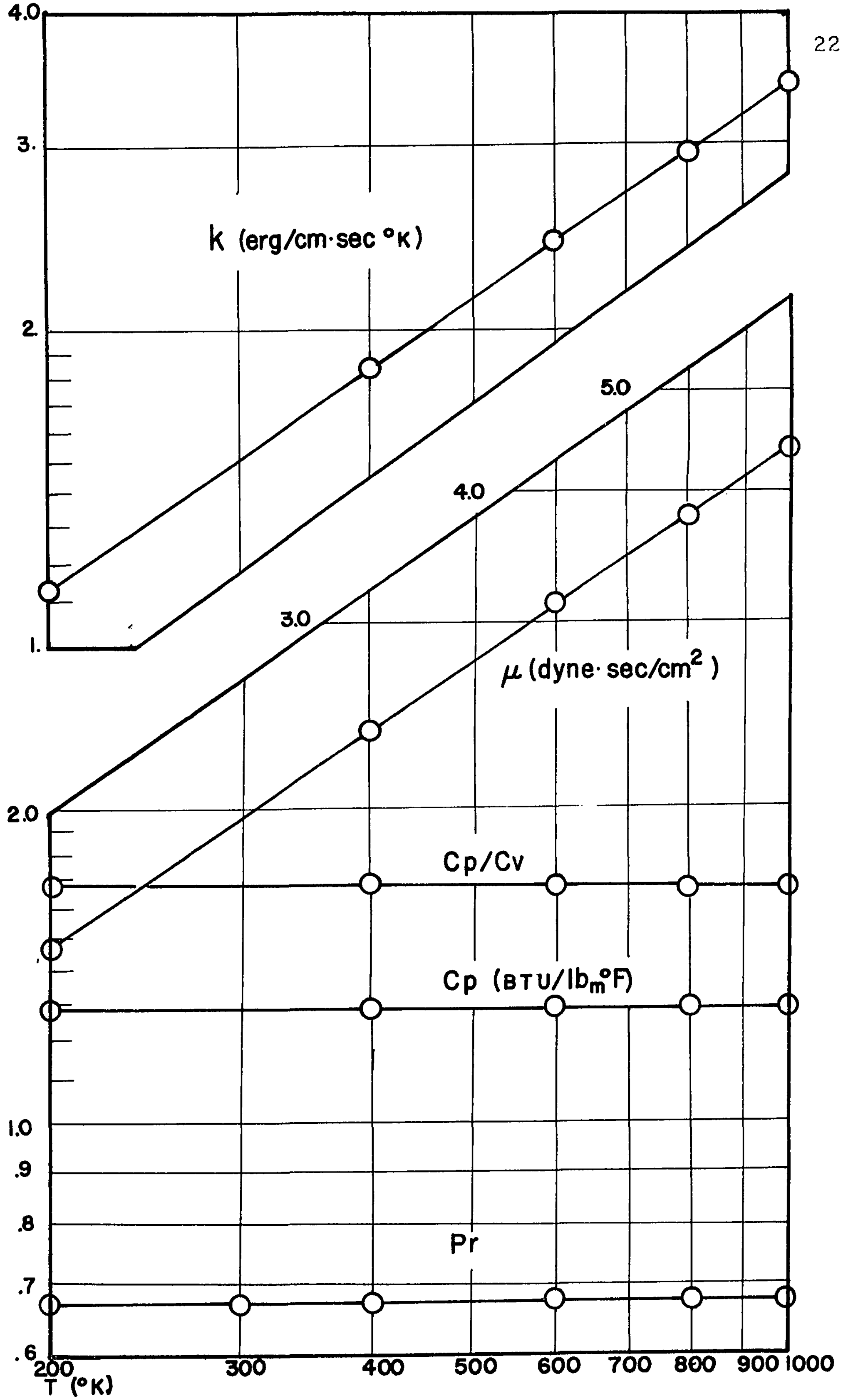

Figure 66. Thermodynamic and transport properties of helium.

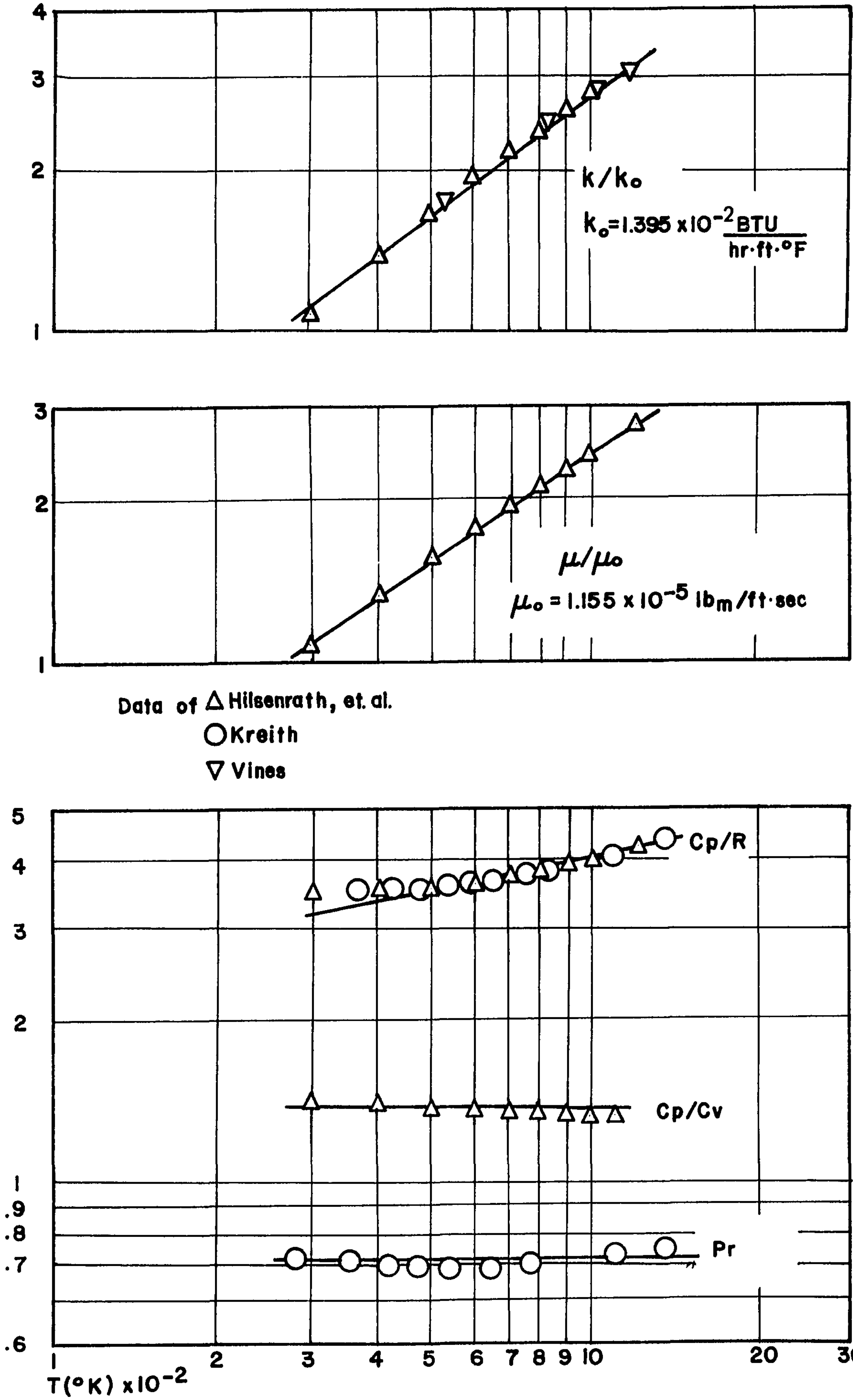

Figure 67. Thermodynamic and transport properties for air.

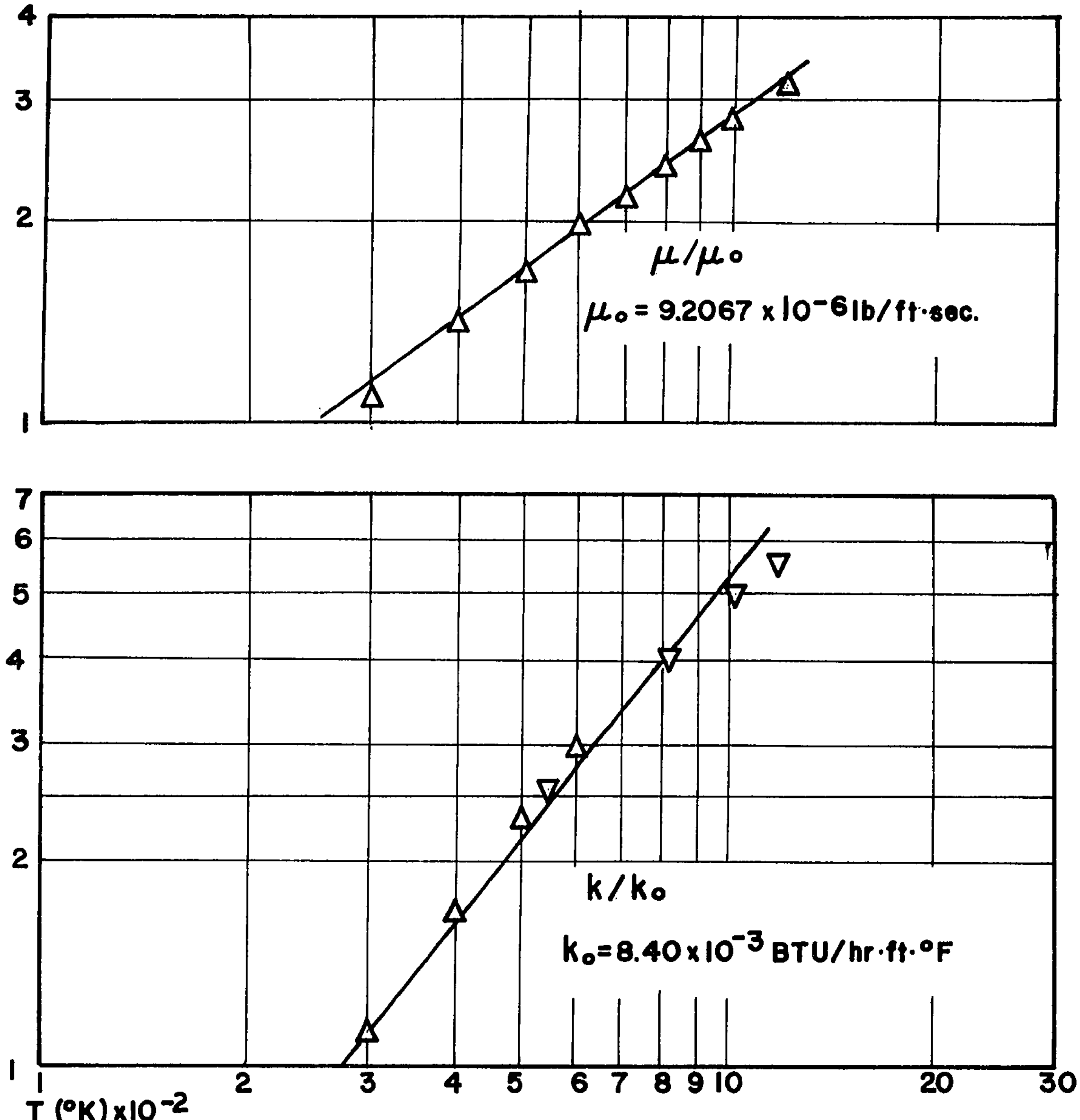

Figure 68. Thermodynamic and transport properties for carbon dioxide.

DATA OF △ Hilsenrath, et. al
▽ Vines

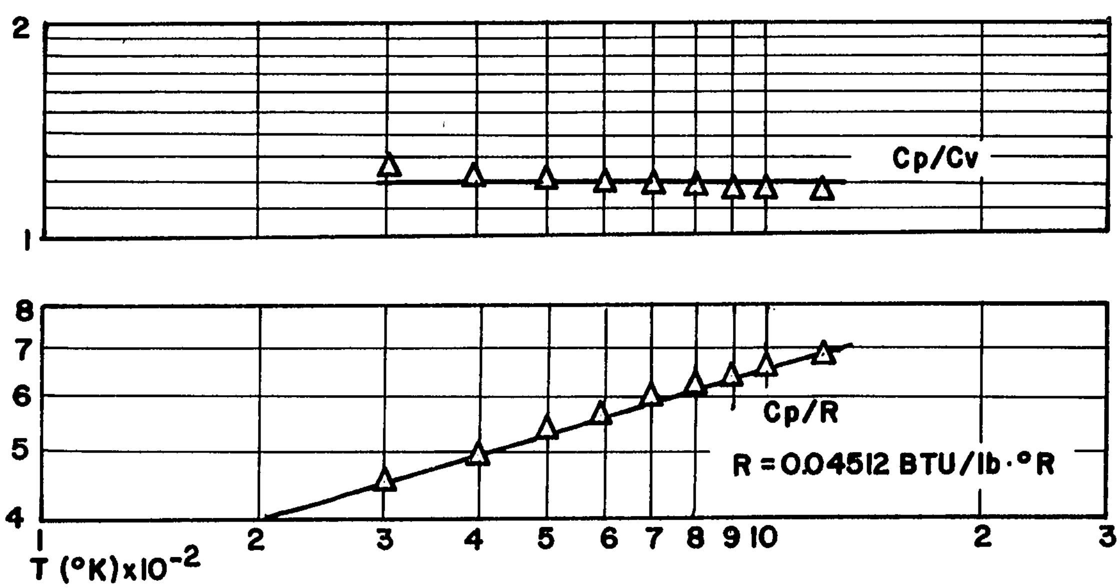

Appendix C

Calorimeter Conductance:

Error in One Dimensional Heat Conduction Equation

Due to Thermocouple Location

A schematic of the calorimeter used to measure local q_w'' is shown in Figure 42. We assume that all thermocouples are homogeneous and thermocouple beads are infinitesmally small. We are trying to determine a maximum range of deviation for the calorimeter conductance defined as

$$K_{cal} = q_w''/(T_i - T_o)$$

due solely to thermocouple bead location. T_i and T_o are the temperatures measured by thermocouples in the inner and outer holes respectively. When a thermocouple with a bead diameter less than the hole diameter is inserted into a calorimeter, the exact location of the thermocouple is unknown. The uncertainty in the thermocouple location is the sum of two uncertainties-- 1.) the location of the thermocouple hole and 2.) the location of the thermocouple in the holes. The holes drilled were 0.030"D. A realistic maximum error in the location of the holes with respect to the tube centerline is 0.005". On the basis of the one dimensional heat conduction equation in cylindrical coordinates;

$$K_{cal} = \frac{k}{r_t \ln(r_i/r_o)}$$

where r_i = radius where the center of the inner thermocouple hole is located

r_o = radius where the center of the outer thermocouple hole is located

r_t = inside radius of tube

k = thermal conductivity of calorimeter material

We assume that the temperature field in the calorimeter is unaffected by the presence of holes, that the conductivity of the calorimeter material is not a function of radius and that the thermocouple bead will be at the temperature of the point of the wall where it is touching. This is not a bad approximation since although the holes were packed with a high conductivity grease, the conductivity of the thermocouples are greater by almost two orders of magnitude than the filler. Also, there was a possibility of voids existing in the packing. The minimum value of conductance occurs with the tolerances and free play of the thermocouples in the holes acting so as to provide a maximum distance between the thermocouple beads. The ratio of minimum calorimeter conductance to that calculated using nominal dimensions can be shown to be,

$$\frac{K_{cal,min}}{K_{cal,nom}} = \frac{\ln\left(\frac{0.4375}{0.2500}\right)}{\ln\left(\frac{0.4375 + 0.015 + 0.005}{0.2500 - 0.015 - 0.005}\right)} = 0.80$$

and the maximum ratio obtainable,

$$\frac{K_{cal,max}}{K_{cal,nom}} = \frac{\ln\left(\frac{0.4375}{0.2500}\right)}{\ln\left(\frac{0.4375 - 0.015 - 0.005}{0.2500 + 0.015 + 0.005}\right)} = 1.28$$

So that the total range of variation can be as large as 48%. In Figure 44 these error limits are shown drawn with respect to the average value of all the calorimeter conductances. While additional uncertainties (i.e. power level during radiation test, uncertainty of thermocouple output) could have been added to increase the limits, there seems to be no reason for doing this since the above uncertainty is sufficient to include all the conductance scatter.

Appendix D

Calorimeter Radiation Calibration

End Effects and Conduction Losses

A. Radiation

For the calibration, a 1/8 inch diameter stainless steel tube was extended down the center of the test section. The section was evacuated with a mechanical vacuum pump and a voltage was applied to the heating element. Knowledge of the power input to the element, assumption of uniform irradiation to the tube inner wall and measurement of the temperature difference corresponding to this known q_w'' allows calculation of the calorimeter conductance K where

$$K = q_w''/\Delta E$$

where ΔE is the corrected difference in thermocouple emf across each calorimeter half. In order to insure proper centering of the heating element, several ceramic spacers were mounted at points midway between the calorimeter locations. These will reduce the radiative heat transfer in two ways. 1.) The viewfactor from the wire to the wall is reduced and 2.) the local temperature of the wire at the spacer is reduced due to thermal conduction through the spacer. Concerning the viewfactor, we consider the geometry and co-ordinate system illustrated in Figure 69. The elemental cylindrical area dA, is at a point directly

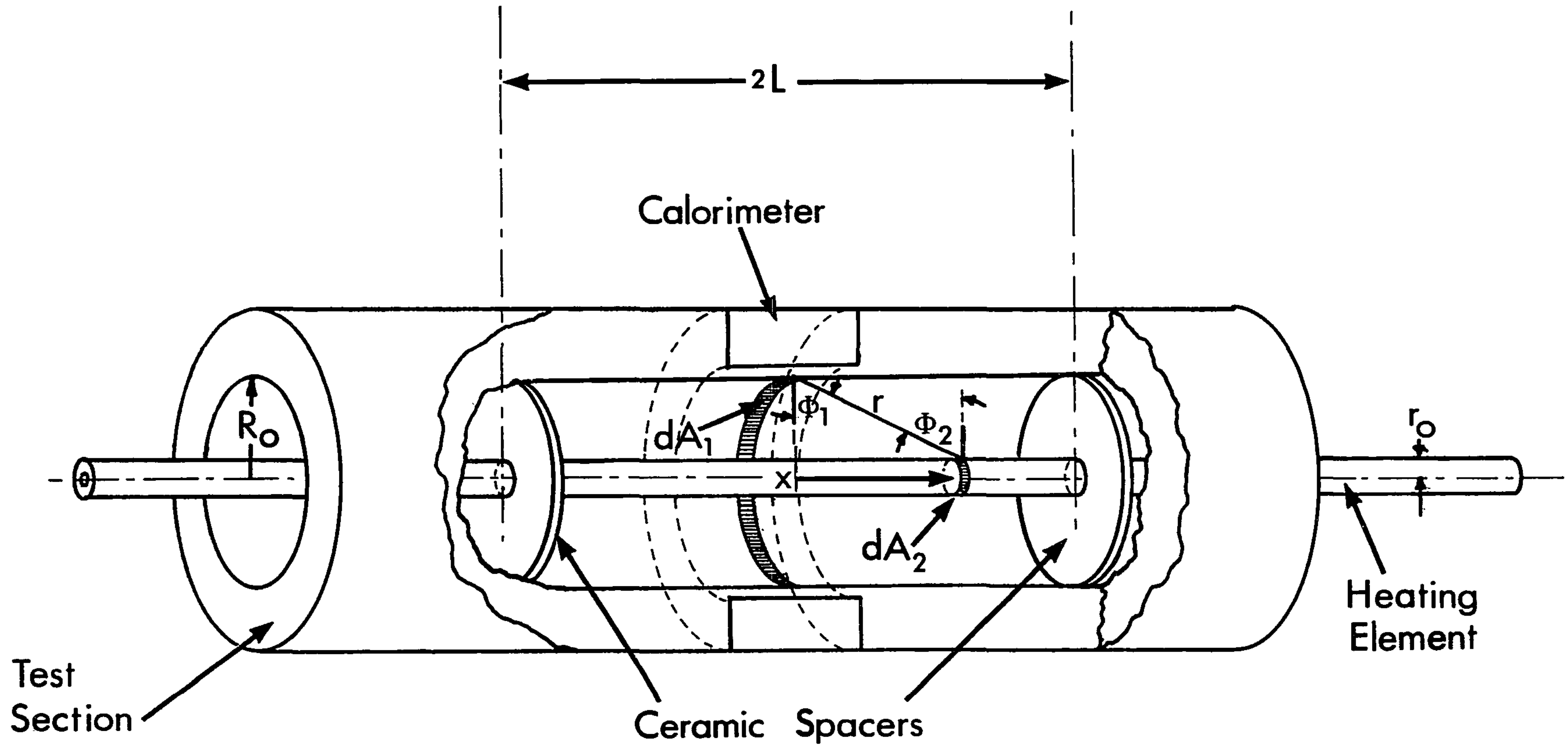

Figure 69. Coordinate system for radiation calibration.

under the calorimeter. The ceramic spacers are mounted at $x=\pm L$ and it is desired to calculate the viewfactor from the finite length of wire between these limits to dA_1. The angle ϕ_1 is the included angle between an inward facing normal from the tube inner wall and a line segment of length r connecting dA_2 and dA_1 where dA_1 is an element of area on the heater. Angle ϕ_2 lies between this same line segment and dA_2. The inside radius of the test section is R_o and r_o is the radius of the heating element. The geometric shape factor from the heater to dA_1 is;

$$A_2F_{2-1} = \left\{\int_{-L}^{L} \frac{\cos\phi_1 \cos\phi_2}{\pi r^2} dA_2\right\} dA_1$$

writing $\cos\phi_1$, $\cos\phi_2$ in terms of geometric quantities;

$$A_2F_{2-1} = \left[\int_{-L}^{L} \frac{R_o^2 r_o dx}{(R_o^2+x^2)^2}\right] dA_2$$

$$= \pi r_o^2 \left[\frac{x}{R_o^2+x^2} + \frac{1}{R_o} \tan^{-1}\left(\frac{x}{R_o}\right)\right] dA_2 \Bigg]_{-L}^{+L}$$

The percentage difference between the shapefactor for L= and the shapefactor for the particular test section dimensions is;

$$\left| \frac{(A_2F_{2-1})_\infty - (A_2F_{2-1})_{L=4.8''}}{(A_2F_{2-1})_{L=\infty}} \right| < 0.01$$

It must be remembered that this does not include reflection or reradiation from the spacer.

B. Conduction Losses

A total of 4 spacers, 1/16 inch thick x 1/8 inch I.D. x 0.294 inch O.D. were used to center the heating wire at the centerline of the test section. Here we attempt to calculate the thermal conduction loss through these spacers from the wire to the wall. First, a temperature of the heating wire must be determined. For radiation between two grey bodies which see only each other, the total heat transfer may be written

$$Q_r = \sigma(T_1^4 - T_2^4)\Big/\left(\frac{\rho_1}{\epsilon_1 A_1} + \frac{1}{A_1} + \frac{\rho_2}{\epsilon_2 A_2}\right)$$

where ρ_1 = reflectivity of heating tube (Ref. 49. Table 2.5 316 s. s. 'as received') = 0.39

α_2 = absorptivity of inside tube wall (taken as equal to that of black enamel) = 0.95 (Ref. 50)

ϵ_1 = emissivity of heating tube = 1-0.61 = 0.39

ϵ_2 = emissivity of inside tube wall = 1-0.95 = 0.05

A_1 = surface area of heating wire = πx(58"L) x (1/8'D)in^2

A_2 = surface area of inside tube wall = π (58"L) x (0.294"D)in^2

T_2 = temperature of inside tube wall = 212 °F = 671 °R

the power input to the heater during the radiation test was 1167 BTU/hr. Using these quantities in the above expression yields T_1 = 1190 °F. For the ceramic spacer, taking the thermal conductivity as being approximately

approximately equal to that of glass (0.40 BTU/hr ft F), the conducted heat transfer through the disks is

$$q_{conduction} = 4 \times \frac{1}{16}'' \times 2\pi \times 0.40 \quad \frac{(1190\,^{\circ}F - 212\,^{\circ}F)}{\ln\left(\frac{0.294}{0.125}\right)} \quad BTU/hr$$

$$= 58 \ BTU/hr$$

This amounts to about 5% of the total heat transfer. However, a correction for this loss was not included in the calibration for two reasons. First, in the vicinity of the spacers, the temperature of the wire is reduced so the wire-to-wall temperature difference is reduced. Second, this analysis assumes perfect thermal contact of wire with spacer and spacer with tube wall. It is probable that the conduction losses are a fraction of the above, but there is no way to calculate this quantity precisely.

Appendix E

Uncertainty Analysis - Nusselt Number, Friction Factor Data

The relationship between the uncertainty interval or precision index w_i of a calculated quantity or dependent variable R and the uncertainty intervals w_i of the independent variables or measured quantities, x_i, is given by (46),

$$w_r^2 = \sum_{i=1}^{n} \left(\frac{\partial R}{\partial x_i} \right)^2 w_i^2 \tag{E.1}$$

Since the uncertainty intervals of most of the instruments whose outputs are combined to produce R are not known, the recommendation of Kline and McClintok (46) will be used. An interval is estimated for each instrument or measurement for which it is felt the probability is 1 to 20 that the true value of the measured quantity lies outside of this interval centered at the measured value. For gages such as for pressure or voltage, the uncertainty is taken as 1/2 of the least division on the dial. For thermocouples, the uncertainty interval is taken as the ISA calibration. Since the uncertainty interval for the wall parameters will vary with each run, the time and effort needed to treat nearly 40 tests and several hundred data points would be prohibitive. Test run #44 was chosen as an example for uncertainty calculations. Since this particular run was one of the highest in terms of pressure drop and local heat fluxes, the uncertainty intervals will be low in relation to those for other runs. If the uncertainty interval for this test can be shown to span most of the data for the lower flux tests, then there is no need to calculate these additional intervals.

The uncertainty in the calorimeter conductances must be known. The expression for the conductance of a calorimeter in terms of experimentally measured quantities in the calibration is,

$$K_i = \frac{EI/2\pi r_o L}{(\Delta e_{i,test} - \Delta e_{i,tare})} \times 3.413 \text{ BTU/hrfT}^2\text{mv}$$

where $\Delta e_{i,test}$ is the difference in thermocouple output across calorimeter i corresponding to an electrical input E x I to the heating wire and $\Delta e_{i,tare}$ is the difference in readings when there is no input to the heating wire. The factor 3.413 is a conversion between watts and BTU/hr. Application of equation E.1. yields

$$\left(\frac{w_{K_i}}{K_i}\right)^2 = \left(\frac{w_E}{E}\right)^2 + \left(\frac{w_I}{I}\right)^2 + \left(\frac{w_{r_o}}{r_o}\right)^2 + 4\left(\frac{w_e}{\Delta e_i}\right)^2$$

The coefficient 4 is present in front of the thermocouple emf term since the differential emf will actually be a combination of 4 thermocouple readings- 2 tare or zero heat flux readings and 2 readings with heat flux. Absolute uncertainty intervals which were deemed appropriate for all significant measured quantities are given in Table E.1. Some word should be mentioned concerning some

Table E.1.

Uncertainty Intervals. Experimentally Measured Quantities

Quantity	Experimental Level	Uncertainty (Absolute)
E	15.1 volts	0.1 V
I	22.6 amps	0.1 amp
T_o	0.294 inches	0.001 inches
L	58.625 inches	0.0625 inches
x_1, x_2	1.75 inches, 11.33in.	0.005 inches
$(\Delta e_{,i})$test - $(\Delta e_{,i})$tare (calibration)	0.055mv (avg.)	0.0010 mv.
M	0.4 - S.C.F.M.	1%
T_o	1670 °R (avg.)	5°R
p_o	order of 8 inches Hg	0.05 inches Hg
p_o - p	order of 0.10 inches H_2O	0.002 inches H_2O

of these quantities. The interval for the thermocouple output w_e may seem to be extremely small, but it should be remembered that we are dealing with a precision rather than an accuracy error in this case. The ISA calibration is essentially an accuracy term. The accuracy error is effectively eliminated through subtraction of the tare readings. The quantity w_e was determined by a test on the instrumentation during an actual run. It was found that ten consecutive readings from the same thermocouple could be included within an interval of 0.0010 mv. However, there were sporadic intervals when electrical interference or power fluctuations would cause a much greater variation. For most calorimeters, these periods were the exception rather than the rule. The Meriam flowmeter was calibrated to within a 0.5% of a Meriam standard flow device. The error in the flow measurement will increase due to errors in measurement of the output pressure and quantities necessary for calculation of correction factors. 1% should be quite representative when these additional uncertainties are considered.

Substitution of the quantities in Table E.1 into the above equation yields for an average conductance of approximately 55.0 BTU/hrft^{2}mv

$$\left(\frac{w_{K_i}}{K_i}\right)_{avg.} = 0.037$$

or a deviation of approximately 3.7%.[1] The expression for the wall heat flux at any point is given by

$$q_w''\Big|_{x_1} = K_i\ (\Delta e_{i,test} - \Delta e_{i,tare})$$

The uncertainty interval for the local heat transfer is

$$\left(\frac{w_{q''}}{q''}\right)^2 \doteq 4\left(\frac{w_e}{(\Delta e_{i,test} - \Delta e_{i,tare})}\right)^2 + \left(\frac{w_{K_i}}{K_i}\right)^2$$

The uncertainty, as can be expected, is a function of the output during the test. For UTV test #44, the uncertainty intervals in the local heat flux are shown in Table E.2. Since the local results presented in the text are averaged from two calorimeters, the uncertainty should be somewhat less than these values. Since the output from the fourth and further calorimeters from the entrance are much smaller, the uncertainty interval is rather large for these fluxes.

This problem is compounded in the calculation for the gas bulk temperature, which besides the local heat transfer rate, is the most important quantity in the evaluation of Nu_m. Since the local heat fluxes are combined in a rather complicated fashion in the integration for the bulk temperature, a simplified analysis is used. Since Nusselt number data is presented only for the first two calorimeters, the uncertainty will be calculated

---

[1]This should not be confused with the uncertainty calculated in Appendix C which applies to the calorimeter before calibration.

Table E.2.

Uncertainty Intervals for Test Run # 44

Local Heat Transfer Rates

Calorimeter		(Δe_i)test - (Δe_i)tare (μV)	K_i^*	q_w'' $\frac{BTU}{hr\,ft^2}$	$\frac{w_{q''}}{\%}$
12	entrance	144.0	45.2	6520	3.85
11		123.1	60.2	7380	4.05
10		37.3	58.5	2180	6.61
9		40.7	59.0	2400	6.10
8		20.3	48.6	988	10.1
7		15.2	63.9	970	13.3
6		11.9	52.2	620	17.0
5		11.5	60.8	700	17.6
4		6.9	57.9	400	29.0
3		8.8	55.7	485	22.9
2	exit	5.9	57.6	340	34.0
1		-0.5	50.0	-25	40.0

*BTU/hr ft^2 mv

only for these two points. We assume that the heat transfer from the gas between the test section entrance and first calorimeter is given by,

$$Q_1 = 2\pi r_o q''_w \big|_{x_1}$$

and up to the second calorimeter by

$$Q_2 = 2\pi r_o (x_2 - x_1) q''_w \Big|_{x_2} + Q_1$$

which represents an integration by means of Simpson's rule. We also make the simplification that the specific heat c_p of the gas is constant so that the bulk temperature may be written as,

$$T_{m1} = T_o - 2\pi r_o x_1 q''_w / \mathring{M} c_p$$

and

$$T_{m2} = T_o - \left(2\pi r_o x_1 q''_w \Big|_{x_1} + (x_2 - x_1) q''_w \Big|_{x_2} \right) / \mathring{M} c_p$$

where M is the mass flow rate, x_1 and x_2 are the locations of calorimeters 1 and 2 respectively. Use of the uncertainty intervals in Table E.2 results in

$$\frac{w_{T_{m1}}}{T_{m1}} = 0.0402 \qquad \frac{w_{T_{m2}}}{T_{m2}} = 0.0545$$

Proceeding in this manner, the uncertainty in the Nusselt numbers at these points are:

$$\frac{w_{Nu_1}}{Nu_1} = 0.078 \qquad \frac{w_{Nu_2}}{Nu_2} = 0.132$$

The bulk temperature enters the computation for the friction factor (eqn. 5.13) by way of the density term. Friction factor data is presented for axial points past the second calorimeter and the uncertainty analysis for the bulk temperature is not extended to this region.

However, the second term in the brackets in equation 5.13, ρ_o/ρ_m rapidly decreases in importance along the tube. For example by the fourth calorimeter in test #40, the axial gradient of this term accounts for less than 25% of the total friction factor. The bulk temperature is asymptotically approaching the limiting value of the exit bulk temperature. This limiting value would tend to bound the error on the negative side of the bulk temperature so that continuation of the preceeding analysis downstream would overestimate the error. The evaluation of derivatives for discrete data can be a risky business such as is performed here for the local friction factor. The limiting error for the derivative is extremely difficult to determine and primarily for this reason an uncertainty analysis is not performed on the local friction factor. The non-dimensionalized pressure drop P easily admits to such an analysis, however. The expression for this quantity in terms of experimentally measured quantities is,

$$P = (2\pi p_o(p_o - p)r_o^{\,2})/RT_o\mathring{M}^2$$

where R is the gas constant for air. The uncertainty interval is given by

$$\left(\frac{w_P}{P}\right)^2 = 2\left(\frac{w_{r_o}}{r_o}\right)^2 + \left(\frac{w_{T_o}}{T_o}\right)^2 + \left(\frac{w_{(p_o-p)}}{p_o-p}\right)^2 + \left(\frac{w_p}{p_o}\right)^2 + 2\left(\frac{w_{\mathring{M}}}{\mathring{M}}\right)^2$$

where we have made a distinction between the uncertainty interval for p_o and p_o-p since the former quantity was measured by an air over mercury manometer and the latter quantity was read with a micromanometer. Using the uncertainty interval used previously for p_o and a 0.001" absolute uncertainty for the micromanometer reading, we obtain the results in Table E.3 for runs #44 and #25. Run #25 is at about the middle of operational parameters run in the Graetz boundary condition test series. We note that the uncertainty level decreases with axial displacement since the pressure defect is an integrated quantity.

Table E.3.

Uncertainty Intervals for Non-Dimensionalized Pressure Drop

Test Run # 44			Test Run # 25		
x^+	P	$\frac{w_P}{P}$ (%)	x^+	P	$\frac{w_P}{P}$
0.0120	0.136	1.69	0.0362	-0.085	4.5
0.0404	0.266	1.66	0.1018	0.039	9.2
0.0919	0.471	1.65	0.1674	0.185	2.5
0.1434	0.648	1.65<	0.2330	0.398	1.88
0.1949	0.807	1.65<	0.2986	0.647	1.73
0.2465	0.969	1.65<	0.3349	0.796	1.70
0.2749	1.083	1.65<			

Appendix F

Computer Program

Solution of Similarity Boundary Layer Equations

The basic initial value integration program (DESP) requires that the simultaneous fourth order equations 4.10 and 4.11 be written as a set of simultaneous first order equations. To this end let,

$$f = f_1$$

$$f' = \frac{df_1}{d\eta} = f_2$$

$$f'' = \frac{df_2}{d\eta} = f_3$$

$$f''' = \left\{\beta(f_2^2 - \rho_e^+/\rho^+) - f_3 f_1 - \lambda' f_3 Pr_0\right\} / \lambda Pr_0$$

$$G = f_4$$

$$G' = \frac{df_4}{d\eta} = f_5$$

$$G'' = \frac{df_5}{d\eta} = \left\{(\gamma_0 - 1) M_0^2 \frac{U_e^{+2}}{H_{2,e}^+}\left(\beta \frac{\rho_e^+}{\rho^+} - 2 Pr_0 \lambda f_3^2\right) - f_5 f_1 - 2 f_5 (\lambda/Pr^+)'\right\} / 2\,(\lambda/Pr^+)$$

The following is a list of variables used in the computer program.

Program name	Meaning

A = exponent in power law for specific heat = a

B = exponent in power law for viscosity =b or

= coefficient of $U_e^+ p/p_0$ - total continuity equation (4.29)

= coefficient of p/p_0 - total momentum equation (4.30)

BETA = $\frac{2\xi}{U_e^+}\frac{dU_e^+}{d\xi}$

BUZZ = $(2\xi)^{1/2} - (2(\xi - \Delta\xi))^{1/2}$

C = exponent in power law for conductivity c or

= term in total continuity equation (4.29)

$$= (2\xi)\left\{\left(\int_0^{\eta_e}\theta(\Omega)d\Omega\right)^2 - 2\int_0^{\eta_e} f'(\eta)\int_0^{\eta}\theta(\Omega)d\Omega\, d\eta\right. \qquad \text{or}$$

C = term in total momentum equation (4.30)

$$= P/p_o U_e^+ \gamma_o M_o^2 \left\{2(2\xi)^{1/2}\left(\int_0^{\eta_e}(f'(\eta))^2 d\eta - \int_0^{\eta_e}\theta(\Omega)d\Omega\right)\right.$$
$$+ 2\gamma_o M_o^2 (2\xi)^{1/2}\int_0^{\eta_e}\theta(\Omega)d\Omega + P/p_o U_e^+ \gamma_o M_o^2$$
$$+ Pr_o \gamma_o M_o^2 \lambda_\omega (f_o''(0) + f''(0))\left((2\xi)^{1/2} - (2(\xi-\Delta\xi))^{1/2}\right)\Big\}$$
$$+ (2\xi) M_o^2 \gamma_o \left\{\left(\int_0^{\eta_e}\theta(\Omega)d\Omega\right)^2 - 2\int_0^{\eta_e}(f'(\eta))^2\int_0^{\eta}\theta(\Omega)d\Omega\, d\eta\right\}$$

where subscript $_o$ refers to values at the last axial step.

COEF1 = $(\gamma_o - 1)M_o^2$

COEF2 = $\gamma_o M_o^2$

COEF3 = $1 + \gamma_o M_o^2$

COEF4 = $\mu_\omega^+ \rho_\omega^+ / \mu_e^+ \rho_e^+$

DELF3 = $\Delta f''(0)$ = perturbation in derivative of velocity at wall

DELF5 = $\Delta G'(0)$ = perturbation in derivative of enthalpy at wall

DETA = $\Delta\eta$ = stepsize in similarity parameter

DZETA = $\Delta\xi$ = stepsize in transformed axial coordinate

ETA = η_e = point where boundary layer growth is assumed to be complete

EXP1 = 1/(A + 1)

EXP2 = (B-A-2)/(A+1)

EXP3 = (B-1)/(A+1)

EXP4 = (C-A-1)/(A+1)

ERRUE = acceptable absolute error $\left|\frac{U^+}{U_e^+}-1\right|$ at $\eta=\eta_e$

ERRHE = acceptable absolute error $\left|\frac{H_2^+}{H_{2,e}^+}-1\right|$ at $\eta=\eta_e$

ERPPO = acceptable absolute difference in two successive interated values of p/p_o at ξ

ERUUE = acceptable aboslute difference in two successive values of $\left|\frac{U^+}{U_e^+}-1\right|$ at $\eta=\eta_e$

FUNC(1,I) $= f((I-1)\Delta\eta)_\xi$

FUNC(2,I) $= f'((I-1)\Delta\eta)_\xi$

FUNC(3,I) $= G((I-1)\Delta\eta)_\xi$

IGRAL1 $= \int_0^{\eta_e}\theta\, d\eta$

IGRAL2 $= \int_0^{\eta_e} f'(\eta)\left(\int_0^{\eta}\theta(\Omega)\,d\Omega\right) d\eta$

IGRAL2 $= \int_0^{\eta_e} f'(\eta)\left(\int_0^{\eta}\theta(\Omega)\,d\Omega\right) d\eta$

IGRAL3 $= \int_0^{\eta_e}(f(\eta))^2 d\eta$ η

IGRAL4 $= \int_0^{\eta_e}(f'(\eta))^2\left(\int_0^{\eta}\theta(\Omega)\,d\Omega\right) d\eta$

GAMMA $= \gamma_0$

MACH $= M_o$

PDIF(1,1) $= \Delta f'(\eta_e)/\Delta f''(o)$

PDIF(1,2) $= \Delta f'(\eta_e)/\Delta G'(o)$

PDIF(2,1) $= \Delta G(\eta_e)/\Delta f''(o)$

PDIF(2,2) $= \Delta G(\eta_e)/\Delta G'(o)$

PPO = p/p_o

PPOO = $(p/p_o)_o$ = value of pressure ratio from last iteration

PPOOO = p/p_o at last axial step

STAR(1) = V^+ (obtained by interpolation from equal η intervals to equal y^+ intervals)

STAR(2) = U^+ (obtained by interpolation from equal η intervals to equal y^+ intervals)

STAR(3) = T/T_0 (obtained by interpolation from equal η intervals to equal y^+ intervals)

TA1W = θ_w^{a+1}

TAW1 = (1-TA1W)

UEO = U_e^+ value of free stream dimensionless velocity from last iteration

UEOO = $U_{e,o}^+$ value of free stream dimensionless velocity from last axial step

UE = U_e^+ value of free stream dimensionless velocity at present step

V = V^+ radial velocity

X = X^+

Y(1) = f

Y(2) = f'

Y(3) = f"

Y(4) = G

Y(5) = G'

YEND1 = $f(\eta_e)$

YEND2 = $f'(\eta_e)$

YEND3 = $G(\eta_e)$

YSRT3 = $f''(0)$

YSRT5 = G'(0) from guess or correction routine

YST3TO = $f''(0)_o$ = value of velocity derivative at wall at last axial step

```
0001                  SUBROUTINE FEOUT1(Y,DY,N,X,SPTYPE,*)
              C
              C       ******************************************************************
              C
              C       THIS SUBROUTINE PULLS OUT VALUES OF U/UE, F ( STREAM FUNCTION )
              C       AND H/HE AT ETA ( END OF THE B.L. ) FOR USE IN CONVERGENCE CHECK
              C       AND CORRECTIVE PROCEDURE
              C
              C       ******************************************************************
              C
0002                  DIMENSION Y(5),DY(5),F(101),FUNC(3,101)
0003                  COMMON F,FUNC,NOFNS,BETA,TA1W,DZETA,PR,COEF1,COEF3,FXP1,EXP2,EXP3,
                     1EXP4,YEND1,YEND2,YEND4,XEND,UE,ZETA,TWTO,ETA,DETA,UECO,COEF2,COEF4
                     1,TAW1,IGRAL1,IGRAL2,IGRAL3,IGRAL4,IGRAL5,II
0004                  REAL IGRAL1,IGRAL2,IGRAL3,IGRAL4,IGRAL5
0005                  LOGICAL SPTYPE
0006                  IF(.NOT.SPTYPE)RETURN
0007                  IF(X.EQ.0)RETURN
0008                  YEND1=Y(1)
0009                  YEND2=Y(2)
0010                  YEND4=Y(4)
0011                  WRITE(6,1)YEND1,YEND2,YEND4
0012                1 FORMAT(20H AT ETA=END, Y(1) = ,F8.4,8H Y(2) = ,F8.4,7H Y(5)= ,F8.4
                     1)
0013                  RETURN
0014                  END
```

```
0001                SUBROUTINE FEOUT2(Y,DY,N,X,SPTYPE,*)
            C
            C       ******************************************************************
            C
            C       THIS SUBROUTINE CALCULATES INTEGRAL PARAMETERS FOR USE IN
            C       INTEGRATED MOMENTUM AND CONTINUITY EQUATIONS.  ALSO STORES
            C       VELOCITY AND ENTHALPY PROFILES FOR PRINTOUT IF THIS HAPPENS TO
            C       SATISFY CONVERGENCE CRITERIA FOR THIS STEP
            C
            C       ******************************************************************
            C
0002                LOGICAL SPTYPE
0003                IF(.NOT.SPTYPE)RETURN
0004                DIMENSION Y(5),DY(5),F(101),FUNC(3,101)
0005                REAL INGRN,IGRAL1,IGRAL2,IGRAL3,IGRAL4,IGRAL5
0006                COMMON F,FUNC,NOFNS,BETA,TA1W,DZETA,PR,COEF1,COEF3,EXP1,EXP2,EXP3,
                   1EXP4,YEND1,YEND2,YEND4,XEND,UE,ZETA,TWTO,ETA,DETA,UECO,COEF2,COEF4
                   1,TAW1,IGRAL1,IGRAL2,IGRAL3,IGRAL4,IGRAL5,II
0007                INGRN=(TA1W+TAW1*Y(4))**EXP1
0008                IF(X.EQ.0.0)GO TO 1
0009                TEMP=TEMP+INGRN
0010                IF(X.EQ.ETA)GO TO 2
0011                IF(KIK.EQ.-1)GO TO 3
0012                CHECK=CHECK+4.0*Y(2)
0013                IGRAL1=IGRAL1+4.0*INGRN
0014                IGRAL2=IGRAL2+4.0*TEMP*Y(2)
0015                IGRAL3=IGRAL3+4.0*Y(2)*Y(2)
0016                KIK=-KIK
0017                IGRAL4=IGRAL4+4.0*Y(2)*Y(2)*TEMP
0018                GO TO 5
0019              1 KIK=1
0020                CHECK=0.0
0021                IGRAL1=0.0
0022                TEMP=INGRN/2.0
0023                IGRAL2=0.0
0024                IGRAL3=0.0
0025                IGRAL4=0.0
```

```
      M=0
    2 IGRAL1=IGRAL1+INGRN
      CHECK=CHECK+Y(2)
      IGRAL2=Y(2)*TEMP+IGRAL2
      IGRAL3=IGRAL3+Y(2)*Y(2)
      IGRAL4=IGRAL4+Y(2)*Y(2)*TEMP
      GO TO 5
    3 IGRAL1=IGRAL1+2.0*INGRN
      CHECK=CHECK+2.0*Y(2)
      IGRAL2=IGRAL2+2.0*TEMP*Y(2)
      IGRAL4=IGRAL4+2.0*Y(2)*Y(2)*TEMP
      IGRAL3=IGRAL3+2.0*Y(2)*Y(2)
      KIK=-KIK
    5 M=M+1
      FUNC(1,M)=Y(1)
      FUNC(2,M)=Y(2)
      FUNC(3,M)=Y(4)
      IF(X.NE.ETA)GO TO 6
      CHECK=CHECK*DETA/3.0
      WRITE(6,100)CHECK,YEND1
  100 FORMAT(8H CHECK =,F8.6,8H CHECK =,F8.6)
      IGRAL1=IGRAL1*DETA/3.0
      IGRAL2=IGRAL2*DETA*DETA/3.0
      IGRAL3=IGRAL3*DETA/3.0
      IGRAL4=IGRAL4*DETA*DETA/3.0
    6 RETURN
      END
```

```
0001            SUBROUTINE FEVAL(Y,X,DY)
           C
           C    ************************************************************
           C
           C    THIS SUBROUTINE EVALUATES THE RIGHT HAND SIDE OF THE BOUNDARY LAYER
           C    EQUATIONS AFTER CONVERSION TO A SET OF SIMULTANEOUS FIRST ORDER
           C    DIFFERENTIAL EQUATIONS AND IS CALLED BY DESP
           C
           C    ************************************************************
           C
0002            DIMENSION Y(5),DY(5),F(101),FUNC(3,101),FPRM(3)
0003            COMMON F,FUNC,NOFNS,BETA,TA1W,DZETA,PR,COEF1,COEF3,EXP1,EXP2,EXP3,
               1EXP4,YEND1,YEND2,YEND4,XEND,UE,ZETA,TWTO,ETA,DETA,UECO,COEF2,COEF4
               1,TAW1,IGRAL1,IGRAL2,IGRAL3,IGRAL4,IGRAL5,II
0004            REAL IGRAL1,IGRAL2,IGRAL3,IGRAL4,IGRAL5
0005            DY(1)=Y(2)
0006            DY(2)=Y(3)
0007            HARCH=TA1W+TAW1*Y(4)
0008            DY(3)=(BETA*(Y(2)*Y(2)-HARCH**EXP1)-Y(3)*Y(1)-2.0*PR*EXP3*HARCH**E
               1XP2*TAW1*Y(3)*Y(5))/(2.0*PR*HARCH**EXP3)
0009            DY(4)=Y(5)
0010            DY(5)=(COEF1*UE*UE*(BETA*HARCH**EXP1*Y(2)-2.0*PR*HARCH**EXP3*Y(3)*
               1Y(3))-2.0*EXP4*HARCH**(EXP4-1.0)*TAW1*Y(5)*Y(5)-Y(5)*Y(1))/(2.0*HA
               1RCH**EXP4)
0011            RETURN
0012            END
```

```
C
C      ******************************************************************
C
C       MAIN PROGRAM
C
C      ******************************************************************
C
C      ******************************************************************
C
C      THIS PROGRAM INTEGRATES THE SIMILARITY DIFFERENTIAL EQUATIONS FOR
C      LAMINAR FLOW OF A GAS IN A TUBE WITH TEMPERATURE DEPENDENT PROPERT
C      IES.
C
C      ******************************************************************
C
C
C      INPUT VARIABLES ARE NAMED AS FOLLOWS
C
C      GAMMA=RATIO OF SPECIFIC HEATS CP/CV
C       MACH=INLET MACH NO.
C      TWTC=INLET WALL TO BULK TEMPERATURE RATIO
C      PR=PRANDTL NO.
C      A=EXPONENT IN POWER LAW FOR SPECIFIC HEAT
C      B=EXPONENT IN POWER LAW FOR VISCOSITY
C      C=EXPONENT IN POWER LAW FOR CONDUCTIVITY
C      DZETA=AXIAL MESH STEP IN TRANSFORMED COORDINATE SYSTEM
C      ETA=VALUE OF TRANSFORMED Y VARIABLE AT WHICH THE VELOCITY AND
C      ENTHALPY BOUNDARY LAYERS ARE ASSUMED TO REACH THEIR FREE STREAM
C      VALUES
C      M=NO. OF AXIAL MESH POINTS AT WHICH SOLUTUIONS WILL BE COMPLETED
C      ERRUE=ACCEPTABLE ABSOLUTE DIFFERENCE BETWEEN NON DIMENSIONALIZED
C      AXIAL VELOCITY U/UE AND 1 AT ETA
C      ERRHE=ACCEPTABLE ABSOLUTE DIFFERENCE BETWEEN NON DIMENSIONALIZED
C      ENTHALPY AND 1 AT ETA
C      ERRPC=ACCEPTABLE ABSOLUTE DIFFERENCE IN TWO SUCCESSIVE VALUES OF
C      THE PRESSURE RATIO AT ZETA
```

```
      REAL MISS1,MISS2,NETA,IGRAL1,IGRAL2,IGRAL3,IGRAL4,IGRAL5,MACH
      REAL SILT
      DIMENSION F(101),FLAP(3),GLAP(3),PDIF(2,2),ERR(3),FUNC(3,101),Y(5)
     1,DN(100),STAR(3),V(100)
      COMMON F,FUNC,NOFNS,BETA,TAIW,DZETA,PR,COEF1,COEF3,EXP1,EXP2,EXP3,
     1EXP4,YEND1,YEND2,YEND4,XEND,UE,ZETA,TWTO,ETA,DETA,UECO,COEF2,COEF4
     1,TAW1,IGRAL1,IGRAL2,IGRAL3,IGRAL4,IGRAL5,II
      EXTERNAL FEVAL,AF,FEOUT1,FEOUT2
      DOUBLE PRECISION B,C,PPOUE,PPO
      LOGICAL FIRST, SPTYPE
      READ(5,1)GAMMA,A,B,C,PR
    1 FORMAT(5F6.4)
      READ(5,2)MACH,TWTO
    2 FORMAT(2F4.2)
      READ(5,3)DZETA,M,N,XEND
    3 FORMAT(E6.2,2I3,F5.2)
      READ(5,8)ERRUE,ERRHE,ERPPO,ERUUE
    8 FORMAT(4F8.5)
C     ECHO CHECK
      WRITE(6,37)GAMMA,A,B,C
   37 FORMAT(9H GAMMA = ,F8.4,5H A = ,F8.4,5H B = ,F8.4,5H C = ,F8.4)
      WRITE(6,38)MACH,TWTO,PR
   38 FORMAT(12H MACH NO. = ,F8.4,8H T/TO = ,F8.4,6H PR = ,F8.4)
      WRITE(6,39)DZETA,M,ETA
   39 FORMAT(9H DZETA = ,F8.4,17H # AXIAL STEPS = ,I4,21H ETA (FREE STRE
     1AM) = ,F8.4)
   40 FORMAT(9H ERRUE = ,E9.3,9H ERRHE = ,E9.3,9H ERPPO = ,E9.3,9H ERUUE
      WRITE(6,40)ERRUE,ERRHE,ERPPO,ERUUE
      TAIW=TWTO**(A+1.0)
      DETA=0.10
      DWS=1.0/320.0
      ETA=XEND
      II=ETA/DETA+2
C
C     ******************************************************************
C
C     CALCULATE COEFFICIENTS AND EXPONENTS WHICH ARE FREQUENTLY USED
C     IN CALCULATIONS
C
C     ******************************************************************
C
```

```
      TAW1=(1.0-TAIW)
      PPOOO=1.00
      COEF1=MACH*MACH
      COEF2=GAMMA*COEF1
      COEF3=1.0+GAMMA*COEF1
      IF(TAW1.EQ.0.0)GO TO 700
      COEF1=(GAMMA-1.0)*COEF1*(A+1.0)/TAW1
      GO TO 701
  700 COEF1=0.0
  701 CONTINUE
      COEF4=TWTO**(B-1.0)
      EXP1=1.0/(1.0+A)
      EXP2=(B-A-2.0)/(A+1.0)
      EXP3=(B-1.0)/(A+1.0)
      EXP4=(C-A-1.0)/(A+1.0)
      NN=5
      H=0.10
      MM=0
      ZETA=0.0
      UFOO=1.0
      XX=0.0
      IGRAL5=0.0
      BETA=0.0
      UE=1.0
   33 XSTART=0.0
      ETA=XEND
      YSRT3=0.332
      IF(TAW1.EQ.0.0)GO TO 702
      YSRT5=(A+1.0)*TWTO**A/TAW1*(1.0-TWTO)*0.332*PR**0.3333
      GO TO 703
  702 YSRT5=0.0
  703 CONTINUE
    5 DELF3=0.001
      DELF5=0.001
      KK=0
      IF(MM.GE.4)DELF3=0.0001
      IF(MM.GE.4)DELF5=0.0001
```

```
    6 Y(3)=YSRT3
      Y(5)=YSRT5
      ETA=XEND
      XSTART=0.00
    7 Y(1)=0.0
      Y(2)=0.0
      Y(4)=0.0
      CALL DESP(ETA,FEVAL,NN,Y,XSTART,ETA,H,ERRUE,AE,FEOUT1,&800)
C
C     ****************************************************************
C
C     CALCULATE PARTIAL DERIVATIVES OF U/UE AND H/HE AT THE OUTER EDGE
C     OF BOUNDARY LAYER WITH RESPECT TO D(U/UE)D(ETA) AND D(H/HE)/D(ETA)
C
C
C     ****************************************************************
C
      ERR1=ABS(1.0-YEND2)
      ERR2=ABS(1.0-YEND4)
      IF(ERR1.LE.ERRUE.AND.ERR2.LE.ERRHE)GO TO 9
      IF(KK.EQ.0)GO TO 10
      IF(KK.EQ.1)GO TO 11
      FLAP(3)=YEND2
      GLAP(3)=YEND4
      GO TO 12
   10 YSRT3=YSRT3+DELF3
      FLAP(1)=YEND2
      KK=KK+1
      GLAP(1)=YEND4
      GO TO 6
   11 YSRT5=YSRT5+DELF5
      FLAP(2)=YEND2
      GLAP(2)=YEND4
      KK=KK+1
      GO TO 6
C
C     ****************************************************************
C
C     SET UP CORRECTION MATRIX TO CALCULATE NEW VALUES OF WALL DERIVATI
C     VES
C
C     ****************************************************************
```

```
0095           PDIF(2,1)=(GLAP(2)-GLAP(1))/DELF3
0096           PDIF(2,2)=(GLAP(3)-GLAP(2))/DELF5
0097           DO 13 I=1,3
0098           MISS1=ABS(1.0-FLAP(I))
0099           MISS2=ABS(1.0-GLAP(I))
0100        13 ERR(I)=SQRT(MISS1**2.0+MISS2**2.0)
0101           I=1
0102           IF(ERR(1).GE.ERR(2))I=2
0103           IF(ERR(I).GE.ERR(3))I=3
0104           IF(I.EQ.1.OR.I.EQ.2)YSRT5=YSRT5-DELF5
0105           IF(I.EQ.1)YSRT3=YSRT3-DELF3
0106           FLAP(1)=FLAP(I)
0107           GLAP(1)=GLAP(I)
0108           KK=1
0109           DET=PDIF(1,1)*PDIF(2,2)-PDIF(1,2)*PDIF(2,1)
0110           DELF3=(PDIF(2,2)*(1.0-FLAP(I))-PDIF(1,2)*(1.0-GLAP(I)))/DET
0111           DELF5=(PDIF(1,1)*(1.0-GLAP(I))-PDIF(2,1)*(1.0-FLAP(I)))/DET
0112           YSRT3=YSRT3+DELF3
0113           GO TO 6
0114         9 Y(1)=0.0
0115           Y(2)=0.0
0116           Y(3)=YSRT3
0117           Y(4)=0.0
0118           Y(5)=YSRT5
0119           KK=0
      C
      C        ***************************************************************
      C
      C        OBTAIN DETAILED BOUNDARY LAYER PROFILES
      C
      C        ***************************************************************
      C
0120           CALL DESP(DETA,FFVAL,NN,Y,XSTART,ETA,H,ERRUF,AE,FEOUT2,&800)
0121        17 IF(MM.NE.0)GO TO 24
0122           ZETA=DZETA
      C
      C        ***************************************************************
      C
      C        SOLVE INTEGRATED CONTINUITY AND MOMENTUM EQUATIONS
      C        FOR U/UF AND P/PO
```

```
C
C     ******************************************************************
C
   24 B=2.0*(2.0*ZETA)**0.5*(YEND1-IGRAL1)-1.0
      C=2.0*ZETA*(IGRAL1**2.0-2.0*IGRAL2)
      PPOUF=(-B+DSQRT(B**2.0-4.0*C))/2.0
      IF(MM.EQ.0)YST3TO=YSRT3
      BUZZ=(2.0*ZETA)**0.5-(2.0*(ZETA-DZETA))**0.5
      B=-COEF3+4.0*PR*COEF2*COEF4*(IGRAL5+BUZZ*(YST3TO+YSRT3)*UEOO/4.0)
      C=PPOUE*COEF2*(2.0*(2.0*ZETA)**0.5*(IGRAL3-IGRAL1)+PPOUE+PR*COEF4*
     1BUZZ*(YST3TO+YSRT3))+COEF2*(2.0*ZETA)*(IGRAL1**2.0-2.0*IGRAL4)
      PPO=(-B+DSQRT(B**2.0-4.0*C))/2.0
      UE=PPOUF/PPO
      WRITE(6,50)UE,PPO
   50 FORMAT(8H U/UO = ,F9.5,8H P/PO = ,F9.5)
C
C     ******************************************************************
C
C     CHECK IF U/UE AND P/PO DIFFER BY LESS THAN SPECIFIED AMOUNT
C     FROM VALUES CALCULATED FOR LAST ITERATION
C
C     ******************************************************************
C
      IF(FIRST.OR.MM.EQ.0) GO TO 18
      ERR5=ABS(UE-UEO)
      ERR6=ABS(PPO-PPOO)
      IF(ERR5.LE.ERUUE.AND.ERR6.LE.ERPPO)GO TO 19
      UEO=UE
      PPOO=PPO
      BETA=2.0*ZETA/UE*(UE-UEOO)/DZETA
      GO TO 5
   18 UEO=UE
      PPOO=PPO
      FIRST=.FALSE.
      BETA=2.0*ZETA/UE*(UE-UEOO)/DZETA
      IF(MM.EQ.0)GO TO 20
C
```

```
C      ***************************************************************
C
C      IF THIS IS X+=0, THEN BOUNDARY LAYERS CAN ONLY BE PRINTED AS
C      FUNCTIONS OF ETA SINCE IN THE Y+-X+ SYSTEM, THE BOUNDARY LAYER
C      THICKNESS IS THEORETICALLY ZERO
C
C      ***************************************************************
C
       GO TO 5
    20 MM=1
       WRITE(6,21)
    21 FORMAT(38H ZETA = 0.0  UF/UO=1.0  P/PO=1.0  X=0 //)
       WRITE(6,22)
    22 FORMAT(35H  ETA      Y(1)      U/UE      H/HE)
       ETA=0.0
       DO 23 I=1,II
       WRITE(6,32)ETA, FUNC(1,I),FUNC(2,I),FUNC(3,I)
    32 FORMAT(2X,F5.2,4X,F8.5,2(2X,F8.5))
    23 ETA=ETA+DETA
       F(J)=FUNC(1,J)
    67 CONTINUE
       YST3TO=YSRT3
       GO TO 33
    19 XX=XX+DZETA/(UF+UEOO)*(PPCOC+PPO)
       WRITE(6,25)ZETA,UE,PPO,XX
    25 FORMAT(8H ZETA = ,F8.5,8H U/UE = ,F8.5,8H P/PO = ,F8.5,6H X =  ,F8
      1.5)
       BETA=2.0*ZETA*(UF-UEOO)/(DZETA*UE)
       NETA=0.0
       DN(1)=0.00
       WRITE(6,28)
       DO 26 I=1,II
       U=FUNC(2,I)*UF
       TEMP=(TA1W+TAW1*FUNC(3,I))**EXP1
       X=NETA
```

```
0173          DO 67 J=1,II
0174          DEX=X/DETA-0.00001
0175          IND=DEX
0176          IND=IND+1
0177          LKJ=II-3
0178          IF(IND.GE.LKJ)IND=LKJ
0179          SILT=IND*DETA-DETA
0180          IF(IND.LE.1)GO TO 60
0181          IND=IND+1
0182          FY=-(X-SILT-DETA)*(X-SILT-2.0*DETA)*(X-SILT-3.0*DETA)*F(IND-1)/6.0
             1+(X-SILT)*(X-SILT-2.0*DETA)*(X-SILT-3.0*DETA)*F(IND)/2.0-(X-SILT)*
             1(X-SILT-DETA)*(X-SILT-3.0*DETA)*F(IND+1)/2.0+(X-SILT)*(X-SILT-DETA
             1)*(X-SILT-2.0*DETA)*F(IND+2)/6.0
0183          FY=FY/DETA**3.0
0184          GO TO 71
0185       60 FY=-X*(X-2.0*DETA)*F(2)/DETA**2.0
0186          FY=FY+X*(X-DETA)*F(3)/(2.0*DETA**2.0)
0187       71 CONTINUE
0188          V(I)=TEMP*UE*(2.0*ZETA)**0.5*((NETA*(1.0-BETA)*FUNC(2,I)-FUNC(1,I)
             1)/(2.0*ZETA))
0189          WRITE(6,31)DN(I),NETA,FUNC(2,I),U,TEMP,FUNC(3,I),V(I)
0190          DN(I+1)=DN(I)+(2.0*ZETA)**0.5*DETA/(UE*PPO)*TEMP
0191          NETA=NETA+DETA
0192       26 CONTINUE
0193       31 FORMAT(1X,F6.4,F8.4,1X,F9.6,4(3X,F9.6))
0194       28 FORMAT(3X,3H Y ,4X,5H NETA,3X,5H U/UE,7X,5H U/UO,7X,5H T/TO,7X,5H
             1H/HE,7X,3H V+//)
0195          LAP=M-1
0196          IF(MM.LT.LAP)GO TO 409
0197          YY=0.00
0198          KLAP=II-2
0199          NOMONS=1
0200      406 DO 401 K=1,KLAP
0201          KULP=K+1
0202          IF(YY.GE.DN(K).AND.YY.LT.DN(KULP))GO TO 402
0203          GO TO 401
```

```
  402 I=K
      GO TO 407
  401 CONTINUE
  407 CONTINUE
C
C     ******************************************************************
C
C     SINCE OUTPUT FROM INTEGRATION ROUTINE IS AT EQUAL ETA INTERVALS
C     IT IS NECESSARY TO INTERPOLATE FOR VALUES OF THE DEPENDENT
C     VARIABLES AT EQUALLY SPACED Y+=1-R/RO VALUES.  USE PARABOLA FIT
C     THRU LAST AND TWO FORWARD TABULATED VALUES OF DEPENDENT VARIABLE
C
C     ******************************************************************
C
      DO 403 J=2,3
      STAR(J)=(YY-DN(I+1))*(YY-DN(I+2))*FUNC(J,I)/((DN(I)-DN(I+1))*(DN(I
     1)-DN(I+2)))+(YY-DN(I))*(YY-DN(I+2))*FUNC(J,I+1)/((DN(I+1)-DN(I))*(
     1DN(I+1)-DN(I+2)))+(YY-DN(I))*(YY-DN(I+1))*FUNC(J,I+2)/((DN(I+2)-DN
     1(I))*(DN(I+2)-DN(I+1)))
  403 CONTINUE
      STAR(1)=(YY-DN(I+1))*(YY-DN(I+2))*V(I)/((DN(I)-DN(I+1))*(DN(I)-DN(
     1I+2)))+(YY-DN(I))*(YY-DN(I+2))*V(I+1)/((DN(I+1)-DN(I))*(DN(I+1)-DN
     1(I+2)))+(YY-DN(I))*(YY-DN(I+1))*V(I+2)/((DN(I+2)-DN(I))*(DN(I+2)-D
     1N(I+1)))
      STAR(2)=UE*STAR(2)
      STAR(3)=(TA1W+TAW1*STAR(3))**EXP1
C     PUNCH PROFILES FOR USE IN FINITE DIFFERENCE PROGRAM
      WRITE(98,404)STAR(2),STAR(1),STAR(3)
      IF(YY.GT.DN(KLAP))GO TO 405
      NOMONS=NOMONS+1
      YY=YY+DWS
  404 FORMAT(F11.7,F11.4,F11.7)
      GO TO 406
  405 CONTINUE
      WRITE(98,408)X,PPO
  408 FORMAT(F7.5,F11.7)
      FISH=(PPO*UE-PPOOO*UEOO)/(2.0*PPO*DZETA)
      WRITE(98,410)NOMONS,UE,FISH
  410 FORMAT(I4,2F8.5)
```

```
  409 CONTINUE
      IF(MM.EQ.M) GO TO 30
      IGRAL5=IGRAL5+0.25*(UE+UEOO)*(YST3TO+YSRT3)*(ZETA**0.5-(ZETA-DZETA
     1)**0.5)
      DO 248 J=1,II
      F(J)=FUNC(1,J)
  248 CONTINUE
C
C     ******************************************************************
C
C     INCREMENT AXIAL DISPLACEMENT
C     AND INITIALIZE PROFILE DERIVATIVES
C
C     ******************************************************************
C
      ZETA=ZETA+DZETA
      YST3TO=YSRT3
      FIRST=.TRUE.
      MM=MM+1
      PPOOO=PPO
      UEOO=UE
      GO TO 24
  800 CALL ERROR
   30 STOP
      END
```

Appendix G

This appendix is a listing of the data reduction program described in Chapter 5. Major I/O and intermediate variables and different stages of the calculations are identified through use of comment cards.

```
C
C     ******************************************************************
C
C     VARIABLE PROPERTY LAMINAR FLOW DATA REDUCTION
C     FINALIZED 6/18/71
C     ALL CURVEFITS ARE OF POLYNOMIAL THIRD DEGREE TYPE A+BX+CX2+DX3
C     ALL THERMOCOUPLE CORRELATIONS ARE FOR 32.2 DEG. F.
C     REFERENCE JUNCTION TEMPERATURE
C
C     THE FOLLOWING SUBSCRIPTS APPLY AS FOLLOWS,
C     1 REFERS TO CU-CON THERMOCOUPLE OUTPUT, RANGE 200 TO 600 DEG F
C     (DEG. F. VS. MV)
C     2 REFERS TO CR-AL THERMOCOUPLE OUTPUT, RANGE 200 TO 1880 DEG. F.
C     (DEG. F. - MV)
C     3 REFERS TO CALIBRATION OF UPSTREAM CR-AL THERMOCOUPLE
C     DEG. F. (TRUE) VS. DEG. F. (MEASURED))
C     4 REFERS TO CU-CON THERMOCOUPLE OUTPUT, RANGE 200 TO 600 DEG F.
C     (DEG. F. - MV)
C     5 REFERS TO TEMPERATURE CORRECTION FACTOR FOR LAMINAR FLOW ELEMENT
C     (CORRECTION FACTOR VS. DEG. F.) RANGE 50-120 DEG. F.
C     ALL TRANSPORT PROPERTY CORRELATIONS OF DATA IN NBS 564
C     6 REFERS TO ABSOLUTE VISCOSITY RATIO VERSUS TEMPERATURE
C     MU/MUO VS. DEG. K
C     RANCE 200-1800 DEG. F.
C     7 REFERS TO THERMAL CONDUCTIVITY RATIO K/KO VS. DEG. K.
C     RANGE 200-1800 DEG. F.  KO=0.01395 BTU/HR FT DEG. F.
C     RANGE 200-1800 DEG. F.
C     8 REFERS TO SPECIFIC HEAT RATIO CP/R VS. DEG. K.
C     RANGE 200-1800 DEG. F. R=GAS CONSTANT=0.0685 BTU/LBM DEG. ;.
C
C     K=NO. OF RUN FROM WHICH TAPE TEST WAS TAKEN
C     II=NO. OF RUN
C     JJ=0 MEANS BLUE MAN. FLUID AT MICROMANOMETER
C     JJ=1 MEANS RED  MAN. FLUID AT MICROMANOMETER
C     KKK=0 MEANS PVUT BOUNDARY CONDITION
C     KKK=1 MEANS UVT BOUNDARY CONDITION
C
C     ******************************************************************
C
```

```
0001          DIMENSION A(9),B(9),C(9),D(9),COND(12),XDC(6),XDP(7),DELP(8),TA(12
             1,2),TT(12,2),IBAD(6),TW(12),FLUX(12),DELT(12),TB(7),PHI(4,4),XXDP(
             18),XXDC(6),RHS(4),PDIV(7),X(7),AAA(100),ANS(4),FFF(2,8)
0002          EQUIVALENCE(PHI,AAA)
0003          DO 1 I=1,8
0004          READ(5,100)A(I),B(I),C(I),D(I)
0005        1 CONTINUE
0006      100 FORMAT(4F12.7)
        C
        C     ************************************************************
        C
        C     READ IN CALORIMETER CONDUCTANCES BEGINNING WITH EXIT BOTTOM
        C     CALORIMETER TO INLET TOP CALORIMETER (BTU/HRFT2 MV(CU-CON))
        C
        C     ************************************************************
        C
0007          READ(5,101)(COND(I),I=1,12)
0008      101 FORMAT(4F8.2)
        C
        C     ************************************************************
        C
        C     READ IN X/D RATIOS WHERE CALORIMETERS ARE LOCATED BEGINNING
        C     WITH CALORIMETER CLOSEST TO EXIT
        C
        C     ************************************************************
        C
0009          READ(5,102)(XXDC(I),I=1,6)
0010      102 FORMAT(3F7.3)
        C
        C     ************************************************************
        C
        C     READ IN X/D RATIOS WHERE PRESSURE TAPS ARE LOCATED
        C     BEGINNING WITH TAP CLOSEST ENTRANCE
        C
        C     ************************************************************
        C
0011          READ(5,157)(XDP(I),I=1,7)
0012      157 FORMAT(F7.3)
0013      507 READ(5,160)II,JJ,KKK,K
0014          WRITE(6,301)
0015      301 FORMAT(1H1)
0016      160 FORMAT(4I4)
0017          IF(II.GT.500)GO TO 508
```

```
C
C     ****************************************************************
C
C     READ IN TEST DATA AS FOLLOWS
C     PATM=ATMOSPHERIC PRESSURE (IN. HG)
C     PFM=PRESSURE DIFFERENTIAL ACCROSS LAMINAR FLOW ELEMENT (IN. H2O)
C     TFM=OUTPUT FROM CU-CON THERMOCOUPLE LOCATED AT FLOW ELEMENT
C     P1=PRESSURE AT STATIC TAP #1 (IN. HG.) LEFT COLLUMN
C     P2=PRESSURE AT STATIC TAP #1 (IN. HG)- RIGHT COLLUMN
C     TUP=OUTPUT FROM UPSTREAM CR-AL THERMOCOUPLE (MV)
C     TBULK = OUTPUT FROM THERMOCOUPLE AT EXIT
C
C     ****************************************************************
C
      READ(5,103)PATM,PFM,TFM,TBULK,P1,P2,TUP
  103 FORMAT(F6.2,F6.3,2F7.4,2F5.2,F7.3)
C
C     ****************************************************************
C
C     READ IN STATIC PRESSURE DROP DATA
C
C     ****************************************************************
C
      IF(KKK)500,500,501
  500 WRITE(6,505)II
      READ(5,105)(DELP(I),I=1,6)
  105 FORMAT(3F6.3)
      GO TO 502
  501 WRITE(6,506)II
      READ(5,504)(DELP(I),I=1,7)
  502 CONTINUE
  504 FORMAT(4F6.3)
  505 FORMAT(/10X,35H PARABOLIC INLET VELOCITY TEST NO. ,I3)
  506 FORMAT(/10X,35H SIMULTANEOUS DEVELOPMENT TEST NO. ,I3)
      WRITE(6,6)K
    6 FORMAT(10X,30H TARE TEST TAKEN FROM RUN NO. ,I3)
C
C     ****************************************************************
C
C     READ IN TARE TEST THERMOCOUPLE READINGS
C
C     ****************************************************************
```

```
                C
0033                  READ(5,104)(TA(I,1),TA(I,2),I=1,12)
                C
                C     ***************************************************************
                C
                C     READ IN THERMOCOUPLE READING FOR TEST WITH GASFLOW (MV)
                C
                C     ***************************************************************
                C
0034                  READ(5,104)(TT(I,1),TT(I,2),I=1,12)
                C     ECHO CHECK
0035              104 FORMAT(2F7.4)
0036                  WRITE(6,805)
0037              805 FORMAT(10X,30H TARE THERMOCOUPLE OUTPUT (MV))
0038                  WRITE(6,808)
0039                  DO 806 I=1,6
0040                  K=I+6
0041                  WRITE(6,807)I,TA(I,1),TA(I,2),K,TA(K,1),TA(K,2)
0042              806 CONTINUE
0043              807 FORMAT(10X,2(2X,I3,2(3X,F8.4)))
0044              808 FORMAT(10X,5H    I,3X,8H TA(I,1),4X,8H TA(I,2),5H   I  ,2X,8H TA(I,
                     11),4X,8H TA(I,2)/)
0045                  WRITE(6,809)
0046              809 FORMAT(10X,30H TEST THERMOCOUPLE OUTPUT (MV))
0047                  WRITE(6,550)
0048              550 FORMAT(10X,5H    I,3X,8H TT(I,1),4X,8H TT(I,2),5H   I  ,2X,8H TT(I,
                     11),4X,8H TT(I,2)/)
0049                  DO 810 I=1,6
0050                  K=I+6
0051                  WRITE(6,807)I,TT(I,1),TT(I,2),K,TT(K,1),TT(K,2)
0052              810 CONTINUE
0053                  WRITE(6,811)PFM
0054              811 FORMAT(10X,42H DIFFERENTIAL PRESSURE -FLOWMETER (IN.) = ,F6.3)
0055                  WRITE(6,812)TFM,TBULK
0056              812 FORMAT(10X,23H FLOWMETER TEMP (MV) = ,F7.4,23H BULK EXIT TEMP (MV)
                     1 = ,F7.4)
0057                  WRITE(6,814)P1,P2
0058              814 FORMAT(10X,27H INLET PRESSURE MAN , LEFT ,F5.2,7H RIGHT ,F5.2,7H I
                     1N. HG)
0059                  WRITE(6,815)TUP
0060              815 FORMAT(10X,25H INLET BULK TEMP CR-AL = ,F7.3)
0061                  WRITE(6,816)
0062              816 FORMAT(10X,27H STATIC PRESSURE DROP (IN.))
```

```
      IF(KKK.EQ.0)GO TO 817
      WRITE(6,819)DELP(1),DELP(2),DELP(3)
  819 FORMAT(10X,9H P0-P2 = ,F6.3,9H P1-P2 = ,F6.3,9H P2-P3 = ,F6.3)
      WRITE(6,820)DELP(4),DELP(5),DELP(6)
  820 FORMAT(10X,9H P2-P4 = ,F6.3,9H P2-P5 = ,F6.3,9H P2-P6 = ,F6.3)
      WRITE(6,821)DELP(7)
  821 FORMAT(10X,9H P2-P7 = ,F6.3)
      GO TO 822
  817 WRITE(6,823)DELP(1),DELP(2),DELP(3)
      WRITE(6,824)DELP(4),DELP(5),DELP(6)
  823 FORMAT(10X,9H P1-P2 = ,F6.3,9H P1-P3 = ,F6.3,9H P1-P4 = ,F6.3)
  824 FORMAT(10X,9H P1-P5 = ,F6.3,9H P1-P5 = ,F6.3,9H P1-P6 = ,F6.3)
  822 CONTINUE
      IF(JJ.EQ.0)GO TO 825
      WRITE(6,826)
      GO TO 827
  825 WRITE(6,828)
  827 CONTINUE
  826 FORMAT(10X,32H RED MANOMETER FLUID SP GR 0.826)
  828 FORMAT(10X,33H BLUE MANOMETER FLUID SP GR 0.797)
C
C     ******************************************************************
C
C     CALCULATE MASS FLOW RATE , MACH AND REYNOLDS NUMBERS
C     QMAS=CORRECTED MASS FLOW RATE (LBM/MIN)
C     TFM=GAS BULK TEMPERATURE AT FLOWMETER
C
C     ******************************************************************
C
      TFM=A(4)+B(4)*TFM+C(4)*TFM**2.0+D(4)*TFM**3.0
      QMAS=0.0751*PFM*4.37/4.00*(A(5)+B(5)*TFM+C(5)*TFM**2.0+D(5)*TFM**3
     1.0)
C
C     ******************************************************************
C
C     CALCULATE INLET REYNOLDS NUMBER
C     TIN=INLET GAS TEMPERATURE=CORRECTED UPSTREAM ADIABATIC DEVELOPMENT
C     SECTION TEMPERATURE
C     TUP=UPSTREAM MIXING CHAMBER GAS TEMPERATURE (DEG. F.)
C
C     ******************************************************************
C
```

```
      TUP=A(2)+B(2)*TUP+C(2)*TUP**2.0+D(2)*TUP**3.0
      TIN=A(3)+B(3)*TUP+C(3)*TUP**2.0+D(3)*TUP**3.0
      WRITE(6,829)TIN
      TIN=TIN+459.7
      SPEC=671.0/TIN
  829 FORMAT(10X,30H INLET TEMPERATURE (DEG. F) = ,F9.2)
      TAP=TIN/1.8
      VISC=0.00001153*(A(6)+B(6)*TAP+C(6)*TAP**2.0)
      TBULK=A(1)+B(1)*TBULK+C(1)*TBULK**2.0+D(1)*TBULK**3.0
C
C     ******************************************************************
C
C     CALCULATE MACH NO. AT INLET
C     DENS=GAS DENSITY AT INLET (LBM/FT3)
C     UIN=GAS VELOCITY AT INLET (FT/SEC)
C
C     ******************************************************************
C
      DENS=0.071*(PATM+P1+P2)/29.92*559.7/TIN
      UIN=576.0*QMAS/(0.294**2.0*3.1415*60.0*DENS)
      VMACH=35.4*QMAS/(DENS*SQRT(2405.0*TIN))
      WRITE(6,106)SPEC,VMACH
  106 FORMAT(10X,9H TW/TO = ,F8.3,12H MACH NO. = ,F6.3)
      CSUBP=0.0685*(A(8)+B(8)*TAP+C(8)*TAP**2.0+D(8)*TAP**3.0)
      CONDP=0.01395*(A(7)+B(7)*TAP+C(7)*TAP**2.0+D(7)*TAP**3.0)
      PR=VISC*CSUBP/CONDP*3600.0
      REYD=4.0*QMAS/(60.0*3.1414*VISC*0.294)*12.0
      WRITE(6,300)PR,REYD
  300 FORMAT(10X,6H PR = ,F8.6,8H REYD = ,F8.1/)
C
C     ******************************************************************
C
C     READ IN CALORIMETERS WHICH ARE BELIEVED TO BE PROVIDING SPURIOUS
C     OUTPUT, N=NUMBER OF SUCH CALORIMETERS
C
C     ******************************************************************
C
      READ(5,108)N
  108 FORMAT(I4)
      IF(N)200,201,200
  200 CONTINUE
```

```
      DO 11 I=1,N
      READ(5,108)IBAD(I)
   11 CONTINUF
  201 CONTINUE
C
C     ******************************************************************
C
C     R1=POSITION(RADIUS) OF INNER THERMOCOUPLE
C     R2=POSITION (RADIUS) OF OUTER THERMOCOUPLE (IN.)
C
C     ******************************************************************
C
      R1=0.2500
      R2=0.4375
      DO 12 I=1,12
C
C     ******************************************************************
C
C     AMP=TEMPERATURE REGISTERED BY INNER THERMOCOUPLE (DEG. F.)
C
C     ******************************************************************
C
      AMP=A(1)+B(1)*TT(I,2)+C(1)*TT(I,2)**2.0+D(1)**TT(I,2)**3.0
      TW(I)=AMP+(TT(I,2)-TT(I,1))/26.0*LOG(R1/0.147)/LOG(R2/R1)
      DELT(I)=TT(I,2)-TT(I,1)-TA(I,2)+TA(I,1)
      FLUX(I)=COND(I)*DELT(I)*1000.0
   12 CONTINUE
C
C     ******************************************************************
C
C     NEXT REMOVE SPURIOUS CALORIMETER READINGS, REPLACE WITH READING
C     OF OPPOSITE CALORIMETER. AT LEAST ONE CALORIMETER MUST BE
C    OPERATIVE AT EACH AXIAL POSITION.  INTEGRATE  HEAT FLUX CURVE TO
C     OBTAIN GAS BULK TEMPERATURE AT EACH AXIAL POSITION
C
C     ******************************************************************
```

```
      IF(N)401,401,400
  400 CONTINUE
      K=N
      DO 13 N=1,K
      KCHEK=(IBAD(N)+1)/2-IBAD(N)/2
      IF(KCHEK)15,15,14
   14 KK=IBAD(N)
      FLUX(KK)=FLUX(KK+1)
      TW(KK)=TW(KK+1)
      GO TO 13
   15 KK=IBAD(N)
      FLUX(KK)=FLUX(KK-1)
      TW(KK)=TW(KK-1)
   13 CONTINUE
  401 CONTINUE
      DO 18 I=1,11,2
      K=(I+1)/2
      FLUX(K)=(FLUX(I)+FLUX(I+1))/2.0
      TW(K)=(TW(I)+TW(I+1))/2.0
   18 CONTINUE
      DO 183 I=1,6
      IF(KKK)180,180,181
C
C     ******************************************************************
C
C     ASSUME COOLING OF THE GAS COMMENCES MIDWAY BETWEEN THE
C     END FACE OF THE PLENUM AND THE COOLING SECTION
C
C     ******************************************************************
C
  181 XDC(I)=XXDC(I)+3.337-3.450
      GO TO 183
  180 XDC(I)=XXDC(I)
  183 CONTINUE
C
C     ******************************************************************
C
C     USE FIRST AND SECOND CALORIMETERS (5 AND 6)
C     REQUIRE CONSERVATION OF ENERGY KNOWING TB(I) AT EXIT OF GAS
C
C     ******************************************************************
```

```
      C
0147        TBULK=(TBULK+459.7)/1.8
      C
      C     ******************************************************************
      C
      C     ASSUME COOLING OF GAS CEASES JUST INSIDE FORWARD FACE OF BULK
      C     TEMPERATURE MEASURING PLENUM 1.25 IN. FROM LAST CALORIMETER
      C     EVALUATE THE TOTAL HEAT TRANSFER FROM THE GAS FROM ENTRANCE
      C     TO EXIT
      C
      C     ******************************************************************
      C
0148        XDCEND=XDC(1)+1.250/0.294
0149        QTOT=(60.0*0.0685*1.8*QMAS)*(A(8)*(TAP-TBULK)+B(8)*(TAP**2.0-TBULK
           1**2.0)/2.0+C(8)*(TAP**3.0-TBULK**3.0)/3.0)
      C
      C     ******************************************************************
      C
      C     HEAT FLUX VARIATION GIVEN BY AA/X**0.425+BB/X**0.39+CC/X**0.25
      C
      C     ******************************************************************
      C
0150        EXP1=0.450
0151        EXP2=0.390
0152        EXP3=0.250
0153        PHI(1,1)=1.0/XDC(6)**EXP1
0154        PHI(2,1)=1.0/XDC(5)**EXP1
0155        PHI(3,1)=XDCEND**(1.0-EXP1)/(1.0-EXP1)
0156        PHI(1,2)=1.0/XDC(6)**EXP2
0157        PHI(2,2)=1.0/XDC(5)**EXP2
0158        PHI(3,2)=XDCEND**(1.0-EXP2)/(1.0-EXP2)
0159        PHI(1,3)=1.0/XDC(6)**EXP3
0160        PHI(2,3)=1.0/XDC(5)**EXP3
0161        PHI(3,3)=XDCEND**(1.0-EXP3)/(1.0-EXP3)
0162        Q1=ABS(FLUX(6))
0163        Q2=ABS(FLUX(5))
0164        Q3=529.9*QTOT
      C
```

```
      C     ******************************************************************
      C
      C     SOLVE FOR AA,BB,CC
      C
      C     ******************************************************************
      C
            DET=PHI(1,1)*(PHI(2,2)*PHI(3,3)-PHI(3,2)*PHI(2,3))-PHI(2,1)*(PHI(1
           1,2)*PHI(3,3)-PHI(1,3)*PHI(3,2))+PHI(3,1)*(PHI(1,2)*PHI(2,3)-PHI(1,
           13)*PHI(2,2))
            AA=(Q1*(PHI(2,2)*PHI(3,3)-PHI(3,2)*PHI(2,3))-Q2*(PHI(1,2)*PHI(3,3)
           1-PHI(1,3)*PHI(3,2))+Q3*(PHI(1,2)*PHI(2,3)-PHI(1,3)*PHI(2,2)))/DET
            BB=(Q2*(PHI(1,1)*PHI(3,3)-PHI(1,3)*PHI(3,1))-Q3*(PHI(1,1)*PHI(2,3)
           1-PHI(2,1)*PHI(1,3))+Q1*(PHI(3,1)*PHI(2,3)-PHI(2,1)*PHI(3,3)))/DET
            CC=(Q3*(PHI(2,2)*PHI(1,1)-PHI(2,1)*PHI(1,2))-Q1*(PHI(2,2)*PHI(3,1)
           1-PHI(3,2)*PHI(2,1))+Q2*(PHI(1,2)*PHI(3,1)-PHI(3,2)*PHI(1,1)))/DET
      C
      C     ******************************************************************
      C
      C     NOW SOLVE ITERATIVELY FOR GAS BULK TEMPERATURES AT EACH CALORIMETE
      C     R LOCATION
      C     QTRAN=TOTAL HEAT TRANSFERRED FROM GAS UP TO POINT XDC(I)
      C     ITERATION COMPLETE WHEN TWO SUCCESSIVE VALUES OF THE BULK
      C     TEMPERATURE ARE WITHIN 1/4 DEG. OF EACH OTHER
      C
      C     ******************************************************************
      C
            DO 31 I=1,6
            QTRAN=2.0*0.147*0.294*3.1414/144.0*(AA*XDC(I)**(1.0-EXP1)/(1.0-EXP
           11)+BB*XDC(I)**(1.0-EXP2)/(1.0-EXP2)+CC*XDC(I)**(1.0-EXP3)/(1.0-EXP
           13))
            TB(I)=TAP
            NI=0
         32 TOLD=TB(I)
            TB(I)=(-QTRAN/(60.0*0.0685*1.8*QMAS)+A(8)*TAP+B(8)*(TAP**2.0-TB(I)
           1**2.0)/2.0+C(8)*(TAP**3.0-TB(I)**3.0)/3.0)/A(8)
            NI=NI+1
            IF(NI.GT.50)GO TO 509
            ERROR=ABS(TB(I)-TOLD)
            IF(ERROR-0.25)31,31,32
         31 CONTINUE
```

```
      WRITE(6,839)
  839 FORMAT(12X,3H X+,4X,6H (X+)M,3X,3H Q+,5X,4H NUM,4X,6H TBULK,2X,6H
     1TW/TB,2X,6H (RE)M)
      WRITE(6,840)
  840 FORMAT(43X,8H DEG. F.)
      DO 23 I=1,6
      TW(I)=TW(I)+459.7
      TAPW=TW(I)/1.8
      CONDP=0.01395*(A(7)+B(7)*TB(I)+C(7)*TB(I)**2.0+D(7)*TB(I)**3.0)
      H=FLUX(I)/(1.8*TB(I)-TW(I))
      BNUSS=H*0.0245/CONDB
C
C     ******************************************************************
C
C     CALCULATE INVERSE GRAETZ PARAMETERS BASED ON INLET AND
C     LOCAL BULK PROPERTIES
C
C     ******************************************************************
C
      XINC=XDC(I)*2.0/(REYD*PR)
      CSUBP=0.0685*(A(8)+B(8)*TB(I)+C(8)*TB(I)**2.0+D(8)*TB(I)**3.0)
      VISCB=0.00001153*(A(6)+B(6)*TB(I)+C(6)*TB(I)**2.0)
      REYB=4.0*12.0*QMAS/(3.1414*0.294*VISCB*60.0)
      XLOC=CONDB*XDC(I)/(REYB*VISCB*CSUBP*1800.0)
      RATIO=TW(I)/(TB(I)*1.8)
      QNON=0.147/12.0*FLUX(I)/(TIN*CONDP)
      TBB=1.8*TB(I)-459.7
      WRITE(6,150)XINC,XLOC,QNON,BNUSS,TBB,RATIO,REYB
  150 FORMAT(10X,3F8.4,F9.4,F8.2,F7.3,F8.1)
   23 CONTINUE
      WRITE(6,830)
  830 FORMAT(/10X,34H NON DIMENSIONALIZED PRESSURE DROP)
      WRITE(6,841)
  841 FORMAT(10X,6H   X+ ,5X,3H P+)
      IF(KKK)172,172,173
  172 DO 8 I=1,6
      XXDP(I+1)=(XDP(I+1)-XDP(1))/(REYD*PR)*2.0
      IF(JJ.EQ.1)DFLP(I)=DFLP(I)*0.826/0.797
      DFLP(I)=32.2*62.4*DFLP(I)/(12.0*DENS*UIN**2.0)
      WRITE(6,107)XXDP(I+1),DFLP(I)
    8 CONTINUE
```

```
      GO TO 174
C
C     ******************************************************************
C
C     ASSUME PRESSURE DROP DATA FOR UVT GIVEN AS PO-P2,P1-P2,
C     P2-P3,P2-P4,P2-P5,P2-P6,P2-P7
C
C     ******************************************************************
C
  173 DO 176 I=3.7
  176 DELP(I)=DELP(I)+DELP(1)
      DELP(1)=DELP(1)-DELP(2)
      DELP(2)=DELP(1)+DELP(2)
      DO 177 I=1,7
      IF(JJ.EQ.1)DELP(I)=DELP(I)*0.826/0.797
      DELP(I)=32.2*62.4*DELP(I)/(12.0*DENS*UIN**2.0)
C
C     ******************************************************************
C
C     ASSUME PRESSURE DROP IN BELLMOUTH GIVEN BY DYNAMIC VELOCITY HEAD
C     ASSUME VELOCITY FIELD DEVELOPMENT BEGINS AT END OF BELLMOUTH
C     NOW DETERMINE LOCAL GRAETZ PARAMETERS CORRESPONDING TO EACH
C     OF THE PRESSURE TAP LOCATIONS
C
C     ******************************************************************
C
      DELP(I)=DELP(I)-0.50
      XXDP(I)=(XDP(I)+3.337)/(REYD*PR)*2.0
  177 WRITE(6,107)XXDP(I),DELP(I)
  107 FORMAT(10X,F8.4,F9.3)
  174 CONTINUE
      IF(KKK.EQ.1)GO TO 110
      XXDP(1)=XDP(1)/(REYD*PR)*2.0
      WRITE(6,158)XXDP(1)
  158 FORMAT(10X,34H POSITION OF FIRST PRESSURE TAP = ,F8.6)
  110 CONTINUE
      IF(KKK.EQ.1)GO TO 411
      GO TO 412
  411 DASP=DELP(1)
      DO 413 I=1,7
      X(I)=XDP(I)+3.337-3.450
      DELP(I)=DELP(I)-DASP
```

```
      XXDP(I)=XDP(I)
  413 CONTINUE
      GO TO 414
  412 DO 415 I=1,6
      ILK=8-I
      ILP=7-I
      DELP(ILK)=DELP(ILP)
      XXDP(I)=XDP(I)
      X(I)=XDP(I)
  415 CONTINUE
      XXDP(7)=XDP(7)
      X(7)=XDP(7)
  414 CONTINUE
      DELP(1)=0.0
C
C     ****************************************************************
C
C     BEGIN ITERATION FOR BULK TEMPERATURES (DEG. K.)
C
C     ****************************************************************
C
      DO 422 I=1,7
      QTRAN=2.0*3.1414*C.147*0.294/144.0*(AA*X(I)**(1.0-EXP1)/(1.0-EXP1)
     1+BB*X(I)**(1.0-EXP2)/(1.0-EXP2)+CC*X(I)**(1.0-EXP3)/(1.0-EXP3))
      TB(I)=TAP
      NI=0
  416 TOLD=TB(I)
      TB(I)=(-QTRAN/(60.0*0.0685*1.8*QMAS)+A(8)*TAP+B(8)*(TAP**2.0-TB(I)
     1**2.0)/2.0+C(8)*(TAP**3.0-TB(I)**3.0)/3.0)/A(8)
      REYP=4.0*12.0*QMAS/(60.0*3.1414*0.294*VISCB)
      NI=NI+1
      IF(NI.GT.50)GO TO 509
      ERROR=ABS(TB(I)-TOLD)
      IF(ERROR-0.25)417,417,416
  417 CONTINUE
C
C     ****************************************************************
C
C     CALCULATE MEAN REYNOLDS NUMBER AND PRANDTL NUMBER AT PRESSURE
C     TAP #1
```

```
C
C     ******************************************************************
C
  422 CONTINUE
      IT=0
  802 CONTINUE
      DUSP=DELP(1)
      IT=IT+1
C
C     ******************************************************************
C
C     NOW FIT THIRD ORDER LFAST SQUARES POLYNOMIAL THROUGH NON
C     DIMENSIONALIZED PRESSURE AS A FUNCTION OF LOCAL GRAFTZ PARAMETER
C     ASSIGN DOUBLE WFIGHT TO DELP(2) IN LEAST SQUARES FIT
C
C     ******************************************************************
C
      DISP=XXDP(2)-XXDP(1)
      DO 700 I=1,4
      DO 701 J=1,4
      PHI(I,J)=DISP**(I+J)
  701 CONTINUE
      RHS(I)=(DELP(2)-DUSP)*DISP**I
  700 CONTINUE
      DO 702 I=1,7
      DISP=XXDP(I)-XXDP(1)
      DO 703 J=1,4
      DO 704 K=1,4
      PHI(J,K)=PHI(J,K)+DISP**(J+K)
  704 CONTINUF
      RHS(J)=RHS(J)+(DELP(I)-DUSP)*DISP**J
  703 CONTINUE
  702 CONTINUE
      IM=4
      L=4
      CALL SPINV(AAA,L,IM,IS)
C
C     ******************************************************************
C
C     NOW CALCULATE DERIVATIVE OF NON-DIMENSIONALIZED PRESSURE
C     DROP AT TAP POINTS WITH RESPECT TO GRAETZ PARAMETER
```

```
      GO TO 507
  510 FORMAT(34H BULK TEMPERATURE DID NOT CONVERGE)
  509 WRITE(6,510)
      GO TO 507
  508 STOP
      END
```

Appendix H. Data

Raw and reduced experimental data is included in this appendix. Tests numbered consecutively are in chronological order. Reynolds numbers well above 2000. Some results in the transition region are included.

PARABOLIC INLET VELOCITY TEST NO. 1
TARE TEST TAKEN FROM RUN NO. 1
TARE THERMOCOUPLE OUTPUT (MV)

I	TA(I,1)	TA(I,2)	I	TA(I,1)	TA(I,2)
1	4.2515	4.2548	7	4.2745	4.2770
2	4.2412	4.2367	8	4.2771	4.2775
3	4.2765	4.2745	9	4.2730	4.2689
4	4.2819	4.2816	10	4.2776	4.2781
5	4.2813	4.2801	11	4.2926	4.2919
6	4.2720	4.2654	12	4.2919	4.2886

TEST THERMOCOUPLE OUTPUT (MV)

I	TT(I,1)	TT(I,2)	I	TT(I,1)	TT(I,2)
1	4.2520	4.2546	7	4.2838	4.2919
2	4.2369	4.2367	8	4.2820	4.2936
3	4.2784	4.2796	9	4.2919	4.3026
4	4.2817	4.2824	10	4.2979	4.3076
5	4.2769	4.2815	11	4.3549	4.3800
6	4.2691	4.2695	12	4.3515	4.3790

DIFFERENTIAL PRESSURE -FLOWMETER (IN.) = 0.300
FLOWMETER TEMP (MV) = 1.0524 BULK EXIT TEMP (MV) = 4.5790
INLET PRESSURE MAN , LEFT 3.45 RIGHT 3.50 IN. HG
INLET BULK TEMP CR-AL = 12.300
STATIC PRESSURE DROP (IN.)
P1-P2 = -0.006 P1-P3 = 0.029 P1-P4 = 0.053
P1-P5 = 0.092 P1-P5 = 0.128 P1-P6 = 0.152
BLUE MANOMETER FLUID SP GR 0.797
INLET TEMPERATURE (DEG. F) = 578.18
TW/TO = 0.647 MACH NO. = 0.011
PR = 0.709698 REYD = 1108.4

X+	(X+)M	Q+	NUM	TBULK DEG. F.	TW/TB	(RE)M
0.4301	0.3360	0.0508	~~9.1205~~	225.66	0.977	1434.2
0.3470	0.2763	0.0563	~~4.7852~~	243.75	0.954	1409.0
0.2640	0.2161	0.1744	~~7.5699~~	272.42	0.916	1371.6
0.1810	0.1541	0.2152	~~5.2384~~	316.66	0.865	1319.5
0.0980	0.0881	0.2566	3.5064	387.46	0.793	1244.0
0.0150	0.0146	0.7027	4.8038	528.66	0.683	1138.6

NON DIMENSIONALIZED PRESSURE DROP

X+	P+
0.0458	-0.061
0.1289	0.322
0.2119	0.574
0.2949	1.000
0.3779	1.401
0.4237	1.662

POSITION OF FIRST PRESSURE TAP = 0.010811

X+	(X+)M	F	F(RE)M	FP	FP(RE)M	(RE)M	TBULK DEG F	TB/TO
0.0193	0.0190	0.00086	0.97	-0.00356	-4.02	1123.8	541.6	0.671
0.0651	0.0608	0.00503	6.03	0.00178	2.13	1199.7	441.7	0.745
0.1481	0.1295	0.00897	11.53	0.00727	9.34	1285.0	347.4	0.832
0.2312	0.1930	0.00931	12.52	0.00822	11.06	1345.8	293.0	0.894
0.3142	0.2536	0.00877	12.19	0.00781	10.85	1390.1	256.5	0.938
0.3972	0.3134	0.01095	15.56	0.01035	14.70	1421.0	233.5	0.969
0.4430	0.3464	~~0.01144~~	~~14.40~~	0.01097	~~15.71~~	~~1433.2~~	221.9	0.981

PARABOLIC INLET VELOCITY TEST NO. 2
TARE TEST TAKEN FROM RUN NO. 2
TARE THERMOCOUPLE OUTPUT (MV)

I	TA(I,1)	TA(I,2)	I	TA(I,1)	TA(I,2)
1	4.1866	4.1866	7	4.2095	4.2111
2	4.1715	4.1690	8	4.2038	4.2110
3	4.2084	4,2091	9	4.2096	4.2094
4	4,2140	4.2119	10	4.2148	4.2134
5	4.2091	4,2082	11	4.2306	4.2316
6	4.2015	4.1968	12	4,2306	4.2294

TEST THERMOCOUPLE OUTPUT (MV)

I	TT(I,1)	TT(I,2)	I	TT(I,1)	TT(I,2)
1	4,1946	4.1959	7	4.2304	4.2421
2	4.1804	4,1807	8	4.2412	4,2412
3	4.2161	4.2206	9	4.2427	4.2579
4	4.2212	4.2221	10	4,2457	4.2578
5	4.2175	4.2244	11	4.3116	4.3475
6	4.2084	4.2091	12	4.3105	4.3492

DIFFERENTIAL PRESSURE -FLOWMETER (IN.) = 0.386
FLOWMETER TEMP (MV) = 0.8435 BULK EXIT TEMP (MV) = 4.9610
INLET PRESSURE MAN , LEFT 2.95 RIGHT 3.05 IN. HG
INLET BULK TEMP CR-AL = 13.249
STATIC PRESSURE DROP (IN.)
P1-P2 = -0.010 P1-P3 = 0.033 P1-P4 = 0.064
P1-P5 = 0.108 P1-P5 = 0.161 P1-P6 = 0.193
BLUE MANOMETER FLUID SP GR 0.797
INLET TEMPERATURE (DEG. F) = 618.91
TW/T_0 = 0.622 MACH NO. = 0.016
PR = 0.712609 RLYD = 1435.1

X+	(X+)M	Q+	NUM	TBULK DEG. F.	TW/TB	(PE)M
0.3307	0.2584	0.0503	~~4.4957~~	240.81	0.953	1866.9
0.2669	0.2135	0.0863	~~4.4247~~	264.99	0.923	1824.6
0.2030	0.1678	0.1263	~~3.7950~~	300.56	0.879	1767.5
0.1392	0.1201	0.2892	~~5.3210~~	352.68	0.824	1693.1
0.0753	0.0687	0.3538	3.9100	432.42	0.751	1597.2
0.0115	0.0113	0.8745	5.2496	581.44	0.647	1462.0

NON DIMENSIONALIZED PRESSURE DROP

X+	P+
0.0352	-0.056
0.0991	0.192
0.1629	0.374
0.2268	0.636
0.2906	0.945
0.3259	1.133

POSITION OF FIRST PRESSURE TAP = 0.008313

X+	(X+)M	F	F(RE)M	FP	IP(RE)4	(RI)M	TBULK DEG F	TB/T_0
0.0148	0.0147	0.00131	1.91	-0.00296	-4.29	1450.6	594.2	0.637
0.0511	0.0474	0.00412	6.33	0.00089	1.37	1535.7	491.3	0.706
0.1139	0.1010	0.00663	10.92	0.00479	7.88	1646.2	387.7	0.793
0.1778	0.1501	0.00668	11.56	0.00541	9.36	1730.4	324.0	0.857
0.2416	0.1965	0.00633	11.37	0.00520	9.33	1795.7	281.0	0.907
0.3055	0.2416	0.00832	15.35	0.00751	13.86	1845.0	251.6	0.944
0.3467	0.2762	~~0.00863~~	~~16.11~~	~~[illegible]~~	~~14.94~~	1866.2	239.8	0.960

PARABOLIC INLET VELOCITY TEST NO. 3
TARE TEST TAKEN FROM RUN NO. 3
TARE THERMOCOUPLE OUTPUT (MV)

I	TA(I,1)	TA(I,2)	I	TA(I,1)	TA(I,2)
1	4.2441	4.2468	7	4.2819	4.2819
2	4.2318	4.2305	8	4.2866	4.2866
3	4.2802	4.2792	9	4.2811	4.2764
4	4.2861	4.2869	10	4.2853	4.2852
5	4.2901	4.2889	11	4.2999	4.2998
6	4.2776	4.2715	12	4.2994	4.2958

TEST THERMOCOUPLE OUTPUT (MV)

I	TT(I,1)	TT(I,2)	I	TT(I,1)	TT(I,2)
1	4.2599	4.2592	7	4.3154	4.3154
2	4.2430	4.2419	8	4.3144	4.3285
3	4.2817	4.2870	9	4.3215	4.3439
4	4.2880	4.2894	10	4.3305	4.3440
5	4.2993	4.3055	11	4.3915	4.4319
6	4.2894	4.2912	12	4.3930	4.4350

DIFFERENTIAL PRESSURE -FLOWMETER (IN.) = 0.442
FLOWMETER TEMP (MV) = 0.9812 BULK EXIT TEMP (MV) = 4.9150
INLET PRESSURE MAN , LEFT 3.40 RIGHT 3.50 IN. HG
INLET BULK TEMP CR-AL = 13.920
STATIC PRESSURE DROP (IN.)
P1-P2 = -0.008 P1-P3 = 0.006 P1-P4 = 0.068
P1-P5 = 0.120 P1-P5 = 0.182 P1-P6 = 0.220
BLUE MANOMETER FLUID SP GR 0.797
INLET TEMPERATURE (DEG. F) = 647.82
TW/TO = 0.606 MACH NO. = 0.018
PP = 0.715244 REYD = 1592.9

X+	(X+)M	Q+	NUM	TBULK DEG. F.	TW/TB	(RE)M
0.2969	0.2295	~~[illegible]~~	~~-3.4035~~	240.22	0.957	2101.4
0.2396	0.1909	0.0827	~~4.1334~~	271.11	0.919	2041.2
0.1823	0.1504	0.1769	~~5.1786~~	310.11	0.872	1972.2
0.1250	0.1075	0.2940	~~5.3976~~	361.29	0.819	1892.0
0.0677	0.0612	0.3414	3.9608	434.14	0.753	1794.8
0.0133	0.0100	0.9652	6.3098	571.63	0.656	1653.2

NON DIMENSIONALIZED PRESSURE DROP

X+	P+
0.0316	-0.037
0.0890	0.029
0.1463	0.313
0.2036	0.556
0.2609	0.839
0.2926	1.016

POSITION OF FIRST PRESSURE TAP = 0.007464

X+	(X+)M	F	F(RE)M	FP	FP(RE)M	(RE)M	TBULK DEG F	TB/TO
0.0133	0.0130	0.00119	1.95	-0.00297	-4.86	1630.5	585.6	0.643
0.0459	0.0420	0.00300	5.19	-0.00004	-0.07	1732.4	436.8	0.710
0.1023	0.0902	0.00538	9.93	0.00376	6.93	1843.8	395.8	0.787
0.1596	0.1345	0.00669	12.92	0.00555	10.72	1931.2	333.7	0.847
0.2169	0.1760	0.00727	14.58	0.00617	12.37	2005.2	289.3	0.897
0.2743	0.2154	0.00767	15.87	0.00690	14.28	2069.5	254.8	0.940
0.3059	0.2364	~~0.00862~~	~~18.12~~	~~0.00777~~	~~16.14~~	2101.5	238.7	0.962

PARABOLIC INLET VELOCITY TEST NO. 9
TARE TEST TAKEN FROM RUN NO. 4
TARE THERMOCOUPLE OUTPUT (MV)

I	TA(I,1)	TA(I,2)	I	TA(I,1)	TA(I,2)
1	4.2389	4.2403	7	4.2861	4.2882
2	4.2224	4.2212	8	4.2854	4.2893
3	4.2684	4.2695	9	4.2837	4.2804
4	4.2749	4.2729	10	4.2885	4.2865
5	4.2898	4.2893	11	4.3042	4.3048
6	4.2812	4.2754	12	4.3039	4.3028

TEST THERMOCOUPLE OUTPUT (MV)

I	TT(I,1)	TT(I,2)	I	TT(I,1)	TT(I,2)
1	4.2400	4.2393	7	4.3055	4.3055
2	4.2849	4.2403	8	4.3100	4.3249
3	4.2851	4.2903	9	4.3101	4.3307
4	4.2900	4.2915	10	4.3180	4.3338
5	4.2998	4.3076	11	4.5058	4.5954
6	4.2904	4.2942	12	4.5301	4.6536

DIFFERENTIAL PRESSURE -FLOWMETER (IN.) = 0.566
FLOWMETER TEMP (MV) = 0.8602 BULK EXIT TEMP (MV) = 4.3450
INLET PRESSURE MAN , LEFT 5.75 RIGHT 5.90 IN. HG
INLET BULK TEMP CR-AL = 14.021
STATIC PRESSURE DROP (IN.)
P1-P2 = 0.001 P1-P3 = 0.002 P1-P4 = 0.002
P1-P5 = 0.003 P1-P5 = 0.004 P1-P6 = 0.005
BLUE MANOMETER FLUID SP GR 0.797
INLET TEMPERATURE (DEG. F) = 652.18
TW/TO = 0.603 MACH NO. = 0.020
PR = 0.715627 REYD = 2067.5

X+	(X+)M	Q+	NUM	TBULK DEG. F.	TW/TB	(RE)M
0.2286	0.1712	-0.5541	-926.1641	211.66	0.997	2811.9
0.1845	0.1351	0.0918	-14.8064	191.29	1.031	2872.5
0.1404	0.1020	0.2137	-26.0078	184.58	1.042	2892.3
0.0962	0.0711	0.2279	-56.1272	199.75	1.020	2846.9
0.0521	0.0409	0.4440	30.8898	257.00	0.939	2689.6
0.0080	0.0073	2.3427	25.2938	458.10	0.745	2297.5

NON DIMENSIONALIZED PRESSURE DROP

X+	P+
0.0244	0.002
0.0685	0.005
0.1126	0.007
0.1568	0.010
0.2009	0.012
0.2253	0.015

MANOMETER LINE BLEW: DUMMY VALUES.

POSITION OF FIRST PRESSURE TAP = 0.005748

X+	(X+)M	F	F(RE)M	FP	FP(RE)M	(RE)M	TBULK DEG F	TB/T
0.0153	0.0096	~~0.00827~~	~~18.67~~	~~0.00009~~	~~0.20~~	2256.2	484.6	0.711
0.0346	0.0288	~~0.00558~~	~~14.18~~	~~0.00008~~	~~0.20~~	2540.0	320.1	0.861
0.0788	0.0596	~~0.00144~~	~~4.00~~	~~0.00006~~	~~0.16~~	2782.5	220.7	0.987
0.1229	0.0898	~~0.00009~~	~~0.27~~	~~0.00005~~	~~0.16~~	2876.8	188.6	1.036
0.1670	0.1217	~~0.00017~~	~~0.48~~	~~0.00007~~	~~0.19~~	2885.2	185.9	1.040
0.2112	0.1564	~~-0.00037~~	~~-1.01~~	~~0.00009~~	~~0.25~~	2841.8	200.1	1.018
0.2355	0.1769	~~-0.00060~~	~~-1.66~~	~~0.00011~~	~~0.31~~	2804.0	213.1	0.998

PARABOLIC INLET VELOCITY TEST NO. 10
TARE TEST TAKEN FROM RUN NO. 4
TARE THERMOCOUPLE OUTPUT (MV)

I	TA(I,1)	TA(I,2)	I	TA(I,1)	TA(I,2)
1	4.2389	4.2403	7	4.2861	4.2882
2	4.2224	4.2212	8	4.2854	4.2893
3	4.2684	4.2695	9	4.2837	4.2804
4	4.2749	4.2729	10	4.2885	4.2865
5	4.2698	4.2893	11	4.3042	4.3048
6	4.2612	4.2754	12	4.3039	4.3028

TEST THERMOCOUPLE OUTPUT (MV)

I	TT(I,1)	TT(I,2)	I	TT(I,1)	TT(I,2)
1	4.2519	4.2546	7	4.2948	4.2948
2	4.2407	4.2390	8	4.2963	4.3071
3	4.2618	4.2859	9	4.3073	4.3259
4	4.2860	4.2868	10	4.3134	4.3281
5	4.2941	4.2995	11	4.4070	4.4512
6	4.2839	4.2858	12	4.4068	4.4641

DIFFERENTIAL PRESSURE -FLOWMETER (IN.) = 0.492
FLOWMETER TEMP (MV) = 0.8700 BULK EXIT TEMP (MV) = 4.6330
INLET PRESSURE MAN , LEFT 4.50 RIGHT 4.65 IN. HG
INLET BULK TEMP CR-AL = 14.025
STATIC PRESSURE DROP (IN.)
P1-P2 = -0.019 P1-P3 = 0.012 P1-P4 = 0.081
P1-P5 = 0.147 P1-P5 = 0.222 P1-P6 = 0.264
BLUE MANOMETER FLUID SP GR 0.797
INLET TEMPERATURE (DEG. F) = 652.35
TW/TO = 0.603 MACH NO. = 0.019
PR = 0.715642 REYD = 1794.8

X+	(X+)M	Q+	NUM	TBULK DEG. F.	TW/TB	(RE)M
0.2634	0.2511	~~0.0074~~	~~1.1892~~	229.64	0.972	2397.4
0.2125	0.1675	0.0701	~~4.2483~~	261.47	0.931	2325.2
0.1617	0.1324	0.1713	~~5.4482~~	302.64	0.880	2241.0
0.1109	0.0949	~~0.1477~~	~~2.7032~~	357.65	0.822	2152.2
0.0600	0.0543	0.4164	4.7837	436.75	0.750	2022.9
0.0092	0.0089	1.1219	7.0979	583.92	0.649	1854.7

NON DIMENSIONALIZED PRESSURE DROP

X+	P+
0.0281	-0.073
0.0789	0.046
0.1298	0.312
0.1806	0.563
0.2314	0.851
0.2595	1.014

POSITION OF FIRST PRESSURE TAP = 0.006621

X+	(X+)M	F	F(RE)M	FP	FP(RE)M	(RE)M	TBULK DEG F	TB/T
0.0118	0.0116	0.00009	0.17	-0.00423	-7.78	1639.3	597.7	0.635
0.0399	0.0373	0.00291	5.66	-0.00031	-0.59	1947.6	493.8	0.704
0.0907	0.0798	0.00614	12.79	0.00435	9.06	2083.2	392.9	0.788
0.1416	0.1186	0.00721	15.80	0.00593	12.99	2190.8	327.9	0.853
0.1924	0.1546	0.00722	16.48	0.00598	13.65	2281.8	280.6	0.907
0.2433	0.1888	0.00778	18.37	0.00687	16.20	2359.6	244.5	0.954
0.2713	0.2071	~~0.00816~~	~~19.56~~	~~0.00729~~	~~17.45~~	2397.6	228.1	0.977

PARABOLIC INLET VELOCITY TEST NO. 11
TARE TEST TAKEN FROM RUN NO. 4
TARE THERMOCOUPLE OUTPUT (MV)

I	TA(I,1)	TA(I,2)	I	TA(I,1)	TA(I,2)
1	4.2389	4.2403	7	4.2861	4.2882
2	4.2224	4.2212	8	4.2854	4.2893
3	4.2684	4.2695	9	4.2837	4.2804
4	4.2749	4.2729	10	4.2885	4.2865
5	4.2898	4.2893	11	4.3042	4.3048
6	4.2612	4.2754	12	4.3039	4.3028

TEST THERMOCOUPLE OUTPUT (MV)

I	TT(I,1)	TT(I,2)	I	TT(I,1)	TT(I,2)
1	4.2530	4.2567	7	4.3034	4.3034
2	4.2421	4.2416	8	4.3039	4.3189
3	4.2809	4.2867	9	4.3199	4.3423
4	4.2882	4.2887	10	4.3274	4.3421
5	4.2991	4.3048	11	4.3866	4.4252
6	4.2899	4.2913	12	4.3818	4.4267

DIFFERENTIAL PRESSURE -FLOWMETER (IN.) = 0.400
FLOWMETER TEMP (MV) = 0.8700 BULK EXIT TEMP (MV) = 4.8980
INLET PRESSURE MAN , LEFT 3.60 RIGHT 3.70 IN. HG
INLET BULK TEMP CR-AL = 13.942
STATIC PRESSURE DROP (IN.)
P1-P2 = -0.015 P1-P3 = 0.011 P1-P4 = 0.058
P1-P5 = 0.118 P1-P5 = 0.175 P1-P6 = 0.210
BLUE MANOMETER FLUID SP GR 0.797
INLET TEMPERATURE (DEG. F) = 648.77
TW/TO = 0.605 MACH NO. = 0.016
PR = 0.715327 REYD = 1461.5

X+	(X+)M	Q+	NUM	TBULK DEG. F.	TW/TB	(RE)M
0.3236	0.2496	0.0327	~~3.9137~~	238.50	0.959	1932.2
0.2611	0.2067	0.0870	~~4.9302~~	264.54	0.927	1885.0
0.1987	0.1632	0.1610	~~4.9567~~	305.15	0.878	1818.0
0.1362	0.1175	0.2311	4.0763	366.55	0.814	1729.7
0.0737	0.0678	0.4186	4.2293	461.70	0.731	1617.8
0.0113	0.0112	0.9355	5.0145	633.84	0.619	1471.6

NON DIMENSIONALIZED PRESSURE DROP

X+	P+
0.0345	-0.084
0.0970	0.062
0.1594	0.323
0.2219	0.655
0.2843	0.970
0.3188	1.169

POSITION OF FIRST PRESSURE TAP = 0.008134

X+	(X+)M	F	F(RE)M	FP	FP(RE)M	(RE)M	TBULK DEG F	TB/TO
0.0145	0.0145	0.00022	0.33	-0.00431	-6.30	1465.5	647.2	0.607
0.0495	0.0468	0.00318	4.92	-0.00038	-0.59	1549.0	531.4	0.678
0.1115	0.0992	0.00680	11.39	0.00462	7.74	1674.9	405.4	0.774
0.1739	0.1464	0.00820	14.55	0.00668	11.85	1774.3	332.6	0.848
0.2364	0.1906	0.00835	15.46	0.00704	13.03	1851.7	282.6	0.905
0.2989	0.2335	0.00882	16.84	0.00786	15.00	1908.5	249.9	0.947
0.3334	0.2572	~~0.00945~~	~~18.25~~	~~0.00879~~	~~16.94~~	1931.5	237.4	0.964

PARABOLIC INLET VELOCITY TEST NO. 12
TARE TEST TAKEN FROM RUN NO. 4
TARE THERMOCOUPLE OUTPUT (MV)

I	TA(I,1)	TA(I,2)	I	TA(I,1)	TA(I,2)
1	4.2389	4.2403	7	4.2861	4.2882
2	4.2224	4.2212	8	4.2854	4.2893
3	4.2684	4.2695	9	4.2837	4.2804
4	4.2749	4.2729	10	4.2885	4.2865
5	4.2898	4.2893	11	4.3042	4.3048
6	4.2612	4.2754	12	4.3039	4.3028

TEST THERMOCOUPLE OUTPUT (MV)

I	TT(I,1)	TT(I,2)	I	TT(I,1)	TT(I,2)
1	4.2514	4.2560	7	4.3007	4.3007
2	4.2421	4.2420	8	4.2986	4.3108
3	4.2839	4.2892	9	4.3105	4.3291
4	4.2895	4.2898	10	4.3163	4.3275
5	4.2992	4.3041	11	4.3813	4.4180
6	4.2884	4.2905	12	4.3809	4.4226

DIFFERENTIAL PRESSURE -FLOWMETER (IN.) = 0.350
FLOWMETER TEMP (MV) = 0.8685 BULK EXIT TEMP (MV) = 4.9670
INLET PRESSURE MAN , LEFT 3.40 RIGHT 3.50 IN. HG
INLET BULK TEMP CR-AL = 13.810
STATIC PRESSURE DROP (IN.)
P1-P2 = -0.010 P1-P3 = 0.021 P1-P4 = 0.055
P1-P5 = 0.[illegible]27 P1-P5 = 0.143 P1-P6 = 0.174
BLUE MANOMETER FLUID SP GR 0.797
INLET TEMPERATURE (DEG. F) = 643.08
TW/TO = 0.608 MACH NO. = 0.014
PR = 0.714832 REYD = 1282.4

X+	(X+)M	Q+	NUM	TBULK DEG. F.	TW/TB	(RE)M
0.3690	0.2657	0.0475	~~4.7991~~	240.35	0.957	1688.0
0.2978	0.2351	0.0793	~~4.9266~~	259.75	0.933	1657.1
0.2266	0.1843	0.1782	~~6.3828~~	292.34	0.893	1608.9
0.1553	0.1320	0.1743	3.6322	344.18	0.836	1549.5
0.0841	0.0759	0.3337	3.9530	428.43	0.757	1447.5
0.0128	0.0126	0.8874	5.3140	595.31	0.641	1312.1

NON DIMENSIONALIZED PRESSURE DROP

X+	P+
0.0393	-0.075
0.1106	0.149
0.1818	0.397
0.2531	0.701
0.3243	1.035
0.3636	1.253

POSITION OF FIRST PRESSURE TAP = 0.009277

X+	(X+)M	F	F(RE)M	FP	FP(RE)M	(RE)M	TBULK DEG F	TB/TO
0.0166	0.0164	0.00068	0.89	-0.00415	-5.39	1300.7	[illegible]10.1	0.628
0.0559	0.0525	0.00406	5.63	0.00045	0.62	1386.4	495.1	0.705
0.1271	0.1112	0.00742	11.10	0.00547	8.18	1495.[illegible]	386.7	0.799
0.1984	0.1649	0.00786	12.38	0.00661	10.42	1575.4	315.2	0.867
0.2696	0.2160	0.00753	12.29	0.00644	10.51	1633.2	274.0	0.915
0.3408	0.2665	0.00934	15.61	0.00863	14.43	1672.3	24[illegible].6	0.948
0.3802	0.2945	~~0.01193~~	~~16.92~~	~~0.00954~~	~~16.17~~	1686.9	239.6	0.961

PARABOLIC INLET VELOCITY TEST NO. 13
TARE TEST TAKEN FROM RUN NO. 4
TARE THERMOCOUPLE OUTPUT (MV)

I	TA(I,1)	TA(I,2)	I	TA(I,1)	TA(I,2)
1	4.2389	4.2403	7	4.2861	4.2882
2	4.2224	4.2212	8	4.2854	4.2893
3	4.2684	4.2695	9	4.2837	4.2804
4	4.2749	4.2729	10	4.2885	4.2865
5	4.2898	4.2893	11	4.3042	4.3048
6	4.2812	4.2754	12	4.3039	4.3028

TEST THERMOCOUPLE OUTPUT (MV)

I	TT(I,1)	TT(I,2)	I	TT(I,1)	TT(I,2)
1	4.2425	4.2455	7	4.2916	4.2916
2	4.2307	4.2289	8	4.3047	4.3047
3	4.2768	4.2803	9	4.3078	4.3191
4	4.2827	4.2821	10	4.3121	4.3226
5	4.2939	4.2978	11	4.3737	4.4082
6	4.2840	4.2845	12	4.3715	4.4099

DIFFERENTIAL PRESSURE -FLOWMETER (IN.) = 0.300
FLOWMETER TEMP (MV) = 0.6968 BULK EXIT TEMP (MV) = 4.5215
INLET PRESSURE MAN , LEFT 3.50 RIGHT 3.70 IN. HG
INLET BULK TEMP CR-AL = 14.020
STATIC PRESSURE DROP (IN.)
P1-P2 = -0.007 P1-P3 = 0.023 P1-P4 = 0.052
P1-P5 = 0.088 P1-P5 = 0.129 P1-P6 = 0.151
BLUE MANOMETER FLUID SP GR 0.797
INLET TEMPERATURE (DEG. F) = 652.14
TW/TO = 0.604 MACH NO. = 0.012
PR = 0.715623 REYD = 1120.2

X+	(X+)M	Q+	NUM	TBULK DEG. F.	TW/TB	(RE)B
0.4220	0.3201	0.0093	~~2.1091~~	223.62	0.980	1505.2
0.3405	0.2639	0.0458	~~4.2703~~	244.32	0.953	1474.9
0.2591	0.2077	0.1402	~~6.1228~~	279.41	0.908	1427.5
0.1776	0.1495	~~0.2690~~	~~1.5680~~	335.45	0.845	1360.8
0.0961	0.0864	0.3113	3.7787	426.56	0.759	1271.3
0.0147	0.0144	0.8157	4.7836	605.61	0.634	1145.0

NON DIMENSIONALIZED PRESSURE DROP

X+	P+
0.0459	-0.067
0.1264	0.217
0.2079	0.485
0.2894	0.822
0.3708	1.210
0.4158	1.419

POSITION OF FIRST PRESSURE TAP = 0.010608

X+	(X+)M	F	F(RE)M	FP	FP(RE)M	(RE)M	TBULK DEG F	TB/T
0.0189	0.0188	0.00135	1.53	-0.00374	-4.25	1134.8	621.3	0.621
0.0639	0.0599	0.00487	5.91	0.00100	1.22	1213.8	496.2	0.703
0.1454	0.1263	0.00849	11.18	0.00635	8.37	1317.6	374.3	0.805
0.2268	0.1862	0.00910	12.70	0.00770	10.74	1394.9	304.1	0.879
0.3083	0.2429	0.00878	12.74	0.00753	10.94	1451.6	259.7	0.934
0.3898	0.2988	0.01045	15.57	0.00960	14.31	1490.1	232.4	0.971
0.4347	0.3300	0.00997	14.99	0.00945	14.21	1504.3	222.8	0.984

PARABOLIC INLET VELOCITY TEST NO. 20
TARE TEST TAKEN FROM RUN NO. 16
TARE THERMOCOUPLE OUTPUT (MV)

I	TA(I,1)	TA(I,2)	I	TA(I,1)	TA(I,2)
1	4.2323	4.2321	7	4.2768	4.2771
2	4.2180	4.2156	8	4.2749	4.2785
3	4.2685	4.2686	9	4.2793	4.2739
4	4.2739	4.2719	10	4.2837	4.2824
5	4.2864	4.2846	11	4.2966	4.2969
6	4.2741	4.2688	12	4.2968	4.2937

TEST THERMOCOUPLE OUTPUT (MV)

I	TT(I,1)	TT(I,2)	I	TT(I,1)	TT(I,2)
1	4.0000	4.0000	7	4.2839	4.2839
2	4.0000	4.0000	8	4.2881	4.2881
3	4.0000	4.0000	9	4.2800	4.2842
4	4.0000	4.0000	10	4.2832	4.2884
5	4.2834	4.2831	11	4.3306	4.3475
6	4.2704	4.2686	12	4.3329	4.3182

DIFFERENTIAL PRESSURE -FLOWMETER (IN.) = 0.394
FLOWMETER TEMP (MV) = 0.8760 BULK EXIT TEMP (MV) = 4.2953
INLET PRESSURE MAN , LEFT 3.70 RIGHT 3.85 IN. HG
INLET BULK TEMP CR-AL = 7.985
STATIC PRESSURE DROP (IN.)
P1-P2 = 0.012 P1-P3 = 0.045 P1-P4 = 0.103
P1-P5 = 0.151 P1-P5 = 0.206 P1-P6 = 0.238
BLUE MANOMETER FLUID SP GR 0.797
INLET TEMPERATURE (DEG. F) = 397.35
TW/TO = 0.783 MACH NO. = 0.014
PR = 0.700698 REYD = 1663.8

X+	(X+)M	Q+	NUM	TBULK DEG. F.	TW/TB	(RE)M
0.2901	0.2472	0.0488	~~7.4312~~	214.23	0.980	1948.3
0.2341	0.2021	0.0363	~~2.8492~~	226.61	0.962	1924.1
0.1781	0.1566	0.1206	~~7.1726~~	244.34	0.952	1891.0
0.1221	0.1101	~~0.2640~~	~~2.1248~~	269.87	0.920	1846.2
0.0661	0.0617	0.2510	4.8183	308.51	0.874	1784.2
0.0101	0.0100	0.6043	6.3163	380.25	0.802	1684.9

NON DIMENSIONALIZED PRESSURE DROP

X+	P+
0.0309	0.089
0.0869	0.338
0.1429	0.766
0.1989	1.122
0.2549	1.532
0.2858	1.775

POSITION OF FIRST PRESSURE TAP = 0.007292

X+	(X+)M	F	F(RE)M	FP	FP(RE)M	(RE)M	TBULK DEG F	TB/TO
0.0130	0.0129	0.00358	8.00	0.00102	3.71	1674.9	386.3	0.794
0.0439	0.0421	0.00529	10.20	0.00342	6.96	1740.2	336.9	0.843
0.0999	0.0917	0.00711	12.91	0.00609	11.06	1815.6	286.9	0.900
0.1559	0.1389	0.00775	14.48	0.00707	13.21	1867.8	255.9	0.939
0.2119	0.1848	0.00790	15.06	0.00732	13.95	1906.3	234.7	0.967
0.2679	0.2300	0.00837	16.20	0.00798	15.44	1934.6	219.8	0.988
0.2988	0.2549	~~0.00843~~	~~17.38~~	~~0.00859~~	~~16.73~~	1946.7	213.7	0.998

PARABOLIC INLET VELOCITY TEST NO. 14
TARE TEST TAKEN FROM RUN NO. 4
TARE THERMOCOUPLE OUTPUT (MV)

I	TA(I,1)	TA(I,2)	I	TA(I,1)	TA(I,2)
1	4.2389	4.2403	7	4.2861	4.2882
2	4.2224	4.2212	8	4.2854	4.2893
3	4.2684	4.2695	9	4.2837	4.2804
4	4.2749	4.2729	10	4.2885	4.2865
5	4.2898	4.2893	11	4.3042	4.3048
6	4.2812	4.2754	12	4.3039	4.3028

TEST THERMOCOUPLE OUTPUT (MV)

I	TT(I,1)	TT(I,2)	I	TT(I,1)	TT(I,2)
1	4.2327	4.2317	7	4.2800	4.2800
2	4.2189	4.2176	8	4.2910	4.2910
3	4.2659	4.2693	9	4.2923	4.3009
4	4.2721	4.2718	10	4.2999	4.3084
5	4.2838	4.2858	11	4.3655	4.3970
6	4.2737	4.2732	12	4.3601	4.3939

DIFFERENTIAL PRESSURE -FLOWMETER (IN.) = 0.251
FLOWMETER TEMP (MV) = 0.8585 BULK EXIT TEMP (MV) = 4.5950
INLET PRESSURE MAN., LEFT 3.70 RIGHT 3.85 IN. HG
INLET BULK TEMP CR-AL = 13.971
STATIC PRESSURE DROP (IN.)
P1-P2 = -0.003 P1-P3 = 0.022 P1-P4 = 0.049
P1-P5 = 0.079 P1-P5 = 0.110 P1-P6 = 0.130
BLUE MANOMETER FLUID SP GR 0.797
INLET TEMPERATURE (DEG. F) = 650.02
TW/TO = 0.605 MACH NO. = 0.010
PR = 0.715437 REYD = 918.0

X+	(X+)M	Q+	NUM	TBULK DEG. F.	TW/TB	(RE)M
0.5151	0.3917	~~0.0264~~	~~5.1940~~	225.16	0.977	1230.4
0.4157	0.3199	0.0484	~~5.0028~~	236.79	0.963	1216.3
0.3162	0.2502	0.1183	~~6.6453~~	264.55	0.926	1184.6
0.2168	0.1796	~~0.0692~~	~~1.8918~~	315.65	0.865	1132.2
0.1174	0.1042	0.2627	3.5455	406.80	0.776	1055.2
0.0179	0.0176	0.7351	4.3993	597.89	0.639	940.9

NON DIMENSIONALIZED PRESSURE DROP

X+	P+
0.0549	-0.045
0.1543	0.304
0.2538	0.687
0.3532	1.115
0.4527	1.554
0.5075	1.836

POSITION OF FIRST PRESSURE TAP = 0.012949

X+	(X+)M	F	F(RE)M	FP	FP(RE)M	(RE)M	TBULK DEG F	TB/TI
0.0231	0.0229	0.00174	1.62	-0.00387	-3.61	931.7	515.2	0.625
0.0780	0.0725	0.00624	6.27	0.00203	2.04	1003.8	479.7	0.715
0.1774	0.1519	0.01077	11.80	0.00863	9.45	1095.7	354.5	0.825
0.2769	0.2239	0.01120	12.99	0.01002	11.62	1159.7	286.5	0.900
0.3763	0.2934	0.01031	12.38	0.00947	11.37	1201.3	248.2	0.949
0.4758	0.3638	0.01199	14.67	0.01183	14.48	1223.7	229.2	0.975
0.5307	0.4040	0.01289	15.85	0.01266	15.56	1229.0	224.9	0.981

PARABOLIC INLET VELOCITY TEST NO. 22
TARE TEST TAKEN FROM RUN NO. 22
TARE THERMOCOUPLE OUTPUT (MV)

I	TA(I,1)	TA(I,2)	I	TA(I,1)	TA(I,2)
1	4.2441	4.2452	7	4.2585	4.2594
2	4.2323	4.2290	8	4.2620	4.2645
3	4.2526	4.2521	9	4.2562	4.2500
4	4.2632	4.2598	10	4.2550	4.2525
5	4.2705	4.2700	11	4.2865	4.2879
6	4.2592	4.2533	12	4.2854	4.2843

TEST THERMOCOUPLE OUTPUT (MV)

I	TT(I,1)	TT(I,2)	I	TT(I,1)	TT(I,2)
1	4.2530	4.2698	7	4.3110	4.3110
2	4.2531	4.2530	8	4.3325	4.3325
3	4.2764	4.2812	9	4.3316	4.3582
4	4.2880	4.2920	10	4.3338	4.3589
5	4.3003	4.3076	11	4.5623	4.6738
6	4.2856	4.2904	12	4.6076	4.7673

DIFFERENTIAL PRESSURE -FLOWMETER (IN.) = 0.576
FLOWMETER TEMP (MV) = 0.8599 BULK EXIT TEMP (MV) = 6.3303
INLET PRESSURE MAN , LEFT 5.80 RIGHT 6.00 IN. HG
INLET BULK TEMP CR-AL = 19.192
STATIC PRESSURE DROP (IN.)
P1-P2 = -0.045 P1-P3 = 0.012 P1-P4 = 0.100
P1-P5 = 0.202 P1-P5 = 0.316 P1-P6 = 0.381
BLUE MANOMETER FLUID SP GR 0.797
INLET TEMPERATURE (DEG. F) = 875.64
TW/TO = 0.502 MACH NO. = 0.023
PR = 0.740267 REYD = 1943.0

X+	(X+)M	Q+	NUM	TBULK DEG. F.	TW/TB	(RE)M
0.2352	0.1813	~~0.1525~~	~~7.4787~~	286.50	0.898	2664.5
0.1898	0.1448	0.1158	7.2150	275.21	0.913	2691.6
0.1444	0.1110	0.1789	9.8246	283.31	0.904	2672.0
0.0990	0.0787	~~0.2287~~	~~0.9936~~	321.52	0.861	2585.4
0.0535	0.0457	0.5172	8.9709	414.89	0.771	2407.2
0.0082	0.0079	2.2255	14.3736	679.30	0.604	2079.4

NON DIMENSIONALIZED PRESSURE DROP

X+	P+
0.0251	-0.110
0.0705	0.029
0.1159	0.245
0.1613	0.496
0.2067	0.777
0.2317	0.938

POSITION OF FIRST PRESSURE TAP = 0.005912

X+	(X+)M	F	F(RE)M	FP	FP(RE)M	(RE)M	TBULK DEG F	TB/TO
0.0106	0.0103	0.00238	4.87	-0.00576	-11.80	2050.2	710.3	0.574
0.0356	0.0320	0.00477	10.81	-0.00102	-2.32	2269.0	504.2	0.697
0.0810	0.0664	0.00727	18.22	0.00526	13.19	2506.5	358.3	0.821
0.1264	0.0986	0.00763	20.10	0.00706	18.61	2635.0	297.6	0.887
0.1718	0.1314	0.00711	19.08	0.00669	17.97	2685.2	276.3	0.913
0.2172	0.1665	0.00738	19.77	0.00788	21.11	2678.9	278.9	0.909
0.2423	0.1872	0.00754	20.05	0.00797	21.19	2658.3	287.5	0.899

PARABOLIC INLET VELOCITY TEST NO. 23
TARE TEST TAKEN FROM RUN NO. 22
TARE THERMOCOUPLE OUTPUT (MV)

I	TA(I,1)	TA(I,2)	I	TA(I,1)	TA(I,2)
1	4.2441	4.2452	7	4.2585	4.2594
2	4.2323	4.2290	8	4.2620	4.2645
3	4.2526	4.2521	9	4.2562	4.2500
4	4.2632	4.2598	10	4.2550	4.2525
5	4.2705	4.2700	11	4.2865	4.2879
6	4.2592	4.2533	12	4.2854	4.2843

TEST THERMOCOUPLE OUTPUT (MV)

I	TT(I,1)	TT(I,2)	I	TT(I,1)	TT(I,2)
1	4.2562	4.2609	7	4.2868	4.2868
2	4.2456	4.2451	8	4.3054	4.3054
3	4.2659	4.2699	9	4.3314	4.3682
4	4.2764	4.2792	10	4.3407	4.3714
5	4.2854	4.2919	11	4.4286	4.4948
6	4.2716	4.2724	12	4.4384	4.5145

DIFFERENTIAL PRESSURE -FLOWMETER (IN.) = 0.505
FLOWMETER TEMP (MV) = 0.8750 BULK EXIT TEMP (MV) = 5.8591
INLET PRESSURE MAN , LEFT 4.70 RIGHT 4.85 IN. HG
INLET BULK TEMP CR-AL = 19.157
STATIC PRESSURE DROP (IN.)
P1-P2 = -0.057 P1-P3 = -0.013 P1-P4 = 0.057
P1-P5 = 0.126 P1-P5 = 0.205 P1-P6 = 0.249
BLUE MANOMETER FLUID SP GR 0.797
INLET TEMPERATURE (DEG. F) = 874.13
TW/TO = 0.503 MACH NO. = 0.021
PR = 0.74071 REYD = 1700.8

X+	(X+)M	Q+	NUM	TBULK DEG. F.	TW/TB	(PE)H
0.2688	0.2054	0.0541	~~3.2080~~	276.94	0.909	2351.5
0.2169	0.1730	0.0977	~~3.1939~~	326.17	0.854	2253.5
0.1650	0.1389	0.1122	~~2.1730~~	397.37	0.783	2132.8
0.1131	0.1013	~~0.9287~~	~~0.3256~~	499.05	0.700	1994.3
0.0612	0.0584	0.6232	4.2617	647.85	0.609	1844.7
0.0093	0.0094	1.1856	4.6779	891.49	0.503	1693.0

NON DIMENSIONALIZED PRESSURE DROP

X+	P+
0.0286	-0.175
0.0805	-0.039
0.1324	0.173
0.1843	0.384
0.2362	0.624
0.2648	0.761

LEAK IN PRESSURE TAP #1.

POSITION OF FIRST PRESSURE TAP = 0.006756

X+	(X+)M	F	F(RE)M	FP	FP(RE)H	(RE)M	TBULK DEG F	TB/TI
0.0121	0.0121	~~0.00296~~	~~4.32~~	~~-0.00742~~	~~-17.50~~	1683.6	897.9	0.491
0.0407	0.0400	0.00222	3.93	-0.00186	-3.29	1706.2	751.2	0.555
0.0926	0.0857	0.00727	13.95	0.00439	8.42	1918.1	565.6	0.655
0.1445	0.1255	0.00782	16.14	0.00568	11.72	2062.8	443.5	0.744
0.1963	0.1609	0.00642	14.08	0.00472	10.34	2193.0	359.4	0.821
0.2482	0.1938	0.00758	17.46	0.00648	14.92	2302.6	299.1	0.885
0.2769	0.2115	0.00808	~~19.00~~	0.00685	~~16.12~~	2352.8	274.8	0.914

PARABOLIC INLET VELOCITY TEST NO. 24
TARE TEST TAKEN FROM RUN NO. 22
TARE THERMOCOUPLE OUTPUT (MV)

I	TA(I,1)	TA(I,2)	I	TA(I,1)	TA(I,2)
1	4.2441	4.2452	7	4.2585	4.2594
2	4.2323	4.2290	8	4.2620	4.2645
3	4.2526	4.2521	9	4.2562	4.2500
4	4.2632	4.2598	10	4.2550	4.2525
5	4.2705	4.2700	11	4.2865	4.2879
6	4.2592	4.2533	12	4.2854	4.2843

TEST THERMOCOUPLE OUTPUT (MV)

I	TT(I,1)	TT(I,2)	I	TT(I,1)	TT(I,2)
1	4.2668	4.2730	7	4.3050	4.3050
2	4.2525	4.2566	8	4.3164	4.3164
3	4.2698	4.2783	9	4.3294	4.3600
4	4.2803	4.2836	10	4.3262	4.3474
5	4.2942	4.3056	11	4.4222	4.4850
6	4.2750	4.2795	12	4.4330	4.5048

DIFFERENTIAL PRESSURE -FLOWMETER (IN.) = 0.451
FLOWMETER TEMP (MV) = 0.8901 BULK EXIT TEMP (MV) = 5.6150
INLET PRESSURE MAN , LEFT 3.90 RIGHT 4.10 IN. HG
INLET BULK TEMP CR-AL = 19.545
STATIC PRESSURE DROP (IN.)
P1-P2 = -0.020 P1-P3 = -0.008 P1-P4 = 0.033
P1-P5 = 0.087 P1-P5 = 0.151 P1-P6 = 0.188
BLUE MANOMETER FLUID SP GR 0.797
INLET TEMPERATURE (DEG. F) = 890.78
TW/TO = 0.497 MACH NO. = 0.020
PR = 0.742262 REYD = 1509.3

X+	(X+)M	Q+	NUM	TBULK DEG. F.	TW/TB	(RE)M
0.3020	0.2287	0.1063	~~7.4237~~	268.90	0.920	2111.3
0.2437	0.1933	0.1399	~~4.9133~~	321.00	0.859	2017.3
0.1854	0.1548	0.1710	3.5238	387.11	0.792	1915.3
0.1271	0.1121	~~0.2282~~	~~0.3647~~	473.64	0.720	1805.6
0.0688	0.0643	0.4367	3.5695	594.65	0.639	1686.5
0.0105	0.0104	1.1010	5.2187	807.97	0.536	1546.0

NON DIMENSIONALIZED PRESSURE DROP

X+	P+
0.0322	-0.073
0.0905	-0.029
0.1488	0.122
0.2071	0.317
0.2654	0.549
0.2975	0.686

POSITION OF FIRST PRESSURE TAP = 0.007591

X+	(X+)M	F	F(RE)M	FP	FP(RE)M	(RE)M	TBULK DEG F	TB/T
0.0135	0.0135	0.00163	2.51	-0.00335	-5.15	1534.8	826.7	0.522
0.0457	0.0441	0.00286	4.64	-0.00102	-1.65	1619.4	579.5	0.590
0.1040	0.0945	0.00472	8.25	0.00234	4.08	1745.2	528.0	0.680
0.1623	0.1394	0.00610	11.33	0.00427	7.94	1859.1	427.1	0.757
0.2206	0.1797	0.00708	13.92	0.00531	10.43	1964.7	351.9	0.828
0.2789	0.2163	0.00793	16.36	0.00655	13.51	2062.6	293.4	0.892
0.3111	0.2354	0.00842	17.78	0.00704	14.88	2113.2	266.4	0.925

PARABOLIC INLET VELOCITY TEST NO. 25
TARE TEST TAKEN FROM RUN NO. 22
TARE THERMOCOUPLE OUTPUT (MV)

I	TA(I,1)	TA(I,2)	I	TA(I,1)	TA(I,2)
1	4.2441	4.2452	7	4.2585	4.2594
2	4.2323	4.2290	8	4.2620	4.2645
3	4.2526	4.2521	9	4.2562	4.2590
4	4.2632	4.2598	10	4.2550	4.2525
5	4.2705	4.2700	11	4.2865	4.2879
6	4.2592	4.2533	12	4.2854	4.2843

TEST THERMOCOUPLE OUTPUT (MV)

I	TT(I,1)	TT(I,2)	I	TT(I,1)	TT(I,2)
1	4.2600	4.2664	7	4.2954	4.2954
2	4.2466	4.2494	8	4.3071	4.3071
3	4.2642	4.2712	9	4.3194	4.3484
4	4.2739	4.2768	10	4.3189	4.3402
5	4.2656	4.2955	11	4.4216	4.4784
6	4.2698	4.2754	12	4.4270	4.4948

DIFFERENTIAL PRESSURE -FLOWMETER (IN.) = 0.400
FLOWMETER TEMP (MV) = 0.8775 BULK EXIT TEMP (MV) = 5.4448
INLET PRESSURE MAN , LEFT 3.25 RIGHT 3.35 IN. HG
INLET BULK TEMP CR-AL = 19.485
STATIC PRESSURE DROP (IN.)
P1-P2 = -0.019 P1-P3 = 0.009 P1-P4 = 0.041
P1-P5 = 0.089 P1-P5 = 0.145 P1-P6 = 0.179
BLUE MANOMETER FLUID SP GR 0.797
INLET TEMPERATURE (DEG. F) = 888.21
TW/TO = 0.498 MACH NO. = 0.018
PR = 0.741920 REYD = 1341.7

X+	(X+)M	Q+	NUM	TBULK DEG. F.	TW/TB	(RE)M
0.3399	0.2557	0.0964	~~7.6644~~	261.78	0.929	1888.0
0.2742	0.2156	0.1235	~~4.8453~~	310.00	0.871	1808.7
0.2086	0.1729	0.1896	~~4.1810~~	376.51	0.802	1715.0
0.1430	0.1253	~~0.2283~~	~~0.3718~~	469.12	0.723	1608.6
0.0774	0.0726	0.4398	3.4752	604.12	0.633	1491.2
0.0118	0.0118	1.0185	4.5037	840.01	0.522	1359.9

NON DIMENSIONALIZED PRESSURE DROP

X+	P+
0.0362	-0.085
0.1018	0.039
0.1674	0.185
0.2330	0.398
0.2986	0.647
0.3349	0.796

POSITION OF FIRST PRESSURE TAP = 0.008543

X+	(X+)M	F	F(RE)M	FP	FP(RE)M	(RE)M	TBULK DEG F	TB/TO
0.0152	0.0152	0.00144	1.95	-0.00378	-5.11	1350.6	859.0	0.509
0.0515	0.0499	0.00359	5.12	-0.00059	-0.84	1426.5	699.8	0.579
0.1171	0.1065	0.00601	9.31	0.00334	5.18	1549.3	529.3	0.679
0.1827	0.1561	0.00676	11.24	0.00481	8.00	1661.2	418.7	0.765
0.2483	0.2004	0.00697	12.28	0.00527	9.29	1761.3	340.4	0.839
0.3139	0.2414	0.00845	15.62	0.00731	13.50	1847.9	283.8	0.903
0.3501	0.2632	~~0.00910~~	~~17.20~~	~~0.00776~~	~~14.65~~	1889.2	259.6	0.934

PARABOLIC INLET VELOCITY TEST NO. 26
TARE TEST TAKEN FROM RUN NO. 22
TARE THERMOCOUPLE OUTPUT (MV)

I	TA(I,1)	TA(I,2)	I	TA(I,1)	TA(I,2)
1	4.2441	4.2452	7	4.2585	4.2594
2	4.2323	4.2290	8	4.2608	4.2608
3	4.2526	4.2521	9	4.2562	4.2500
4	4.2632	4.2598	10	4.2550	4.2525
5	4.2705	4.2700	11	4.2865	4.2879
6	4.2592	4.2533	12	4.2854	4.2843

TEST THERMOCOUPLE OUTPUT (MV)

I	TT(I,1)	TT(I,2)	I	TT(I,1)	TT(I,2)
1	4.2568	4.2615	7	4.2884	4.2884
2	4.2460	4.2464	8	4.3015	4.3015
3	4.2677	4.2734	9	4.3134	4.3378
4	4.2774	4.2805	10	4.3178	4.3331
5	4.2869	4.2925	11	4.4057	4.4581
6	4.2716	4.2748	12	4.4124	4.4724

DIFFERENTIAL PRESSURE -FLOWMETER (IN.) = 0.353
FLOWMETER TEMP (MV) = 0.8656 BULK EXIT TEMP (MV) = 5.1777
INLET PRESSURE MAN , LEFT 3.15 RIGHT 3.30 IN. HG
INLET BULK TEMP CR-AL = 19.124
STATIC PRESSURE DROP (IN.)
P1-P2 = -0.011 P1-P3 = 0.007 P1-P4 = 0.046
P1-P5 = 0.088 P1-P5 = 0.138 P1-P6 = 0.167
BLUE MANOMETER FLUID SP GR 0.797
INLET TEMPERATURE (DEG. F) = 872.71
TW/TO = 0.504 MACH NO. = 0.016
PR = 0.739886 REYD = 1190.8

X+	(X+)M	Q+	NUM	TBULK DEG. F.	TW/TB	(RE)M
0.3840	0.2665	0.0625	~~6.1007~~	251.82	0.942	1684.5
0.3098	0.2412	0.1159	~~5.2034~~	297.24	0.886	1616.3
0.2357	0.1927	0.1527	3.8357	356.38	0.822	1539.4
0.1616	0.1396	~~0.9049~~	~~6.0000~~	435.83	0.750	1453.1
0.0875	0.0804	0.3347	3.1135	550.53	0.666	1355.2
0.0134	0.0131	0.9371	4.7688	765.67	0.553	1231.4

NON DIMENSIONALIZED PRESSURE DROP

X+	P+
0.0409	-0.064
0.1150	0.041
0.1892	0.266
0.2633	0.509
0.3374	0.793
0.3783	0.962

POSITION OF FIRST PRESSURE TAP = 0.009652

X+	(X+)M	F	F(RE)M	FP	FP(RE)M	(RE)M	TBULK DEG F	TB/TO
0.0172	0.0170	0.00178	2.17	-0.00361	-4.41	1221.0	780.0	0.539
0.0581	0.0553	0.00379	4.91	-0.00032	-0.41	1297.7	633.6	0.614
0.1323	0.1179	0.00633	8.89	0.00399	5.61	1404.1	486.9	0.710
0.2064	0.1735	0.00760	11.36	0.00590	8.82	1495.6	392.8	0.788
0.2805	0.2239	0.00825	13.01	0.00658	10.37	1577.0	324.7	0.856
0.3546	0.2704	0.00936	15.43	0.00812	13.39	1649.4	273.0	0.917
0.3956	0.2949	~~0.01005~~	~~16.93~~	~~0.00883~~	~~14.89~~	1685.6	249.7	0.947

PARABOLIC INLET VELOCITY TEST NO. 27
TARE TEST TAKEN FROM RUN NO. 22
TARE THERMOCOUPLE OUTPUT (MV)

I	TA(I,1)	TA(I,2)	I	TA(I,1)	TA(I,2)
1	4.2441	4.2452	7	4.2585	4.2594
2	4.2323	4.2290	8	4.2608	4.2608
3	4.2526	4.2521	9	4.2562	4.2500
4	4.2632	4.2598	10	4.2550	4.2525
5	4.2705	4.2700	11	4.2865	4.2879
6	4.2592	4.2533	12	4.2854	4.2843

TEST THERMOCOUPLE OUTPUT (MV)

I	TT(I,1)	TT(I,2)	I	TT(I,1)	TT(I,2)
1	4.2580	4.2616	7	4.2848	4.2848
2	4.2463	4.2458	8	4.2855	4.2978
3	4.2655	4.2700	9	4.3061	4.3274
4	4.2734	4.2754	10	4.3121	4.3275
5	4.2840	4.2875	11	4.4010	4.4500
6	4.2702	4.2728	12	4.4075	4.4643

DIFFERENTIAL PRESSURE -FLOWMETER (IN.) = 0.300
FLOWMETER TEMP (MV) = 0.8576 BULK EXIT TEMP (MV) = 4.7686
INLET PRESSURE MAN , LEFT 3.20 RIGHT 3.35 IN. HG
INLET BULK TEMP CR-AL = 19.233
STATIC PRESSURE DROP (IN.)
P1-P2 = -0.008 P1-P3 = 0.015 P1-P4 = 0.040
P1-P5 = 0.082 P1-P5 = 0.123 P1-P6 = 0.147
BLUE MANOMETER FLUID SP GR 0.797
INLET TEMPERATURE (DEG. F) = 877.40
TW/TO = 0.502 MACH NO. = 0.013
PR = 0.740497 REYD = 1011.8

X+	(λ+)M	Q+	NUM	TBULK DEG. F.	TW/TB	(RE)M
0.4515	0.3311	0.0453	~~7.5606~~	235.17	0.964	1456.2
0.3644	0.2774	0.0944	~~6.0348~~	273.33	0.915	1404.7
0.2772	0.2220	0.1419	~~4.4438~~	330.98	0.848	1336.5
0.1900	0.1621	0.1911	3.2463	416.86	0.766	1252.4
0.1029	0.0944	0.3348	3.1384	549.69	0.666	1153.5
0.0157	0.0156	0.8764	4.1453	800.84	0.538	1035.1

NON DIMENSIONALIZED PRESSURE DROP

X+	P+
0.0481	-0.063
0.1353	0.120
0.2224	0.316
0.3096	0.652
0.3968	0.974
0.4449	1.164

POSITION OF FIRST PRESSURE TAP = 0.011350

X+	(λ+)M	F	F(RE)M	FP	FP(RE)M	(RE)M	TBULK DEG F	TB/TI
0.0203	0.0202	0.00287	2.95	-0.00309	-3.17	1026.5	822.8	0.524
0.0684	0.0653	0.00484	5.31	0.00016	0.17	1096.6	648.3	0.606
0.1555	0.1376	0.00756	9.09	0.00476	5.73	1203.3	475.1	0.719
0.2427	0.2005	0.00917	11.87	0.00716	9.26	1294.7	369.4	0.810
0.3299	0.2575	0.01007	13.81	0.00815	11.17	1370.9	299.2	0.885
0.4170	0.3115	0.01103	15.78	0.00953	13.64	1430.7	252.1	0.944
0.4652	0.3410	~~0.01114~~	~~16.24~~	~~0.01015~~	~~14.79~~	1456.5	233.6	0.969

PARABOLIC INLET VELOCITY TEST NO. 28
TARE TEST TAKEN FROM RUN NO. 22
TARE THERMOCOUPLE OUTPUT (MV)

I	TA(I,1)	TA(I,2)	I	TA(I,1)	TA(I,2)
1	4.2441	4.2452	7	4.2585	4.2594
2	4.2323	4.2290	8	4.2608	4.2562
3	4.2526	4.2521	9	4.2562	4.2500
4	4.2632	4.2598	10	4.2550	4.2525
5	4.2705	4.2700	11	4.2865	4.2879
6	4.2592	4.2533	12	4.2854	4.2843

TEST THERMOCOUPLE OUTPUT (MV)

I	TT(I,1)	TT(I,2)	I	TT(I,1)	TT(I,2)
1	4.2522	4.2556	7	4.2769	4.2769
2	4.2372	4.2366	8	4.2804	4.2926
3	4.2533	4.2568	9	4.2990	4.3140
4	4.2650	4.2654	10	4.3062	4.3198
5	4.2776	4.2803	11	4.3921	4.4362
6	4.2654	4.2662	12	4.4000	4.4484

DIFFERENTIAL PRESSURE -FLOWMETER (IN.) = 0.251
FLOWMETER TEMP (MV) = 0.8621 BULK EXIT TEMP (MV) = 4.8686
INLET PRESSURE MAN , LEFT 3.45 RIGHT 3.50 IN. HG
INLET BULK TEMP CR-AL = 19.160
STATIC PRESSURE DROP (IN.)
P1-P2 = -0.007 P1-P_3 = 0.019 P1-P4 = 0.042
P1-P5 = 0.076 P1-P5 = 0.109 P1-P6 = 0.090
BLUE MANOMETER FLUID SP GR 0.797
INLET TEMPERATURE (DEG. F) = 874.26
TW/T_U = 0.503 MACH NO. = 0.011
PR = 0.740087 REYD = 846.8

X+	(X+)M	Q+	NUM	TBULK DEG. F.	TW/TB	(RE)M
0.5398	0.3970	0.0430	~~6.4119~~	237.66	0.960	1214.7
0.4356	0.3300	0.0710	~~4.9591~~	267.82	0.921	1180.5
0.3314	0.2633	0.1122	~~3.8409~~	321.05	0.859	1126.7
0.2272	0.1926	0.2619	~~4.6783~~	407.48	0.774	1054.2
0.1230	0.1128	0.3022	2.8358	548.20	0.667	965.3
0.0188	0.0187	0.7712	3.5008	818.24	0.530	860.8

NON DIMENSIONALIZED PRESSURE DROP

X+	P+
0.0575	-0.083
0.1617	0.220
0.2660	0.486
0.3702	0.871
0.4744	1.256
0.5319	1.036

LEAK IN PRESSURE
TAP #7

POSITION OF FIRST PRESSURE TAP = 0.013570

X+	(X+)M	F	F(RE)M	FP	FP(RE)M	(RE)M	TBULK DEG F	TB/TU
0.0242	0.0242	0.00413	3.53	-0.00214	-1.83	853.6	940.9	0.516
0.0818	0.0783	0.00531	4.86	0.00033	0.30	914.3	654.8	0.603
0.1860	0.1640	0.00924	9.34	0.00628	6.34	1010.4	468.5	0.724
0.2902	0.2380	0.01309	14.28	0.01109	12.10	1091.3	359.0	0.820
0.3944	0.3057	~~0.01225~~	~~14.14~~	~~0.01052~~	~~12.15~~	1154.6	290.9	0.895
0.4986	0.3719	~~0.00121~~	~~1.45~~	~~0.00008~~	~~0.10~~	1198.4	250.2	0.946
0.5561	0.4091	~~0.01097~~	~~13.34~~	~~0.01169~~	~~[illegible]~~	1214.3	236.6	0.965

PARABOLIC INLET VELOCITY TEST NO. 29
TARE TEST TAKEN FROM RUN NO. 29
TARE THERMOCOUPLE OUTPUT (MV)

I	TA(I,1)	TA(I,2)	I	TA(I,1)	TA(I,2)
1	4.2514	4.2527	7	4.2568	4.2559
2	4.2370	4.2350	8	4.2588	4.2613
3	4.2604	4.2609	9	4.2714	4.2654
4	4.2713	4.2708	10	4.2768	4.2744
5	4.2822	4.2818	11	4.3079	4.3085
6	4.2731	4.2671	12	4.3064	4.3066

TEST THERMOCOUPLE OUTPUT (MV)

I	TT(I,1)	TT(I,2)	I	TT(I,1)	TT(I,2)
1	4.2739	4.2824	7	4.3231	4.3231
2	4.2621	4.2677	8	4.3221	4.3447
3	4.2789	4.2890	9	4.3504	3.4001
4	4.2909	4.2972	10	4.3573	4.3886
5	4.3105	4.3270	11	4.5043	4.6031
6	4.2889	4.2948	12	4.5019	4.6098

DIFFERENTIAL PRESSURE -FLOWMETER (IN.) = 0.461
FLOWMETER TEMP (MV) = 0.8049 BULK EXIT TEMP (MV) = 5.9850
INLET PRESSURE MAN , LEFT 4.10 RIGHT 4.30 IN. HG
INLET BULK TEMP CR-AL = 26.550
STATIC PRESSURE DROP (IN.)
P1-P2 = -0.038 P1-P3 = -0.002 P1-P4 = 0.006
P1-P5 = 0.097 P1-P5 = 0.123 P1-P6 = 0.163
BLUE MANOMETER FLUID SP GR 0.797
INLET TEMPERATURE (DEG. F) = 1181.18
TW/TO = 0.409 MACH NO. = 0.022
PR = 0.756968 REYD = 1487.5

X+	(X+)M	Q+	NUM	TBULK DEG. F.	TW/TB	(RE)M
0.2890	0.2248	0.0946	~~6.6022~~	286.22	0.899	2148.6
0.2332	0.1937	0.1112	~~3.5981~~	365.60	0.814	2012.2
0.1774	0.1571	0.1489	~~2.6736~~	461.62	0.729	1880.7
0.1216	0.1143	0.2341	~~2.6196~~	582.09	0.646	1754.5
0.0658	0.0651	0.4726	3.3670	744.76	0.560	1633.4
0.0101	0.0102	1.2920	5.4383	1030.24	0.459	1514.5

NON DIMENSIONALIZED PRESSURE DROP

X+	P+
0.0308	-0.109
0.0866	-0.007
0.1424	0.016
0.1982	0.276
0.2540	0.349
0.2848	0.462

POSITION OF FIRST PRESSURE TAP = 0.007265

X+	(X+)M	F	F(RE)M	FP	FP(RE)M	(RE)M	TBULK DEG F	TB/TO
0.0130	0.0131	0.00131	1.97	-0.00444	-6.69	1506.0	1056.8	0.443
0.0438	0.0442	0.00302	4.76	-0.00149	-2.35	1572.3	857.1	0.510
0.0996	0.0962	0.00525	8.87	0.00245	4.14	1691.2	659.8	0.602
0.1553	0.1420	0.00626	11.37	0.00403	7.31	1814.7	517.8	0.687
0.2111	0.1814	0.00639	12.42	0.00410	7.97	1943.4	411.0	0.771
0.2669	0.2149	0.00631	13.11	0.00449	9.32	2077.2	324.0	0.857
0.2977	0.2311	~~0.00903~~	~~19.43~~	~~0.00695~~	~~4.96~~	2153.1	282.3	0.905

PARABOLIC INLET VELOCITY TEST NO. 30
TARE TEST TAKEN FROM RUN NO. 29
TARE THERMOCOUPLE OUTPUT (MV)

I	TA(I,1)	TA(I,2)	I	TA(I,1)	TA(I,2)
1	4.2514	4.2527	7	4.2568	4.2559
2	4.2370	4.2350	8	4.2588	4.2613
3	4.2604	4.2609	9	4.2714	4.2654
4	4.2713	4.2708	10	4.2768	4.2744
5	4.2822	4.2818	11	4.3079	4.3085
6	4.2731	4.2671	12	4.3064	4.3066

TEST THERMOCOUPLE OUTPUT (MV)

I	TT(I,1)	TT(I,2)	I	TT(I,1)	TT(I,2)
1	4.2696	4.2761	7	4.3120	4.3120
2	4.2568	4.2610	8	4.3157	4.3343
3	4.2740	4.2828	9	4.3378	4.3806
4	4.2860	4.2919	10	4.3459	4.3738
5	4.2913	4.3036	11	4.4939	4.5793
6	4.2728	4.2799	12	4.4784	4.5777

DIFFERENTIAL PRESSURE -FLOWMETER (IN.) = 0.402
FLOWMETER TEMP (MV) = 0.8140 BULK EXIT TEMP (MV) = 5.5973
INLET PRESSURE MAN , LEFT 3.40 RIGHT 3.60 IN. HG
INLET BULK TEMP CR-AL = 26.325
STATIC PRESSURE DROP (IN.)
P1-P2 = -0.024 P1-P3 = -0.010 P1-P4 = 0.020
P1-P5 = 0.071 P1-P5 = 0.129 P1-P6 = 0.162
BLUE MANOMETER FLUID SP GR 0.797
INLET TEMPERATURE (DEG. F) = 1172.28
TW/TO = 0.411 MACH NO. = 0.020
PR = 0.755439 REYD = 1296.4

X+	(X+)M	0+	NUM	TBULK DEG. F.	TW/TB	(RE)M
0.3322	0.2547	0.0738	~~6.4213~~	271.57	0.917	1896.2
0.2681	0.2195	0.1005	~~3.5903~~	348.51	0.831	1776.0
0.2040	0.1784	0.1651	~~3.2029~~	443.76	0.743	1657.3
0.1398	0.1303	~~0.1889~~	~~2.2165~~	565.70	0.656	1541.2
0.0757	0.0746	0.4280	3.1092	733.12	0.565	1428.8
0.0116	0.0117	1.1569	4.3422	1028.42	0.458	1319.4

NON DIMENSIONALIZED PRESSURE DROP

X+	P+
0.0354	-0.087
0.0995	-0.035
0.1637	0.072
0.2278	0.257
0.2920	0.468
0.3274	0.587

POSITION OF FIRST PRESSURE TAP = 0.008352

X+	(X+)M	F	F(RE)M	FP	FP(RE)M	(RE)M	TBULK DEG F	TB/T
0.0149	0.0151	0.00225	2.95	-0.00368	-4.83	1311.9	1055.5	0.443
0.0503	0.0507	0.00337	4.62	-0.00133	-1.82	1372.4	849.6	0.513
0.1144	0.1100	0.00513	7.61	0.00220	3.26	1482.7	641.3	0.610
0.1786	0.1616	0.00659	10.52	0.00427	6.82	1596.9	500.4	0.700
0.2427	0.2057	0.00779	13.35	0.00545	9.34	1714.2	373.2	0.788
0.3069	0.2434	0.00885	16.22	0.00704	12.92	1833.7	307.9	0.875
0.3423	0.2618	~~0.00941~~	~~17.89~~	~~0.00738~~	~~[illegible]~~	1900.1	267.8	0.923

PARABOLIC INLET VELOCITY TEST NO. 31
TARE TEST TAKEN FROM RUN NO. 29
TARE THERMOCOUPLE OUTPUT (MV)

I	TA(I,1)	TA(I,2)	I	TA(I,1)	TA(I,2)
1	4.2514	4.2527	7	4.2568	4.2559
2	4.2370	4.2350	8	4.2588	4.2613
3	4.2604	4.2609	9	4.2714	4.2654
4	4.2713	4.2708	10	4.2768	4.2744
5	4.2822	4.2818	11	4.3079	4.3085
6	4.2731	4.2671	12	4.3064	4.3066

TEST THERMOCOUPLE OUTPUT (MV)

I	TT(I,1)	TT(I,2)	I	TT(I,1)	TT(I,2)
1	4.2689	4.2731	7	4.3056	4.3056
2	4.2562	4.2582	8	4.3310	4.3310
3	4.2783	4.2839	9	4.3355	4.3710
4	4.2873	4.2908	10	4.3397	4.3665
5	4.2869	4.2966	11	4.4898	4.5752
6	4.2727	4.2782	12	4.4751	4.5669

DIFFERENTIAL PRESSURE -FLOWMETER (IN.) = 0.305
FLOWMETER TEMP (MV) = 0.8158 BULK EXIT TEMP (MV) = 5.4096
INLET PRESSURE MAN , LEFT 3.50 RIGHT 3.65 IN. HG
INLET BULK TEMP CR-AL = 26.710
STATIC PRESSURE DROP (IN.)
P1-P2 = -0.017 P1-P3 = -0.008 P1-P4 = 0.032
P1-P5 = 0.073 P1-P5 = 0.121 P1-P6 = 0.151
BLUE MANOMETER FLUID SP GR 0.797
INLET TEMPERATURE (DEG. F) = 1187.49
TW/TO = 0.407 MACH NO. = 0.015
PR = 0.748056 REYD = 982.3

X+	(X+)M	Q+	NUM	TBULK DEG. F.	TW/TB	(RE)M
0.4370	0.3517	0.0444	~~5.0054~~	258.82	0.933	1455.4
0.3527	0.2777	0.0615	3.6631	298.79	0.885	1403.9
0.2683	0.2243	0.1432	~~4.2918~~	372.86	0.806	1322.0
0.1839	0.1561	~~0.3076~~	~~0.1184~~	495.72	0.704	1216.3
0.0996	0.0974	0.4075	3.2735	697.47	0.583	1099.1
0.0152	0.0154	1.1026	4.2987	1085.32	0.441	992.3

NON DIMENSIONALIZED PRESSURE DROP

X+	P+
0.0466	-0.105
0.1339	-0.050
0.2153	0.200
0.2997	0.460
0.3840	0.760
0.4306	0.950

POSITION OF FIRST PRESSURE TAP = 0.010986

X+	(X+)M	F	F(RE)M	FP	FP(RE)M	(RE)M	TBULK DEG F	TB/T
0.0196	0.0198	0.00219	2.16	-0.00526	-5.19	987.0	1118.5	0.426
0.0662	0.0668	0.00458	4.76	-0.00152	-1.58	1040.8	850.3	0.513
0.1506	0.1419	0.00804	9.30	0.00429	4.96	1156.8	583.2	0.644
0.2349	0.2041	0.01003	12.74	0.00750	9.53	1269.9	426.6	0.758
0.3193	0.2587	0.01091	14.89	0.00884	12.07	1364.7	330.7	0.850
0.4036	0.3115	0.01185	16.97	0.01082	15.49	1431.7	275.1	0.914
0.4502	0.3417	~~0.01301~~	~~18.94~~	~~0.01210~~	~~17.61~~	1455.2	257.5	0.937

PARABOLIC INLET VELOCITY TEST NO. 32
TARE TEST TAKEN FROM RUN NO. 29
TARE THERMOCOUPLE OUTPUT (MV)

I	TA(I,1)	TA(I,2)	I	TA(I,1)	TA(I,2)
1	4.2514	4.2527	7	4.2568	4.2559
2	4.2370	4.2350	8	4.2588	4.2613
3	4.2604	4.2609	9	4.2714	4.2654
4	4.2713	4.2708	10	4.2768	4.2744
5	4.2822	4.2818	11	4.3079	4.3085
6	4.2731	4.2671	12	4.3064	4.3066

TEST THERMOCOUPLE OUTPUT (MV)

I	TT(I,1)	TT(I,2)	I	TT(I,1)	TT(I,2)
1	4.2572	4.2608	7	4.2924	4.2924
2	4.2464	4.2464	8	4.3164	4.3164
3	4.2725	4.2776	9	4.3186	4.3527
4	4.2824	4.2836	10	4.3310	4.3546
5	4.2745	4.2821	11	4.4771	4.5564
6	4.2631	4.2705	12	4.4572	4.5475

DIFFERENTIAL PRESSURE -FLOWMETER (IN.) = 0.304
FLOWMETER TEMP (MV) = 0.8088 BULK EXIT TEMP (MV) = 4.6971
INLET PRESSURE MAN , LEFT 3.65 RIGHT 3.80 IN. HG
INLET BULK TEMP CR-AL = 27.051
STATIC PRESSURE DROP (IN.)
P1-P2 = -0.014 P1-P3 = -0.003 P1-P4 = 0.037
P1-P5 = 0.073 P1-P5 = 0.114 P1-P6 = 0.137
BLUE MANOMETER FLUID SP GR 0.797
INLET TEMPERATURE (DEG. F) = 1200.87
TW/TO = 0.404 MACH NO. = 0.015
PR = 0.750376 REYD = 979.1

X+	(X+)M	Q+	NUM	TBULK DEG. F.	TW/TB	(RE)M
0.4372	0.3247	0.0269	~~0.0152~~	235.41	0.964	1484.9
0.3528	0.2776	0.0418	~~2.0122~~	295.71	0.888	1404.3
0.2684	0.2262	0.1651	~~4.7081~~	381.35	0.797	1310.5
0.1840	0.1672	~~0.0076~~	~~0.1142~~	503.90	0.697	1207.5
0.0996	0.0974	0.3590	2.9800	688.61	0.587	1100.6
0.0152	0.0155	1.0398	4.3687	1040.08	0.454	996.6

NON DIMENSIONALIZED PRESSURE DROP

X+	P+
0.0460	-0.090
0.1310	-0.020
0.2154	0.236
0.2998	0.457
0.3841	0.719
0.4307	0.864

POSITION OF FIRST PRESSURE TAP = 0.010989

X+	(X+)M	F	F(RE)M	FP	FP(RE)M	(RE)M	TBULK DEG F	TB/TO
0.0196	0.0199	0.00213	2.11	-0.00499	-4.95	990.3	1072.8	0.438
0.0662	0.0667	0.00461	4.82	-0.00108	-1.13	1046.3	824.7	0.523
0.1520	0.1423	0.00795	9.16	0.00454	5.23	1152.8	585.4	0.643
0.2350	0.2058	0.00960	12.07	0.00710	8.93	1258.3	436.7	0.749
0.3194	0.2601	0.01008	13.68	0.00763	10.36	1357.1	334.6	0.846
0.4038	0.3086	0.01068	15.42	0.00892	12.89	1444.6	262.7	0.930
0.4593	0.3341	~~0.01130~~	~~14.79~~	~~0.00969~~	~~14.41~~	1486.7	232.7	0.970

PARABOLIC INLET VELOCITY TEST NO. 33
TARE TEST TAKEN FROM RUN NO. 29
TARE THERMOCOUPLE OUTPUT (MV)

I	TA(I,1)	TA(I,2)	I	TA(I,1)	TA(I,2)
1	4.2514	4.2527	7	4.2568	4.2559
2	4.2470	4.2350	8	4.2588	4.2613
3	4.2604	4.2609	9	4.2714	4.2654
4	4.2713	4.2708	10	4.2768	4.2744
5	4.2822	4.2818	11	4.3079	4.3085
6	4.2731	4.2671	12	4.3064	4.3066

TEST THERMOCOUPLE OUTPUT (MV)

I	TT(I,1)	TT(I,2)	I	TT(I,1)	TT(I,2)
1	4.2698	4.2632	7	4.2883	4.3015
2	4.2470	4.2471	8	4.2977	4.3132
3	4.2718	4.2756	9	4.3148	4.3402
4	4.2615	4.2828	10	4.3285	4.3501
5	4.2769	4.2814	11	4.4664	4.5419
6	4.2659	4.2675	12	4.4500	4.5306

DIFFERENTIAL PRESSURE -FLOWMETER (IN.) = 0.253
FLOWMETER TEMP (MV) = 0.8010 BULK EXIT TEMP (MV) = 4.4556
INLET PRESSURE MAN , LEFT 3.80 RIGHT 4.00 IN. HG
INLET BULK TEMP CR-AL = 27.156
STATIC PRESSURE DROP (IN.)
P1-P2 = -0.008 P1-P3 = 0.013 P1-P4 = 0.042
P1-P5 = 0.069 P1-P5 = 0.104 P1-P6 = 0.124
BLUE MANOMETER FLUID SP GR 0.797
INLET TEMPERATURE (DEG. F) = 1204.97
TW/TO = 0.403 MACH NO. = 0.012
PR = 0.751092 REYD = 815.5

X+	(X+)M	Q+	NUM	TBULK DEG. F.	TW/TB	(RE)M
0.5244	0.3850	0.0205	~~0.9247~~	223.51	0.981	1251.7
0.4232	0.3243	0.0339	~~3.3565~~	266.28	0.924	1201.3
0.3219	0.2635	0.0933	~~3.6073~~	341.60	0.837	1125.9
0.2207	0.1964	0.1803	3.2626	464.14	0.727	1031.0
0.1195	0.1161	0.3304	2.9339	664.56	0.599	926.4
0.0182	0.0185	0.9573	3.9162	1059.97	0.448	827.7

NON DIMENSIONALIZED PRESSURE DROP

X+	P+
0.0559	-0.073
0.1571	0.117
0.2583	0.387
0.3596	0.635
0.4608	0.956
0.5167	1.138

POSITION OF FIRST PRESSURE TAP = 0.013182

X+	(X+)M	F	F(RE)M	FP	FP(RE)M	(RE)M	TBULK DEG F	TB/T[illegible]
0.0235	0.0239	0.00351	2.89	-0.00437	-3.60	822.5	1095.7	0.432
0.0794	0.0800	0.00674	5.89	0.00033	0.29	873.6	817.7	0.526
0.1806	0.1683	0.01038	10.15	0.00654	6.39	978.0	551.0	0.665
0.2819	0.2405	0.01120	12.08	0.00853	9.21	1079.0	395.4	0.786
0.3831	0.3030	0.01101	12.83	0.00857	9.99	1165.0	299.0	0.885
0.4843	0.3527	0.01331	16.34	0.01173	14.41	1228.2	241.3	0.958
0.5402	0.3765	~~0.01440~~	~~16.74~~	~~0.01215~~	~~15.46~~	1251.9	221.9	0.985

SIMULTANEOUS DEVELOPMENT TEST NO. 34
TARE TEST TAKEN FROM RUN NO. 34
TARE THERMOCOUPLE OUTPUT (MV)

I	TA(I,1)	TA(I,2)	I	TA(I,1)	TA(I,2)
1	4.2480	4.2506	7	4.2506	4.2534
2	4.2569	4.2332	8	4.2502	4.2555
3	4.2569	4.2571	9	4.2510	4.2486
4	4.2596	4.2591	10	4.2543	4.2539
5	4.2628	4.2613	11	4.2746	4.2777
6	4.2498	4.2452	12	4.2785	4.2789

TEST THERMOCOUPLE OUTPUT (MV)

I	TT(I,1)	TT(I,2)	I	TT(I,1)	TT(I,2)
1	4.2598	4.2668	7	4.2730	4.2819
2	4.2495	4.2481	8	4.2710	4.2844
3	4.2654	4.2692	9	4.2772	4.2924
4	4.2694	4.2705	10	4.2824	4.2949
5	4.2770	4.2801	11	4.3700	4.4158
6	4.2605	4.2594	12	4.3774	4.4300

DIFFERENTIAL PRESSURE -FLOWMETER (IN.) = 0.408
FLOWMETER TEMP (MV) = 0.9218 BULK EXIT TEMP (MV) = 4.5610
INLET PRESSURE MAN , LEFT 3.60 RIGHT 3.70 IN. HG
INLET BULK TEMP CR-AL = 14.855
STATIC PRESSURE DROP (IN.)
P0-P2 = 0.162 P1-P2 = 0.049 P2-P3 = 0.074
P2-P4 = 0.131 P2-P5 = 0.189 P2-P6 = 0.241
P2-P7 = 0.275
RED MANOMETER FLUID SP GR 0.826
INLET TEMPERATURE (DEG. F) = 688.22
TW/TO = 0.585 MACH NO. = 0.017
PR = 0.718946 REYD = 1455.7

X+	(λ+)M	Q+	NUM	TBULK DEG. F.	TW/TB	(RE)M
0.3230	0.2433	0.0704	~~3.7774~~	227.33	0.975	1979.3
0.2600	0.2031	0.0593	~~3.7764~~	260.96	0.931	1916.3
0.1982	0.1604	0.0936	~~3.1372~~	301.93	0.880	1847.1
0.1358	0.1148	0.1587	~~3.2241~~	354.35	0.824	1769.2
0.0734	0.0653	0.3057	3.8436	428.33	0.756	1675.8
0.0110	0.0106	0.9984	6.8047	575.94	0.653	1534.1

NON DIMENSIONALIZED PRESSURE DROP

X+	P+
0.0145	0.186
0.0490	0.437
0.1114	0.816
0.1738	1.114
0.2362	1.413
0.2986	1.681
0.3330	1.856

X+	(λ+)M	F	F(RE)M	FP	FP(RE)M	(RE)M	TBULK DEG F	TB/TO
0.0145	0.0141	0.01229	18.68	0.00822	12.48	1519.4	592.0	0.639
0.0490	0.0451	0.01078	17.42	0.00788	12.74	1615.3	482.7	0.713
0.1114	0.0965	0.00841	14.49	0.00697	12.00	1723.0	387.3	0.793
0.1738	0.1437	0.00753	13.61	0.00651	11.77	1807.1	326.2	0.855
0.2362	0.1877	0.00776	14.58	0.00668	12.57	1880.1	280.3	0.908
0.2986	0.2290	0.00820	15.95	0.00748	14.55	1945.9	243.3	0.955
0.3330	0.2508	~~0.00895~~	~~17.71~~	~~0.00811~~	~~16.06~~	1979.8	225.7	0.980

SIMULTANEOUS DEVELOPMENT TEST NO. 35
TARE TEST TAKEN FROM RUN NO. 34
TARE THERMOCOUPLE OUTPUT (MV)

I	TA(I,1)	TA(I,2)	I	TA(I,1)	TA(I,2)
1	4.2480	4.2506	7	4.2506	4.2534
2	4.2369	4.2332	8	4.2502	4.2555
3	4.2569	4.2571	9	4.2510	4.2486
4	4.2596	4.2591	10	4.2543	4.2539
5	4.2628	4.2613	11	4.2746	4.2777
6	4.2498	4.2452	12	4.2785	4.2789

TEST THERMOCOUPLE OUTPUT (MV)

I	TT(I,1)	TT(I,2)	I	TT(I,1)	TT(I,2)
1	4.2488	4.2553	7	4.2628	4.2700
2	4.2401	4.2375	8	4.2639	4.2724
3	4.2569	4.2606	9	4.2684	4.2785
4	4.2599	4.2594	10	4.2711	4.2815
5	4.2662	4.2690	11	4.3580	4.3972
6	4.2519	4.2509	12	4.3613	4.4098

DIFFERENTIAL PRESSURE -FLOWMETER (IN.) = 0.350
FLOWMETER TEMP (MV) = 0.9268 BULK EXIT TEMP (MV) = 4.3294
INLET PRESSURE MAN , LEFT 3.80 RIGHT 4.00 IN. HG
INLET BULK TEMP CR-AL = 14.785
STATIC PRESSURE DROP (IN.)
P0-P2 = 0.150 P1-P2 = 0.031 P2-P3 = 0.065
P2-P4 = 0.128 P2-P5 = 0.150 P2-P6 = 0.199
P2-P7 = 0.236
RED MANOMETER FLUID SP GR 0.826
INLET TEMPERATURE (DEG. F) = 685.19
TW/TB = 0.586 MACH NO. = 0.014
PR = 0.718056 REYD = 1249.5

X+	(X+)M	Q+	NUM	TBULK DEG. F.	TW/TB	(RE)M
0.3765	0.2812	~~0.0517~~	~~20.3291~~	218.47	0.988	1712.0
0.3038	0.2347	0.0396	~~3.1470~~	251.42	0.942	1657.6
0.2310	0.1854	0.0914	~~3.4758~~	291.31	0.892	1598.3
0.1583	0.1326	~~0.0868~~	~~1.9779~~	342.20	0.836	1531.4
0.0856	0.0755	0.2570	3.4729	414.26	0.768	1450.8
0.0129	0.0123	0.8841	6.2880	561.87	0.661	1324.9

NON DIMENSIONALIZED PRESSURE DROP

X+	P+	
0.0169	0.272	
0.0571	0.496	
0.1298	0.962	
0.2025	1.269	
0.2752	1.570	
0.3480	1.917	POOR RESPONSE
0.3881	2.183	

X+	(X+)M	F	F(RE)M	FP	FP(RE)M	(RE)M	TBULK DEG F	TB/T
0.0169	0.0163	0.01107	14.52	0.00687	9.02	1311.6	578.5	0.647
0.0571	0.0521	0.01125	15.72	0.00830	11.60	1397.8	467.8	0.724
0.1298	0.1115	0.00971	14.48	0.00830	12.39	1491.6	374.2	0.805
0.2025	0.1661	0.00796	12.45	0.00697	10.90	1564.0	314.9	0.867
0.2752	0.2169	~~0.00746~~	~~12.78~~	~~0.00676~~	~~11.00~~	1626.5	270.2	0.920
0.3480	0.2646	~~0.01141~~	~~19.20~~	~~0.01059~~	~~17.82~~	1683.1	234.2	0.968
0.3881	0.2898	~~0.0132~~	~~22.75~~	~~0.01245~~	~~21.34~~	1712.5	216.8	0.993

SIMULTANEOUS DEVELOPMENT TEST NO. 36
TARE TEST TAKEN FROM RUN NO. 34
TARE THERMOCOUPLE OUTPUT (MV)

I	TA(I,1)	TA(I,2)	I	TA(I,1)	TA(I,2)
1	4.2480	4.2506	7	4.2506	4.2534
2	4.2369	4.2332	8	4.2502	4.2555
3	4.2569	4.2571	9	4.2510	4.2486
4	4.2596	4.2591	10	4.2543	4.2539
5	4.2628	4.2613	11	4.2746	4.2777
6	4.2498	4.2452	12	4.2785	4.2789

TEST THERMOCOUPLE OUTPUT (MV)

I	TT(I,1)	TT(I,2)	I	TT(I,1)	TT(I,2)
1	4.2542	4.2562	7	4.2613	4.2674
2	4.2417	4.2399	8	4.2607	4.2674
3	4.2588	4.2605	9	4.2681	4.2749
4	4.2622	4.2614	10	4.2706	4.2796
5	4.2538	4.2560	11	4.3518	4.3884
6	4.2363	4.2359	12	4.3570	4.4013

DIFFERENTIAL PRESSURE -FLOWMETER (IN.) = 0.300
FLOWMETER TEMP (MV) = 0.9209 BULK EXIT TEMP (MV) = 4.2962
INLET PRESSURE MAN , LEFT 3.90 RIGHT 4.10 IN. HG
INLET BULK TEMP CR-AL = 14.788
STATIC PRESSURE DROP (IN.)
P0-P2 = 0.113 P1-P2 = 0.033 P2-P3 = 0.045
P2-P4 = 0.083 P2-P5 = 0.119 P2-P6 = 0.164
P2-P7 = 0.192
RED MANOMETER FLUID SP GR 0.826
INLET TEMPERATURE (DEG. F) = 685.32
TW/TO = 0.586 MACH NO. = 0.012
PR = 0.718669 REYD = 1071.8

X+	(X+)M	Q+	NUM	TBULK DEG. F.	TW/TB	(RE)M
0.4389	0.3271	0.0163	~~8.4848~~	216.45	0.991	1471.6
0.3541	0.2716	0.0134	~~1.1011~~	243.98	0.952	1432.0
0.2693	0.2137	0.0903	~~4.0531~~	279.32	0.906	1385.7
0.1846	0.1527	~~0.2567~~	~~1.4470~~	327.04	0.852	1329.9
0.0998	0.0671	0.2237	3.3197	398.50	0.782	1258.5
0.0150	0.0143	0.8135	5.9517	553.76	0.666	1141.5

NON DIMENSIONALIZED PRESSURE DROP

X+	P+
0.0197	0.282
0.0665	0.604
0.1513	1.048
0.2361	1.419
0.3209	1.765
0.4057	2.201
0.4525	2.483

X+	(X+)M	F	F(RE)M	FP	FP(RE)M	(RE)M	TBULK DEG F	TB/T
0.0197	0.0190	0.01551	17.51	0.01097	12.39	1129.1	571.7	0.651
0.0665	0.0603	0.01325	16.03	0.01008	12.20	1209.9	453.8	0.735
0.1513	0.1285	0.00980	12.70	0.00834	10.81	1295.2	358.3	0.821
0.2361	0.1913	0.00900	12.21	0.00799	10.85	1357.4	301.1	0.883
0.3209	0.2505	0.01046	14.73	0.00933	13.13	1408.0	260.4	0.933
0.4057	0.3069	0.01310	19.00	0.01231	17.85	1450.6	229.4	0.975
0.4525	0.3372	~~0.01396~~	~~20.54~~	~~0.01328~~	~~19.54~~	1471.5	215.1	0.995

SIMULTANEOUS DEVELOPMENT TEST NO. 37
TARE TEST TAKEN FROM RUN NO. 34
TARE THERMOCOUPLE OUTPUT (MV)

I	TA(I,1)	TA(I,2)	I	TA(I,1)	TA(I,2)
1	4.2480	4.2506	7	4.2506	4.2534
2	4.2369	4.2332	8	4.2502	4.2555
3	4.2569	4.2571	9	4.2510	4.2486
4	4.2596	4.2591	10	4.2543	4.2539
5	4.2628	4.2613	11	4.2746	4.2777
6	4.2498	4.2452	12	4.2785	4.2789

TEST THERMOCOUPLE OUTPUT (MV)

I	TT(I,1)	TT(I,2)	I	TT(I,1)	TT(I,2)
1	4.2491	4.2508	7	4.2644	4.2699
2	4.2351	4.2327	8	4.2644	4.2717
3	4.2576	4.2579	9	4.2695	4.2741
4	4.2607	4.2580	10	4.2724	4.2798
5	4.2537	4.2545	11	4.3512	4.3835
6	4.2387	4.2376	12	4.3550	4.3936

DIFFERENTIAL PRESSURE -FLOWMETER (IN.) = 0.250
FLOWMETER TEMP (MV) = 0.9384 BULK EXIT TEMP (MV) = 4.2608
INLET PRESSURE MAN., LEFT 4.10 RIGHT 4.30 IN. HG
INLET BULK TEMP CR-AL = 14.959
STATIC PRESSURE DROP (IN.)
P0-P2 = 0.074 P1-P2 = 0.023 P2-P3 = 0.035
P2-P4 = 0.068 P2-P5 = 0.096 P2-P6 = 0.127
P2-P7 = 0.148
RED MANOMETER FLUID SP GR 0.826
INLET TEMPERATURE (DEG. F) = 692.72
TW/T_0 = 2.582 MACH NO. = 0.010
PR = .719379 REYD = 888.4

X+	(X+)M	Q+	NUM	TBULK DEG. F.	TW/TB	(RE)M
0.5290	0.3927	0.0062	4.1657	214.85	0.993	1225.5
0.4268	0.3256	-0.0245	-2.6570	240.67	0.957	1194.5
0.3246	0.2559	0.0649	3.1885	274.34	0.912	1157.4
0.2224	0.1527	-0.0543	~~1.4935~~	320.57	0.859	1111.7
0.1202	0.1042	0.1837	2.8848	391.20	0.789	1052.0
0.0181	0.0171	0.7012	5.2505	550.02	0.669	951.1

NON DIMENSIONALIZED PRESSURE DROP

X+	P+
0.0237	0.215
0.0802	0.543
0.1823	1.035
0.2845	1.504
0.3867	1.903
0.4889	2.348
0.5453	2.641

X+	(X+)M	F	F(RE)M	FP	FP(RE)M	(RE)M	TBULK DEG F	TB/T
0.0237	0.0228	0.01519	14.28	0.01046	9.84	940.2	568.9	0.653
0.0802	0.0722	0.01413	14.28	0.01085	10.97	1010.6	446.9	0.741
0.1823	0.1537	0.01171	12.68	0.01028	11.13	1082.8	351.3	0.828
0.2845	0.2289	0.01068	12.12	0.00976	11.07	1134.3	295.3	0.890
0.3867	0.3000	0.01123	13.20	0.01019	11.98	1175.3	254.2	0.938
0.4889	0.3682	0.01303	15.75	0.01237	14.96	1209.1	226.9	0.978
0.5453	0.4049	~~0.01455~~	~~17.83~~	~~0.01391~~	~~17.04~~	1225.4	213.6	0.998

SIMULTANEOUS DEVELOPMENT TEST NO. 38
TARE TEST TAKEN FROM RUN NO. 38
TARE THERMOCOUPLE OUTPUT (MV)

I	TA(I,1)	TA(I,2)	I	TA(I,1)	TA(I,2)
1	4.2515	4.2548	7	4.2601	4.2629
2	4.2418	4.2361	8	4.2594	4.2622
3	4.2601	4.2605	9	4.2577	4.2544
4	4.2628	4.2606	10	4.2592	4.2584
5	4.2585	4.2561	11	4.2890	4.2923
6	4.2387	4.2384	12	4.2936	4.2954

TEST THERMOCOUPLE OUTPUT (MV)

I	TT(I,1)	TT(I,2)	I	TT(I,1)	TT(I,2)
1	4.2712	4.2760	7	4.2928	4.3063
2	4.2577	4.2591	8	4.2957	4.3105
3	4.2753	4.2806	9	4.3047	4.3283
4	4.2781	4.2812	10	4.3106	4.3339
5	4.2832	4.2905	11	4.4675	4.5483
6	4.2719	4.2749	12	4.4770	4.5744

DIFFERENTIAL PRESSURE -FLOWMETER (IN.) = 0.500
FLOWMETER TEMP (MV) = 0.9405 BULK EXIT TEMP (MV) = 4.9550
INLET PRESSURE MAN , LEFT 6.80 RIGHT 7.00 IN. HG
INLET BULK TEMP CR-AL = 19.485
STATIC PRESSURE DROP (IN.)
P0-P2 = 0.262 P1-P2 = 0.054 P2-P3 = 0.092
P2-P4 = 0.140 P2-P5 = 0.216 P2-P6 = 0.311
P2-P7 = 0.350
RED MANOMETER FLUID SP GR 0.826
INLET TEMPERATURE (DEG. F) = 888.21
TW/TO = 0.498 MACH NO. = 0.019
PR = 0.741920 REYD = 1663.6

X+	(X+)M	Q+	NUM	TBULK DEG. F.	TW/TB	(RE)M
0.2739	0.2023	0.0579	~~7.4212~~	243.33	0.954	2382.3
0.2210	0.1701	0.0915	~~4.9535~~	286.22	0.900	2287.5
0.1681	0.1357	0.1293	~~3.4735~~	341.80	0.837	2184.5
0.1152	0.0981	0.2001	~~3.4517~~	416.65	0.767	2065.4
0.0623	0.0565	0.4454	4.6152	526.37	0.682	1926.9
0.0094	0.0092	1.4193	7.7514	745.64	0.565	1739.9

NON DIMENSIONALIZED PRESSURE DROP

X+	P+
0.0123	0.223
0.0415	0.409
0.0944	0.727
0.1473	0.894
0.2002	1.161
0.2532	1.490
0.2824	1.625

X+	(X+)M	F	F(RE)M	FP	FP(RE)M	(RE)M	TBULK DEG F	TB/TI
0.0123	0.0121	0.01237	21.32	0.00729	12.56	1723.3	768.5	0.547
0.0415	0.0391	0.00988	18.22	0.00612	11.27	1842.8	602.1	0.629
0.0944	0.0830	0.00698	13.94	0.00501	10.00	1996.8	465.2	0.726
0.1473	0.1222	0.00718	15.25	0.00576	12.23	2124.3	376.0	0.804
0.2002	0.1579	~~0.00818~~	~~20.07~~	~~0.00744~~	~~16.64~~	2235.7	312.0	0.870
0.2532	0.1910	~~0.00967~~	~~22.57~~	~~0.00852~~	~~19.96~~	2335.3	263.4	0.929
0.2824	0.2085	~~0.00921~~	~~19.56~~	~~0.00719~~	~~17.14~~	2383.6	241.3	0.958

SIMULTANEOUS DEVELOPMENT TEST NO. 39
TARE TEST TAKEN FROM RUN NO. 38
TARE THERMOCOUPLE OUTPUT (MV)

I	TA(I,1)	TA(I,2)	I	TA(I,1)	TA(I,2)
1	4.2515	4.2548	7	4.2601	4.2629
2	4.2418	4.2381	8	4.2594	4.2622
3	4.2601	4.2605	9	4.2577	4.2544
4	4.2628	4.2606	10	4.2592	4.2584
5	4.2585	4.2561	11	4.2890	4.2923
6	4.2387	4.2384	12	4.2936	4.2954

TEST THERMOCOUPLE OUTPUT (MV)

I	TT(I,1)	TT(I,2)	I	TT(I,1)	TT(I,2)
1	4.2690	4.2735	7	4.2893	4.3015
2	4.2559	4.2569	8	4.2919	4.3062
3	4.2725	4.2775	9	4.3000	4.3210
4	4.2765	4.2799	10	4.3066	4.3273
5	4.2811	4.2873	11	4.4347	4.5069
6	4.2708	4.2735	12	4.4471	4.5371

DIFFERENTIAL PRESSURE -FLOWMETER (IN.) = 0.452
FLOWMETER TEMP (MV) = 0.9432 BULK EXIT TEMP (MV) = 5.2625
INLET PRESSURE MAN , LEFT 7.10 RIGHT 7.30 IN. HG
INLET BULK TEMP CR-AL = 19.738
STATIC PRESSURE DROP (IN.)
P0-P2 = 0.215 P1-P2 = 0.043 P2-P3 = 0.075
P2-P4 = 0.114 P2-P5 = 0.169 P2-P6 = 0.219
P2-P7 = 0.257
RED MANOMETER FLUID SP GR 0.826
INLET TEMPERATURE (DEG. F) = 899.05
TW/TO = 0.494 MACH NO. = 0.017
PR = 0.743367 REYD = 1499.1

X+	(X+)M	Q+	NUM	TBULK DEG. F.	TW/TB	(RE)M
0.3034	0.2265	~~0.0514~~	~~4.8434~~	254.86	0.938	2129.3
0.2448	0.1902	~~0.0905~~	~~4.1572~~	297.83	0.886	2048.0
0.1862	0.1514	0.1060	~~2.8192~~	353.08	0.826	1956.6
0.1276	0.1093	0.1810	~~2.9778~~	427.08	0.758	1853.1
0.0690	0.0628	0.3926	3.9770	535.23	0.676	1732.6
0.0104	0.0101	1.2694	6.8863	752.38	0.561	1566.5

NON DIMENSIONALIZED PRESSURE DROP

X+	P+
0.0136	0.235
0.0460	0.418
0.1046	0.740
0.1632	0.906
0.2218	1.143
0.2804	1.354
0.3127	1.517

X+	(X+)M	F	F(RE)M	FP	FP(RE)M	(RE)M	TBULK DEG F	TB/T
0.0136	0.0134	0.01142	17.74	0.00638	9.91	1553.6	775.3	0.544
0.0460	0.0433	0.00998	16.56	0.00627	10.41	1659.1	615.8	0.625
0.1046	0.0924	0.00736	13.20	0.00545	9.78	1793.3	474.9	0.719
0.1632	0.1363	0.00626	11.91	0.00490	9.34	1904.1	387.0	0.793
0.2218	0.1764	0.00674	13.49	0.00530	10.61	2001.0	323.5	0.858
0.2804	0.2137	~~0.00813~~	~~17.31~~	~~0.00726~~	~~15.16~~	2087.1	275.0	0.914
0.3127	0.2333	~~0.00960~~	~~20.45~~	~~0.00859~~	~~18.31~~	2130.4	252.8	0.943

SIMULTANEOUS DEVELOPMENT TEST NO. 40
TARE TEST TAKEN FROM RUN NO. 38
TARE THERMOCOUPLE OUTPUT (MV)

I	TA(I,1)	TA(I,2)	I	TA(I,1)	TA(I,2)
1	4.2515	4.2548	7	4.2601	4.2629
2	4.2418	4.2381	8	4.2594	4.2622
3	4.2601	4.2605	9	4.2577	4.2544
4	4.2628	4.2606	10	4.2592	4.2584
5	4.2585	4.2561	11	4.2890	4.2923
6	4.2387	4.2384	12	4.2936	4.2954

TEST THERMOCOUPLE OUTPUT (MV)

I	TT(I,1)	TT(I,2)	I	TT(I,1)	TT(I,2)
1	4.2700	4.2745	7	4.2859	4.2973
2	4.2579	4.2579	8	4.2915	4.3046
3	4.2724	4.2754	9	4.2980	4.3158
4	4.2761	4.2804	10	4.3049	4.3231
5	4.2813	4.2852	11	4.4312	4.4980
6	4.2695	4.2729	12	4.4430	4.5296

DIFFERENTIAL PRESSURE -FLOWMETER (IN.) = 0.402
FLOWMETER TEMP (MV) = 0.9492 BULK EXIT TEMP (MV) = 4.9625
INLET PRESSURE MAN , LEFT 7.50 RIGHT 7.60 IN. HG
INLET BULK TEMP CR-AL = 20.009
STATIC PRESSURE DROP (IN.)
P0-P2 = 0.169 P1-P2 = 0.027 P2-P3 = 0.070
P2-P4 = 0.100 P2-P5 = 0.160 P2-P6 = 0.216
P2-P7 = 0.238
RED MANOMETER FLUID SP GR 0.826
INLET TEMPERATURE (DEG. F) = 910.65
TW/TO = 0.490 MACH NO. = 0.015
PR = 0.744935 REYD = 1328.4

X+	(X+)M	Q+	NUM	TBULK DEG. F.	TW/TB	(PE)M
0.3416	0.2520	0.0419	~~5.4378~~	243.61	0.953	1912.7
0.2756	0.2118	0.0803	~~4.1825~~	285.87	0.900	1839.3
0.2096	0.1687	0.0888	~~2.6639~~	340.05	0.839	1756.9
0.1436	0.1219	0.1618	~~2.9249~~	412.70	0.770	1663.4
0.0777	0.0701	0.3426	3.7291	519.76	0.687	1553.4
0.0117	0.0114	1.1798	6.6380	742.03	0.566	1399.2

NON DIMENSIONALIZED PRESSURE DROP

X+	P+
0.0153	0.275
0.0518	0.423
0.1178	0.806
0.1838	0.969
0.2497	1.297
0.3157	1.604
0.3522	1.721

X+	(X+)M	F	F(RE)M	FP	FP(RE)M	(RE)M	TBULK DEG F	TB/T
0.0153	0.0151	0.01117	15.48	0.00587	8.14	1385.0	766.5	0.548
0.0518	0.0485	0.00986	14.64	0.00599	8.90	1485.3	600.8	0.633
0.1178	0.1030	0.00817	13.14	0.00625	10.06	1609.1	459.9	0.730
0.1838	0.1519	0.00836	14.30	0.00702	12.01	1709.6	373.3	0.806
0.2497	0.1965	0.00935	16.80	0.00787	14.15	1797.0	311.1	0.871
0.3157	0.2379	0.00913	17.11	0.00804	15.08	1874.6	263.4	0.929
0.3522	0.2596	~~0.00736~~	~~14.00~~	~~0.00635~~	~~12.15~~	1913.8	241.6	0.958

SIMULTANEOUS DEVELOPMENT TEST NO. 41
TARE TEST TAKEN FROM RUN NO. 43
TARE THERMOCOUPLE OUTPUT (MV)

I	TA(I,1)	TA(I,2)	I	TA(I,1)	TA(I,2)
1	4.2620	4.2628	7	4.2620	4.2642
2	4.2484	4.2461	8	4.2638	4.2660
3	4.2640	4.2648	9	4.2650	4.2612
4	4.2679	4.2664	10	4.2667	4.2656
5	4.2572	4.2555	11	4.2964	4.3000
6	4.2390	4.2391	12	4.2989	4.3015

TEST THERMOCOUPLE OUTPUT (MV)

I	TT(I,1)	TT(I,2)	I	TT(I,1)	TT(I,2)
1	4.2643	4.2677	7	4.2800	4.2879
2	4.2521	4.2513	8	4.2829	4.2930
3	4.2644	4.2705	9	4.2903	4.3046
4	4.2719	4.2741	10	4.2972	4.3130
5	4.2774	4.2811	11	4.4124	4.4685
6	4.2676	4.2689	12	4.4271	4.5025

DIFFERENTIAL PRESSURE -FLOWMETER (IN.) = 0.351
FLOWMETER TEMP (MV) = 0.9462 BULK EXIT TEMP (MV) = 4.6932
INLET PRESSURE MAN , LEFT 7.80 RIGHT 8.00 IN. HG
INLET BULK TEMP CR-AL = 19.223
STATIC PRESSURE DROP (IN.)
P0-P2 = 0.135 P1-P2 = 0.000 P2-P3 = 0.052
P2-P4 = 0.092 P2-P5 = 0.122 P2-P6 = 0.163
P2-P7 = 0.191
RED MANOMETER FLUID SP GR 0.826
INLET TEMPERATURE (DEG. F) = 876.97
TW/TO = 0.502 MACH NO. = 0.012
PR = 0.740441 REYD = 1170.5

X+	(X+)M	Q+	NUM	TBULK DEG. F.	TW/TB	(RE)M
0.3901	0.2854	0.0341	6.3012	233.05	0.967	1687.9
0.3147	0.2395	0.0814	5.2597	272.67	0.916	1625.8
0.2394	0.1908	0.0625	2.0650	325.43	0.854	1553.0
0.1640	0.1382	0.1197	2.2674	398.20	0.783	1466.0
0.0887	0.0797	0.3162	3.4842	507.21	0.695	1366.8
0.0133	0.0130	1.0316	5.7448	730.14	0.570	1227.7

NON DIMENSIONALIZED PRESSURE DROP

X+	P+
0.0175	~~0.508~~
0.0591	~~0.508~~
0.1345	~~0.896~~
0.2098	~~1.191~~
0.2852	~~1.418~~
0.3605	~~1.720~~
0.4021	~~1.929~~

LEAK IN MANOMETER

X+	(X+)M	F	F(RE)M	FP	FP(RE)M	(RE)M	TBULK DEG F	TB/T
0.0175	0.0172	~~0.00298~~	~~3.62~~	~~-0.00232~~	~~-2.82~~	1215.3	753.6	0.554
0.0591	0.0553	~~0.00734~~	~~9.83~~	~~0.00364~~	~~4.74~~	1394.6	589.7	0.640
0.1345	0.1170	~~0.01164~~	~~15.08~~	~~0.00863~~	~~12.24~~	1418.2	446.1	0.742
0.2098	0.1720	~~0.00836~~	~~13.38~~	~~0.00743~~	~~11.22~~	1510.3	358.5	0.821
0.2852	0.2222	~~0.00882~~	~~10.83~~	~~0.00525~~	~~8.34~~	1585.7	297.0	0.888
0.3605	0.2691	~~0.01092~~	~~18.09~~	~~0.00964~~	~~15.97~~	1656.0	251.4	0.945
0.4021	0.2941	~~0.01216~~	~~20.54~~	~~0.01122~~	~~18.94~~	1688.7	231.2	0.972

SIMULTANEOUS DEVELOPMENT TEST NO. 42
TARE TEST TAKEN FROM RUN NO. 43
TARE THERMOCOUPLE OUTPUT (MV)

I	TA(I,1)	TA(I,2)	I	TA(I,1)	TA(I,2)
1	4.2620	4.2628	7	4.2620	4.2642
2	4.2484	4.2461	8	4.2638	4.2660
3	4.2640	4.2648	9	4.2650	4.2612
4	4.2679	4.2664	10	4.2667	4.2656
5	4.2572	4.2555	11	4.2964	4.3000
6	4.2390	4.2391	12	4.2989	4.3015

TEST THERMOCOUPLE OUTPUT (MV)

I	TT(I,1)	TT(I,2)	I	TT(I,1)	TT(I,2)
1	4.2661	4.2685	7	4.2779	4.2856
2	4.2532	4.2520	8	4.2830	4.2925
3	4.2706	4.2727	9	4.2880	4.2988
4	4.2745	4.2752	10	4.2949	4.3076
5	4.2652	4.2664	11	4.4018	4.4491
6	4.2454	4.2486	12	4.4158	4.4878

DIFFERENTIAL PRESSURE -FLOWMETER (IN.) = 0.300
FLOWMETER TEMP (MV) = 0.9510 BULK EXIT TEMP (MV) = 4.2465
INLET PRESSURE MAN , LEFT 8.10 RIGHT 8.30 IN. HG
INLET BULK TEMP CR-AL = 19.269
STATIC PRESSURE DROP (IN.)
P0-P2 = 0.094 P1-P2 = 0.024 P2-P3 = 0.032
P2-P4 = 0.068 P2-P5 = 0.091 P2-P6 = 0.134
P2-P7 = 0.144
RED MANOMETER FLUID SP GR 0.826
INLET TEMPERATURE (DEG. F) = 878.94
TW/TO = 0.501 MACH NO. = 0.010
PR = 0.740599 REYD = 999.3

X+	(X+)M	Q+	NUM	TBULK DEG. F.	TW/TB	(RE)M
0.4568	0.3282	0.0226	~~17.3350~~	216.07	0.992	1466.5
0.3685	0.2757	0.0319	~~2.9262~~	255.34	0.938	1411.2
0.2803	0.2198	0.0540	~~2.1685~~	306.39	0.875	1347.9
0.1921	0.1592	0.1127	~~2.4708~~	375.83	0.803	1274.8
0.1038	0.0920	0.2577	3.1961	479.90	0.715	1187.0
0.0156	0.0151	0.9203	5.5040	702.05	0.584	1060.3

NON DIMENSIONALIZED PRESSURE DROP

X+	P+
0.0205	0.225
0.0692	0.472
0.1574	0.805
0.2457	1.171
0.3339	1.410
0.4221	1.853
0.4709	1.956

X+	(X+)M	F	F(RE)M	FP	FP(RE)M	(RE)M	TBULK DEG F	TB/T
0.0205	0.0200	0.01450	15.20	0.00894	9.37	1048.4	727.0	0.566
0.0692	0.0639	0.01203	13.62	0.00800	9.05	1131.8	559.9	0.659
0.1574	0.1349	0.00913	11.25	0.00720	8.87	1231.8	421.5	0.762
0.2457	0.1981	0.00954	12.51	0.00823	10.79	1311.1	338.0	0.842
0.3339	0.2559	0.01120	15.44	0.00973	13.42	1378.9	279.0	0.909
0.4221	0.3097	0.01054	15.16	0.00951	13.68	1437.9	234.4	0.968
0.4709	0.3381	~~0.00661~~	~~9.70~~	~~0.00564~~	~~8.27~~	~~1464.2~~	214.2	0.997

SIMULTANEOUS DEVELOPMENT TEST NO. 43
TARE TEST TAKEN FROM RUN NO. 43
TARE THERMOCOUPLE OUTPUT (MV)

I	TA(I,1)	TA(I,2)	I	TA(I,1)	TA(I,2)
1	4.2620	4.2628	7	4.2620	4.2642
2	4.2484	4.2461	8	4.2638	4.2660
3	4.2640	4.2648	9	4.2650	4.2612
4	4.2679	4.2664	10	4.2667	4.2656
5	4.2572	4.2555	11	4.2964	4.3000
6	4.2390	4.2391	12	4.2989	4.3015

TEST THERMOCOUPLE OUTPUT (MV)

I	TT(I,1)	TT(I,2)	I	TT(I,1)	TT(I,2)
1	4.2627	4.2644	7	4.2724	4.2789
2	4.2486	4.2476	8	4.2768	4.2850
3	4.2677	4.2706	9	4.2839	4.2929
4	4.2711	4.2714	10	4.2907	4.3012
5	4.2621	4.2641	11	4.3892	4.4325
6	4.2468	4.2470	12	4.4065	4.4715

DIFFERENTIAL PRESSURE -FLOWMETER (IN.) = 0.252
FLOWMETER TEMP (MV) = 0.9521 BULK EXIT TEMP (MV) = 4.3865
INLET PRESSURE MAN , LEFT 8.50 RIGHT 8.70 IN. HG
INLET BULK TEMP CR-AL = 19.484
STATIC PRESSURE DROP (IN.)
P0-P2 = 0.070 P1-P2 = -0.011 P2-P3 = 0.031
P2-P4 = 0.041 P2-P5 = 0.075 P2-P6 = 0.108
P2-P7 = 0.122
RED MANOMETER FLUID SP GR 0.826
INLET TEMPERATURE (DEG. F) = 888.17
TW/TO = 0.498 MACH NO. = 0.009
PR = 0.741915 REYD = 837.2

X+	(X+)M	Q+	NUM	TBULK DEG. F.	TW/TB	(RE)M
0.5443	0.3926	0.0188	~~8.0035~~	220.39	0.985	1226.3
0.4391	0.3271	0.0349	~~3.5324~~	251.73	0.943	1189.3
0.3340	0.2593	0.0363	~~1.6767~~	295.73	0.887	1142.6
0.2289	0.1973	0.0895	~~2.2334~~	359.66	0.819	1084.0
0.1237	0.1084	0.2144	2.9237	461.41	0.729	1008.7
0.0186	0.0180	0.8229	5.0786	693.42	0.587	893.7

NON DIMENSIONALIZED PRESSURE DROP

X+	P+
0.0244	0.697
0.0825	0.538
0.1876	0.990
0.2928	1.149
0.3979	1.650
0.5030	2.138
0.5611	2.346

X+	(X+)M	F	F(RE)M	FP	FP(RE)M	(RE)M	TBULK DEG F	TB/TI
0.0244	0.0238	-0.00050	-0.44	-0.00647	-5.71	882.8	720.4	0.569
0.0825	0.0755	0.00458	4.40	0.00029	0.28	959.3	543.0	0.670
0.1876	0.1587	0.01066	11.16	0.00873	9.15	1047.7	403.5	0.778
0.2928	0.2333	0.01263	14.06	0.01137	12.66	1113.6	324.4	0.857
0.3979	0.3026	0.01284	14.97	0.01134	13.22	1165.7	271.7	0.918
0.5030	0.3689	~~0.01491~~	~~18.00~~	~~0.01377~~	~~16.63~~	~~1207.3~~	234.7	0.967
0.5611	0.4047	~~0.01219~~	~~14.95~~	~~0.01144~~	~~14.03~~	~~1226.4~~	219.0	0.990

SIMULTANEOUS DEVELOPMENT TEST NO. 44
TARE TEST TAKEN FROM RUN NO. 44
TARE THERMOCOUPLE OUTPUT (MV)

I	TA(I,1)	TA(I,2)	I	TA(I,1)	TA(I,2)
1	4.2534	4.2600	7	4.2434	4.2474
2	4.2462	4.2426	8	4.2468	4.2485
3	4.2621	4.2614	9	4.2591	4.2546
4	4.2661	4.2650	10	4.2603	4.2588
5	4.2647	4.2651	11	4.3038	4.3068
6	4.2573	4.2524	12	4.3030	4.3076

TEST THERMOCOUPLE OUTPUT (MV)

I	TT(I,1)	TT(I,2)	I	TT(I,1)	TT(I,2)
1	4.2700	4.2761	7	4.3007	4.3199
2	4.2555	4.2578	8	4.2981	4.3201
3	4.2756	4.2837	9	4.3268	4.3630
4	4.2796	4.2854	10	4.3222	4.3570
5	4.2671	4.2982	11	4.5335	4.6596
6	4.2725	4.2795	12	4.5178	4.6664

DIFFERENTIAL PRESSURE -FLOWMETER (IN.) = 0.508
FLOWMETER TEMP (MV) = 0.9780 BULK EXIT TEMP (MV) = 5.4841
INLET PRESSURE MAN , LEFT 4.70 RIGHT 4.85 IN. HG
INLET BULK TEMP CR-AL = 27.375
STATIC PRESSURE DROP (IN.)
p0-p2 = 0.310 p1-p2 = 0.053 p2-p3 = 0.083
p2-p4 = 0.155 p2-p5 = 0.219 p2-p6 = 0.285
p2-p7 = 0.331
BLUE MANOMETER FLUID SP GR 0.797
INLET TEMPERATURE (DEG. F) = 1213.49
TW/TO = 0.401 MACH NO. = 0.023
PR = 0.752584 REYD = 1599.6

X+	(X+)M	Q+	NUM	TBULK DEG. F.	TW/TB	(RE)M
0.2667	0.2047	~~0.0344~~	~~3.0412~~	266.27	0.924	2357.4
0.2151	0.1751	~~0.1034~~	~~4.3960~~	332.97	0.847	2224.8
0.1636	0.1417	~~0.1445~~	~~3.4394~~	417.28	0.765	2087.6
0.1121	0.1034	0.2288	3.1752	528.31	0.681	1946.3
0.0606	0.0594	0.4964	4.1730	687.56	0.587	1809.1
0.0091	0.0093	1.6269	7.3769	1000.08	0.469	1640.6

NON DIMENSIONALIZED PRESSURE DROP

X+	P+
0.0120	0.136
0.0404	0.266
0.0919	0.471
0.1434	0.648
0.1949	0.807
0.2465	0.969
0.2749	1.083

X+	(X+)M	F	F(RE)M	FP	FP(RE)M	(RE)M	TBULK DEG F	TB/TI
0.0120	0.0122	0.01010	16.45	0.00414	6.75	1621.9	1032.7	0.450
0.0404	0.0407	0.00910	15.67	0.00455	7.84	1723.5	804.5	0.531
0.0919	0.0875	0.00709	13.27	0.00460	8.60	1871.7	599.1	0.634
0.1434	0.1283	~~0.00433~~	~~13.76~~	~~0.00446~~	~~8.98~~	2115.0	466.4	0.724
0.1949	0.1638	~~0.00610~~	~~14.62~~	~~0.00473~~	~~10.14~~	2154.1	372.3	0.807
0.2465	0.1950	~~0.00778~~	~~17.84~~	~~0.00611~~	~~13.94~~	2283.8	297.6	0.887
0.2749	0.2106	~~0.00948~~	~~20.94~~	~~0.00733~~	~~17.31~~	2361.1	263.0	0.929

SIMULTANEOUS DEVELOPMENT TEST NO. 45
TARE TEST TAKEN FROM RUN NO. 44
TARE THERMOCOUPLE OUTPUT (MV)

I	TA(I,1)	TA(I,2)	I	TA(I,1)	TA(I,2)
1	4.2534	4.2600	7	4.2434	4.2474
2	4.2462	4.2426	8	4.2468	4.2485
3	4.2621	4.2614	9	4.2591	4.2546
4	4.2661	4.2650	10	4.2603	4.2588
5	4.2647	4.2651	11	4.3038	4.3068
6	4.2573	4.2524	12	4.3030	4.3076

TEST THERMOCOUPLE OUTPUT (MV)

I	TT(I,1)	TT(I,2)	I	TT(I,1)	TT(I,2)
1	4.2692	4.2686	7	4.2899	4.3060
2	4.2485	4.2530	8	4.2912	4.3098
3	4.2706	4.2776	9	4.3161	4.3468
4	4.2741	4.2794	10	4.3142	4.3458
5	4.2801	4.2887	11	4.5146	4.6271
6	4.2665	4.2724	12	4.4949	4.6291

DIFFERENTIAL PRESSURE -FLOWMETER (IN.) = 0.452
FLOWMETER TEMP (MV) = 0.9829 BULK EXIT TEMP (MV) = 5.3726
INLET PRESSURE MAN , LEFT 5.00 RIGHT 5.25 IN. HG
INLET BULK TEMP CR-AL = 27.220
STATIC PRESSURE DROP (IN.)
P0-P2 = 0.245 P1-P2 = 0.036 P2-P3 = 0.068
P2-P4 = 0.127 P2-P5 = 0.175 P2-P6 = 0.237
P2-P7 = 0.272
BLUE MANOMETER FLUID SP GR 0.797
INLET TEMPERATURE (DEG. F) = 1207.46
TW/TO = 0.402 MACH NO. = 0.020
PR = 0.751528 REYD = 1422.8

X+	(X+)M	Q+	NUM	TBULK DEG. F.	TW/TB	(RE)M
0.3002	0.2292	~~0.0133~~	~~1.4207~~	261.78	0.929	2104.9
0.2422	0.1959	~~0.0938~~	~~4.1853~~	326.38	0.853	1989.1
0.1842	0.1586	0.1247	~~2.9927~~	409.95	0.772	1566.0
0.1262	0.1159	0.1872	~~2.4459~~	522.05	0.685	1736.9
0.0682	0.0667	0.4548	3.8285	684.90	0.588	1602.4
0.0102	0.0104	1.4619	6.5485	1003.81	0.467	1457.8

NON DIMENSIONALIZED PRESSURE DROP

X+	P+
0.0135	0.169
0.0455	0.283
0.1035	0.499
0.1615	0.687
0.2195	0.842
0.2774	1.038
0.3095	1.150

X+	(X+)M	F	F(RE)M	FP	FP(RE)M	(RE)M	TBULK DEG F	TB/TO
0.0135	0.0137	0.00955	13.82	0.00352	5.10	1447.6	1036.5	0.449
0.0455	0.0458	0.00896	13.71	0.00433	6.63	1530.6	804.3	0.531
0.1035	0.0983	0.00742	12.39	0.00485	8.10	1668.3	594.3	0.637
0.1615	0.1437	0.00674	12.13	0.00481	8.66	1799.9	461.3	0.729
0.2195	0.1832	0.00713	13.73	0.00505	9.72	1925.9	365.2	0.814
0.2774	0.2182	~~0.00834~~	~~17.04~~	~~0.00671~~	~~12.73~~	2045.4	292.0	0.894
0.3095	0.2359	~~0.00870~~	~~18.33~~	~~0.00720~~	~~15.10~~	2108.0	258.7	0.935

SIMULTANEOUS DEVELOPMENT TEST NO. 46
TARE TEST TAKEN FROM RUN NO. 44
TARE THERMOCOUPLE OUTPUT (MV)

I	TA(I,1)	TA(I,2)	I	TA(I,1)	TA(I,2)
1	4.2534	4.2600	7	4.2434	4.2474
2	4.2462	4.2426	8	4.2468	4.2485
3	4.2621	4.2614	9	4.2591	4.2546
4	4.2661	4.2650	10	4.2603	4.2588
5	4.2647	4.2651	11	4.3038	4.3068
6	4.2573	4.2524	12	4.3030	4.3076

TEST THERMOCOUPLE OUTPUT (MV)

I	TT(I,1)	TT(I,2)	I	TT(I,1)	TT(I,2)
1	4.2602	4.2651	7	4.2830	4.2969
2	4.2450	4.2482	8	4.2850	4.3026
3	4.2656	4.2714	9	4.3085	4.3350
4	4.2705	4.2736	10	4.3083	4.3348
5	4.2754	4.2823	11	4.4998	4.6054
6	4.2631	4.2676	12	4.4814	4.6048

DIFFERENTIAL PRESSURE -FLOWMETER (IN.) = 0.402
FLOWMETER TEMP (MV) = 0.9822 BULK EXIT TEMP (MV) = 5.0653
INLET PRESSURE MAN , LEFT 5.35 RIGHT 5.50 IN. HG
INLET BULK TEMP CR-AL = 27.290
STATIC PRESSURE DROP (IN.)
P0-P2 = 0.230 P1-P2 = 0.033 P2-P3 = 0.057
P2-P4 = 0.108 P2-P5 = 0.151 P2-P6 = 0.201
P2-P7 = 0.232
BLUE MANOMETER FLUID SP GR 0.797
INLET TEMPERATURE (DEG. F) = 1210.19
TW/TO = 0.402 MACH NO. = 0.018
PR = 0.752005 REYD = 1265.4

X+	(X+)M	Q+	NUM	TBULK DEG. F.	TW/TB	(RE)M
0.3373	0.2547	0.0361	~~5.0722~~	250.05	0.944	1893.1
0.2722	0.2175	0.0709	~~3.6817~~	311.56	0.870	1791.3
0.2070	0.1759	0.1038	~~2.8132~~	390.29	0.789	1683.4
0.1418	0.1286	0.1647	~~2.5947~~	495.63	0.703	1569.2
0.0767	0.0742	0.3839	3.5594	650.15	0.606	1447.0
0.0115	0.0117	1.3529	6.4270	967.99	0.478	1305.5

NON DIMENSIONALIZED PRESSURE DROP

X+	P+
0.0151	0.180
0.0511	0.317
0.1163	0.548
0.1814	0.757
0.2466	0.936
0.3118	1.138
0.3478	1.265

X+	(X+)M	F	F(RE)M	FP	FP(RE)M	(RE)M	TBULK DEG F	TB/TO
0.0151	0.0155	0.01071	13.87	0.00437	5.66	1295.1	1002.8	0.459
0.0511	0.0511	0.00987	13.61	0.00508	7.01	1379.2	766.4	0.548
0.1163	0.1091	0.00792	11.94	0.00542	8.18	1507.5	563.8	0.656
0.1814	0.1594	0.00721	11.72	0.00536	8.70	1625.1	438.5	0.748
0.2466	0.2034	0.00777	13.49	0.00562	9.76	1735.9	348.2	0.831
0.3118	0.2424	0.00891	16.40	0.00715	13.15	1840.6	278.9	0.909
0.3478	0.2622	~~0.00978~~	~~18.54~~	~~0.00832~~	~~15.77~~	1895.7	247.1	0.950

SIMULTANEOUS DEVELOPMENT TEST NO. 47
TARE TEST TAKEN FROM RUN NO. 44
TARE THERMOCOUPLE OUTPUT (MV)

I	TA(I,1)	TA(I,2)	I	TA(I,1)	TA(I,2)
1	4.2522	4.2530	7	4.2532	4.2563
2	4.2373	4.2355	8	4.2550	4.2582
3	4.2550	4.2550	9	4.2562	4.2523
4	4.2588	4.2529	10	4.2592	4.2569
5	4.2603	4.2585	11	4.2923	4.2976
6	4.2518	4.2485	12	4.2937	4.3006

TEST THERMOCOUPLE OUTPUT (MV)

I	TT(I,1)	TT(I,2)	I	TT(I,1)	TT(I,2)
1	4.2593	4.2616	7	4.2764	4.2878
2	4.2451	4.2467	8	4.2790	4.2941
3	4.2585	4.2616	9	4.2982	4.3206
4	4.2613	4.2654	10	4.3026	4.3256
5	4.2709	4.2761	11	4.4837	4.5782
6	4.2604	4.2641	12	4.4645	4.5805

DIFFERENTIAL PRESSURE -FLOWMETER (IN.) = 0.350
FLOWMETER TEMP (MV) = 0.9795 BULK EXIT TEMP (MV) = 4.7076
INLET PRESSURE MAN , LEFT 5.70 RIGHT 5.90 IN. HG
INLET BULK TEMP CR-AL = 27.513
STATIC PRESSURE DROP (IN.)
P0-P2 = 0.156 P1-P2 = 0.031 P2-P3 = 0.048
P2-P4 = 0.088 P2-P5 = 0.124 P2-P6 = 0.167
P2-P7 = 0.190
BLUE MANOMETER FLUID SP GR 0.797
INLET TEMPERATURE (DEG. F) = 1218.85
TW/TO = 0.400 MACH NO. = 0.015
PR = 0.753525 REY_D = 1101.6

X+	(X+)M	Q+	NUM	TBULK DEG. F.	TW/TB	(RE)M
0.3868	0.2885	0.0313	~~6.7599~~	236.68	0.962	1570.1
0.3120	0.2471	0.0874	~~5.2561~~	299.22	0.883	1576.7
0.2373	0.2005	0.0921	~~2.6853~~	380.04	0.799	1477.3
0.1626	0.1471	0.1291	~~2.1043~~	488.93	0.708	1372.2
0.0879	0.0852	0.3446	3.2219	649.25	0.607	1260.8
0.0132	0.0135	1.1991	5.6405	977.22	0.475	1135.1

NON DIMENSIONALIZED PRESSURE DROP

X+	P+
0.0174	0.183
0.0586	0.352
0.1333	0.613
0.2080	0.835
0.2827	1.031
0.3575	1.265
0.3987	1.387

X+	(X+)M	F	F(RE)M	FP	FP(RE)M	(RE)M	TBULK DEG F	TB/TO
0.0174	0.0177	0.01230	13.85	0.00584	6.58	1125.9	1012.7	0.456
0.0586	0.0587	0.01094	13.12	0.00602	7.22	1199.8	769.8	0.546
0.1333	0.1250	0.00844	11.10	0.00584	7.69	1315.8	559.7	0.659
0.2080	0.1820	0.00789	11.24	0.00596	8.48	1423.7	429.8	0.755
0.2827	0.2314	0.00885	13.50	0.00661	10.09	1525.8	336.7	0.843
0.3575	0.2749	0.00970	15.74	0.00783	12.70	1622.1	265.9	0.926
0.3987	0.2969	~~0.00948~~	~~16.19~~	~~0.00817~~	~~13.67~~	1672.7	233.7	0.969

SIMULTANEOUS DEVELOPMENT TEST NO. 48
TARE TEST TAKEN FROM RUN NO. 44
TARE THERMOCOUPLE OUTPUT (MV)

I	TA(I,1)	TA(I,2)	I	TA(I,1)	TA(I,2)
1	4.2522	4.2530	7	4.2532	4.2563
2	4.2373	4.2355	8	4.2550	4.2582
3	4.2550	4.2550	9	4.2562	4.2523
4	4.2588	4.2529	10	4.2592	4.2569
5	4.2603	4.2585	11	4.2923	4.2976
6	4.2518	4.2485	12	4.2937	4.3006

TEST THERMOCOUPLE OUTPUT (MV)

I	TT(I,1)	TT(I,2)	I	TT(I,1)	TT(I,2)
1	4.2535	4.2554	7	4.2711	4.2836
2	4.2381	4.2389	8	4.2742	4.2828
3	4.2574	4.2616	9	4.2911	4.3102
4	4.2635	4.2646	10	4.2972	4.3176
5	4.2660	4.2698	11	4.4494	4.5307
6	4.2569	4.2597	12	4.4440	4.5463

DIFFERENTIAL PRESSURE -FLOWMETER (IN.) = 0.305
FLOWMETER TEMP (MV) = 0.9816 BULK EXIT TEMP (MV) = 4.4946
INLET PRESSURE MAN , LEFT 6.00 RIGHT 6.25 IN. HG
INLET BULK TEMP CR-AL = 27.000
STATIC PRESSURE DROP (IN.)
P0-P2 = 0.110 P1-P2 = 0.025 P2-P3 = 0.038
P2-P4 = 0.068 P2-P5 = 0.096 P2-P6 = 0.132
P2-P7 = 0.152
BLUE MANOMETER FLUID SP GR 0.797
INLET TEMPERATURE (DEG. F) = 1198.87
TW/TO = 0.405 MACH NO. = 0.013
PR = 0.750029 REYD = 960.7

X+	(X+)M	Q+	NUM	TBULK DEG. F.	TW/TB	(RE)M
0.4454	0.3283	0.0240	~~7.5382~~	228.10	0.974	1467.4
0.3594	0.2808	0.0755	~~5.1737~~	288.04	0.896	1387.1
0.2733	0.2281	0.0779	~~2.4242~~	368.10	0.810	1298.7
0.1873	0.1679	0.1020	~~1.7128~~	478.59	0.715	1203.1
0.1012	0.0976	0.3140	2.9363	643.56	0.609	1101.2
0.0152	0.0155	1.0505	4.8555	977.34	0.474	988.9

NON DIMENSIONALIZED PRESSURE DROP

X+	P+
0.0200	0.130
0.0675	0.313
0.1535	0.595
0.2396	0.813
0.3256	1.025
0.4117	1.284
0.4592	1.437

X+	(X+)M	F	F(RE)M	FP	FP(RE)M	(RE)M	TBULK DEG F	TB/TO
0.0200	0.0204	0.01281	12.57	0.00632	6.20	981.0	1512.3	0.456
0.0675	0.0673	0.01141	11.94	0.00642	6.71	1046.1	767.6	0.547
0.1535	0.1430	0.00875	10.08	0.00605	6.97	1151.6	551.2	0.664
0.2396	0.2074	0.00808	10.11	0.00613	7.67	1250.2	418.3	0.765
0.3256	0.2630	0.00925	12.42	0.00716	9.61	1342.2	324.9	0.856
0.4117	0.3125	0.01096	15.64	0.00945	13.48	1426.5	255.8	0.939
0.4592	0.3379	~~0.01173~~	~~17.23~~	~~0.01028~~	~~15.11~~	1469.4	225.3	0.981

SIMULTANEOUS DEVELOPMENT TEST NO. 49
TARE TEST TAKEN FROM RUN NO. 44
TARE THERMOCOUPLE OUTPUT (MV)

I	TA(I,1)	TA(I,2)	I	TA(I,1)	TA(I,2)
1	4.2522	4.2530	7	4.2532	4.2563
2	4.2373	4.2355	8	4.2550	4.2582
3	4.2550	4.2550	9	4.2562	4.2523
4	4.2588	4.2529	10	4.2592	4.2569
5	4.2603	4.2585	11	4.2923	4.2976
6	4.2518	4.2485	12	4.2937	4.3006

TEST THERMOCOUPLE OUTPUT (MV)

I	TT(I,1)	TT(I,2)	I	TT(I,1)	TT(I,2)
1	4.2541	4.2554	7	4.2657	4.2747
2	4.2388	4.2360	8	4.2689	4.2801
3	4.2562	4.2592	9	4.2857	4.3000
4	4.2604	4.2613	10	4.2932	4.3101
5	4.2647	4.2666	11	4.4329	4.5030
6	4.2557	4.2567	12	4.4315	4.5241

DIFFERENTIAL PRESSURE -FLOWMETER (IN.) = 0.252
FLOWMETER TEMP (MV) = 0.9918 BULK EXIT TEMP (MV) = 4.2700
INLET PRESSURE MAN , LEFT 6.10 RIGHT 6.20 IN. HG
INLET BULK TEMP CR-AL = 26.650
STATIC PRESSURE DROP (IN.)
P0-P2 = 0.076 P1-P2 = 0.076 P2-P3 = 0.076
P2-P4 = 0.052 P2-P5 = 0.080 P2-P6 = 0.108
P2-P7 = 0.138
BLUE MANOMETER FLUID SP GR 0.797
INLET TEMPERATURE (DEG. F) = 1185.13
TW/TO = 2.408 MACH NO. = 0.011
PR = 0.747047 REY$_D$ = 793.5

X+	(X+)M	Q+	NUM	TBULK DEG. F.	TW/TB	(RE)M
0.5409	0.3934	0.0098	7.2664	217.66	0.989	1223.6
0.4364	0.3328	0.0670	6.7112	264.22	0.926	1169.6
0.3319	0.2692	0.0537	2.1838	333.84	0.845	1101.0
0.2274	0.1987	0.0915	1.8442	438.28	0.747	1019.1
0.1230	0.1167	0.2684	2.7903	604.69	0.631	925.6
0.0185	0.0187	0.9289	4.3811	957.83	0.480	819.3

NON DIMENSIONALIZED PRESSURE DROP

X+	P+
0.0243	~~-0.509~~
0.0820	~~0.329~~
0.1865	~~1.159~~
0.2910	~~0.897~~
0.3954	~~1.203~~
0.4999	~~1.508~~
0.5576	~~1.843~~

MISREADING

X+	(X+)M	F	F(RE)M	FP	FP(RE)M	(RE)M	TBULK DEG F	TB/TO
0.0243	0.0247	~~0.04388~~	~~35.63~~	~~0.03684~~	~~29.92~~	812.1	995.0	0.462
0.0820	0.0810	~~0.02984~~	~~26.07~~	~~0.02438~~	~~21.30~~	873.7	734.5	0.562
0.1865	0.1699	~~0.00809~~	~~7.87~~	~~0.00520~~	~~5.06~~	972.5	510.4	0.692
0.2910	0.2448	~~0.00192~~	~~2.03~~	~~-0.00006~~	~~-0.07~~	1060.3	380.4	0.800
0.3954	0.3108	~~0.00921~~	~~10.46~~	~~0.00720~~	~~8.17~~	1135.6	295.5	0.889
0.4999	0.3721	~~0.01995~~	~~23.88~~	~~0.01877~~	~~22.47~~	1196.9	238.4	0.962
0.5576	0.4053	~~0.02350~~	~~28.78~~	~~0.02241~~	~~27.44~~	1224.4	215.7	0.995

SIMULTANEOUS DEVELOPMENT TEST NO. 50
TARE TEST TAKEN FROM RUN NO. 50
TARE THERMOCOUPLE OUTPUT (MV)

I	TA(I,1)	TA(I,2)	I	TA(I,1)	TA(I,2)
1	4.2401	4.2410	7	4.2516	4.2531
2	4.2275	4.2261	8	4.2534	4.2571
3	4.2532	4.2537	9	4.2551	4.2513
4	4.2566	4.2561	10	4.2566	4.2560
5	4.2602	4.2597	11	4.2872	4.2896
6	4.2523	4.2489	12	4.2875	4.2904

TEST THERMOCOUPLE OUTPUT (MV)

I	TT(I,1)	TT(I,2)	I	TT(I,1)	TT(I,2)
1	4.2564	4.2594	7	4.2730	4.2835
2	4.2421	4.2427	8	4.2751	4.2874
3	4.2599	4.2620	9	4.2911	4.3067
4	4.2622	4.2649	10	4.2930	4.3112
5	4.2719	4.2769	11	4.4286	4.4910
6	4.2609	4.2626	12	4.4202	4.5001

DIFFERENTIAL PRESSURE -FLOWMETER (IN.) = 0.402
FLOWMETER TEMP (MV) = 0.9756 BULK EXIT TEMP (MV) = 4.6890
INLET PRESSURE MAN , LEFT 7.50 RIGHT 7.70 IN. HG
INLET BULK TEMP CR-AL = 19.589
STATIC PRESSURE DROP (IN.)
P0-P2 = 0.155 P1-P2 = 0.031 P2-P3 = 0.048
P2-P4 = 0.093 P2-P5 = 0.133 P2-P6 = 0.176
P2-P7 = 0.206
BLUE MANOMETER FLUID SP GR 0.797
INLET TEMPERATURE (DEG. F) = 892.67
TW/TO = 0.496 MACH NO. = 0.015
PR = 0.742513 REY$_D$ = 1330.0

X+	(X+)M	Q+	NUM	TBULK DEG. F.	TW/TB	(RE)M
0.3423	0.2504	0.0342	~~6.0527~~	234.11	0.965	1924.0
0.2762	0.2118	0.0431	~~2.4088~~	282.44	0.903	1838.8
0.2101	0.1695	0.0944	~~2.7250~~	341.92	0.837	1748.4
0.1439	0.1227	0.1561	~~2.6657~~	418.55	0.764	1651.1
0.0778	0.0706	0.3457	3.5833	526.89	0.681	1541.9
0.0117	0.0114	1.1146	6.1711	740.03	0.566	1395.6

NON DIMENSIONALIZED PRESSURE DROP

X+	P+
0.0154	0.189
0.0519	0.361
0.1180	0.626
0.1841	0.878
0.2503	1.098
0.3164	1.337
0.3529	1.500

X+	(X+)M	F	F(RE)M	FP	FP(RE)M	(RE)M	TBULK DEG F	TB/TO
0.0154	0.0151	0.01036	14.32	0.00536	7.41	1382.2	762.7	0.550
0.0519	0.0488	0.00942	13.91	0.00574	8.47	1476.4	606.2	0.630
0.1180	0.1038	0.00765	12.22	0.00570	9.10	1596.5	466.9	0.725
0.1841	0.1528	0.00707	12.01	0.00559	9.49	1698.6	377.4	0.802
0.2503	0.1970	0.00769	13.77	0.00600	10.75	1792.0	316.4	0.872
0.3164	0.2372	0.00905	17.00	0.00759	14.26	1879.6	257.0	0.937
0.3529	0.2579	~~0.01304~~	~~19.34~~	~~0.00846~~	~~17.07~~	1925.8	231.7	0.971

SIMULTANEOUS DEVELOPMENT TEST NO. 51
TARE TEST TAKEN FROM RUN NO. 50
TARE THERMOCOUPLE OUTPUT (MV)

I	TA(I,1)	TA(I,2)	I	TA(I,1)	TA(I,2)
1	4.2401	4.2410	7	4.2516	4.2531
2	4.2275	4.2261	8	4.2534	4.2571
3	4.2532	4.2537	9	4.2551	4.2513
4	4.2566	4.2561	10	4.2566	4.2560
5	4.2602	4.2597	11	4.2872	4.2896
6	4.2523	4.2489	12	4.2875	4.2904

TEST THERMOCOUPLE OUTPUT (MV)

I	TT(I,1)	TT(I,2)	I	TT(I,1)	TT(I,2)
1	4.2543	4.2564	7	4.2646	4.2750
2	4.2394	4.2391	8	4.2689	4.2802
3	4.2573	4.2609	9	4.2834	4.2971
4	4.2615	4.2662	10	4.2886	4.3032
5	4.2673	4.2699	11	4.4134	4.4704
6	4.2579	4.2588	12	4.4123	4.4906

DIFFERENTIAL PRESSURE -FLOWMETER (IN.) = 0.352
FLOWMETER TEMP (MV) = 0.9962 BULK EXIT TEMP (MV) = 4.4663
INLET PRESSURE MAN , LEFT 7.80 RIGHT 7.90 IN. HG
INLET BULK TEMP CR-AL = 19.650
STATIC PRESSURE DROP (IN.)
P0-P2 = 0.126 P1-P2 = 0.000 P2-P3 = 0.042
P2-P4 = 0.081 P2-P5 = 0.113 P2-P6 = 0.152
P2-P7 = 0.177
BLUE MANOMETER FLUID SP GR 0.797
INLET TEMPERATURE (DEG. F) = 895.28
TW/T_U = 0.495 MACH NO. = 0.013
PR = 0.742862 REYD = 1160.8

X+	(X+)M	Q+	NUM	TRULK DEG. F.	TW/TB	(RE)M
0.3920	0.2540	0.0191	~~5.4577~~	225.08	0.978	1695.5
0.3163	0.2392	0.0742	~~5.3026~~	267.83	0.921	1627.4
0.2406	0.1907	0.0647	~~2.2860~~	320.32	0.859	1554.2
0.1648	0.1377	0.1470	3.0165	388.46	0.791	1473.4
0.0891	0.0792	0.2787	3.4042	487.36	0.709	1378.5
0.0134	0.0129	1.0491	6.4253	700.23	0.585	1233.0

NON DIMENSIONALIZED PRESSURE DROP

X+	P+
0.0176	0.423
0.0594	0.423
0.1351	0.733
0.2109	1.019
0.2866	1.253
0.3623	1.539
0.4041	1.720

X+	(X+)M	F	F(RE)M	FP	FP(RE)M	(RE)M	TBULK DEG F	TB/TU
0.0176	0.0172	0.00333	4.08	-0.00210	-2.57	1224.0	725.3	0.567
0.0594	0.0548	0.00687	9.06	0.00300	3.96	1318.4	562.9	0.657
0.1351	0.1164	0.00948	13.53	0.00769	10.97	1426.6	432.1	0.753
0.2109	0.1716	0.00866	13.10	0.00738	11.17	1513.1	351.7	0.828
0.2866	0.2220	0.00750	11.92	0.00597	9.49	1589.5	292.5	0.893
0.3623	0.2684	0.01025	17.02	0.00905	15.03	1659.6	245.4	0.953
0.4041	0.2926	~~0.01103~~	~~18.71~~	~~0.00997~~	~~16.92~~	1696.7	223.0	0.984

Appendix I

Derivation of the Similar Boundary Layer Equations

When the thermal or velocity boundary layer thickness on a body of revolution is small when compared to the local radius of the body, then the energy, continuity and momentum equations (2.30, 2.31, 2.32) may be written with the radius terms removed;

$$\rho^+ u^+ \frac{\partial u^+}{\partial x^+} + \rho^+ v^+ \frac{\partial u^+}{\partial r^+} = \frac{dp}{dx^+} + 2 Pr_0 \frac{\partial}{\partial r^+} \mu^+ \frac{\partial u^+}{\partial r^+} \tag{I.1}$$

$$\frac{\partial}{\partial x^+}(\rho^+ u^+) + \frac{\partial}{\partial r}(\rho^+ v^+) = 0 \tag{I.2}$$

$$\rho^+ u^+ \frac{\partial H_2^+}{\partial x^+} + \rho^+ v^+ \frac{\partial H_2}{\partial r^+} = 2 \frac{\partial}{\partial r^+} \frac{k^+}{c_p^+} \frac{\partial H_2}{\partial r^+} - (\gamma_o - 1) M_0^2 \left(u^+ \frac{dp}{dx^+} - 2 Pr_0 \mu^+ \left(\frac{\partial u^+}{\partial r^+} \right)^2 \right) \tag{I.3}$$

where the usual form of the dissipation term in the energy equation has been retained. The stream function ψ is introduced to eliminate the continuity equation;

$$\frac{\partial \psi}{\partial x^+} = -\rho^+ v^+ \tag{I.4}$$

$$\frac{\partial \psi}{\partial y^+} = \rho^+ u^+ \tag{I.5}$$

We introduce the transformation to new independent variables;

$$\xi = \int_0^{x^+} C \rho_e^+ \mu_e^+ u_e^+ \, dx^+ \tag{I.6}$$

$$\eta = \frac{u_e^+}{\sqrt{2\xi}} \int_0^{y^+} \rho_e^+ \, dy^+ \tag{I.7}$$

where $y^+ = 1 - r^+$ represents the dimensionless displacement from the tube wall and C is a constant. Subscript e refers to quantities at the edge of the boundary layer or in the central core. We also introduce two new dependent variables;

$$u^+/u_e^+ = f'(\eta) \qquad (I.8)$$

$$H^+/H_{2,e}^+ = G(\eta) \qquad (I.9)$$

Expanding the axial derivative in terms of the new independent variables,

$$\frac{\partial}{\partial x^+} = \frac{\partial \xi}{\partial x^+}\frac{\partial}{\partial \xi} + \frac{\partial \eta}{\partial x^+}\frac{\partial}{\partial \eta} \qquad (I.10)$$

and the radial derivative,

$$\frac{\partial}{\partial y^+} = -\frac{\partial}{\partial r^+} = \frac{\partial \eta}{\partial y^+}\frac{\partial}{\partial \eta} + \frac{\partial \xi}{\partial y^+}\frac{\partial}{\partial \xi} \qquad (I.11)$$

It can be shown that the stream function ψ is is related to the velocity function f by,

$$\psi = \sqrt{2\xi}\, f$$

From the stream function we may solve for the radial velocity,

$$v^+ = -\frac{1}{\rho^+}\frac{\partial \psi}{\partial x^+} = -\frac{1}{\rho^+}\left(\frac{\partial \xi}{\partial x^+}\frac{f}{\sqrt{2\xi}} + \frac{\partial \eta}{\partial x^+}\frac{\partial}{\partial \eta}\left(\sqrt{2\xi}\, f\right)\right) \qquad (I.12)$$

$$= \frac{C\rho_e^+\mu_e^+u_e^+}{\rho^+}\left(\frac{\eta f'}{\sqrt{2\xi}} - \frac{f}{\sqrt{2\xi}} - \frac{\eta f'\sqrt{2\xi}}{u_e^+}\frac{\partial u_e^+}{\partial \xi}\right) \qquad (I.13)$$

where primes denote differentiation with respect to η. We consider each term in the momentum equation separately. Starting with the first term on the left hand side of equation I.1.;

$$\rho^+u^+\frac{\partial u^+}{\partial x^+} = \rho^+u^+\left(\frac{\partial \xi}{\partial x^+}\frac{\partial u^+}{\partial \xi} + \frac{\partial \eta}{\partial x^+}\frac{\partial u^+}{\partial \eta}\right) \qquad (I.14)$$

$$= \rho^+u^+\left(\frac{\partial \xi}{\partial x^+}\frac{\partial}{\partial \xi}(u_e^+f') + \frac{\partial (u_e^+f')}{\partial \eta}\frac{\partial \eta}{\partial \xi}\frac{\partial \xi}{\partial x^+}\right) \qquad (I.15)$$

We note that ξ is a function only of the axial coordinate x^+ since all quantities of which it is composed are functions only of the axial coordinate. Continuing the expansion;

$$\rho^+u^+\frac{\partial u^+}{\partial x^+} = C\rho_e^+\mu_e^+u_e^+\rho^+\left(u_e^+f'^2\frac{\partial u_e^+}{\partial \xi} + \eta f'f''u_e^+\frac{\partial u^+}{\partial \xi} - \eta\frac{ff''}{2\xi}u_e^{+2}\right) \qquad (I.16)$$

In the solution of the boundary layer equations at the tube wall, the convention for the sign of the transverse velocity v^+ was reversed. A positive value is away from the tube wall. This is in accordance with usual boundary layer convention.

$$\rho^+ v^+ \frac{\partial U^+}{\partial y^+} = C \rho_e^+ \mu_e^+ U_e^+ \rho^+ \left(\frac{\eta f'}{\sqrt{2\xi}} - f' \eta \frac{\sqrt{2\xi}}{U_e^+} \frac{\partial U_e^+}{\partial \xi} - \frac{f}{\sqrt{2\xi}} \right) U_e^+ f'' \frac{\rho^+ U_e^+}{\sqrt{2\xi}} \qquad (I.17)$$

Next consider,

$$\frac{\partial}{\partial r^+} \mu^+ \frac{\partial U^+}{\partial r^+} = \frac{\partial}{\partial y^+} \mu^+ \frac{\partial U^+}{\partial y^+} \qquad (I.18)$$

$$= \frac{\partial \eta}{\partial y^+} \frac{\partial}{\partial \eta} \left(\mu^+ \frac{\partial \eta}{\partial y^+} \frac{\partial U^+}{\partial \eta} \right)$$

$$= \frac{\partial U^+}{\partial \eta} \frac{\partial \mu^+}{\partial \eta} \left(\frac{\partial \eta}{\partial y^+} \right)^2 + \mu^+ \frac{\partial^2 \eta}{\partial \eta \partial y^+} \frac{\partial U^+}{\partial \eta} \frac{\partial \eta}{\partial y^+} + \mu^+ \left(\frac{\partial \eta}{\partial y^+} \right)^2 \frac{\partial^2 U^+}{\partial \eta^2}$$

$$= \frac{\rho^+ U_e^{+3}}{2\xi} \left(\frac{\partial \mu^+}{\partial \eta} \rho^+ f'' + \mu^+ f'' \frac{\partial \rho^+}{\partial \eta} + \mu^+ \rho^+ f''' \right) \qquad (I.19)$$

$$= \frac{\rho^+ U_e^{+3}}{2\xi} \left(\mu^+ \rho^+ f'' \right)' \qquad (I.20)$$

The pressure gradient term becomes;

$$\frac{dP}{dx^+} = \frac{d}{dx^+} \left(\frac{p_o - p}{\rho_o U_o^2} \right) = - \frac{dp}{dx^+} \Big/ \rho_o U_o^2 \qquad (I.21)$$

Since we are assuming the flow in the core is inviscid (i.e. potential flow),

$$\frac{dp}{dx^+} = -\rho_e U_e \frac{dU_e}{dx^+} \qquad (I.22)$$

$$\frac{dP}{dx^+} = \rho_e U_e \frac{dU_e}{dx^+} \Big/ \rho_o U_o^2 = \rho_e^+ U_e^+ \frac{dU_e^+}{dx^+} \qquad (I.23)$$

$$\frac{dP}{d\xi}=\frac{dP}{dx^+}\frac{dx^+}{d\xi}=\rho_e^+U_e^+\frac{dU_e^+}{C\rho_e^+U_e^+\mu_e^+dx^+}=\rho_e^+U_e^+\frac{dU_e^+}{d\xi} \tag{I.24}$$

After combining all terms in the momentum equation and after division by a common factor $C\rho_e\rho\mu_eU_e/2\xi$, many terms are found to cancel. The final result is;

$$\frac{2\xi}{U_e^+}\frac{\partial U_e^+}{\partial\xi}\left(f'-\frac{\rho_e^+}{\rho^+}\right)=\frac{2Pr_o}{C\mu_e^+\rho_e^+}\left(\mu^+\rho^+f''\right)'+ff'' \tag{I.25}$$

Drawing the constant term $C\mu_e^+\rho_e^+$ within the differential in the first term on the right hand side of this equation;

$$\frac{2\xi}{U_e^+}\frac{\partial U_e^+}{\partial\xi}\left(f'-\frac{\rho_e}{\rho}\right)=2Pr_o\left(\lambda f''\right)'+ff'' \tag{I.26}$$

where

$$\lambda=\frac{\mu^+\rho^+}{C\mu_e^+\rho_e^+} \tag{I.27}$$

For the energy equation, the free stream or "core" enthalpy is considered as being invariant with axial distance;

$$\frac{\partial H_{2,e}^+}{\partial\xi}=\frac{\partial H_{2,e}^+}{\partial x^+}=0 \tag{I.28}$$

Again considering separate terms in the energy equation;

$$\rho^+U^+\frac{\partial H_2^+}{\partial x^+}=\rho^+U_e^+f'H_{2,e}^+\frac{\partial G}{\partial\eta}\frac{\partial\eta}{\partial\xi}\frac{\partial\xi}{\partial x^+} \tag{I.29}$$

$$=C\rho_e^+\rho^+\mu_e^+U_e^{+2}H_{2,e}^+G'\left(\frac{\eta}{U_e^+}\frac{\partial U^+}{\partial\xi}-\frac{\eta}{2\xi}\right) \tag{I.30}$$

$$\rho^+V^+\frac{\partial H_2^+}{\partial y^+}=\rho^+V^+\frac{\partial H_2^+}{\partial\eta}\frac{\partial\eta}{\partial y^+} \tag{I.31}$$

$$=C\rho_e^+\mu_e^+U_e^+\left(\frac{\eta f'}{\sqrt{2\xi}}-\frac{f}{\sqrt{2\xi}}-\eta f'\frac{\sqrt{2\xi}}{U_e^+}\frac{\partial U_e^+}{\partial\xi}\right)\left(\frac{\rho^+U_e^+}{\sqrt{2\xi}}\right)H_{2,e}^+G' \tag{I.32}$$

$$\frac{\partial}{\partial y^+}\left(\frac{k^+}{c_p^+}\frac{\partial H_2^+}{\partial y^+}\right)=\frac{\partial\eta}{\partial y^+}\frac{\partial}{\partial\eta}\left(\frac{k^+}{c_p^+}\frac{\partial\eta}{\partial y^+}\frac{\partial H_2^+}{\partial\eta}\right) \tag{I.33}$$

$$=\left(\frac{\rho^+U_e^+}{\sqrt{2\xi}}\right)^2 H_{2,e}^+G'\frac{\partial}{\partial\eta}\left(\frac{k^+}{c_p^+}\right)+\left(\frac{\rho^+U_e^+}{\sqrt{2\xi}}\right)\frac{k^+}{c_p^+}\frac{U_e^+}{\sqrt{2\xi}}H_{2,e}^+G'\frac{\partial\rho^+}{\partial\eta}$$

$$+\left(\frac{\rho^+U_e^+}{\sqrt{2\xi}}\right)^2\frac{k^+}{c_p^+}H_{2,e}^+G'' \tag{I.34}$$

$$=\frac{\rho^+U_e^+}{2\xi}H_{2,e}^+\left[\rho^+G'\frac{\partial}{\partial\eta}\left(\frac{k^+}{c_p^+}\right)+\frac{k^+}{c_p^+}G'\frac{\partial\rho^+}{\partial\eta}+\rho^+\frac{k^+}{c_p^+}G''\right] \tag{I.35}$$

$$=\frac{\rho^+U_e^{+2}H_{2,e}^+}{2\xi}\left(\rho^+G\frac{k^+}{c_p^+}\right)' \tag{I.36}$$

$$U^+\frac{dP}{dX^+}=C\rho_e^+\mu_e^+U_e^{+3}f'\frac{dU_e^+}{d\xi} \tag{I.37}$$

After combining these terms into a single expression, many terms are seen to cancel. The final result is;

$$2\left(\frac{\rho^+U_e^{+2}H_{2,e}^+}{2\xi}\right)\left(\rho^+\frac{k^+}{c_p^+}G'\right)'+\frac{\rho^+U_e^+H_{2,e}^+}{2\xi}C\rho_e^+\mu_e^+G'f$$
$$=(\gamma_0-1)M_0^2\left[U_e^{+4}\rho_e^{+2}\mu_e^+f'\frac{C}{U_e^+}\frac{\partial U_e^+}{\partial\xi}-2Pr_0U_e^{+4}f''^2\frac{\rho^{+2}}{2\xi}\right] \tag{I.39}$$

Dividing by a common factor $C\rho_e^+\mu_e^+/2\xi$ yields;

$$2\left(\frac{\rho^+G'\frac{k^+}{c_p^+}}{C\rho_e^+\mu_e^+}\right)'+G'f=(\gamma_0-1)M_0^2\left[\frac{\rho_e^+}{\rho^+}\frac{U_e^{+2}}{H_{2,e}^+}f'\frac{2\xi}{U_e^+}\frac{dU_e^+}{d\xi}-2Pr_0\frac{\rho^+}{\rho_e^+}\frac{\mu^+}{C\mu_e^+}\frac{U_e^{+2}}{H_{2,e}^+}f''^2\right] \tag{I.40}$$

Let

$$\beta=\frac{2\xi}{U_e^+}\frac{dU_e^+}{d\xi} \tag{I.41}$$

$$Pr^+=c_p^+\mu^+/k^+ \tag{I.42}$$

The final form of the equation becomes

$$2\left(\frac{\lambda G'}{\mathrm{Pr}^+}\right)' + G'f = (\gamma_0 - 1)M_0^2\left[\frac{\rho_e}{\rho}\frac{U_e^{+2}}{H_{2,e}^+}\beta f' - 2\,\mathrm{Pr}_0\lambda\frac{U_e^{+2}}{H_{2,e}^+}f''^2\right] \qquad (I.43)$$

VITA

Norman Zethward Shilling, son of Edward Shilling and Bessie Arlene Jenkins was born in   on

.

He graduated from Lyndhurst High School, Lyndhurst, New Jersey in 1962 and attended Stevens Institute of Technology and Newark College of Engineering. He received his B.S. in M.E. from the latter institution with the designation Summa Cum Laude in June, 1966. He was elected to membership in Pi Tau Sigma and Tau Beta Pi honor societies.

In September of 1966 he entered Massachusetts Institute of Technology holding a National Science Foundation Traineeship. He was nominated and elected to the MIT chapter of Sigma Xi in May of 1967. His M.S. thesis topic was "Dynamic Compensation Techniques for Plenum Fluid Suspensions". He completed requirements for his M.S. in M.E. in August 1967.

On September 2, 1967 he married Mary Eleanor Powell of Lyndhurst, New Jersey and subsequently returned to Newark College of Engineering as a doctoral candidate in the Department of Mechanical Engineering. While completing requirements for the D.Sc. degree he was the recipient of NASA research and NDEA teaching fellowships. He began work on the present dissertation in June of 1969. All experimental work was performed in the Mechanical Engineering Department laboratories during the period from September 1969 to August 1971. Support was provided by the Foundation for the Advancement of Graduate Study in Engineering.